UNIVERSITY OF
BIRMINGHAM

DRY HEAT TREATMENT OF FLOUR: ADDRESSING QUALITY AND SAFETY IMPLICATIONS

by

SILVIA KEPPLER

A thesis submitted to
The University of Birmingham
for the degree of
DOCTOR OF PHILOSOPHY

School of Chemical Engineering
The University of Birmingham
February 2017

Abstract

High ratio cake formulations such as sponges and cupcakes are well appreciated by the market due to their favourable attributes like sweet taste, moist mouthfeel, and tender texture. To bake a successful cake of such kind, it is necessary to change flour functionality. This can be done by dry heat treatment. The aim of this work was to investigate the dry heat treatment of flour and to implement it on a novel thermal processing equipment, the Revtech system, for the production of high ratio cake flour.

For this purpose, flour was heat treated in lab-scale experiments at accurately controlled time-temperature conditions. The effect of heat on flour functionality was evaluated with a variety of analytical methods, e.g. the Rapid-Visco-Analyser (RVA) or the rheometer.

The Revtech system is presented for the continuous heat treatment of flour. Particles are conveyed through helical pipes by vibrations and the pipe walls are heated by resistive heating. Residence time distributions were determined as a function of process parameters and shown to be narrow. The residence time was generally found to increase during extended periods of operation, which was related to the deposition of a powder layer inside the pipe. Temperature distributions of pipe and flour flow were characterised. After flour heat treatment in the Revtech equipment, high ratio cakes were baked and analysed. A method was developed to compare the results to lab-scale experiments. The time-temperature history of flour was described in terms of equivalent, constant treatment times and temperatures, which may be correlated to cake quality attributes. The approach is industrially relevant for the development of a cake flour specification and the facilitation of process validation.

"Life is what happens to you while you are busy making other plans"

John Lennon (1940 - 1980)

Acknowledgements

This project was an amazing journey for me and it greatly enriched my life. I am deeply grateful to all the people who accompanied me along the way.

First I would like to thank my supervisor at the University of Birmingham, Prof. Peter Jonathan Fryer for his brilliance, guidance, and patience and for teaching me and believing in me. I am also grateful to my second academic supervisor, Prof. Serafim Bakalis for welcoming me at the University and for his continued support. I would also like to express my gratitude to my advisor at Campden BRI, Dr Craig Leadley for his positivity and guidance and for always having my best interests at heart.

I am most thankful to the entire Campden BRI family and my colleagues at the School of Chemical Engineering for their never ending support; special thanks to Prof. Philip Richardson, Sarabjit Sahi, and Keith Jewel. I would also like to thank Lynn Draper for making everything just a little bit easier.

I am particularly grateful for the collaboration with my colleagues at the Indian Institute of Science in Bengaluru. I would like to thank Prof. Prabhu Nott, S.V.S.S.R. Phanikanth, and Peter Varun D'souza.

I would like to express gratitude to Martin Mitzkat and the whole team of Revtech process systems for the productive collaboration.

My special thanks are extended to the Biotechnology and Biological Sciences Research Council (BBSRC) for the generous funding of my project.

A person who has influenced my work in a major way is Dr John Chubb. I am most grateful for his contribution, his encouragement, and his kind words. He helped me through one of the most difficult periods of my PhD journey.

I am also indebted to Neil Griffith. Large parts of the experimental work could only take place because of his commitment.

I would like to thank all my friends who are always there for me. Special thanks to Ana, Charlotte, Domenico, Eleni, Emma, Ioanna, Lais, Laura, Luke, Matty, and Stepfi. I do not know what I would do without you!

I would like to express heartfelt thanks to Fotis.

Most of all, I would not be where I am today without my family. Thanks a million for your support and help and care in all situations.

Table of Contents

List of Figures

Chapter 2: Literature review

Chapter 3: Effect of temperature and time on flour functionality

Chapter 4: Residence time of flour and grains in the Revtech

Chapter 5: Heat treatment of flour in the Revtech

List of Tables

Chapter 2: Literature review

Chapter 3: Effect of temperature and time on flour functionality

Chapter 4: Residence time of flour and grains in the Revtech

Chapter 5: Heat treatment of flour in the Revtech

Abbreviations

GPI	Gluten performance index
PV	Peak viscosity
RTD	Residence time distribution
RVA	Rapid-Visco-Analyser
SEM	Scanning electron microscope
SRC	Solvent retention capacity

Nomenclature

Symbol	Parameter	Unit
a	thermal diffusivity	m^2/s
c_p	specific heat	J/kgK
h	heat transfer coefficient	$W/(m^2K)$
k	thermal conductivity	W/(m K)
m	mass	kg
$\dot{m}$	flow rate	kg/h
r	radius	m
t	time	s
v	velocity	m/s
x	axial distance	m
L	length	m
N	microbial count	/
$\dot{Q}$	heat flux	W
R^2	coefficient of determination	/
S	microbial survivors	/
T	temperature	°C, K
V	volume	m^3
X	colour value	/
Y	colour value	/
Z	colour value	/
α	angle	°, rad
β	angle	°, rad
δ	distance	m
μ	dynamic viscosity	Pas
ν	kinematic viscosity	m^2/s
ρ	bulk density	kg/m^3
φ	reaction rate	1/s

1 Introduction

Traditional cakes such as pound cakes require equal amounts of sugar, flour, eggs, and fat and exhibit a coarse texture and a limited shelf life (Catterall, 2000). Montzheimer (1931) discovered that chlorine gas improved the baking performance of flour in that it is more tolerant to high sugar concentrations in the formulation (Guy and Pithawala, 1981). Thereafter, high ratio cakes with sugar to flour ratios of 1.0 - 1.4 were developed. These cakes exhibit a higher level of sweetness, a moist mouthfeel, a fine texture, and a long shelf life. Hence, high ratio cake formulations such as sponges, cupcakes, or gateaux cakes are widespread in industry and proved very successful in the packaged cake market due to their good eating and keeping qualities (Guy and Pithawala, 1981; Hodge, 1975).

The production of successful high ratio cakes requires the use of cake flour. Cake flour is flour which has been treated to alter its functionality to carry more water and sugar leading to the desired cake quality attributes (Collyer, 1968; Cook, 2002). The most effective method for this purpose is to expose flour to chlorine gas up to levels of 2500 mg/kg (Bent et al., 1997). This is referred to as flour chlorination. Whilst it is common practice in countries like the USA, Canada, or Australia, chlorination is banned in Europe due to health concerns (Catterall, 2000; Cauvain and Young, 2009; Kent, 1994). The dry heat treatment of flour was accepted as an alternative process. The potential of dry heat treatment in replacing chlorination is significant as it is a physical flour modification receiving increased consumer acceptance in comparison to the chemical modification with chlorine gas. Flour heat treatment is therefore the focus of this work.

Little has been published about the mechanism of both treatments on flour on a molecular level. Flour components such as starch, protein, lipids, or arabinoxylans are organised in a complex manner and show manifold interactions. It is therefore challenging to determine the specific effects on each category and to distinguish between them. However, it is widely accepted that starch properties are affected in that starch granule swelling is facilitated allowing for the development of the desired cake structure (Alexander, 1939; Chamberlain, 1962; Gough et al., 1977; Guy and Pithawala, 1981). The evaluation of treatment effects is not trivial and hence, the success of flour treatment is commonly assessed by baking a cake.

Flour is industrially heat treated in batch processes or continuous systems. Bulk quantities and a low thermal conductivity of flour present challenges in achieving optimal, uniform, and reproducible results. The Revtech equipment is presented here as a novel technological solution for the continuous heat treatment of flour.

The overall goal of this work is to investigate the dry heat treatment of flour and to implement it on the Revtech equipment for the production of high ratio cake flour. For that purpose, it is necessary to obtain an understanding about treatment times and temperature distributions in the system. For process validation, it is important to identify relevant reactions (e.g. functionality alterations, microbial inactivation) taking place in the material during heat treatment and to determine reaction rates.

The objectives of this study are:

i) to investigate changes in flour functionality induced by heat treatment,

ii) to characterise residence times of particles in the Revtech equipment,

iii) to examine temperature profiles in the system, and

iv) to evaluate integrated effects of time and temperature after the heat treatment of flour in the Revtech device.

The aim of this work is to characterise the Revtech equipment and to show how it might be used. The results obtained in chapters 3 - 5 are not directly applicable to industrial machines.

The thesis consists of 6 chapters and is structured in the following way:

Chapter 2 – Literature review

An overview is given of the production, composition, and processing of wheat flour. The production of high ratio cake flour by chlorination and by dry heat treatment is explained in detail and the technology of cake making is described. Furthermore, the Revtech system, which is used for the continuous heat treatment of flour in this study, is characterised.

Chapter 3 – Effect of temperature and time on flour functionality

The effect of heat treatment on flour functionality was studied in accurately controlled laboratory scale experiments. Various analytical methods such as the Rapid-Visco-Analyser (RVA), the rheometer, or solvent retention capacity (SRC) tests were used to examine the effect of heat on functional properties and interactions of flour components.

Chapter 4 – Residence time of flour and grains in the Revtech

Treatment times are critical for the outcome of a thermal process. Therefore, flour was conveyed continuously through the Revtech system and treatment times were investigated. Residence time distributions were determined depending on process parameters. Residence time dynamics were examined over extended periods of operation.

Additionally, residence times of barley grains passing through the machine were studied due to the increasing interest in microbial inactivation of low water activity products such as nuts, seeds, or pulses.

Chapter 5 – Heat treatment of flour in the Revtech

Temperature distributions of product flow and pipe wall are shown and the integrated effects of treatment times and temperatures after flour heat treatment were studied. Flour was heat treated in the Revtech system at various processing conditions and analysed by baking high ratio cakes. In addition, the effects of heat treatment on flour functionality were assessed by analytical methods and compared to lab-scale results.

Chapter 6 – Conclusions and future work

A summary of results is presented and the industrial relevance is pointed out. Recommendations for future work are provided.

This work has been published in the following scientific papers, which are provided in full length in the appendix:

- Palgan, I., Limburn, R., Maguire, E., Keppler, S. (2015). "Challenges in validation of processes for low water activity foods." *New Food Magazine*, 18 (3), 58-62
- Keppler, S., Bakalis, S., Leadley, C.E., and Fryer, P.J. (2016). "A systematic study of the residence time of flour in a vibrating apparatus used for thermal processing." *Innovative Food Science and Emerging Technologies*, 33, 462-471.
- Keppler, S., Bakalis, S., Leadley, C.E., and Fryer, P.J. (2016). "Processing of barley grains in a continuous vibrating conveyor." *Journal of Food Engineering*, 187, 114-123.
- Keppler, S., Bakalis, S., Leadley, C.E., and Fryer, P.J. "Quantifying the effect of heat treatment on flour functionality." in preparation for submission to *Journal of Food Engineering*

This work has been presented at the following conferences:

- Keppler, S., Bakalis, S., Leadley, C.E., and Fryer, P.J. (2014). Study of the motion and residence time of particulate goods in a vibrating device used for thermal processing. *Conference of Food Engineering* (CoFE), Omaha, NE, USA (Oral presentation)
- Keppler, S., Bakalis, S., Leadley, C.E., and Fryer, P.J. (2015). Dynamics of the residence time of barley grains in a vibrating apparatus. *International Congress of Engineering and Food* (ICEF12), Quebec City, Canada (Oral presentation)

- Keppler, S., Bakalis, S., Leadley, C.E., and Fryer, P.J. (2015). Residence time dynamics of flour in a vibrating apparatus. *Institute of Food Technologists* (IFT15), Chicago, IL, USA (Poster presentation)
- Keppler, S., Bakalis, S., Leadley, C.E., and Fryer, P.J. (2016). Evaluation of the suitability of heat treated flour in high ratio cakes. *American Association of Cereal Chemists* (AACC), Savannah, GA, USA (Oral presentation)
- Keppler, S., Bakalis, S., Leadley, C.E., and Fryer, P.J. (2016). Dry heat treatment of flour in a novel tubular heating apparatus. *European Federation of Food Science and Technology* (EFFoST), Vienna, Austria (Oral presentation)
- Keppler, S., Bakalis, S., Leadley, C.E., and Fryer, P.J. (2017). Uniform heat treatment of particles for sustainable food processing. *Q-Safe International Conference*, Ermoupoli, Greece (Poster presentation)
- Keppler, S., Bakalis, S., Leadley, C.E., and Fryer, P.J. (2017). Uniform heat treatment of particles for sustainable food processing. *1st International Conference on Sustainable Energy and Resource Use in Food Chains (ICSEF)*, Old Windsor, England (Oral presentation)

2 Literature review

The aim of this project is the successful heat treatment of flour in a novel system for the production of high ratio cake flour. This chapter reviews the basics of flour production, composition, and processing. Subsequently, the principles of cake baking are described and the necessity of flour treatment for the production of high ratio cakes is explained. High ratio cakes were developed after it was found that flour chlorination improved its functionality. Hence, the process of flour chlorination and the effect on flour components and functionality is shown. The focus of this work lies on the alternative process, the dry heat treatment of flour, which is explained in detail in the following section. This chapter is completed by presenting the equipment used in this study for the heat treatment of flour.

2.1 Wheat flour

2.1.1 Production

Wheat has been cultivated for about 10 000 years (Cornell, 2012). Today, it is the second largest cereal crop grown in the world (730 million tonnes in 2014) that is only exceeded by the cultivation of maize (1020 million tonnes in 2014) (FAOSTAT, 2016; Manley et al., 2011).

The structure of a wheat grain is shown in Figure 2-1. The wheat germ represents only 2 - 3% by weight of the kernel, the bran characterises the outer layers of the grain and makes up

approx. 8% (Cornell, 2012). The endosperm represents the major part (80 - 85%) of the kernel consisting of a mixture of protein and starch (Cornell, 2012).

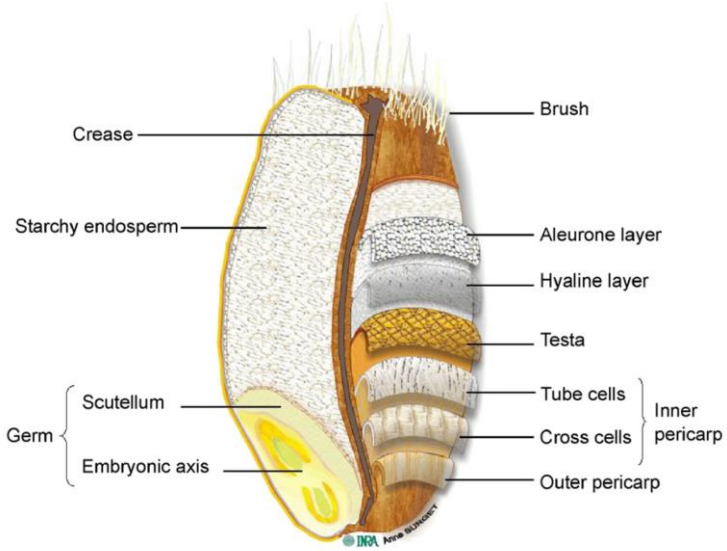

Figure 2-1: Structure of a wheat grain, showing component tissues (Saulnier et al., 2007)

Wheat kernels are typically milled before further processing (Miskelly et al., 2010). The aim of milling is the efficient separation of bran and germ from the grain's endosperm and to reduce the particle size of the endosperm to flour (Miskelly et al., 2010).

Before milling, wheat is cleaned by means of separators, combinators, magnets and aspirators and it is conditioned through water addition for efficient separation and correct moisture content of the product (Miskelly et al., 2010). Milling can be divided in three steps (Miskelly et al., 2010):

i) Breaking: A series of pairs of break rolls open the grain and scrape the bran to release endosperm particles.

ii) Separation on particle size and density: A number of sieves separate bran, semolina, and flour.

iii) Reduction: The size of endosperm chunks is reduced and the required level of starch damage is achieved in reduction roll passages. Mechanically damaged starch absorbs up to three times more water than undamaged starch, which plays a significant role in various applications.

The major mill products are flour, semolina, bran, germ, and pollard (remaining fine bran, endosperm, and germ materials from the 'reduction' step; used for animal feed) (Miskelly et al., 2010).

2.1.2 Composition

Wheat flour is essentially made of the endosperm, which is the major part (80 - 85%) of the wheat kernel (Cornell, 2012; Miskelly et al., 2010). Its composition is displayed in Table 2-1 and discussed in detail below.

Table 2-1: Composition of the wheat kernel's endosperm (Manley et al. 2011)

Component	%
Moisture	14.0
Protein	9.6
Fat	1.4
Ash	0.7
Carbohydrate by difference	74.3
Starch	72.0
Hemicellulose	1.8
Sugars	1.1
Cellulose	0.2
Total carbohydrate	74.1

2.1.2.1 Starch

Starch is formed by photosynthesis (Cornell, 2012). About 10^{11} tonnes of carbon dioxide are converted into organic polymers such as starch and cellulose annually (Cornell, 2012).

Composition

Starch is formed in cereals and other plants to store energy in their seeds or tubers (Guy et al., 2007). It is the predominant component of wheat flour (ca. 70 - 75%) and it is organised in granules that vary in shape, size, structure, and chemical composition (Da Rosa Zavareze and Guerra Dias, 2011; Manley et al., 2011). Two types and sizes of starch granules can be distinguished in wheat (Manley et al., 2011). The large, lenticular (A-type) granules have dimensions of 25 - 40 µm, while the small, spherical (B-type) granules have a diameter of typically up to 10 µm (Buleon et al., 1998; Manley et al., 2011; Ross, 2012). Starch consists

mainly of two glucose polymers, amylose and amylopectin macromolecules (Da Rosa Zavareze and Guerra Dias, 2011; Manley et al., 2011). The ratio of amylose and amylopectin depends on the botanical origin of the starch (Manley et al., 2011). For common wheat starch, amylose contents between 17% and 29% have been reported (Buleon et al., 1998; Manley et al., 2011; Ross, 2012).

i) Amylose is the smaller one of the two polymers with a size of about 250 - 1 000 D-glucose units (Ross, 2012). It is a linear molecule composed of D-glucose units linked by α-1,4 glycosidic bonds with a small number of branches (Da Rosa Zavareze and Guerra Dias, 2011; Ross, 2012) (see Figure 2-2). Its linear nature renders it insoluble in cold water (Ross, 2012). The linear amylose chain has a helical structure, which is formed with hydrogen atoms in the interior of the helix and hydroxyl groups on the outside (Da Rosa Zavareze and Guerra Dias, 2011). It is the hydrogen atoms in the interior of the helix that make amylose hydrophobic and enables it to form complexes with free fatty acids, component glycerides of fatty acids, iodine and some alcohols (Da Rosa Zavareze and Guerra Dias, 2011). Furthermore, it complexes with fats and emulsifiers in foods such as mono- and diglycerides (Da Rosa Zavareze and Guerra Dias, 2011).

ii) Amylopectin is a highly branched macromolecule and much larger than amylose (5 000 - 50 000 D-glucose units) (Da Rosa Zavareze and Guerra Dias, 2011; Ross, 2012) (see Figure 2-2). It is too large to be truly soluble, but it forms hydrated colloidal suspensions (Ross, 2012). The linear chains consist of 10 - 60 D-glucose monomers that are linked by α-1,4 glycosidic bonds. Additionally, there are side chains with 15 - 45 glucose units which are connected to the linear chains by α-1,6 glycosidic bonds (Da Rosa Zavareze and Guerra Dias, 2011).

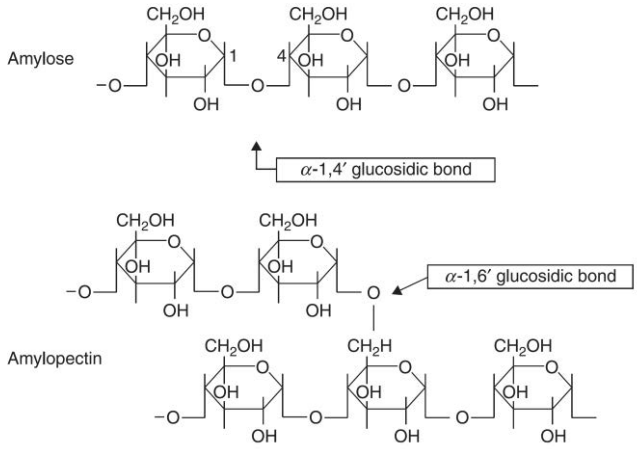

Figure 2-2: Structure of amylose and amylopectin macromolecules (Cornell, 2012)

Starch granules show a high degree of molecular organisation (Da Rosa Zavareze and Guerra Dias, 2011). During development of the plant seed, starch granules are formed as hollow spheres with starch polymers in the outer walls. Amylopectin molecules crystallise overnight and the sphere shrinks. The next day, new polymers form on the outside and shrink again the following night. This sequence continues until the granule is filled with polymers (Guy, 2006). Figure 2-3 shows the internal, concentrically layered granule structure (Zeeman et al., 2010). Repeating layers of crystallised terminal chains of amylopectin are altered with amorphous layers of amylose and amylopectin branch points resulting in a semicrystalline structure (Da Rosa Zavareze and Guerra Dias, 2011; Manley et al., 2011; Ross, 2012). The amorphous zone is less dense, more susceptible to enzymatic attacks and absorbs more water at temperatures below the gelatinisation temperature (Da Rosa Zavareze and Guerra Dias, 2011).

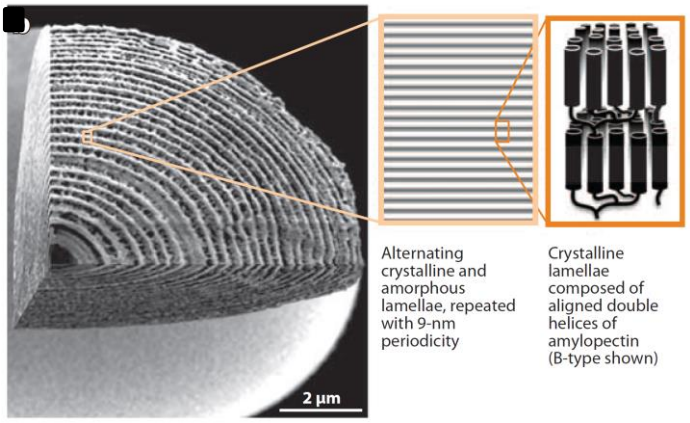

Figure 2-3: Internal growth-ring structure of a starch granule (Zeeman et al., 2010)

Next to glucose polymers, 1 - 2% minor components can be found either on the surface or inside the starch granules (Gough et al., 1977; Manley et al., 2011). These are mainly lipids (0.8 - 1.2%) and proteins (< 0.6 %) (Manley et al., 2011; Ross, 2012). The lipids associated with the starch are generally polar and occur prevalently inside the starch granules (Manley et al., 2011). They can occur either free or as amylose-lipid complexes (Manley et al., 2011). The starch surface lipids are mainly glycolipids and triacylglycerols (Manley et al., 2011). Starch associated proteins occur mainly at the surface of the starch granules, although starch granule internal proteins have been reported (Manley et al., 2011).

Functionality

The functionality of starch in an excess amount of water is most important in many food applications although in low water systems like cakes, competition for the available water between the starch, protein, and arabinoxylans is an important consideration. Starch granules absorb up to 30% of their dry weight of water and thereby swell slightly (ca. 5% volume

increase) (Manley et al., 2011). If starch is physically damaged by the milling process, it can absorb 100% of its own weight of water (Manley et al., 2011). This swelling process is reversible below a certain temperature called 'gelatinisation temperature' (Manley et al., 2011). The gelatinisation temperature depends on multiple factors such as botanical origin of the starch, amount of water present, pH, and types and concentrations of salt, sugar, fat, and protein (Guy, 2006; Hesso et al., 2015). When the starch suspension is heated at or above this temperature, the molecular order of the granules is irreversibly destroyed (Manley et al., 2011; Ross, 2012). This is called gelatinisation (Manley et al., 2011). Loss of birefringence (crystallinity) is one of the indicators of starch gelatinisation (Ross, 2012). Gelatinisation changes include extensive swelling of the starch granules and folding and leaching of amylose out of the granule (Gough et al., 1977). The phenomenon is driven by the relaxation of the amorphous regions from their hard, vitreous, glassy state, to a malleable rubbery state characterised by increased molecular mobility and free volume due to the combination of increased temperature and plasticisation by water (Ross, 2012). Concurrently, amylopectin is hydrated and its chains are pushed apart to create granule swelling (Ross, 2012).

The events that occur following starch gelatinisation during further heating are referred to as pasting (Manley et al., 2011; Ross, 2012). These include further swelling of the granules, granule distortion, amylose leaching out of the granules, and continued water uptake by the granule remnants (Hesso et al., 2015). These phenomena contribute to a significant viscosity increase and it is said that a starch paste is formed (Manley et al., 2011). Under conditions of shear, the granules can be completely disrupted and a molecular dispersion of starch molecules can be created (Ross, 2012). During starch gelatinisation and pasting the presence of free starch lipids may give rise to amylose-lipid complex formation (Hesso et al., 2015; Manley et al., 2011). These complexes can alter the gelatinisation temperature and the texture

and viscosity profile of the paste (Da Rosa Zavareze and Guerra Dias, 2011). Paste viscosity is directly related to starch behaviour in many food products (Guy, 2006). It is often used to give insights into flour performance (Guy, 2006).

During cooling of the amorphous starch paste, the starch polysaccharides reassociate to a more ordered (or even crystalline) structure (Manley et al., 2011). After few hours, very stable amylose crystallites are formed between the amylose molecules that leached out during pasting which creates a gel structure (Guy, 2006; Manley et al., 2011). The linear structure of the amylose is the reason for its insolubility in cold water and its higher propensity to crystallise in comparison to amylopectin (Ross, 2012). The recrystallisation of amylopectin side chains, often referred to as retrogradation, is a much slower process requiring several days or weeks and takes place within the gelatinised granules or granule remnants (Manley et al., 2011).

2.1.2.2 Non-starch polysaccharides

Non-starch polysaccharides like cellulose, arabinoxylan, β-D-glucan and arabinogalactan peptides are minor constituents of wheat flour (Manley et al., 2011). It also contains small levels (< 3%) of mono-, di-, and oligosaccharides such as glucose, fructose, sucrose, raffinose, and glucofructans (Manley et al., 2011).

In wheat, arabinoxylans predominate among the non-starch carbohydrates (2.2 wt%) (Kiszonas et al., 2013; Saulnier et al., 2007). They predominantly make up the thin walls surrounding the cells in the starchy endosperm (Izydorczyk and Biliaderis, 1995; Saulnier et

al., 2007). Arabinoxylans are composed of the pentoses arabinose and xylose and hence they are often referred to as pentosans (Saulnier et al., 2007).

Arabinoxylans consist of β-1,4 linked D-xylopyranosyl residues as a backbone substituted with monomeric α-L-arabinofuranose (Kiszonas et al., 2013). α-D-glucuronic acid is found as side chains and hydroxycinnamic acids, ferulic and p-coumaric acids, are found as esters (Saulnier et al., 2007). Ferulic acid only represents about 0.5% of arabinoxylans by weight but has significant effects on arabinoxylans' molecular weight and solubility, as well as on viscosity and gelation of wheat batters and doughs (Kiszonas et al., 2013). An unsubstituted β-1,4 linked D-xylopyranosyl chain forms a 3-fold, left-handed helix, and in the solid state it appears as an extended, twisted ribbon (Izydorczyk and Biliaderis, 1995). This can be important for the functionality of arabinoxylans.

Arabinoxylans can be empirically subdivided into water-extractable and water-unextractable fractions (Kiszonas et al., 2013). Between one quarter and one third of the arabinoxylans molecules in wheat flour are extractable in water at room temperature; a large portion of cereal arabinoxylans cannot be extracted from the cell wall material with water (Izydorczyk and Biliaderis, 1995; Kiszonas et al., 2013; Saulnier et al., 2007). The reason water-unextractable arabinoxylans are not water extractable is not fully understood (Kiszonas et al., 2013). Both arabinoxylan fractions show a high level of structural heterogeneity (Kiszonas et al., 2013).

Influence on rheological properties of dough, retrogradation of starch, and bread quality has been reported (Izydorczyk and Biliaderis, 1995). High water absorption capacity of arabinoxylans has been observed (Izydorczyk and Biliaderis, 1995; Kiszonas et al., 2013). Water-extractable arabinoxylans stabilise the liquid film around the gas cells in a dough,

thereby increasing gas retention during baking and stabilising the dough foam (Hoseney, 1984; Kiszonas et al., 2013). The addition of water-extractable arabinoxylans to dough has been shown to increase the dough consistency and stiffen the dough (Kiszonas et al., 2013).

2.1.2.3 Proteins

Wheat flour is unique amongst cereals in that, when mixed with water, it can form a dough capable of retaining gases to create highly aerated and palatable structures. This is due to the storage proteins (gluten) forming a network that allows for the retention of gas bubbles during baking of a dough to give open textures and pleasant eating products (Manley et al., 2011). This allows wheat to be processed into a range of products such as breads, other baked goods (including cakes and biscuits), pasta and noodles, and other processed foods (Shewry, 2009).

Proteins are present as discrete particles in the wheat endosperm and as interstitial material (Cornell, 2012). The classification of wheat protein is challenging due to their heterogeneous character (Gil, 2012). In the 1970s and 1980s, proteins were first classified on the basis of both their molecular structure and their solubility properties (Mills et al., 2012). One of the first classifications is known as the 'Osborne fractionation' subdividing wheat proteins in albumins, globulins, prolamins, and glutelins (Mills et al., 2012; Shewry, 2009). It is based on differential solubility of proteins in a variety of solvents (Mills et al., 2012). Analytical techniques such as electrophoresis, chromatography, and mass spectrometry are valuable for protein separation (Cornell, 2012; Gil, 2012).

Wheat flour proteins are divided here into gluten and non-gluten proteins (Cornell, 2012; Manley et al., 2011) (see Figure 2-4). The non-gluten proteins (15 - 20% of total protein)

contain albumins (water-extractable) and globulins (unextractable in water, but extractable in dilute salt solutions) (Manley et al., 2011). These are mainly monomeric proteins and physiologically active or structural proteins (Manley et al., 2011).

The gluten fraction (80 - 85% of total protein) are the major storage proteins in wheat (Manley et al., 2011). They can be divided into gliadins and glutenins and form a continuous matrix surrounding the starch granules (Cornell, 2012; Manley et al., 2011). Their low levels of amino acids with charged side chains and high hydrophobicity render them lowly soluble in water or dilute salt solutions (Manley et al., 2011). The gliadins consist of monomeric proteins, whereas the glutenins are polymers with high molecular weight and low molecular weight sub-units (Cornell, 2012; Manley et al., 2011).

Equal amounts of glutenins and gliadins make up the viscoelastic mixture of the wheat gluten complex of a dough (Cornell, 2012). The glutenins are responsible for its elasticity (Cornell, 2012). The three-dimensional network of gluten molecules is formed through disulphide bonding, hydrogen bonding, and hydrophobic interactions (Cornell, 2012).

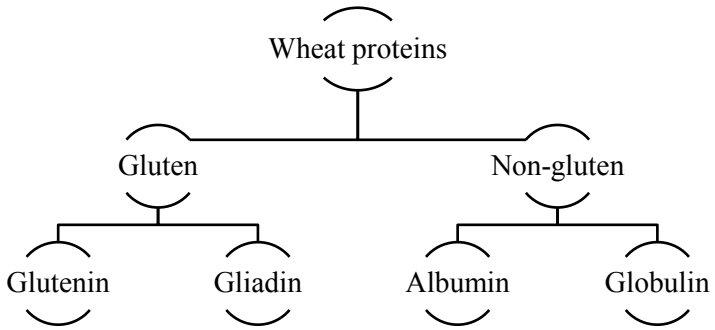

Figure 2-4: Classification of wheat flour proteins (Manley et al., 2011)

2.1.2.4 Lipids

Wheat flour only contains approx. 2% lipids, but this fraction is of special importance because of the lipids' ability to associate with proteins and with starch due to their amphipathic nature (Cornell, 2012; Gough et al., 1977; Manley et al., 2011). Comparable levels of polar and non-polar lipids are present in flour (Manley et al., 2011). Approx. 25% of the flour lipids are associated with the starch granule (see section 2.1.2.1) (Manley et al., 2011). The non-starch lipids consists predominantly of triacylglycerols and other non-polar lipids, glycolipids and phospholipids (Cornell, 2012; Manley et al., 2011).

2.1.3 Processing

Wheat flour is unique in its functional properties and can be used in a variety of applications. Using flour to make bread is probably the earliest form of food processing (Cauvain, 2001). The origins of bread making were suggested to be 8 000 BC in the Middle East, but it is possible that it may have been produced even several thousands of years earlier (Hutkins, 2008). The first pasta was probably consumed in Italy around 600 BC (Marchylo, 2001). Asian noodle processing can be traced back over 6 000 years to northern China (Hatcher, 2001). Today, noodles are well appreciated as convenience food all over the world. Further wheat products include breakfast cereals, biscuits, crackers, and cookies. The focus of this work is the production of cakes, which is described in detail in the following section.

2.2 Cake technology

Cakes made with equal amounts of flour, fat, sugar, and eggs are referred to as low ratio cakes or pound cakes (Catterall, 2000). This is the traditional way of making cakes. They tend to dry quickly and have a coarse texture and a limited shelf life (Catterall, 2000). In contrast are high ratio cake recipes with an increased level of sugar. Typically, they are characterised by a sugar to flour ratio of 1.0 - 1.4 (Guy and Pithawala, 1981). These cakes exhibit a longer shelf life, a fine texture, more sweetness, and a moist crumb (Catterall, 2000). Hence, they became the standard commercial method of baking in countries such as Australia, America, Canada, Japan, and the UK (Catterall, 2000).

A characteristic formulation of a high ratio cake batter is displayed in Table 2-2. It is critical to use special cake flour that has been treated by chlorination or heat treatment to modify its functionality (see sections 2.3 and 2.4). The ingredients can be divided in two main categories (Catterall, 2000):

i) Structure formers: Those ingredients, such as flour and egg, that provide structural components (primarily starch and protein).

ii) Texture contributors. This section can be sub-divided into two:

- Ingredients that lighten and aerate the cake, such as sugar, fat, and baking powder; and
- Ingredients that reduce aeration and make the cake heavier, such as milk and other liquids.

Table 2-2: Typical formulation of a high ratio cake (Campden BRI, 2012)

Ingredient	%
Cake flour	100
Caster sugar	115
White shortening	58
Paste emulsifier	2
Skimmed milk powder	7
Salt	1
Baking powder	3.75
Water	55
Liquid whole egg	80
Glycerine	8

2.2.1 Cake baking process

A cake is a porous system created by increasing the temperature of highly-aerated emulsions (Meza et al., 2011). The batter for a high ratio cake can be prepared by a single-stage, all-in mixing method (Campden BRI, 2012; Cauvain and Young, 2009). All liquids are placed into a mixing bowl, followed by the dry ingredients and fat and emulsifier on top. The ingredients are mixed until the desired batter density is reached (Campden BRI, 2012).

An oil in water emulsion is created during batter preparation with air bubbles entrapped in the fat phase and other ingredients dissolved or dispersed in the water phase (Bent et al., 1997). The central step of batter preparation is the mechanical dispersion of air into the continuous liquid phase (Cook, 2002; Meza et al., 2011).

The batter is placed into cake tins, which are then transferred into a preheated oven. In the early phases of baking, batter viscosity decreases due to temperature effects (see Figure 2-5).

As the fat melts during baking the entrapped air bubbles are released into the aqueous phase (Cook, 2002). Air cells expand due to water evaporation, CO_2 production, and heat expansion. The viscosity of the batter increases as baking continues due to starch gelatinisation and protein coagulation (see Figure 2-5) (Cook, 2002; Shelke et al., 1990). First, starch granules (1 - 40 μm) gelatinise and swell extensively to 2 - 2.4 times their original diameter when the temperature of the batter reaches 80 - 90°C. This increases the batter viscosity and leads to the formation of a rigid gel-like structure by inter-granular contacts (Guy and Pithawala, 1981). Second, some of the egg proteins are denatured by the increasing temperature and form aggregates and polymeric forms of the native proteins (Guy and Pithawala, 1981). It is the swollen starch granules surrounded by the agglomerated protein that creates the firm structure of the cake batter during baking (Guy and Pithawala, 1981). Hence, a cake can be presented as a system with a bricks and mortar structure (Gough et al., 1977). The starch granules describe the bricks which are bound together by the surrounding proteins characterising the mortar (Gough et al., 1977). With increasing solidification of the cake batter, the previously introduced air bubbles burst due to increasing internal pressure. The viscous foam structure sets and is transformed into an open 'sponge' configuration with connected air cells distributed evenly throughout the cake (Cook, 2002; Meza et al., 2011). The rupture of these air cells or bubbles occurs in the outer layers of the batter and moves progressively towards the centre of the cake as the temperature rises (Cook, 2002). This renders the cake structure strong enough to withstand the stresses that are exerted upon it during cooling and the desired crumb structure can be achieved (Flick et al., 2015; Gough et al., 1977).

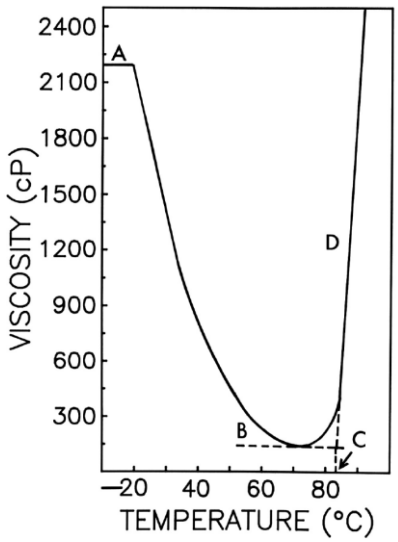

Figure 2-5: Viscosity-temperature profile of a cake during heating. (A) Viscosity at ambient temperature (B) Minimum viscosity of heated batters (C) Onset temperature of rapid viscosity increase and (D) Rapid viscosity increase (Shelke et al., 1990)

Hence, the main principle of cake baking is the expansion of the air cells in combination with the setting of the cake structure. If the cake is baked for insufficient time or formulation changes are made, the air bubbles in the batter might not rupture and no open sponge structure can be created. After removal from the oven, air cells shrink due to cooling of the gas and the cake collapses, leaving a zone of dense cake crumb (Catterall, 2014; Cook, 2002).

As mentioned earlier, the use of specially treated cake flour is crucial for baking a successful high ratio cake. Cakes made from untreated and treated flours behave in a similar way until the final stages of baking (up to 85°C). However, in case of untreated flour, the starch granules do not swell sufficiently for the air cells to rupture. Treated starch granules swell more extensively providing the required structure for the air cells to burst (Gough et al., 1977). Hence, the batter made with treated flour solidifies and the air cells rupture, whereas

this has not been observed for batters of untreated flour resulting in collapse of the crumb structure (Guy and Pithawala, 1981).

From an engineering perspective, baking is a simultaneous heat and mass transfer process, which causes a gradual increase in temperature and dehydration of the product (Hesso et al., 2015). Heat can be supplied to the product by natural or forced convection, conduction, radiation, and condensation of injected steam (Flick et al., 2015). Inside the product, heat is transferred by conduction from the surface to the core (Flick et al., 2015). Additionally, convective heat transfer occurs due to mass transfer and the evaporation of water near the surface and condensation of water near the core due to the temperature gradient also induces heat transfer (Flick et al., 2015). The mass transfer of water is the most important one (Flick et al., 2015). It principally migrates from the core of the product to the surface due to the difference in temperature (Flick et al., 2015). Numerous reactions such as volume increase, starch gelatinisation, protein denaturation, and surface browning take place (Flick et al., 2015; Hesso et al., 2015). The interactions between various phenomena during bread baking are shown in Figure 2-6 and can be largely transferred to cake baking.

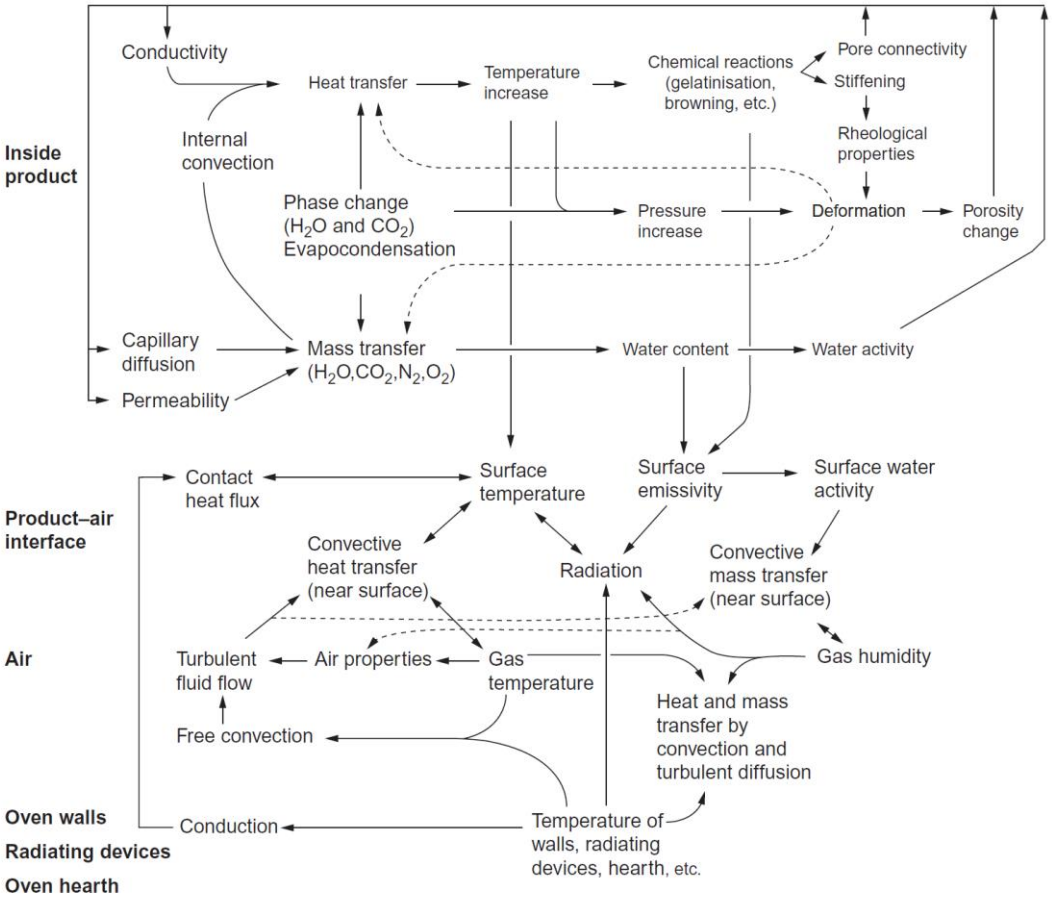

Figure 2-6: Coupled phenomena during bread making (Flick et al., 2015)

2.2.2 Role of ingredients

Flour and egg are responsible for the cake structure as explained in the previous section. The role of ingredients other than flour and egg are discussed below.

The addition of sugar serves several purposes:

i) It stabilises the foam by controlling the viscosity of the continuous phase, which prevents the air bubbles from coalescing and keeps the starch granules suspended (Cook, 2002).

ii) High sugar content is responsible for increased starch gelatinisation and protein denaturation temperatures in the batter by affecting protein and starch hydration (Cook, 2002; Gough et al., 1977; Hesso et al., 2015; Jacobsberg and Daniels, 1974; Meza et al., 2011). It was reported that the gelatinisation temperature rose from normal 52 - 61°C to about 90°C in concentrated sucrose solutions (Bean and Yamazaki, 1973; Gough et al., 1977). By retarding the setting of the structure, sugar increases the extent to which the air cells expand during baking, which contributes to volume and texture of the cake (Cook, 2002; Meza et al., 2011).

iii) The high sugar content limits the formation of a gluten network (Meza et al., 2011). In the production of bread, the development of a gluten network is indispensable for the elastic structure of the final product. However, a gluten network is not desired in the fine structure of a cake.

iv) It allows crust colour to develop at lower temperatures as it lowers the caramelisation point of the cake batter (Cook, 2002).

v) It contributes anti-staling properties to the cake due to its water binding ability (Cook, 2002).

Emulsifiers ensure the homogeneous dispersal of fats and help suspend the ingredients in the batter (Cook, 2002). The shortening serves three major functions in the cake, the entrapment of air during the mixing process, the physical interference with the continuity of starch and protein particles, and the emulsification of the liquid in the formulation (Sahin, 2008). In addition, fats and emulsifiers can form complexes between lipid and amylose during baking which delays the transport of water into the starch granule (Sahin, 2008). This delays gelatinisation, thereby allowing more time for the air bubbles in the batter to expand.

Chemical aerating agents are used to promote the expansion of initial air cells during baking (Cook, 2002). When sodium acid pyrophosphate (leavening acid) is combined with the appropriate level of sodium bicarbonate, carbon dioxide gas is released (Cook, 2002). Baking powders with a slow rate of reaction were found to give the best baking results (Cook, 2002). The later the release of gas before the cake structure sets, the greater the potential for trapping its volume-increasing properties (Cook, 2002).

Hydrocolloids may be added to the formulation for the improvement of cake volume, texture, increased moisture retention during baking and the prevention of staling (Sahin, 2008). For example, the addition of xanthan gum to a batter can increase the viscosity, thereby permitting better aeration during the mixing stage (Cook, 2002).

2.2.3 High ratio cake flour

The purpose of a flour specification is to agree with the supplier on levels of measurable parameters of the flour depending on its application (Manley et al., 2011). This presupposes that critical parameters are known in relation to the function of the flour in different processes (Manley et al., 2011). This is not the case for high ratio cake flour. A cake needs to be baked to evaluate the success of any flour treatment. However, there are certain criteria that have a positive effect on cake quality.

Wheat can be classified into soft and hard varieties, which largely depends on protein content (Cornell, 2012). Soft wheat flour is generally used for the production of high ratio cake flour.

i) When hard wheat is milled, the grain shatters causing the endosperm to fall apart into gritty, angular, clean edged particles (Manley et al., 2011; Stewart, 1969). The

starch granules are often damaged resulting in high water absorption characteristics (Manley et al., 2011). Hard types tend to have high protein contents (10 - 14%) and are usually spring wheats (Manley et al., 2011).

ii) When soft wheat is milled, the endosperm cells break down into rough, irregular, fluffy masses showing detached cellular material with many fine fragments (Stewart, 1969). It results in less damaged starch and in a lower water absorption (Al-Dmoor, 2013; Manley et al., 2011). Their protein levels are typically low or very low (8 - 11%) and their protein gives gluten that is less elastic and resistant to deformation and more extensible before being broken (Manley et al., 2011; Sahin, 2008). Soft wheat contains a higher proportion (by weight) of finer endosperm particles (Stewart, 1969).

The following criteria were reported for a good high ratio cake flour (Stewart, 1969):

i) Adequate treatment:

Physical or chemical flour treatments such as chlorination, heat treatment, or acetylation lead to improved functionality of cake flour.

ii) Reasonably fine granularity:

Flour particle size is important for cake quality (Cauvain and Muir, 1974; Collyer, 1968; Hodge, 1975). Flour particles vary in size (0 - 125 µm) (Stewart, 1969). Pin milling, air classification, or screens can be used to separate flour in fractions with different particle sizes (Cauvain and Muir, 1974; Stewart, 1969).

For high ratio cake baking, a fine flour particle size in a range of 15 - 35 µm has shown to deliver optimum results (Catterall, 2000; Cauvain and Muir, 1974; Cook, 2002; Hodge, 1975; Nicholas et al., 1978; Stewart, 1969). No difference was

detected whether the particle size reduction step was made before or after flour treatment (Cauvain and Muir, 1974; Hodge, 1975; Nicholas et al., 1978).

iii) Protein content:

The protein level of flour suitable for the production of high ratio cakes is typically between 6% and 11% (Al-Dmoor, 2013; Catterall, 2000; Cauvain and Muir, 1974; Nicholas et al., 1978). Nicholas et al. (1978) specified that high ratio products with good baking properties can be achieved with both high protein (12.5%) and low protein (7%) flour if the protein is appropriately denatured. Some authors reported that the protein level is of rather little significance for the cake quality (Cauvain and Muir, 1974; Hodge, 1975).

iv) In addition, low alpha amylase activity is required and the absence of bran ensures a good colour of the cake (Stewart, 1969).

2.3 Flour chlorination

High ratio cakes made from untreated flour collapse after baking (Collyer, 1968). This is due to the inability of starch granules to swell sufficiently in batters with high sugar concentrations (Collyer, 1968). The cake structure does not set and the air cells do not rupture, but contract during cooling resulting in a collapsed cake (Catterall, 2000). Collapsed cakes exhibit a poorer colour and an adverse structure characterised by less tenderness and a coarser texture (Catterall, 2000; Collyer, 1968; Tsen et al., 1971).

Montzheimer (1931) aimed to improve the colour of flour by using chlorine gas, when he found it also improved the baking performance of flour in that it became more tolerant to high sugar concentrations (Guy and Pithawala, 1981). As a result, high ratio cakes were developed and became successful on the packaged cake market due to their good eating and keeping qualities (Guy and Pithawala, 1981).

Chlorine treatment of flour improves the structure forming properties and prevents the cake from collapsing (Collyer, 1968; Kulp et al., 1985). Chlorine is added to flour at a rate of typically between 5 and 10 oz per sack (280 lb) (1100 - 2200 ppm), so that the pH of a defined flour-water-suspension is reduced to between 4 and 5 (Catterall, 2014; Hodge, 1975; Kulp et al., 1985; Russo and Doe, 1970; Tsen et al., 1971). Chlorine gas reacts with water from the flour to create hydrochloric acid and hypochlorite (Kulp et al., 1985) (see Eq. 2 - 1). The hydrochloric acid is responsible for the decreased pH and the hypochlorite is a powerful oxidant that reacts further with the flour components (Kulp et al., 1985).

$Cl_2 + H_2O \rightarrow HClO + HCl$ **Eq. 2 – 1**

It was found that after chlorination, 1/3 of the chlorine was absorbed by the free flour oil, 1/2 by the protein and only 1/7 to 1/5 by the starch fraction of flour (Chamberlain, 1962; Collyer, 1968; Gough et al., 1977). The chlorine levels found in the starch fraction were suggested to result from the bound lipid contents (Gough et al., 1977).

The broad reactivity of chlorine with flour components makes it difficult to resolve the key question: 'Which chemical reaction or reactions of chlorine is important for a certain bakery application?' (Kulp et al., 1985; Tsen et al., 1971). However, the increased acidity after chlorination is not the improving factor in flour (Kulp et al., 1985). Even after neutralisation of the flour with calcium carbonate, the improving effect of chlorine was still retained (Kulp et al., 1985).

2.3.1 Effect on flour components

2.3.1.1 Starch

It was reported that chlorination of the starch fraction is responsible for the improving effect on flour functionality (Catterall, 2000; Chamberlain, 1962; Collyer, 1968; Gough et al., 1977).

It was shown that only 20% of chlorine was absorbed by the starch fraction, which was unexpected because starch is the major component (approx. 75%) of flour (Chamberlain, 1962). It was also demonstrated that when starch replaced flour in a cake formulation, only 20% of the chlorine required by flour was needed for starch to obtain optimum high ratio cakes (Collyer, 1968). Hence, it was concluded that the effect of chlorine on starch was most important for the improved baking performance of flour after chlorination.

Another experiment showed that chlorinated starch and untreated dried gluten produced cakes and cake growth curves almost identical with those produced by chlorinated flour (Russo and Doe, 1970). These findings suggested that chlorination of other flour components was less important for the improving effect on flour functionality.

However, no chemical attack upon the starch molecules was observed (Gough et al., 1977). It was suggested that chlorine reacts with the non-carbohydrate material on the surfaces of starch granules such as proteins and lipids (see section 2.3.1.2) (Collyer, 1968; Gough et al., 1977). This interaction induces the change in starch behaviour (Collyer, 1968). However, at large chlorine doses mechanisms were proposed for the breakdown of starch molecules by oxidation and depolymerisation (Guy and Pithawala, 1981; Kulp et al., 1985; Kulp and Tsen, 1972; Whistler et al., 1966).

No apparent erosion of the granule structure was observed (Gough et al., 1977). The starch granules remained unaffected by chlorination indicating that the treatment did not weaken the granule structure (Kulp et al., 1985).

2.3.1.2 Lipids

The lipid fraction in flour can either be free oil or it is associated with starch or proteins, most likely as phospholipids and lipoproteins (Gough et al., 1977). Halogens such as chlorine can react with lipids either by addition to the unsaturated compounds or by oxidation (Gough et al., 1977; Kulp et al., 1985).

Chlorination of the non-starch materials on the starch granule surface such as lipids and proteins appears to be a key factor for the improvement of cake flour (Gough et al., 1977).

These materials might form a limiting barrier to extensive gelatinisation changes on the starch granule surface, which might be altered by chlorination resulting in the functional changes observed in the starch fraction that lead to the improvement of baking performance of flour (Gough et al., 1977).

Donelson et al. (1984) suggested that the entire lipid fraction is responsible for the improving action of chlorination. The authors fractionated untreated soft wheat cake flour in lipids, starch, tailing, gluten, and solubles. Each fraction was substituted by its chlorinated counterpart and a cake was baked. When the lipid fraction was interchanged, the cake resembled a chlorinated one even though the blend was less than 1% chlorinated (Donelson et al., 1984). The substitution of all the other fractions one at a time resulted in a collapsed cake with a concave surface (Donelson et al., 1984). On the other hand, when fractions of chlorinated flour were used and interchanged with their unchlorinated counterparts, all cakes resembled the cake made from chlorinated flour except when the lipids were changed by the untreated fraction (Donelson et al., 1984).

2.3.1.3 Proteins

Chlorination affects flour proteins in numerous ways; most importantly the gluten fraction is altered so that the development of a gluten network in the cake is reduced. Alteration of proteins on the starch granule surface might be of importance for flour improvement by chlorination (Gough et al., 1977). However, the alteration of other flour fractions is more important for the improving effect of chlorination on flour functionality (Chamberlain, 1962; Gough et al., 1977).

Numerous alterations, both hydrolytic and oxidative, of the protein fraction in flour take place during chlorination (Chamberlain, 1962; Tsen et al., 1971). Oxidative denaturation occurs as well as fragmentation (Kulp et al., 1985). Both inter- and intramolecular hydrogen bonds of the protein molecules are gradually broken by the action of chlorine causing an increased dispersibility of proteins (Guy, 2006; Tsen et al., 1971). Decreased protein solubility at high chlorination levels suggests that oxidation predominates over fragmentation (Kulp et al., 1985).

Evidence was found that chlorine reacts with sulphur-containing amino acids which results in the softening and weakening of gluten (Collyer, 1968; Gough et al., 1977; Harrel, 1952). Gluten proteins tend to be solubilised (Tsen et al., 1971).

Amides, peptide, and disulphide bonds are split and part of the cysteine and methionine can be oxidised (Collyer, 1968; Tsen et al., 1971). Some of the histidine and tyrosine was also destroyed (Collyer, 1968). Additionally, sulfhydryl groups of proteins are oxidised by chlorination to disulphide groups (Tsen et al., 1971).

2.3.2 Effect on flour functionality

The most significant effects of chlorination on flour functionality are:

- The improved swelling behaviour of starch granules after gelatinisation (Chamberlain, 1962; Gough et al., 1977), and
- the improvement of hydration capacity and dispersion of gluten in the cake batter (Alexander, 1939; Collyer, 1968).

The combined effect creates a flour that is able to carry much larger quantities of sugar and water than untreated flour (Collyer, 1968; Cook, 2002). It increases batter viscosity allowing for the development of a fine bubble structure in the batter and it allows the cake structure to solidify in the final stages of baking and prevents the cake from collapsing (Catterall, 2000; Gough et al., 1977).

2.3.2.1 Starch granule swelling

Increased swelling of treated starch granules at ambient temperature has been reported. Figure 2-7 shows that chlorinated starch granules are enlarged in water at both 25°C and 65°C in comparison to untreated samples (Chamberlain, 1962; Cornford, 1961). Others stated no difference in the size of starch granules after chlorination (Alexander, 1939; Gough et al., 1977; Kulp et al., 1985; Kulp and Tsen, 1972). No clear conclusions can be drawn.

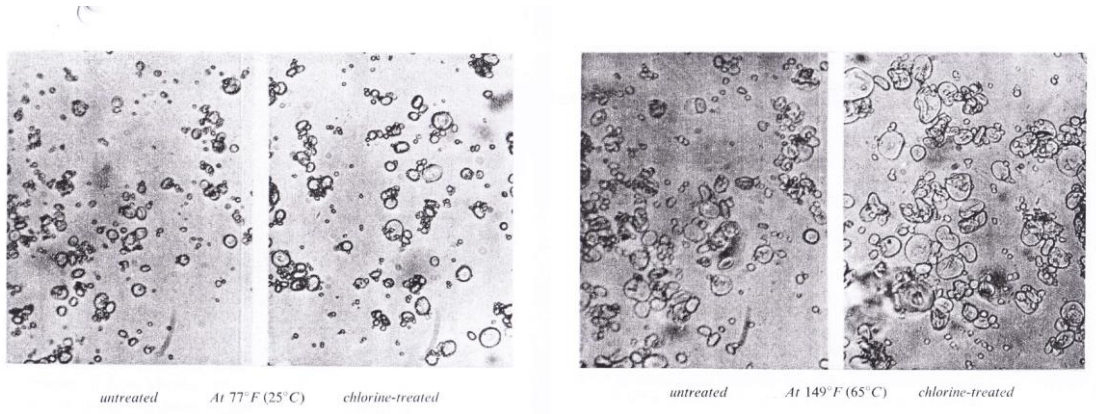

Figure 2-7: The microscopical appearance of suspensions of chlorine-treated and untreated starch in water, at 25°C and 65°C (Chamberlain, 1962)

2.3.2.2 Gelatinisation and pasting of starch

The gelatinisation temperature of starch is not affected by chlorine treatment (Cauvain and Muir, 1974; Guy and Pithawala, 1981; Jacobsberg and Daniels, 1974). Starch granules retained birefringence at all levels of chlorine treatment (Kulp and Tsen, 1972). It was therefore suggested that chlorine did not affect crystalline regions of the granules, but was confined to the surface and amorphous areas (Kulp and Tsen, 1972). The improving effect of chlorine treatment on flour functionality was suggested to be related to the post gelatinisation swelling process (Gough et al., 1977; Guy and Pithawala, 1981).

The pasting temperature of starch is lowered by chlorination (Kulp and Tsen, 1972; Russo and Doe, 1970). In addition, the rise in viscosity was accelerated between 50°C and 75°C for chlorinated flour (Kulp and Tsen, 1972). The authors suggested that the effect was caused by interaction of starch with other flour components (Kulp and Tsen, 1972). The starch granule surface might be 'activated' by chlorine facilitating the formation of starch-lipid or starch-protein complexes resulting in stabilisation of the cake batter during baking (Kulp and Tsen, 1972). Gough et al. (1977) suggested the presence of a limiting barrier to extensive gelatinisation or pasting changes on the surface of the starch granules consisting of non-carbohydrate material (see Figure 2-8). This molecular arrangement is changed by chlorine treatment to a disordered state where water absorption by the starch granule is facilitated (Gough et al., 1977).

The increased swelling of starch granules was then suggested to overcome the dilution effect of sugar and water in the cake batter, bringing sufficient starch granules into contact to establish a strong structure in the cake batter during baking that allows for the rupture of the air cells and the development of the desired cake structure (Hodge, 1975).

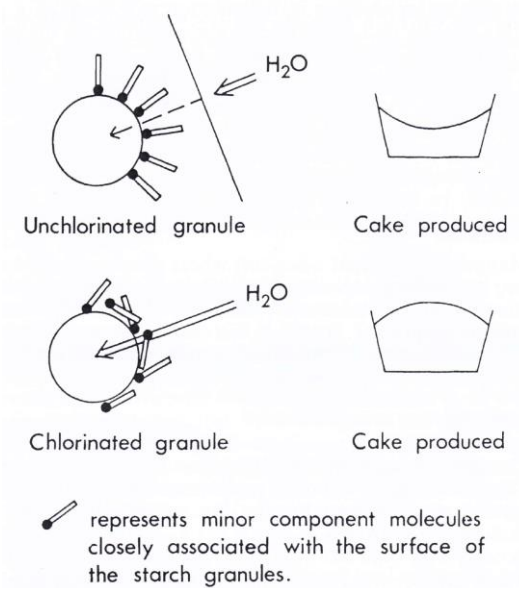

Figure 2-8: Scheme to represent a theory of chlorine action upon wheat starch granules in flour (Gough et al., 1977)

Several authors reported that the peak viscosity was not affected by chlorination unless very high doses were used (Gough et al., 1977; Jacobsberg and Daniels, 1974). At high treatment levels (8 oz Cl_2 per cwt), the peak viscosity or thickening power was reduced due to starch fragmentation (Kulp et al., 1985). In contrast, increasing peak viscosity with increasing levels of chlorination were reported by others (Kulp and Tsen, 1972; Telloke, 1986).

The effect of accelerated pasting changes might appear insignificant, however it was emphasised that any change in viscosity in the post-gelatinisation phase might play an important role considering that gelatinisation is delayed in a cake batter until a temperature of about 90°C is reached (due to a high sugar concentration) and the maximum temperature attained is only 100°C (Gough et al., 1977).

2.3.2.3 Dough properties

Stretching properties of a dough formed of flour and water can be assessed by means of an extensograph. Extensibility of the dough and the resistance to extension can be measured. A farinograph can be used to measure resistance of a dough to rotating mixer blades while a dough is formed, developed, and broken down.

A strengthening effect of dough in the farinograph was observed at lower chlorine levels (1 - 2 oz. Cl_2 per cwt) followed by weakening of the dough at higher levels (Kulp et al., 1985). The strengthening of the dough was attributed to oxidation of sulfhydryl groups and the weakening to cleavage of peptide bonds in high molecular proteins (Kulp et al., 1985). Furthermore, an increase in water absorption of farinograph doughs was observed with increasing chlorine treatment (Tsen et al., 1971). This was attributed to increased hydration capacities of starch granules (Tsen et al., 1971).

Doughs made with untreated flour were highly extensible and showed low resistance in the extensograph (Harrel, 1952). When treated with chlorine, flour gradually lost extensibility and became more resistant to extension, which was attributed to oxidation (Harrel, 1952).

2.3.2.4 Bleaching effect

Chlorine produces hypochlorite which oxidises flour pigments (xanthophyll with small amounts of carotene) which are present in the lipid fraction (Gough et al., 1977; Kulp et al., 1985). This oxidation causes the bleaching effect of the colour (Gough et al., 1977).

2.3.3 Alternative processes

After health concerns were raised, flour chlorination was banned in the EU in the year 2000 (Catterall, 2000). Several alternatives were proposed (Catterall, 2000; Gough et al., 1977):

i) Alternative flour treatments:

- Acetylation of flour by either ketene or acetic anhydride produced cakes that were almost indistinguishable from the chlorinated control. This method is based on the principle that proteins on the starch granule surface had their hydrophilic charge removed by acetylation. This results in a hydrophobic starch granule surface enabling the production of high ratio cakes (Catterall, 2000). However, due to its chemical nature, concerns about its acceptability to the public were raised and the process is not commercially available (Catterall, 2000).
- It was found that heat treatment of flour had the same improving effect as chlorination (Donelson et al., 1984). Proposed principles and limitations are discussed in section 2.4.

ii) Specialised ingredients:

Starches, fibre, gums, protein, chemicals, or emulsifiers can be combined with untreated flour to enhance batter viscosity and to create satisfactory high ratio cakes (Catterall, 2000).

iii) Recipe adjustments:

Using the basic knowledge of the function of the ingredients, it may be possible to amend recipes to increase the sugar and liquid contents while using untreated flour (Catterall, 2000).

iv) Novel methods:

The knowledge that a high ratio cake has to change from a foam in the batter stage to an open structure (sponge) at the end of baking is exploited.

- Microencapsulation of sodium bicarbonate uses the CO_2 from sodium bicarbonate as a 'foam breaking' agent, facilitating the conversion from a foam to a sponge. Problems occurred finding a satisfactory CO_2 delivery system (Catterall, 2000).
- Another approach is to physically shock the cake as soon as it is removed from the oven to disrupt the air bubbles in the product, i.e. by dropping the tray onto a solid surface. Problems occurred with the reproducibility of the results (Catterall, 2000).

2.4 Dry heat treatment of flour

Several flour treatments were considered as an alternative to chlorination. Dry heat treatment with or without the addition of specialised ingredients appeared to be most promising for the production of high ratio cakes (Catterall, 2000).

The key elements of flour improvement by heat treatment were suggested to be (Guy et al., 2007; Guy and Pithawala, 1981):

i) Increased water absorption and improved swelling behaviour of starch granules resulting in a higher batter viscosity in the critical stage of baking when starch gelatinises and protein coagulates. This allows for mutual contact of the starch granules leading to the development of the desired cake structure.

ii) Increased interactions between starch and egg protein resulting in firmer batter gels.

Research suggests that all flour components are affected by dry heat treatment (Nicholas et al., 1978). It is largely recognised that the major effect of flour improvement relates to the starch fraction whose performance is significantly altered after the treatment (Gough et al., 1977; Guy et al., 2007). The modification of starch functionality was attributed to changes in the surface layers of the granules involving proteins and lipids (Cook, 2002).

Mangels (1934) showed in 1934 that the dry heat treatment of starch (80 - 100°C for 8 hours) increased its swelling capacity after gelatinisation in dilute sodium hydroxide solution. About half a century later, the first heat treated cake flour was sold in the UK in the early 1980's (Catterall, 2000). The basis formed the patent of Doe and Russo (1968). Patents of Cauvain et

al. (1976), Hanamoto and Bean (1979), and Gusek (1994) followed specifying and developing the process (Catterall, 2000).

The main weaknesses of heat treated flour are the lack of any bleaching effect and the possible development of a cooked flavour during flour processing (Catterall, 2000).

2.4.1 Effect on flour components

The effect of heat treatment on flour components is not fully understood (Chesterton et al., 2015). Presumably, all flour components (e.g. starch, proteins, and lipids) are affected by the treatment. However, physical and chemical changes are hard to detect (Nicholas et al., 1978).

The most significant changes in flour after heat treatment seem to occur in the protein fractions (Nicholas et al., 1978). Structural changes in proteins as a result of heating include denaturation (cleavage of ionic, hydrogen, and van der Waals bonds) and crosslinking through oxidation of soluble sulfhydryl groups to produce insoluble disulphide bridges (Riganakos and Kontominas, 1994). The denaturation of both gluten and non-gluten protein plays a significant role in the changes in flour functionality after heat treatment:

i) It is widely accepted that both dry heat treatment and chlorination work in a similar way to improve flour functionality by changing the non-starch material on the surface of the starch granules (Catterall, 2000; Collyer, 1968; Guy et al., 2007; Nicholas et al., 1978). The protein on the starch granule surface might form a barrier in native flour that hinders water absorption and hence swelling of the starch granules (Nicholas et al., 1978). This might be aided by bound lipids on the starch granule's surface (Nicholas et al., 1978). This barrier could be degraded by

partial heat denaturation of the proteins allowing the starch granules to swell more easily and to a greater extent (Gough et al., 1977; Nicholas et al., 1978; Van Steertegem et al., 2013). As a result, improved contact between starch granules could be established in the batter supporting a strong structure around the air cells and preventing cake collapse (Guy and Pithawala, 1981).

In addition, these proteins are of the albumen type that generally has a complex folded structure enclosing an "oily" core of hydrophobic amino-acids (Catterall, 2000; Nicholas et al., 1978). The structure is kept in place by a delicate network of bonds which, when disrupted, irreversibly expose the hydrophobic core. As the proteins are attached to the starch surface, the effect is to make the granule more hydrophobic (Catterall, 2000; Seguchi and Yamada, 1988). Hydrophobic starch granules might bind to the membrane of air bubbles in the cake batter, thus stabilising the bubbles (Seguchi and Yamada, 1988). Consequently, hydrophobic starch granules could contribute to the stability of cake batter and to the improvement of cake structure (Seguchi and Yamada, 1988).

ii) Whereas the denaturation of albumin and globulin is desirable, the severe destruction of the gluten component gliadin is detrimental to the cake structure (Nicholas et al., 1978). The reason is its ability to bind water and to stabilise the liquid phase of the batter during the early stages of baking (20 - 80°C). Heat treatment prevents the gluten protein from swelling due to covalent disulphide cross-links and polymerisation and thereby affects its hydration properties (Van Steertegem et al., 2013). Consequently, if gluten protein is too severely damaged, a loss in batter stability results (Nicholas et al., 1978).

Hence, the aim of flour heat treatment is to denature the small globular proteins on the surface of the starch granules and to prevent excessive denaturation of the gliadins (Guy et al., 2007; Nicholas et al., 1978). At optimum conditions of heat treatment, albumins and globulins were denatured by 5 - 50% and gliadins were denatured by 5 - 35% (Nicholas et al., 1978). The level of denaturation was suggested to be more important to the flour's functionality after heat treatment than the initial or final level of undenatured proteins in flour (Nicholas et al., 1978). When the maximum level of denaturation is exceeded, baking qualities deteriorated (Nicholas et al., 1978).

The moisture level in flour plays a significant role in achieving the required degree of denaturation of the particular proteins (Nicholas et al., 1978). The heat treatment promotes the denaturation of gliadin with increasing moisture content of flour (Nicholas et al., 1978). Steam treatment of flour thus results in almost complete denaturation of gliadins, which then makes the flour unsuitable for high ratio cakes (Nicholas et al., 1978). It is therefore crucial that the conditions of heat treatment are chosen adequately to produce a controlled denaturation process that provides the desired denaturation levels (Nicholas et al., 1978).

Flour lipids were not chemically changed by heat treatment, but their physical interaction with other flour components might be altered (Guy and Mair, 1993; Morrison, 1978).

No difference in the morphology of the starch granules was observed between untreated and heat treated starch granules under the microscope and it was concluded that heat treatment did not affect the structure of wheat starch (Gough et al., 1977; Ozawa et al., 2009; Russo and Doe, 1970). In contrast, cavities were detected on corn starch granules after drying at elevated temperatures (Whistler et al., 1958). A higher percentage of granules showing such cavitation was found at lower levels of moisture content (Whistler et al., 1958).

More recently, the impact of heat treatment on solvent accessibility of arabinoxylans was proposed, but no clear conclusions could be drawn (Van Steertegem et al., 2013). Some pentosans are known to contribute to water absorption of flour and viscosity of doughs and batters (Cornell, 2012). They generally increase loaf volume and improve crumb and crust characteristics (Cornell, 2012). Hence, changes in the arabinoxylan fraction due to heat treatment could affect flour functionality.

2.4.2 Effects on flour functionality

Heat treatment of flour improves its functionality with regard to cake baking properties. Starch properties are altered without destroying its granular structure (Gough et al., 1977; Russo and Doe, 1970). The non-starch material present on the starch granule surface is of major importance for the functional changes in flour after heat treatment (Guy and Pithawala, 1981).

2.4.2.1 Batter viscosity and air retention

Cake batters made with heat treated flour show a higher viscosity than batters made with untreated flour, which in turn helps to trap and subdivide air in the batter during mixing (Meza et al., 2011; Sahin, 2008). This was attributed to protein denaturation (Anson and Mirsky, 1932; Gough et al., 1977; Guy et al., 2007; Sahin, 2008). The viscosity profile during mixing, processing and baking is critical to the performance of the finished product (Catterall, 2000).

Furthermore, the hydrophobicity of starch increases during heat treatment due to changes in starch granule surface proteins (Gough et al., 1977; Meza et al., 2011; Ozawa et al., 2009). The hydrophobic starch granules bind to the air cell interfaces and stabilise the air bubbles in cake batters (Meza et al., 2011; Seguchi and Yamada, 1988). The increased hydrophobicity and the increased amount of protein that may be absorbed on the surface of the starch granules was reported to be the reason for a significantly better air retention in foams made from heat treated flour than those made from untreated flour (Meza et al., 2011).

2.4.2.2 Gelatinisation and pasting of starch

The gelatinisation temperature of starch did not change after heat treatment (Guy et al., 2007; Jacobsberg and Daniels, 1974). On a molecular level, the starch granules start to swell at the same point in the baking process for both treated and untreated flour (Guy and Pithawala, 1981).

However, one of the key elements of flour heat treatment is the increased swelling ability of starch granules in high sugar concentrations after gelatinisation resulting in increased stability of the cake structure during baking (Collyer, 1968; Guy et al., 2007; Nicholas et al., 1978). The reason for this is presumably the denaturation of globular proteins on the surface of the starch granules (see section 2.4.1) (Nicholas et al., 1978). Consequently, the pasting properties of starch changed after heat treatment:

- An earlier pasting time was reported for heat treated flour (Ozawa et al., 2009).
- The pasting temperature of starch decreased with increasing temperature of heat treatment from 150°C onwards (Russo and Doe, 1970).

- A significant increase in peak viscosity was observed for dry heat treated cake flour in comparison to untreated flour (Guy et al., 2007; Ozawa et al., 2009; Van Steertegem et al., 2013). This was attributed to the improved swelling of starch granules after heat treatment (Guy et al., 2007; Ozawa et al., 2009). Ozawa et al. (2009) suggested the gluten to be the reason for the increase in viscosity. Van Steertegem et al. (2013) attributed the increase in peak viscosity upon longer and more severe heat treatment to more extensive cross-linking within the proteins that allows the rigidified flour particle to swell longer and to withstand external shear.

2.4.2.3 Gelation of cake batter

The gel forming properties of batters made with heat treated flour are significantly altered in comparison to batters made with untreated flour (Guy and Pithawala, 1981). This was determined by compression tests. Batters made with heat treated flour firmed earlier in the baking process, quicker, and eventually resulted in stronger gels (Guy and Pithawala, 1981). The findings showed that the swelling process of the starch granules is altered after heat treatment, so that they swell more quickly and more extensively than untreated granules (Guy and Pithawala, 1981). This is in agreement with the modified starch pasting behaviour after heat treatment in the previous section.

In addition, the interaction of egg proteins with starch increased in heat treated flour in comparison to untreated flour which resulted in rapid increase in firmness and higher firmness values of the batters (Guy and Pithawala, 1981).

2.4.2.4 Dough properties

Heat treatment affects gluten hydration and dough development (Van Steertegem et al., 2013). Heat treated flour particles hydrate more slowly, probably owing to a more rigid structure as formed by the cross-linked gluten proteins (Van Steertegem et al., 2013). At a certain level of heat treatment a complete lack of gluten network formation was observed (Van Steertegem et al., 2013).

2.4.3 Industrial heat treatment process

The industrial heat treatment of flour can be divided into several processing steps. Typically, flour is first dried and then heat treated, which is explained in detailed below. After heat treatment, the flour is cooled down in a stream of air. The flour moisture is adjusted back to the desired level (e.g. 12%) during rehydration, which can be done by spraying water onto the flour and mixing it. Finally, a milling step is applied to break up agglomerates which might have formed during rehydration (Chesterton et al., 2015; Greatbatch, 2015; Guy, 2006; Poole, 2014).

2.4.3.1 Drying

The drying step is commonly done in a stream of hot air (e.g. fluidised bed dryer) with the intention of reaching the flour target temperature quickly (Greatbatch, 2015; Guy and Mair, 1993). The flour moisture is reduced to below 4 - 7% (Chesterton et al., 2015; Guy and Mair, 1993; Neill et al., 2012). Several explanations are suggested as to why the drying step is important for the success of the treatment:

i) Facilitation of the process: Water is gently removed from flour to prevent lumping (agglomeration) during heat treatment in the next step (Guy and Mair, 1993).

ii) Prevention of starch gelatinisation during subsequent heat treatment (Greatbatch, 2015; Sahi, 2015).

iii) Protection of the proteins: Heating flour at high moisture contents results in excessive denaturation of wheat proteins (Guy and Mair, 1993) (see section 2.4.1). The proteins were suggested to have a function in providing viscosity and bubble control in the batter (Guy and Mair, 1993). After denaturation, their function is decreased and the batter destabilises (Nicholas et al., 1978). By gentle removal of water prior to heat treatment, protein denaturation is reduced and flour functionality is improved in the cake batter.

iv) Prevention of off-flavours and poor colours (Catterall, 2014).

2.4.3.2 Heat treatment

After the drying step, the flour is held at the desired temperature for the time period required to achieve the desired product characteristics (Chesterton et al., 2015). This is commonly done in rotating drums or heated conveyors, where the target temperature of flour is maintained through contact with the equipment (Greatbatch, 2015; Guy and Mair, 1993). Examples of suitable equipment for the heat treatment of flour are (Nicholas et al., 1978):

i) Rotating drums (either batch wise or continuously), or

ii) continuous screw conveyors, where screw and jacket are provided with passages for the circulation of a heating medium, or

iii) mechanically agitated beds via a heated surface, or

iv) stirred expanded beds, or

v) microwave heating, or

vi) heating during a grinding or milling process.

The relevant process parameters are treatment time and temperature (Guy and Mair, 1993). Typical treatment conditions are 120 - 140°C for 0 - 30 min usually involving a drying step (Chesterton et al., 2015; Doe and Russo, 1970; Guy and Mair, 1993; Neill et al., 2012; Nicholas et al., 1978; Thomasson et al., 1995). Treatments at lower temperatures generally require longer holding times, whereas at higher temperatures no holding time may be necessary (Nicholas et al., 1978). Russo and Doe (1970) suggested that holding time is not critical at an optimum treatment temperature of 120°C. The time-temperature conditions should be chosen so that optimal protein denaturation can be achieved (see section 2.4.1) (Nicholas et al., 1978). Overheating should be avoided as it results in starch dextrinisation and subsequently in the development of colour and off-taste in the product (Doe and Russo, 1970; Germaine et al., 2004; Nicholas et al., 1978). The use of inert gas was reported as a factor that can be controlled for the improved success of the treatment (Guy and Mair, 1993).

2.5 Equipment for flour heat treatment used in this work

The dry heat treatment of flour is industrially applied in continuous and batch systems such as rotating drums or screw conveyors (see section 2.4.3). The low thermal conductivity of flour and bulk quantities present challenges for the uniform heat treatment with reproducible results. In this work, the Revtech system (Revtech Process Systems, Loriol-sur-Drôme, France) was investigated for the continuous heat treatment of flour with the overall goal to bake successful high ratio cakes. The advantages of this novel technology are (Revtech Process Systems, 2016):

i) A uniform treatment due to a thin layer of material passing through the system and the distinctive mixing action of the material in the helical device.

ii) It is a highly flexible and customised process that allows to precisely adjust treatment times and temperatures.

Figure 2-9 shows the pilot plant Revtech equipment located at Campden BRI (Chipping Campden, UK). Figure 2-10 shows a 3D schematic of the system. The main components are:

Hopper

A hopper (A) with a conveyor screw attached at the bottom contains the raw material. A debridger is in place to consistently fill the screw. The screw conveys the particles from the hopper to the bottom of the heating spiral. The screw speed adjusts the product flow. Two controlling mechanisms are in place to adjust the screw speed:

- When the screw is empty, the screw speed is pre-set depending on the bulk density of the material.
- When the screw is filled with product, the screw feeder speed is controlled by a check-weigher to keep the flow rate constant should the bulk density change.

Heating spiral

The heating spiral (B) has a length of 34.4 m, an internal diameter of 84.5 mm and an inclination of 2.83°. The pipe walls are electrically heated by resistive heating (Joule effect). A low voltage (30 V) is applied directly to the steel pipe, heating it up as the current runs through the material from the positive to the negative electrode. A positive electrode is located in the middle of the spiral and negative electrodes are located at the inlet and at the outlet of the pipe. Hence, the current runs from the middle of the spiral towards the inlet and the outlet. The pipe is insulated on the outside to reduce heat loss. Eight temperature probes are built into the heating spiral, located in shafts welded to the bottom of the pipe. Probe 1 is located after half a loop from the inlet of the spiral (at 2 m axial distance), after which there is one probe in each loop (approx. 4.05 m per loop). Probe 8 is located in loop 8 (at 30.4 m axial distance), 4 m before the outlet of the pipe.

Two off balance motors (G) are attached on opposite sides of the inner construction of the spiral at an adjustable angle with the horizontal. The motors rotate at a given frequency and create vibrations due to off balance weights. Two weights can be adjusted towards each other and depending on their angle an uneven distribution of mass is created around the axis of

rotation. As a result, vibrations are created. By these vibrations, particles pass continuously from the bottom to the top of the spiral. The vibrations can be controlled by changing:

- *Motor angle*. The movement of the motor is perpendicular to the motor axis. Adjustment of the motor angle β affects the velocity components of the motors in horizontal and vertical direction. This is shown in Figure 2-11 and the components are defined in equations 2 - 2 and 2 - 3. With increasing angle β, which ranges between 10° and 50° ($\alpha = 90° - \beta$), the horizontal velocity component increases, whereas the vertical one decreases.

$$v_x = v \cdot cos(\alpha) \qquad \textbf{Eq. 2 - 2}$$

$$v_y = v \cdot sin(\alpha) \qquad \textbf{Eq. 2 - 3}$$

- *Motor speed*. This controls the vibrational frequency of the oscillations and can be adjusted between 600 rpm (10 Hz) and 740 rpm (12.3 Hz).
- *Off balance motor setting*. This influences the amplitude of the vibrations and can be set between 0% and 100%.

The device is designed so that it is possible to inject steam into the heating pipe, but this feature has not been used for the dry heat treatment in this work.

Cooling spiral

The top of the heating spiral is connected to the bottom of a cooling spiral (D) by a flexible plastic pipe (C). The cooling spiral has a length of 40 m, an inner diameter of 83 mm and an

inclination of 2.33°. Cold air from a chiller is introduced into the pipe via 10 injection ports (H) to cool down the material passing through. The bottom four loops of the spiral are insulated. Analogous to the heating spiral, off balance motors are attached to create vibrations to convey the material through the spiral. The treated product leaves the equipment through a short plastic pipe at point E.

Extraction manifold

The atmosphere of both spirals can be extracted via extraction tubes to the extraction manifold (F).

Residence times of particles passing through the machine are investigated in chapter 4. Temperature distributions of product flow and pipe wall are characterised in chapter 5. Integrated effects of time and temperature on flour functionality after the heat treatment are also presented in chapter 5. The success of flour heat treatment is assessed by baking high ratio cakes and by analytical methods. The results are compared to laboratory scale experiments.

a)

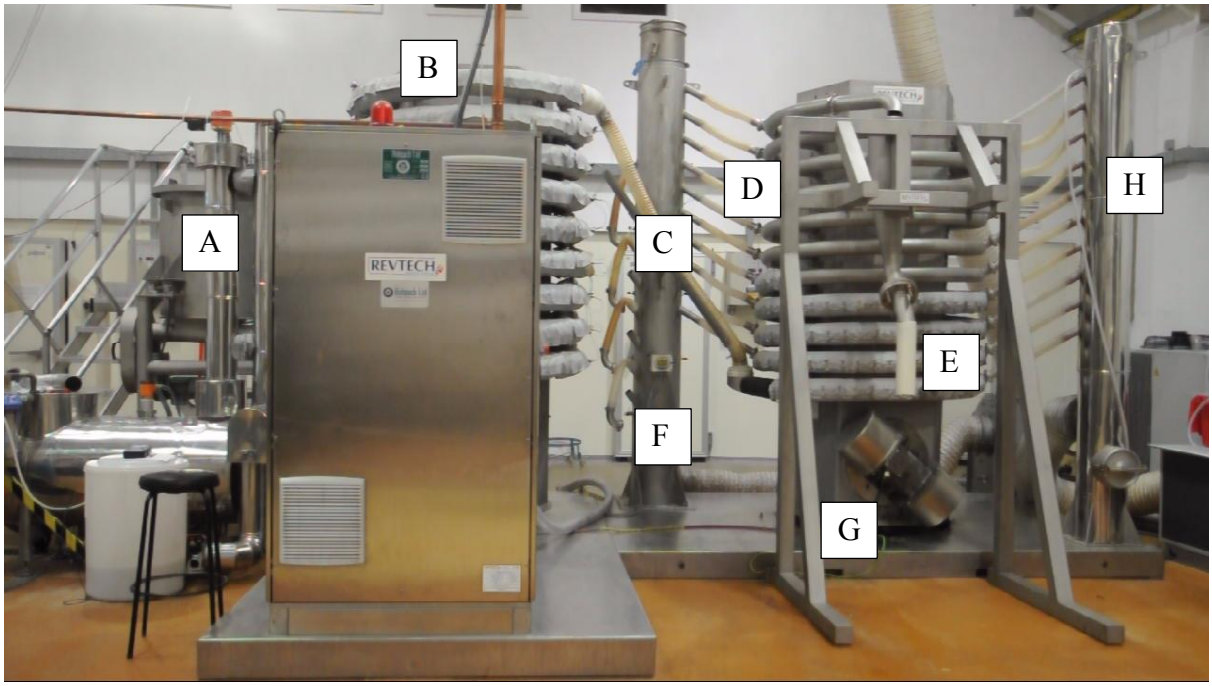

b)

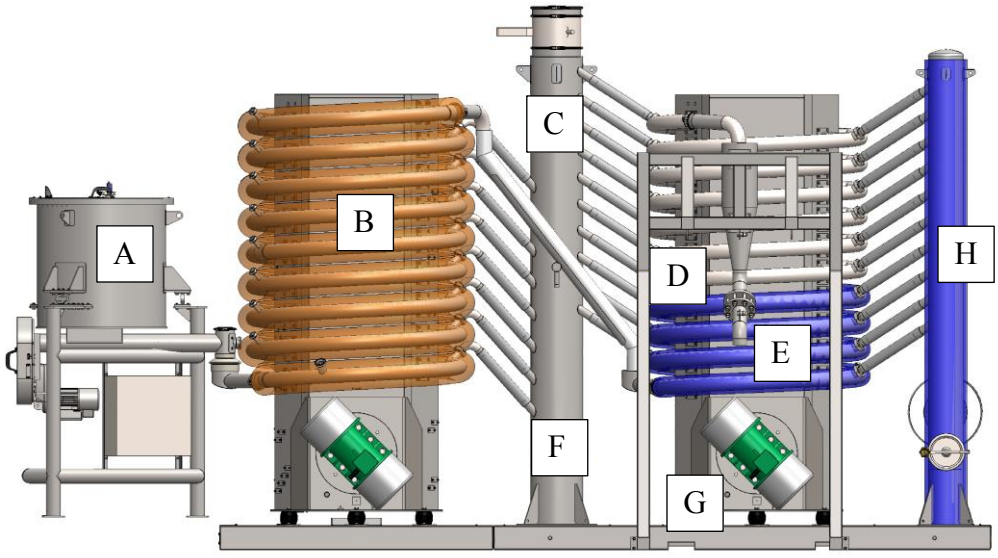

Figure 2-9: Pilot plant Revtech equipment. A) Hopper. B) Heating spiral. C) Flexible connection pipe. D) Cooling spiral. E) Product outlet. F) Extraction manifold. G) Off balance motor. H) Injection ports for cold air. a) Photograph b) Schematic

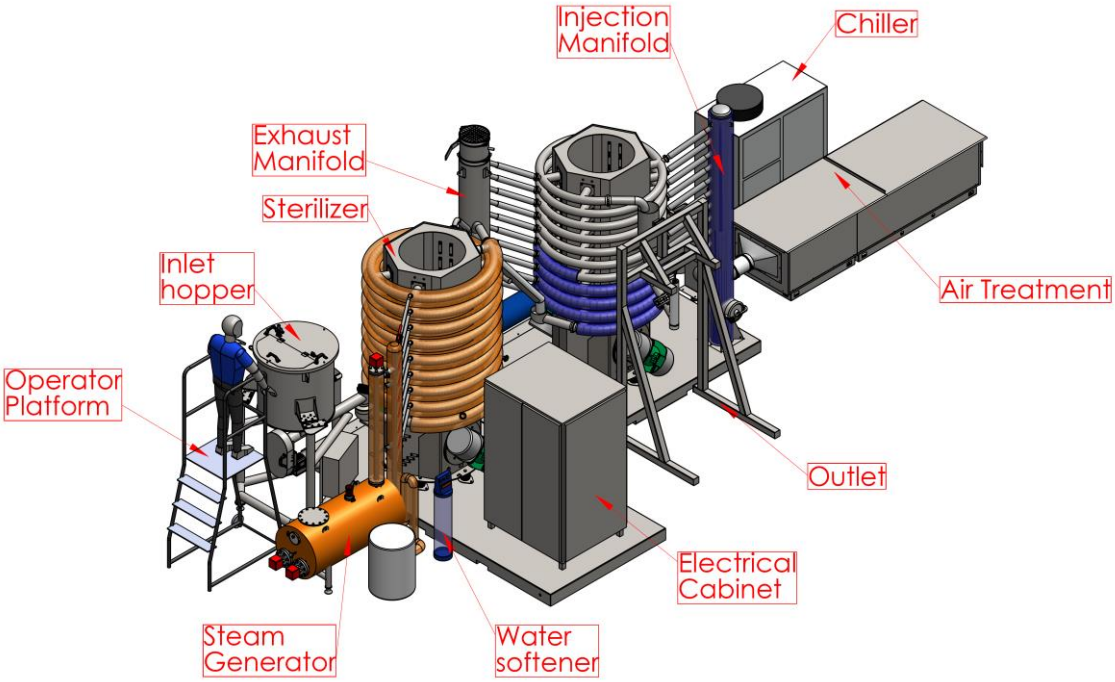

Figure 2-10: 3D schematic of the Revtech system

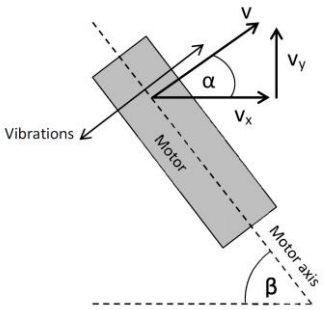

Figure 2-11: Relation between total velocity (v) of the Revtech motor movement, velocity components in horizontal and vertical direction (v_x, v_y), and motor angle to the horizontal (β)

3 Effect of temperature and time on flour functionality

3.1 Introduction

As discussed in chapter 2, flour functionality needs to be changed to successfully bake a high-ratio cake. This can be achieved by chlorination or dry heat treatment (see chapter 2). The work presented here focuses on the dry heat treatment of flour. Understanding the changes in functionality of flour after heat treatment is critical for baking a good quality cake. The interactions of the flour components need to be strong enough in the batter, so that air bubbles are entrapped and stabilised. At elevated temperatures during baking, the structure must be sufficiently strong, so that air cells burst and the desired cake texture can develop (see chapter 2).

This chapter investigates the alterations in flour functionality after heat treatment as measured by analytical methods such as the Rapid-Visco-Analyser (RVA), the rheometer, solvent retention capacity (SRC) tests, and the rheomixer. The RVA provides information about starch granule swelling and the viscosity of a flour-water system at elevated temperature. Both the SRC and rheology tests contribute to the understanding about interactions between flour polymers at ambient temperature. Hydration of proteins and gluten development can be assessed at ambient temperature in the rheomixer.

Research shows that all flour components are affected by dry heat treatment (Nicholas et al., 1978). It is largely recognised that the major effect of flour improvement relates to the starch fraction, whose performance is significantly altered after the treatment (Gough et al., 1977;

Guy et al., 2007). The modification of the function of starch has been attributed to changes in the surface layers of the granules which involves the proteins and lipids in that layer (Cook, 2002). Changes in the gluten fraction were also observed (Meza et al., 2011; Nicholas et al., 1978). More recently, the impact of heat treatment on the solvent accessibility of arabinoxylans was suggested (Van Steertegem et al., 2013).

The hypotheses for the impact of dry heat treatment on flour components are:

i) Facilitation of starch granule swelling (Cook, 2002; Guy and Pithawala, 1981; Nicholas et al., 1978). This was attributed to partial denaturation of the proteins on the granules' surfaces which are thought to form a barrier hindering water absorption into the granule. This is investigated here by means of:

   - *Oscillatory rheology:* To test the viscoelastic properties of a flour-water slurry at ambient temperature. Higher starch granule swelling can affect the network forming properties and the ability to store energy.
   - *Solvent retention capacity (SRC) tests:* To examine the swelling ability of the various flour polymers.
   - *Rapid-Visco-Analyser (RVA) tests:* To investigate the viscosity of a flour-water mixture at elevated temperatures, after gelatinisation. A higher degree of granule swelling can result in higher viscosities.

ii) Impact on gluten proteins (Meza et al., 2011; Nicholas et al., 1978; Van Steertegem et al., 2013). Gluten hydration was reported to decrease with increasing heat treatment up to a complete lack of gluten formation due to cross-

linked proteins (Van Steertegem et al., 2013). This was investigated here by means of:

- *Rheomixer:* To investigate gluten hydration and dough development.
- *Rapid-Visco-Analyser (RVA) tests:* Disulphide cross-links in the gluten proteins may rigidify the flour particle and allow it to swell longer and to withstand external shear in such a way that RVA peak viscosity increases (Van Steertegem et al., 2013).

iii) Impact on solvent accessibility of arabinoxylans (Van Steertegem et al., 2013). An increase of 34% in swelling behaviour in sucrose SRC tests was reported after heat treatment at 100°C for 5 h (Van Steertegem et al., 2013). This was investigated here by means of:

- *Solvent retention capacity (SRC) tests:* To investigate the swelling behaviour of arabinoxylans.
- *Oscillatory rheology:* The increased swelling behaviour of arabinoxylans at ambient temperature may affect the viscoelastic properties of flour-water slurries.

So far, cake quality (e.g. volume, colour, sensory attributes) has not been correlated with any analytical method. Assessment of the success of any treatment is largely achieved by characterising the quality of a baked cake. The combination of different analytical methods may allow for a unique characterisation of the heat treatment (e.g. treatment time and temperature) a flour sample has received which may be correlated with cake quality. It could

lead to a cost- and time-saving technique to characterise heat treated flour. This is further investigated in chapter 5.

The aim of this chapter is to test the hypotheses for the impact of dry heat treatment on flour components and to contribute to a better understanding of the mechanism of flour heat treatment.

3.2 Materials and methods

3.2.1 Materials

Three commercially available soft wheat flours were used for the experiments, denoted I, II, and III respectively. The flours had a protein content of 7.7 - 8.8%, a moisture content of 12.5 - 14.4%, and a Hagberg falling number of 230 - 330 s. The main difference was in particle size with flour II showing a significantly smaller particle size than flours I and III (see Figure 3-1). Flour I was provided by Campden BRI (Chipping Campden, UK). Flours II and III were generously provided by Heygates Ltd. (Northampton, UK). All analytical methods below were conducted within a short period of time, so that the effect of storage conditions is negligible. One batch per flour was used for all experiments.

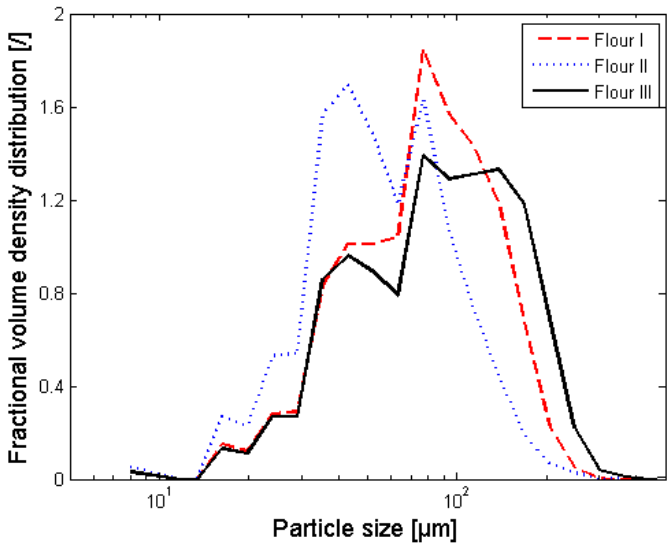

Figure 3-1: Particle size distributions of flour I, II, and III

3.2.2 Heat treatment

Heat treatment was done by sieving flour onto a quadratic hotplate (Stuart SD 162, Stuart Equipment, UK) with an area of 234 cm^2. Flour has a low thermal conductivity (e.g. 0.17 W/m K) (Tiwari et al. 2011). It is therefore critical to maintain a small thickness of the flour layer that is to be heated to ensure a short come-up time to temperature and a constant temperature of the flour throughout the treatment. A layer thickness of less than 1 mm was achieved by sieving 7 ± 0.2 g flour onto the hotplate.

K-type thermocouples were taped to the surface of the hotplate with aluminium tape to measure the temperature. The left half of the hotplate exhibited a narrower temperature distribution in comparison to the entire hotplate. The temperature variation between the centre and the left side (corner points) was 2 - 3°C whereas it was 4 - 7 °C between the centre and the right side (corner points) for temperature setpoints of 110 - 170°C. The centre was the hottest point of the hotplate and was used as setpoint temperature. The whole hotplate was used for treatments of flour I and II; only the left half was used for treatments of flour III. The advantage of using the entire hotplate is that more material can be treated in the same time period and used for e.g. moisture determination or further analysis. The advantage of only using the left half of the hotplate is a more accurate and uniform treatment.

When the whole hotplate is used, the temperature dropped by approx. 5°C (setpoint 130°C) after loading with flour, but recovered to the setpoint within less than one minute. This was followed by a brief overshoot in temperature of approx. 3°C. After 2 - 3 min, the temperature profile was constant with time. An accurate heat treatment was achieved with this method.

Typically, heat treatment was applied at temperatures between 110°C and 200°C for times between 1 and 30 min. Figure 3-2 depicts equilibrium moisture contents of flour III after heat treatment at different temperature setpoints with an approximated exponential curve. It was found in preliminary experiments that the equilibrium moisture content was achieved after 2 - 5 min at all temperatures.

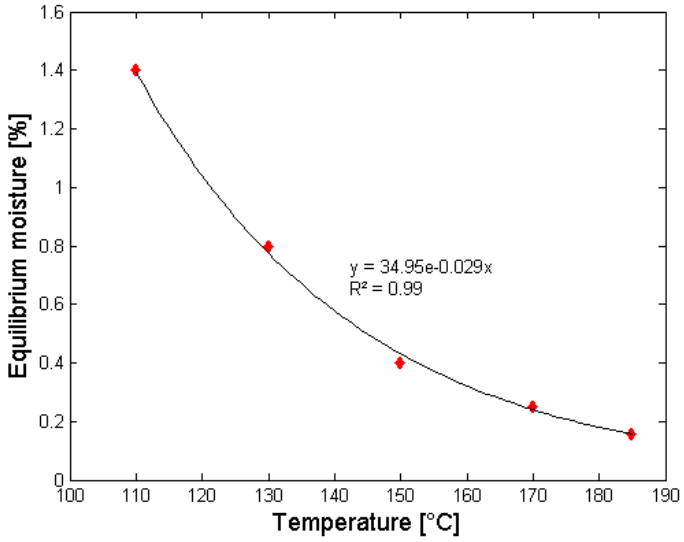

Figure 3-2: Equilibrium moisture contents of flour III after heat treatment on a hotplate at different temperature setpoints with approximated exponential curve

Temperature profiles were applied in some cases. Figure 3-3 shows temperature data and setpoint for a temperature profile between 110°C and 150°C with a 10°C temperature step and a 4 min time step. There is a come up time once the temperature setpoint is changed followed by a minor overshoot in temperature. This behaviour was reproducible (data not shown).

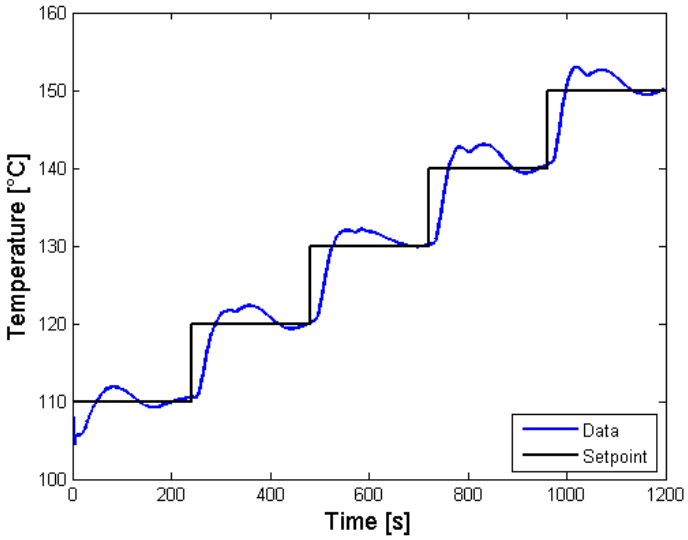

Figure 3-3: Stepwise temperature profile of hotplate loaded with flour; setpoint and data.

3.2.3 Moisture determination

The moisture content of flour samples was measured to accurately compensate for differences in moisture content when performing RVA tests and rheology tests (see sections 3.2.5 and 3.2.6). The moisture content was determined in a convection oven at 130°C according to AACCI Approved Method 44-15.02 (1999) (note: silica gel was used as desiccant).

3.2.4 Scanning electron microscopy

A scanning electron microscope (SEM) EVO 60 (Carl Zeiss AG, Germany) was used to analyse heat treated samples of flour I. The powders were stuck onto a stub using carbon tape and gold coated using an Agar Auto Sputter Coater before putting them into the SEM. The SEM was then pumped to vacuum and images were taken at various magnifications.

3.2.5 Rapid-Visco-Analyser (RVA) tests

Starch-pasting behaviour was studied in the Rapid-Visco-Analyser (RVA 4500, Perten Instruments (Hägersten, Sweden)). The sensitivity of RVA results to the applied heat treatment conditions of the flour was investigated in different solvents. In the sample canister, flour samples (3.0 g dm) were added to 25 g of different liquids: (i) deionized water, (ii) 50% w/w sucrose in water, (iii) 5% w/w lactic acid in water and (iv) 5% w/w sodium carbonate in water. Flours I, II, and III were analysed by this method. The exact moisture content of the sample was determined (see section 3.2.3) and was compensated for to a standard of 14% by the addition of deionised water to the container. The sucrose solution was prepared at least 12 h in advance to ensure complete dissolution. Coated cans were used for the 5% sodium carbonate solution to prevent corrosion of the aluminium canisters. The temperature profile applied was Standard 1 method (AACCI Approved Method 76-21.01, 1999). RVA results such as pasting temperature, peak viscosity, holding strength, setback, and final viscosity were calculated from the data by a software program (ThermoCline for Windows version 3). Viscosity is measured in Centipoise (cP); 1 cP = 1 mPas. Some variability in the results was introduced by different dispersion characteristics of flour in the various liquids. Incomplete dispersion and deposition on the container walls (particularly in 50% sucrose solution) causes variability in RVA parameters.

A typical RVA profile of flour in water is shown in Figure 3-4. During heating, the order of the starch granules is irreversibly destroyed, they swell to many times their original size and amylose leaches out of the granules (Ross 2012) (see chapter 2). The shear forces caused by these swollen granules squeezing past one another result in an increase in viscosity in the RVA (Perten Instruments, 2010). Granule swelling and polymer leaching cause the viscosity

to increase whereas granule rupture and polymer alignment cause the viscosity to decrease (Perten Instruments, 2010). At the equilibrium of the two processes, the 'peak viscosity' occurs (Crosbie and Ross, 2007). As stirring continues, the starch granules undergo further disruption due to the shear forces and the polymers undergo alignment (Crosbie and Ross, 2007; Perten Instruments, 2010). This period is usually accompanied by a reduction in viscosity, which eventually reached a minimum value, which is known as 'holding strength', 'hot paste viscosity', or 'trough' (Perten Instruments, 2010). The starch molecules reassociate during cooling, which usually leads to the formation of a gel (Crosbie and Ross, 2007; Perten Instruments, 2010). The viscosity increases and stabilises at a 'final viscosity' (Perten Instruments, 2010).

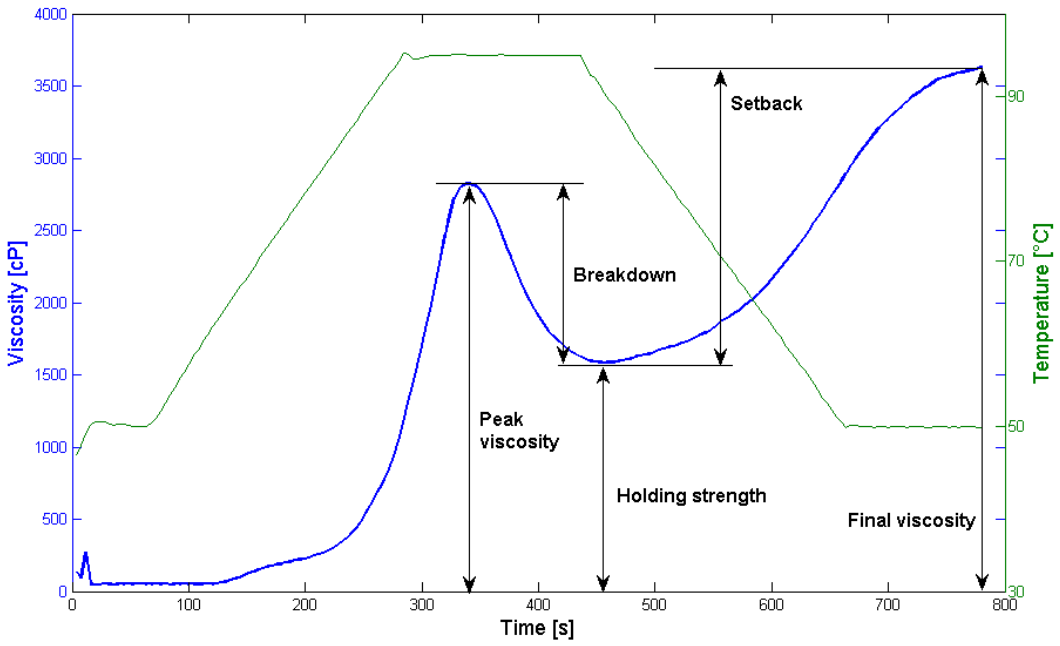

Figure 3-4: Typical Rapid Visco Analysis (RVA) profile of a heat treated flour sample (150°C, 15 min) in water

3.2.6 Small deformation oscillatory measurements

The viscoelastic properties of flour-water slurries were studied on a rheometer (Ares, type 902-30004 (Rheometric Scientific Ltd., Hampshire, UK)) using a parallel plate setup (50 mm diameter, 2 mm gap).

Flour I (15 ± 0.1 g, 14% moisture) was mixed with 20 g of deionised water manually with a spatula for 1 min. Similarly to the RVA tests, the sample mass was corrected on a dry matter basis for varying moisture contents of the heat treated flour. To exclude the effect of time, all samples were loaded onto the rheometer 3 min after mixing. After loading, the edges of the sample were trimmed with a spatula and the sample was held for 1 min before the measurement started. The temperature was controlled at 20°C. Strain sweeps were performed (frequency of 1 Hz and strain range from 0.007 to 188.8%) to identify the linear viscoelastic region. A strain of 0.1% was imposed and frequency sweeps were conducted between 0.1 Hz and 20 Hz. The elastic moduli at a frequency of 5 Hz were compared.

3.2.7 Solvent retention capacity

The solvent retention capacity (SRC) test is a solvation assay for flours that is based on the enhanced swelling behaviour of individual polymer networks in selected single diagnostic solvents which are used to predict the functional contribution of each individual flour component (Kweon et al., 2009). The solvents were deionized water, 5% w/w lactic acid in water, 5% w/w sodium carbonate in water, and 50% w/w sucrose in water. Flour I was used for these experiments. The SRC tests were performed according to AACCI Approved Method 56-11.02 (2009).

Flour (5 ± 0.050 g) was mixed with 25 g of solvent in 50 ml centrifuge tubes. The flour was then left to solvate for 20 min during which the tubes were vigorously shaken every 5 min. The samples were centrifuged at 1000 x g for 15 min. The supernatant was discarded and the tubes were left upside down to dry for 10 min. The pellet was weighed and the SRC was calculated by Eq. 3-1.

$$\%\mathrm{SRC} = \left[\frac{\text{pellet wt}}{\text{flour wt}} - 1\right] \cdot \left[\frac{86}{100 - \%\text{flour moisture}}\right] \cdot 100 \qquad \textbf{Eq. 3-1}$$

The pellet of the lactic acid SRC of the untreated flour sample was very soft and losses occurred during the drying step. Hence, it is possible that the lactic acid SRC of the untreated flour sample was underestimated.

3.2.8 Rheomixer

Flour I was subjected to torque-time analysis in the rheomixer to compare its dough development and protein quality after heat treatment. The rheomixer (Reologica Instruments AB (Lund, Sweden)) consists of an instrumented planetary pin mixer, a microprocessor unit for signal conditions and software for data acquisition. It is described in Anderson (2003) and is designed to be similar to a mixograph (AACCI Approved Method 54-40.02, 1999). The equipment has a removable bowl (for 10 g flour) that has 3 fixed pins and is located in a water jacket to allow constant temperature mixing. Mixing action is provided by 2 pairs of driven pins that are lowered into the bowl and are set rotating. When dough is mixed in the

apparatus, a twisting action is imparted to the bowl (a torque), the extent of which is recorded as a voltage by an accompanying computer. The primary output is a torque-time trace. The instrument was calibrated such that 1.0 V output equals 220 g/cm (0.0216 Nm).

Flour (10 ± 0.1 g) was added into a tempered (30°C) rheomixer bowl, which was then covered with Parafilm and put into a water bath at 30°C for at least 5 min. Three grooves were made into the flour that were connected in the middle of the bowl where 9 g of deionised water was added. The bowl was then transferred into the rheomixer where the dough was developed at a speed of 93 ± 2 rpm for 10 min.

3.2.9 Response surface modelling

Response surfaces present a response variable (e.g. peak viscosity in the RVA or elastic modulus in the rheometer) depending on independent process variables such as treatment time and temperature. It is therefore possible to predict the response variable for any given set of process variables within the chosen operating window.

Data is collected at discrete time-temperature-combinations. A two-step model is used in this study to calculate the response variable at all temperatures for all times. The general approach is as follows:

Step 1: An equation is fitted to the data of the response variable for each temperature setpoint depending on treatment time. Coefficients and constants of the fitted equations are determined depending on temperature.

Step 2: The response variable is calculated for all temperatures depending on time by using the same equation structure as for the data and the obtained coefficients and constants.

A three dimensional surface and two dimensional contour lines can be plotted depending on process parameters.

3.2.9.1 RVA peak viscosity in water

The RVA peak viscosity profile of heat treated flour in water is characterised by an increase followed by a decrease with time for all temperatures.

i) Modelling of the increase in peak viscosity with time:
   - Logarithmic curves are fitted to the peak viscosity data with time for each temperature setpoint of the form: $PV = a \cdot \ln(t) + b$, where PV is the peak viscosity, t is the treatment time and a and b are constants.
   - Constants a and b depend linearly on temperature ($R^2 = 0.99$).
   - The peak viscosity can be calculated for all other temperatures (here 5°C steps) by using logarithmic curves with fitted constants a and b.

ii) As the peak viscosity decreases with time, the turning point is calculated in minutes by an exponential equation depending on temperature ($R^2 = 0.97$).

iii) Modelling of the decrease in peak viscosity with time:
   - First order polynomials are fitted to the peak viscosity data with time for each temperature setpoint.

- Gradient and intercept of the linear equations followed an exponential curve (R^2 = 0.99) and a second order polynomial (R^2 = 0.85), respectively, depending on treatment temperature.
- The decrease in peak viscosity with time can be calculated for all other temperatures (here 5°C steps) by using linear equations with fitted gradients and intercepts.

3.2.9.2 RVA peak viscosity in 50% sucrose solution

The RVA peak viscosity of heat treated flour in 50% sucrose solution was observed to depend linearly on treatment time at each treatment temperature (R^2 = 0.93 - 0.99). The gradient of the first order polynomial was approximated by an exponential curve depending on temperature. The intercept of the first order polynomial was approximated by a second order polynomial for different temperatures. By means of linear equations for the peak viscosity over time, the peak viscosity can be calculated for all temperatures.

3.2.9.3 Elastic modulus of flour-water slurries in the rheometer

The elastic modulus of flour-water slurries was observed to depend linearly on the treatment time at each temperature setpoint (R^2 = 0.95 - 0.99). The gradient could be accurately approximated with an exponential curve depending on temperature (R^2 = 0.99). The intercept was approximated by two straight lines, one from 70 - 170°C and one from 180 - 200°C. The elastic modulus was calculated accordingly by means of linear equations for temperatures between 70°C and 200°C in 10°C steps.

3.3 Results and discussion

3.3.1 Scanning electron microscopy

Figure 3-5 shows typical scanning electron microscope (SEM) photographs of untreated and heat treated (170°C for 15 min) flour. The large, lenticular A-type and the small, spherical B-type starch granules are visible. The material surrounding the granules is mainly gluten protein.

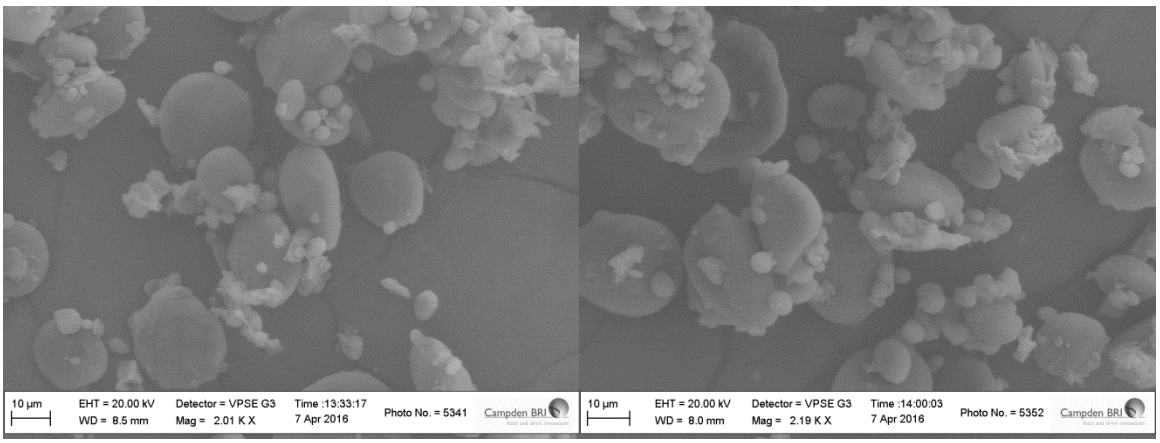

Figure 3-5: SEM micrographs of untreated flour (left) and heat treated flour (170°C, 15 min) (right)

No differences could be detected between the untreated control and the heat treated samples. This is in agreement with Russo and Doe (1970) who reported no differences in superficial structure of starch granules after heat treatment as studied by SEM. Hence, the changes in flour functionality caused by heat treatment as discussed below are not a result of changes in the morphology of flour components.

3.3.2 Rapid-Visco-Analyser tests in different fluids

3.3.2.1 In water

Constant temperature

The pasting behaviour of starch at elevated temperature is evaluated in the RVA. The peak viscosity is used in this study to assess the effect of heat treatment on flour. It is a measure for the viscosity at the equilibrium of two processes: i) granule swelling and polymer leaching on one hand, which increases viscosity and ii) granule rupture and polymer alignment on the other hand, which decreases viscosity (Crosbie and Ross, 2007).

Figure 3-6 shows the effect of treatment time and temperature on the peak viscosity of heat treated samples of flours I, II, and III. Different lines of the same colour depict different temperature setpoints; 110°C, 130°C, 150°C, and 170°C from the bottommost line to the top line. Different flours have different initial peak viscosities and heat treatment causes different change in peak viscosity over time. The peak viscosities of flour I increase from 2400 cP to approx. 2900 cP. The initial peak viscosities of flour II and III are significantly lower at 1400 - 1500 cP indicating reduced swelling of starch granules in comparison to flour I. However, the peak viscosities of flours II and III increase to a greater extent relatively to the initial value, up to 2300 cP and 2800 cP, respectively. The results suggest a greater swelling potential of the starch granules in comparison to flour I. This might depend on wheat variety, harvest year, composition, or age. For example, flour I was considerably older when treatment and measurements were done in comparison to flours II and III. Flours II and III were produced in the same process with the same grist, but flour III had a bigger particle size

distribution (see section 3.2.1). This could cause small compositional changes, which in turn might be responsible for the differences in peak viscosity.

At all temperatures measured, the peak viscosity first increases with increasing treatment time before it reaches a maximum and then declines at longer treatment times. The graph shows times up to 30 min, but the decreasing trend for long times and lower temperatures was confirmed in preliminary experiments (data not shown). The maximum peak viscosity is reached at shorter times for higher process temperatures: i.e. Flour I: 2 min at 170°C against 12 min at 150°C. Figure 3-7 shows the effect of heat treatment on flour I in more detail with best-fit lines. Peak viscosities are in the order of 2400 - 2900 cP; the pooled standard deviation was measured to be ± 31 cP across all temperature-time combinations. Freezing and thawing did not have an effect on peak viscosity (data not shown).

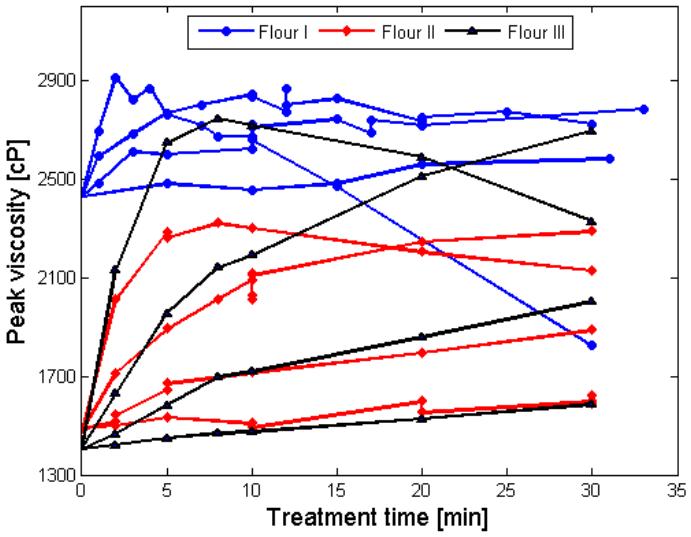

Figure 3-6: Effect of treatment time and temperature on the RVA peak viscosity of flour I, II and III in water. Data with connected lines. Different lines of the same colour depict different temperature setpoints; 110°C, 130°C, 150°C, and 170°C from the bottommost line to the top line.

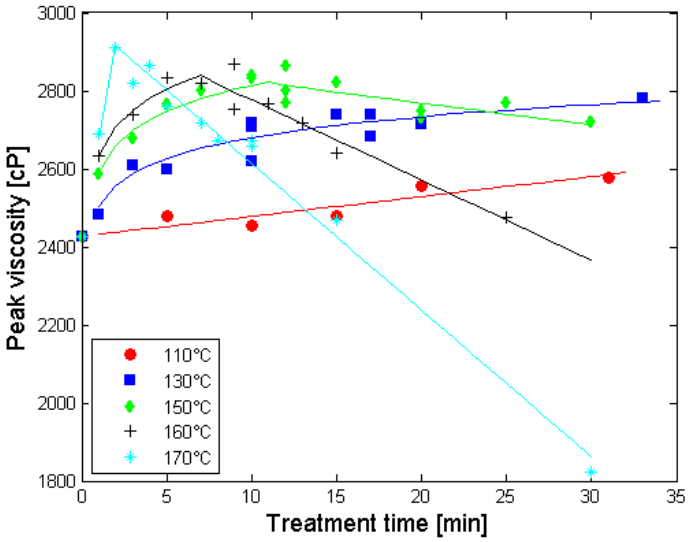

Figure 3-7: Effect of treatment time and temperature on the RVA peak viscosity of flour I in water (with fitted exponential and straight lines)

The temperature dependence of the time at which the maximum peak viscosity is obtained is presented in Figure 3-8a for flour I. An exponential curve can be fitted to the data. The increase in peak viscosity over time is shown in Figure 3-8b; it appears logarithmic as demonstrated in the presented example of 130°C.

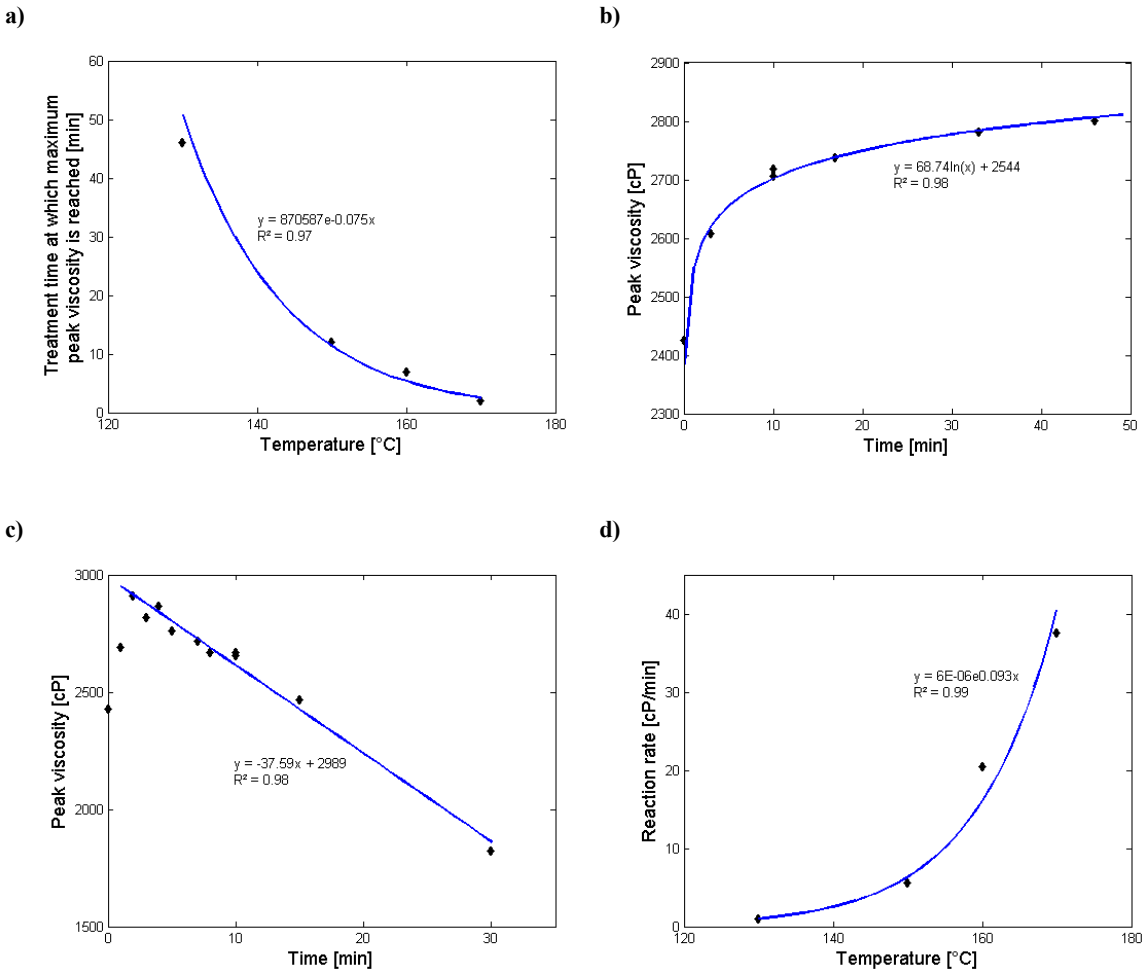

Figure 3-8: Flour I. a) Treatment time after which maximum peak viscosity is reached for different temperatures b) Peak viscosity as a function of treatment time at 130°C c) Peak viscosity as a function of treatment time at 170°C d) Slope of decreasing part of peak viscosity curves at different temperatures. Equations in the figures are best-fit lines.

The increase in peak viscosity over time suggests either that the swelling of the granules is facilitated by the heat treatment or that granule disruption by external shear forces is delayed giving the granules more time to swell. Nicholas et al. (1978) stated that the starch granules swell more easily in heat treated samples due to partial denaturation of the proteins on the granules surface which are thought to form a barrier hindering water absorption into the granule (Cook, 2002; Guy and Pithawala, 1981). Van Steertegem et al. (2013) reported that

the peak viscosity increased upon longer and more severe heat treatment due to covalent disulphide cross-links in the gluten proteins. The polymerised protein rigidifies the flour particle and allows it to swell longer and to withstand external shear in such a way that the RVA peak viscosity increases (Van Steertegem et al., 2013).

In contrast to the increase in peak viscosity with processing time at 130°C, the decrease in peak viscosity is linear with increasing process time as shown in Figure 3-8c at 170°C. A line can be fitted to the data; the slope of that line is plotted as a function of temperature in Figure 3-8d and an exponential curve can be fitted to the slopes.

The decreasing peak viscosity after a certain treatment time indicates less swelling of the starch granules over time. This might be due to fragmentation of starch or due to changes in the granule surface by extreme heat treatment that prevent or delay water uptake. Furthermore, starch granules might become more susceptible to shear. Earlier granule rupture and polymer alignment might result in a low peak viscosity.

Figure 3-9 shows the response surface and contour lines of the RVA peak viscosity of heat treated samples of flour I as a function of treatment time and temperature.

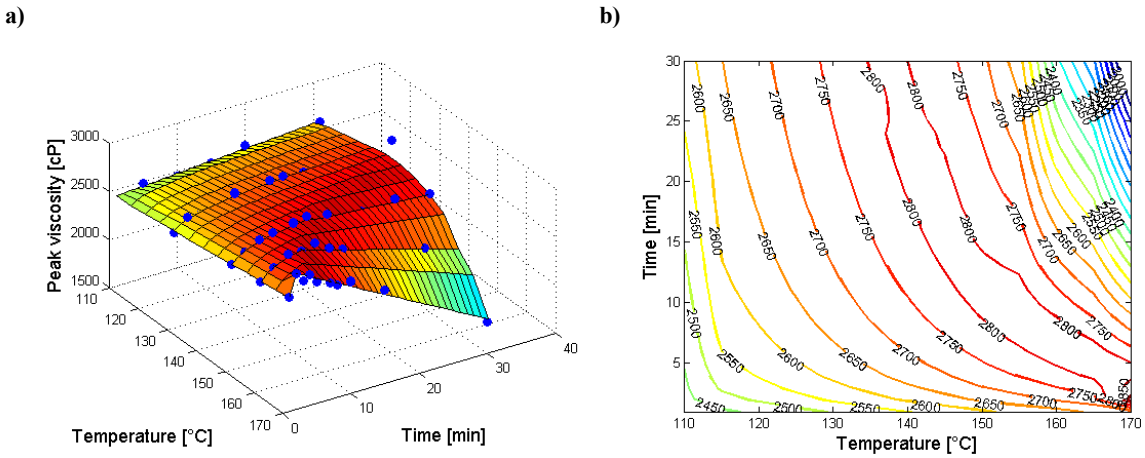

Figure 3-9: RVA peak viscosity in centipoise (cP) of flour I treated at different treatment times and temperatures. a) Response surface with data points (blue). b) Contour lines.

Temperature profiles

The effect of constant temperatures on the RVA peak viscosity of flour was assessed above. In industrial processes, the applied temperatures are commonly not constant and/or show a come up and cooling down time. Hence, this section investigates the peak viscosity of flour samples after stepwise temperature profiles have been applied. Table 3-1 shows the implemented conditions. Temperatures range from 110°C to 170°C with steps of 10 - 20°C and times steps are 2, 4, and 6 min. Flour II was used for the experiments.

Table 3-1: Stepwise temperature profiles applied to flour II on a hotplate

Sample number	Minimum temperature [°C]	Maximum temperature [°C]	Temperature step [°C]	Time step [min]
1	110	150	10	4
2	110	150	20	4
3	110	170	10	2
4	110	170	10	4
5	110	170	20	4
6	110	150	20	6
7	110	150	10	2

After a temperature profile has been applied to a flour sample, the peak viscosity can be calculated by taking the increase in peak viscosity from constant temperature experiments at the required temperature and for the required time and by adding up these values according to the applied profile. However, the change in peak viscosity at constant temperatures is not constant with time (see Figure 3-7). There are three ways of determining the values of change in peak viscosity over time:

Model I: The increase in peak viscosity for the required temperature and time is taken from the beginning of the peak viscosity curves at constant temperature for all temperatures. (see Figure 3-10a).

Model II: The increase in peak viscosity for the required temperature and time is taken from the peak viscosity curves at constant temperatures after the time period the sample has been treated for at other temperatures (see Figure 3-10b).

Model III: The increase in peak viscosity for the required temperature and time is taken from the peak viscosity curves at constant temperatures. The increase in peak viscosity for the lowest temperature is taken from the beginning of the curves. This value is used as starting point on the peak viscosity curve of the next temperature and the new peak viscosity is taken after the required time step. This is repeated for all temperature steps (see Figure 3-10c).

a)

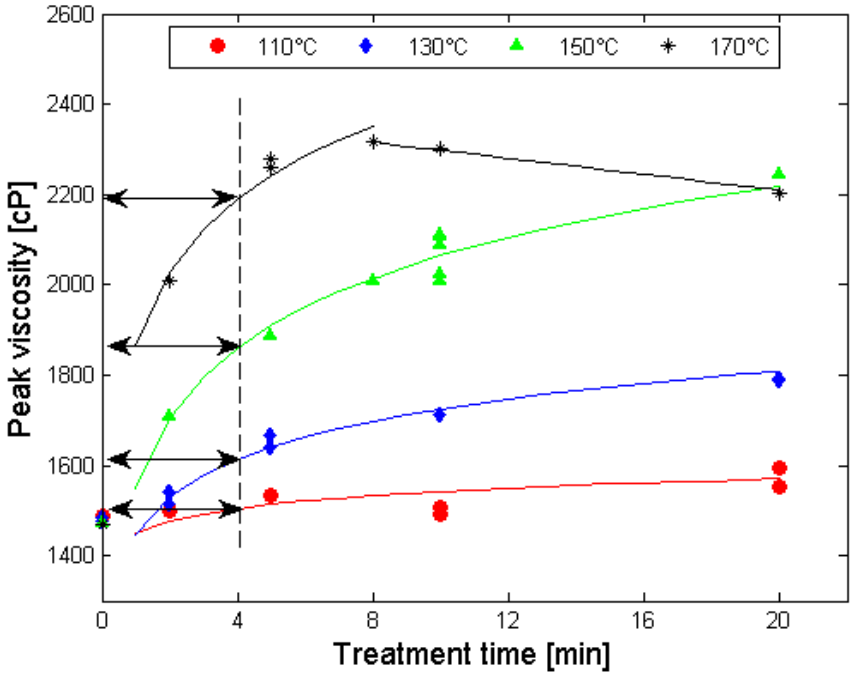

Figure 3-10: RVA peak viscosity of heat treated flour II at constant temperatures and models to calculate peak viscosity of heat treated flour II after stepwise temperature profiles have been applied. a) Model I b) Model II c) Model III.

b)

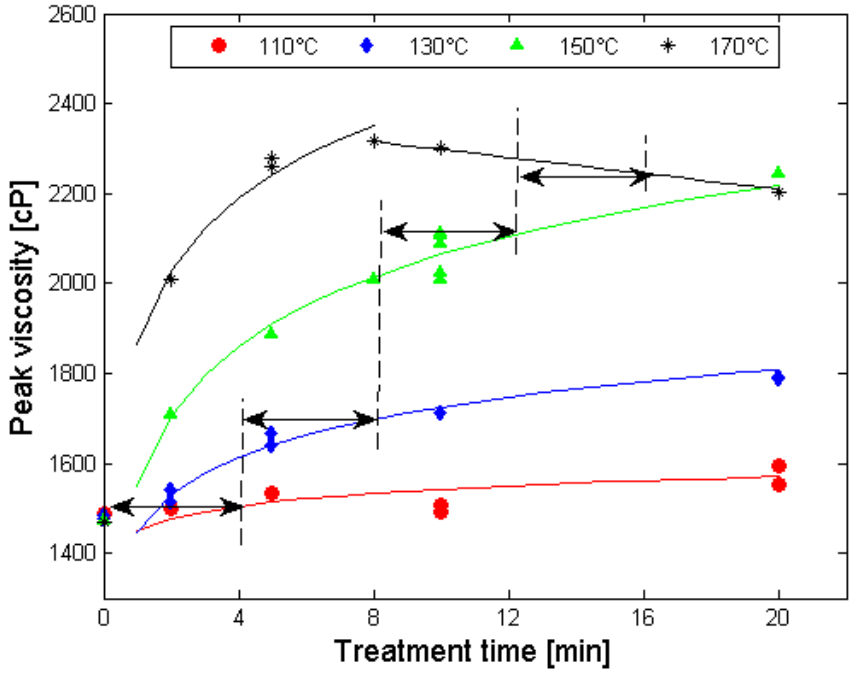

c)

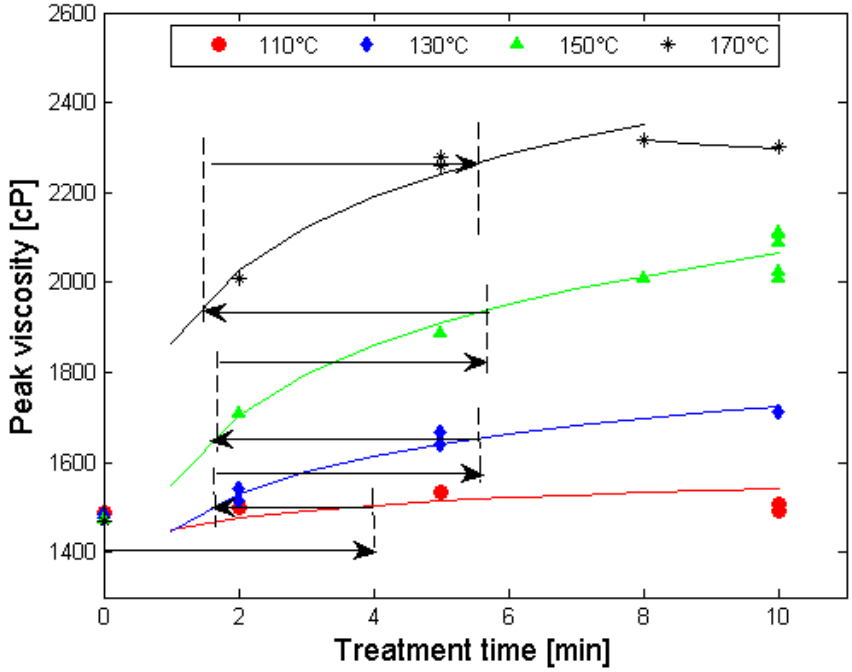

Figure 3-10 (continued): RVA peak viscosity of heat treated flour II at constant temperatures and models to calculate peak viscosity of heat treated flour II after stepwise temperature profiles have been applied. a) Model I b) Model II c) Model III.

Reasons for inaccuracies include:

i) There are no direct measurements available for temperatures of 120°C, 140°C, and 160°C. The values need to be interpolated.

ii) The change of temperature setpoints is not instantaneous but continuous.

iii) After the setpoint is reached, the temperature exceeds the setpoint by a few degrees.

Figure 3-11 depicts the measured data of the peak viscosity and the calculated values of models I, II, and III for 7 temperature profiles (see Table 3-1). Model I largely overestimates the data and model II significantly underestimates it. Model III fits the data accurately (R^2 = 0.92). It might be used to predict peak viscosities of flour in industrial heat treatment processes where non-constant temperature profiles are applied. This is further investigated in chapter 5.

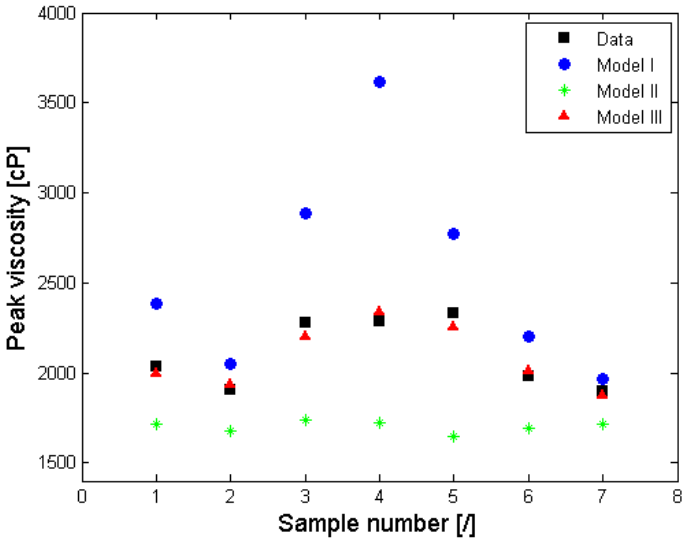

Figure 3-11: Comparison of data and models I, II, and III for RVA peak viscosity of samples of flour II after stepwise temperature profiles have been applied.

3.3.2.2 In 50% sucrose solution

To distinguish between treatment conditions it is preferable to obtain large differences in the observed parameter (here: peak viscosity) after various heat treatments. Kweon et al. (2010) reported a greater difference in the RVA profiles for different levels of flour chlorination when 50% sucrose solution was used instead of water. This phenomenon was therefore investigated for heat treated flour samples as presented below.

The effect of treatment time at 150°C on the RVA traces of flour I in 50% sucrose solution is shown in Figure 3-12. The shape of the profile is significantly different from the one in water (see Figure 3-4). In agreement with Kweon et al. (2010), the profile shows that starch breakdown is negligible in sucrose solution, i.e. the traces do not decrease with time (compare Figure 3-4 and Figure 3-12). According to Kweon et al. (2010), viscosity development in the second-stage granule-swelling process is retarded and hence there is insufficient time for the subsequent disruption process, before cooling and setback.

There is a greater differentiation between the investigated conditions in comparison to the RVA using water (see Figure 3-7). This indicates that the mechanism that increases the peak viscosity in water is more efficient in sucrose. Sucrose might stabilise the starch granules against disruption, thereby increasing the peak viscosity. Kweon et al. (2010) suggested that the exaggerated swelling of arabinoxylans in solvent retention capacity (SRC) tests, which was also observed for the heat treated samples in this study (see section 3.3.3), could be responsible for the exaggerating effect in the RVA profiles.

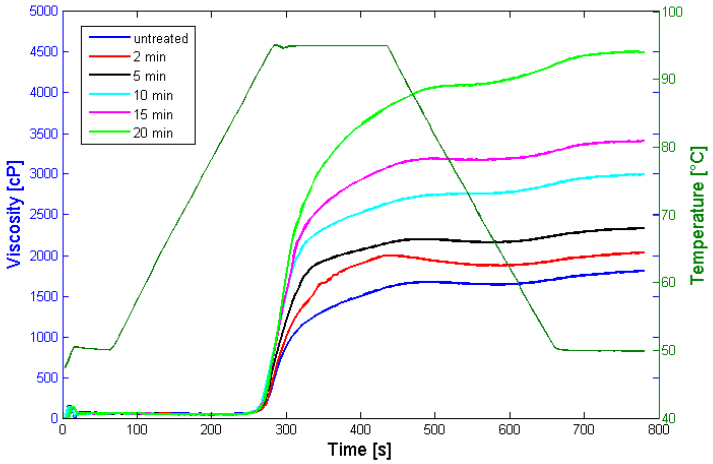

Figure 3-12: RVA profiles in 50% sucrose solution of flour I treated at 150°C for different times

As there is no maximum, the "peak" viscosity is taken during the holding time at 95°C at 7 min. Figure 3-13 plots this viscosity as a function of process time and temperature for flours I, II, and III. Different lines of the same colour depict different temperature setpoints; 110°C, 130°C, 150°C, and 170°C from the bottommost to the top line. Similar to the results in water (see Figure 3-6), the initial value of peak viscosity and the rate of change in peak viscosity are different for different flours. Three observations were different from those in water (see Figure 3-6):

i) The peak viscosity increased with treatment time at all temperatures for all flours. No decrease could be observed at the applied conditions.

ii) The initial level of peak viscosity of flours II and III is significantly higher in 50% sucrose solution in comparison to water. This suggests facilitated starch granule swelling in 50% sucrose solution. In contrast, starch in flour I appears to swell more easily in water.

iii) After heat treatment, the increase of the peak viscosity is significantly higher for flour I in comparison to flours II and III. The peak viscosity of flour I ranges between 1600 cP and 7100 cP. It increases from 6900 cP to 9400 cP for flour II and from 8000 cP to 11000 cP for flour III. The findings suggest that the potential of starch granule swelling of flour I is higher in 50% sucrose solution than in water. Flours II and III show an opposite trend on a relative scale.

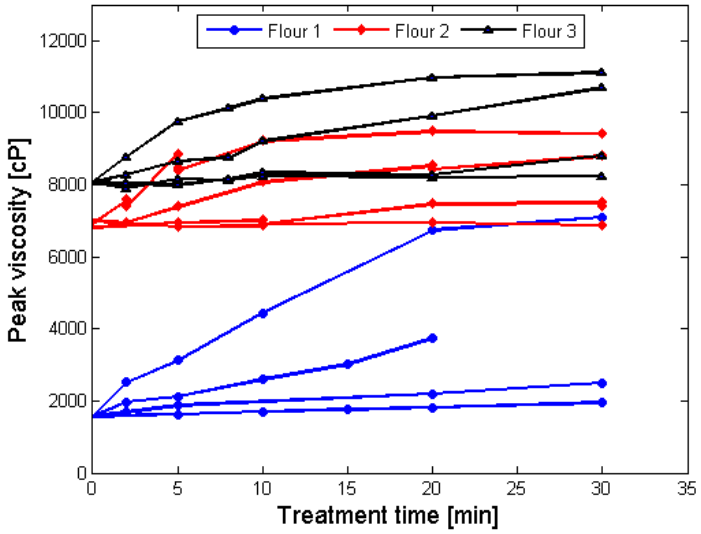

Figure 3-13: Effect of treatment time and temperature on the RVA peak viscosity of flour I, II and III in 50% sucrose solution. Data with connected lines. Different lines of the same colour depict different temperature setpoints; 110°C, 130°C, 150°C, and 170°C from the bottommost line.

Figure 3-14 depicts the effect of heat treatment on the peak viscosity of flour I in more detail. First order polynomials can be approximated to the data for all temperatures over time. The data for flours II and III has a more curved shape. The pooled standard deviation of the peak viscosity was ± 133 cP across all temperature-time combinations. It is higher in comparison to

the standard deviation for the measurements in water (± 31 cP). This is due to difficult dispersion of flour in 50% sucrose solution in comparison to water. Small lumps of flour can be found on the container wall after RVA measurement.

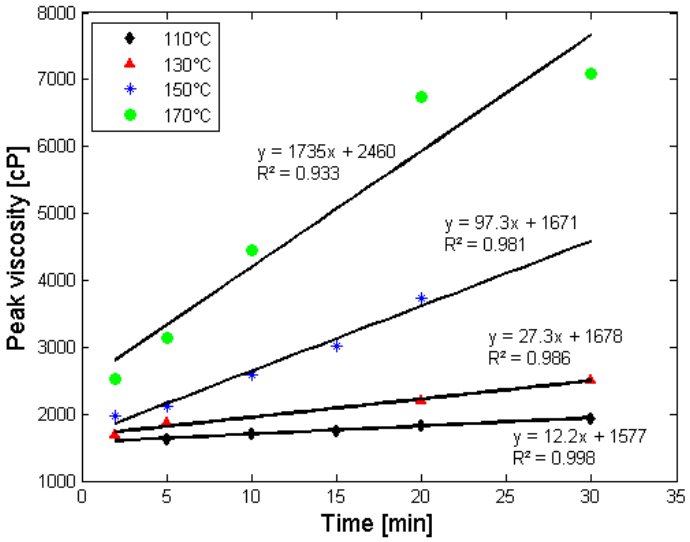

Figure 3-14: RVA peak viscosity in 50% sucrose solution of heat treated samples of flour I (110 - 170°C, 2 - 30 min)

Response surface and contour lines of the peak viscosity of flour samples treated at different time-temperature combinations is presented in Figure 3-15. This can be compared to Figure 3-9 to show the differences in peak viscosity of heat treated flour samples in water and sucrose solutions. In water the lowest value is obtained at high temperatures and long times, whereas in 50% sucrose solution the lowest value is at low temperatures and short times.

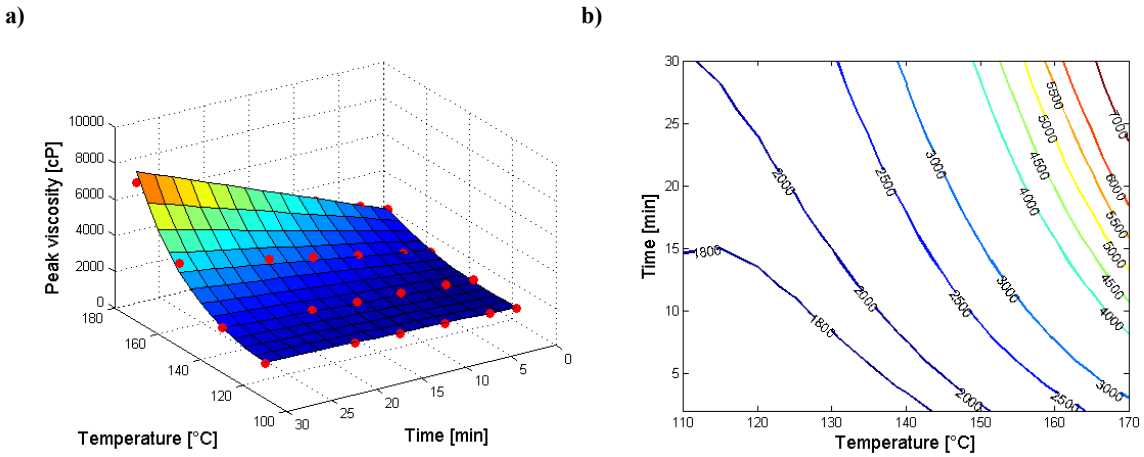

Figure 3-15: RVA peak viscosity of flour I treated at different treatment times and temperatures in 50% sucrose solution: a) Response surface with data points (red) b) Contour lines.

3.3.2.3 In 5% lactic acid

The effect of heat treatment on flour was tested in the RVA at acidic conditions. Figure 3-16 shows the RVA profile of flour I treated at 170°C for different times in 5% lactic acid solution.

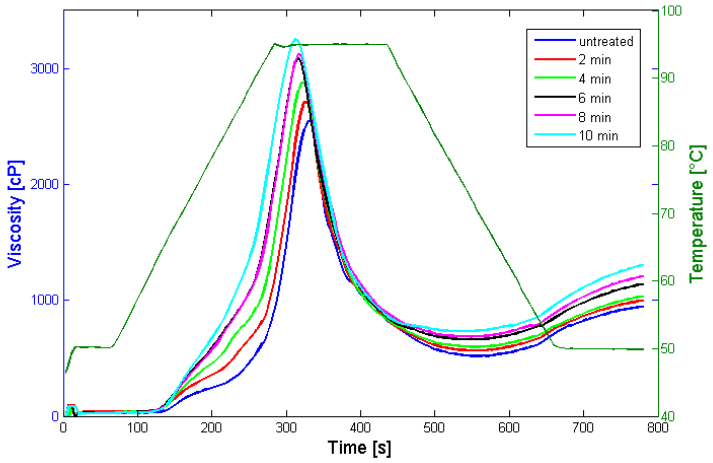

Figure 3-16: RVA profiles in 5% lactic acid solution of heat treated samples of flour I (170°C, 2 - 10 min)

The shape of the trace is similar to the one in water (see Figure 3-4), in that there is a marked peak viscosity followed by a trough and an increase to the final viscosity. The increasing part of the profiles shifts to the left with increasing treatment severity indicating that the swelling process of the starch granules is facilitated. The holding strength is significantly lower in lactic acid solution compared with water. The breakdown viscosity (difference between peak viscosity and holding strength) lies between 950 cP and 1190 cP for heat treated flour (170°C for 2 - 10 min) in water; it is 2030 - 2520 cP in lactic acid. This suggests that disruption of starch granules (starch breakdown process) is more severe in the acidic environment.

In contrast to the profiles in water, but in agreement with those in 50% sucrose solution, the peak viscosity increased linearly with treatment time (data not shown). The results indicate that the mechanism that is destabilising the system in water after long treatment times (see section 3.3.2.1) is delayed, balanced or compensated for by sucrose or lactic acid.

The rate at which the granules were disrupted after the peak viscosity was reached was identical at all treatment times, as can be seen in the overlapping curves. Moreover, the peak viscosity for all treatment times lies on an extended straight line of the decreasing part of all curves.

3.3.2.4 In 5% sodium carbonate

Complementary to the previous section, the effect of heat treatment on flour was tested here in the RVA at alkaline conditions. Figure 3-17 shows RVA profiles of untreated and heat treated samples of flour I. Temperatures between 100°C and 130°C were applied for 10 - 20 min. The level of peak viscosity is higher than in water, 50% sucrose solution, and 5%

lactic acid solution. The most significant difference to previous results is that there is no difference between untreated and heat treated flour samples. These findings suggest either that

i) changes in flour that occur during heat treatment are reversed by 5% sodium carbonate solution, or

ii) changes induced by heat treatment can also be achieved by the alkaline environment in a short time. Thereby, all transformations are accomplished to a maximum in the RVA solution causing equivalent traces; or

iii) the RVA test in sodium carbonate is insensitive to changes induced by heat treatment.

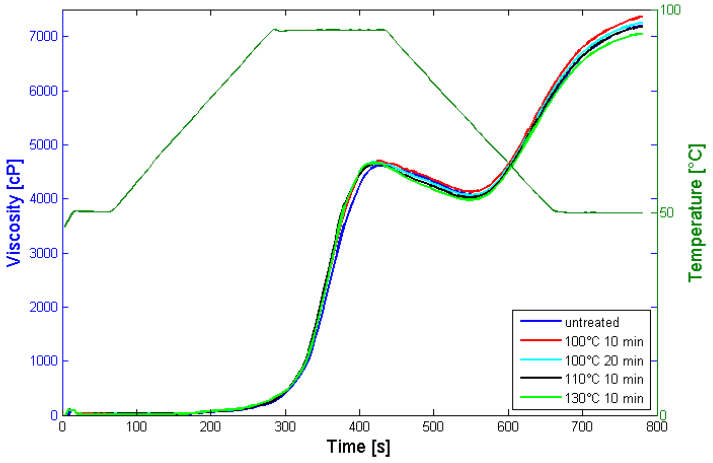

Figure 3-17: RVA profiles in 5% sodium carbonate of heat treated samples of flour I

3.3.2.5 Flour ageing and heat treatment

The effect of flour ageing on cake quality can be significant. It is known that storing flour at ambient temperature results in improved volume and grain of cakes (Clements and Donelson,

1982; Johnson and Hoseney, 1980). Clements and Donelson (1982) found cakes baked from untreated flour that was aged for 9 weeks exceeded oven expansion from chlorinated flour. Russo and Doe (1970) reported that the baking properties of a 5 years old starch were satisfactory without heat treatment and heat treatment brought about no change. These changes occurring in stored flour can be accelerated by heat (Johnson and Hoseney, 1980).

The effect of flour aging in comparison to flour heat treatment on the RVA peak is assessed here. The development of the peak viscosity of untreated flour I in water over a time period of almost 2 years is shown in Figure 3-18a. Flour was stored in paper bags at ambient temperature. A straight line can be fitted to the data over the observed time period. The peak viscosity increased significantly from 1360 cP to 2550 cP, which is almost double its initial value. These results indicate considerable changes in flour during storage at ambient temperature.

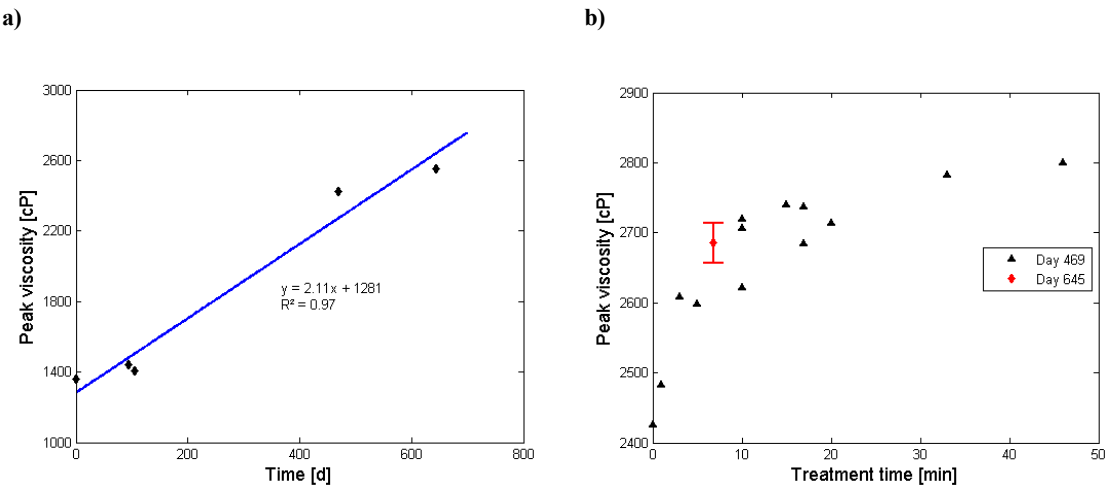

Figure 3-18: RVA peak viscosity of a) Untreated flour I after aging at ambient temperature b) Heat treated Flour I (at 130°C, different times) after aging the untreated flour at ambient temperature.

Figure 3-18b compares peak viscosities of heat treated flour samples treated after storing the flour at ambient conditions for 469 days and approximately 6 months later. Whereas, as shown in Figure 3-18a, the peak viscosity of the untreated raw material increased by 130 cP over this time, the peak viscosity of the heat treated samples is not significantly different. This suggests that the heat treatment increases the peak viscosity to a certain level rather than by a specific amount.

In addition to the improved cake quality after storing flour for extended periods of time (Clements and Donelson, 1982; Johnson and Hoseney, 1980), these findings prove that flour ageing increases RVA peak viscosity. It is shown that ageing and heat treatment cause similar changes in the flour regarding RVA peak viscosity, but at different rates.

3.3.3 Solvent retention capacity

The SRC test is a solvation assay for flours based on the enhanced swelling behaviour of individual polymer networks in selected single diagnostic solvents which are used to predict the functional contribution of each individual flour component (Kweon et al., 2011). Water is used to evaluate the overall swelling behaviour of all network-forming components; 5% lactic acid SRC is related to glutenin network forming and gluten strength; 5% sodium carbonate solution favours swelling behaviour of damaged starch; and sucrose SRC assesses the swelling behaviour of water-accessible arabinoxylans (Kweon et al., 2009).

Figure 3-19 shows the SRC of all four solvents for samples of flour I treated at 150°C for different times. The water SRC increases over time, which reflects the overall improvement of swelling ability of the flour polymers after heat treatment. This is in agreement with literature

(Van Steertegem et al., 2013). Lactic acid SRC showed a maximum around 5 min treatment time after which it decreased slowly. The results indicate an increase in swelling ability of the gluten proteins in the first 5 min of heat treatment. In contrast, Van Steertegem et al. (2013) reported decreasing lactic acid SRC indicating a decreased swelling ability of the gluten network. Similarly to the lactic acid SRC, the sodium carbonate SRC has a maximum around 5 min treatment time, after which it changed only marginally indicating that the effect of heat treatment on swelling behaviour of the damaged starch was limited (Kweon et al., 2009; Van Steertegem et al., 2013). The biggest impact of heat treatment was observed in sucrose SRC, which increased linearly by approximately 40% after 20 min treatment time. Van Steertegem et al. (2013) suggested that the solvent accessibility of arabinoxylans was impacted by heat treatment. The drastic increase in sucrose SRC was also reported for chlorinated flour (Kweon et al., 2009).

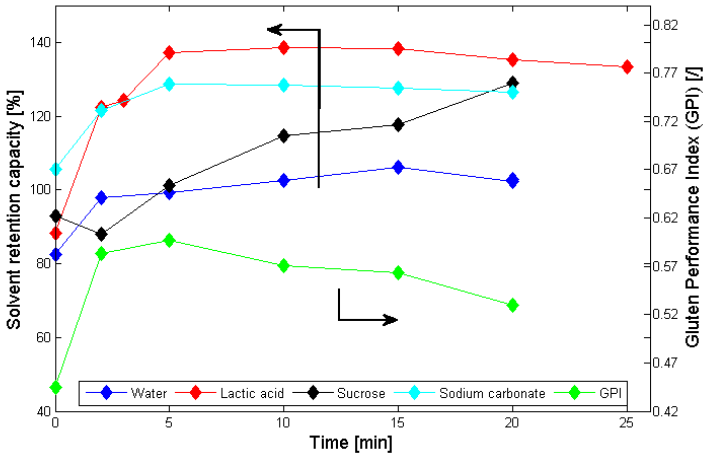

Figure 3-19: Solvent retention capacity (SRC) of flour I treated at 150°C for different times

The Gluten Performance Index (GPI) (see Eq. 3-2) was described by Kweon et al. (2009) as a better predictor of gluten functionality than lactic acid SRC alone. It describes the overall performance capability of glutenin in the environment of other modulating networks (Kweon et al., 2011). GPI is defined as:

$$\text{GPI} = \frac{\text{Lactic acid SRC}}{\text{Sodium carbonate SRC+Sucrose SRC}} \qquad \textbf{Eq. 3-2}$$

The GPI, also shown in Figure 3-19, increased up to 5 min, then it decreased with increasing treatment time. This is mostly due to the significant increase of sucrose SRC rather than the decrease in lactic acid SRC. These results suggest an optimum heat treatment time for optimum gluten network formation and protein hydration.

The water SRC for different treatment times and temperatures is shown in Figure 3-20. It follows a linearly increasing trend in the observed period of time at all temperatures. It demonstrates the improvement of swelling ability of the flour polymers with increasing treatment intensity. This may cause larger contact areas and increased interactions of the various flour components after heat treatment. These findings are in agreement with the increased elastic behaviour of heat treated flour in the rheological study (see section 3.3.4). The results at 150°C (see Figure 3-19) suggest that this is mainly due to the increase in the swelling behaviour of the arabinoxylans. The lactic acid SRC also showed a significant increase after heat treatment. However, the initial value might be underestimated (see section 3.2.7). The rate of the increase in water SRC over time increased exponentially with increasing treatment temperature (data not shown).

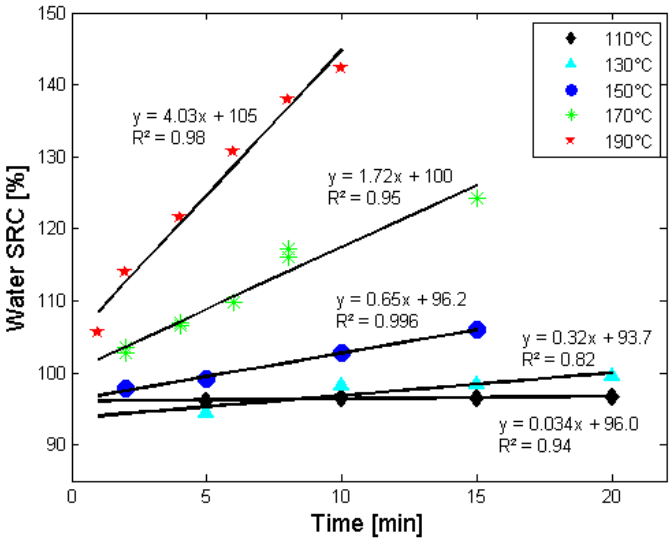

Figure 3-20: Water SRC of flour I treated at different temperatures for different times

The lactic acid SRC developed differently at different treatment temperatures. At 190°C it increased slightly with process time (data not shown), at 170°C it had a maximum at very short times before it increased slowly over time (data not shown) and at 150°C, it is shown in Figure 3-19. A new parameter is empirically created that puts the difference between lactic acid SRC and water SRC in relation to water SRC (see Eq. 3-3).

$$\frac{Lactic\ acid\ SRC - Water\ SRC}{Water\ SRC} \qquad \textbf{Eq. 3-3}$$

It characterises the difference in swelling behaviour of glutenins in comparison to the overall swelling ability of flour polymers. The result is standardised by the overall swelling capacity

of flour polymers. Only the section of the lactic acid SRC is evaluated where the slope is monotonic.

This parameter is plotted against treatment time for different temperatures in Figure 3-21. Logarithmic curves can be approximated. No clear conclusions can be drawn, but it might help in further studies to characterise the heat treatment a flour sample has received.

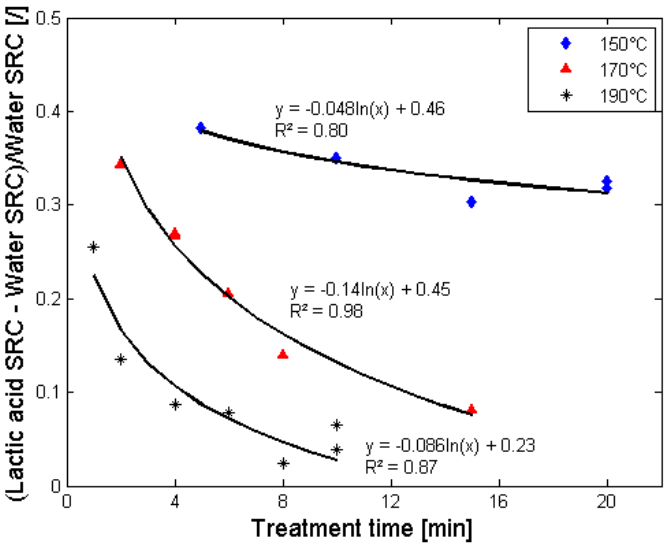

Figure 3-21: Relation between (Lactic acid SRC-Water SRC)/Water SRC of heat treated flour I and treatment time at different temperatures with best-fit curves

3.3.4 Small deformation oscillatory measurements

The rheological measurements evaluate the viscoelastic behaviour of a flour-water slurry to understand the interactions between flour components. The storage modulus relates to the elastic component indicating the amount of energy stored. The elastic flow characterises a reversible deformation. The loss modulus relates to the viscous component indicating the

amount of energy dissipated through generated heat. Viscous flow characterises irreversible deformation (Miri, 2010).

Figure 3-22 shows the effect of treatment time (150°C) on the storage (G') and loss (G'') moduli of heat treated samples of flour I. The elastic component dominates. Both moduli increase with increasing treatment time. Flour samples treated at temperatures between 110°C and 200°C for a constant time of 5 min display significantly higher storage moduli than loss moduli in all cases (data not shown). Both moduli increase with increasing temperature.

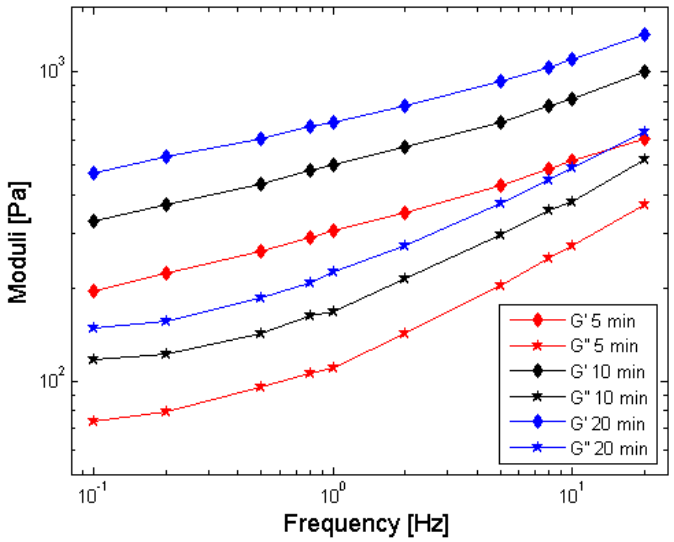

Figure 3-22: Effect of heat treatment time (at 150°C) on elastic (G') and viscous (G'') moduli of a flour-water slurry (flour I)

The time and temperature dependence of the elastic modulus at an oscillation frequency of 5 Hz of the flour-water slurries is shown in Figure 3-23a and as a response surface in Figure 3-23b. The elastic behaviour of the samples increased linearly in the observed period of time

for all temperatures. The rate of the increase in elastic modulus over time is constant at a given temperature, but increases exponentially with increasing temperature (R^2 = 0.99, data not shown). When the logarithm of the reaction rate is plotted against the reciprocal temperature, an activation energy of -96.4 kJ/mol is obtained.

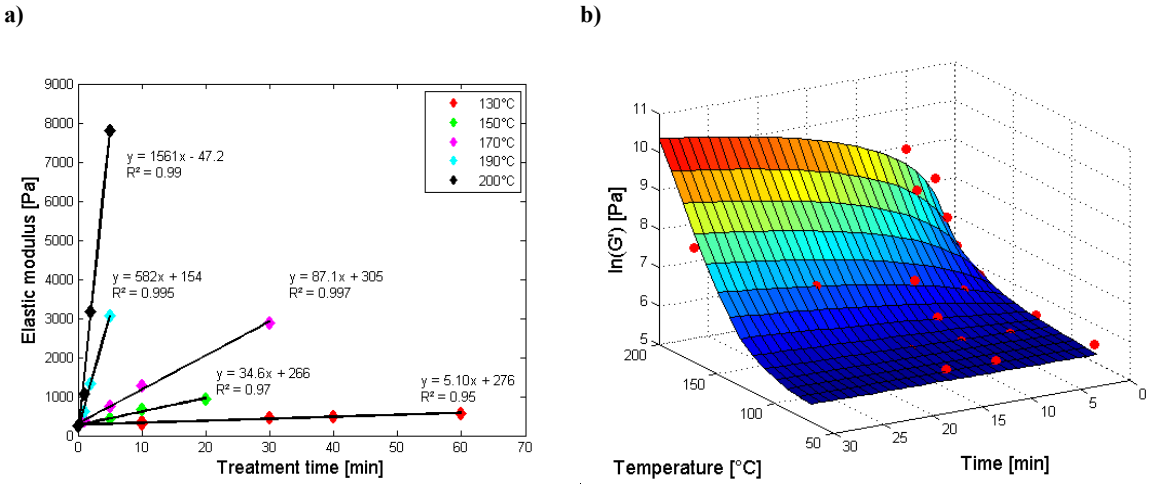

Figure 3-23: a) Elastic modulus of heat treated flour samples (130 - 200°C, 1 - 60 min) in water at 5 Hz b) Response surface of the elastic modulus of heat treated flour samples in water depending on treatment temperature and time with data points (R^2 = 0.85).

The results suggest that more severe heat treatments cause increased interactions of flour components, so that the system is able to store more energy at ambient temperature. Possible explanations include:

i) The proteins on the starch granule surface form a barrier and hinder water absorption into the untreated granule (Nicholas et al., 1978). The barrier might be degraded by partial denaturation of the proteins allowing the starch granules to

swell more easily at ambient temperature. Increased swelling of polymers might allow for more contact areas, interactions, and the ability to store more energy.

ii) Heat treatment impacts on the arabinoxylan fraction of flour. It is the component whose swelling behaviour in the SRC test increases most upon heat treatment (see section 3.3.3). This is also suggested by Van Steertegem et al. (2013).

In a continuous heating process, the product flow has a process specific residence time distribution as it is passing through the equipment (see chapter 4). To evaluate the impact of the width of the residence time distribution on flour functionality, it is important to understand the changes in functionality of flour mixtures containing flours that were treated for different times. For that reason, untreated flour was combined with heat treated flour (190°C for 5 min) and the elastic modulus was measured.

Figure 3-24 shows the elastic modulus G' of untreated flour (heat treated flour fraction = 0), heat treated flour, and various combinations. The elastic modulus is not a linear function of the heat treated flour fraction suggesting the untreated flour is the dominant component. These findings indicate that less treated samples decrease the rheological results to a more significant degree than treated samples cause an increase.

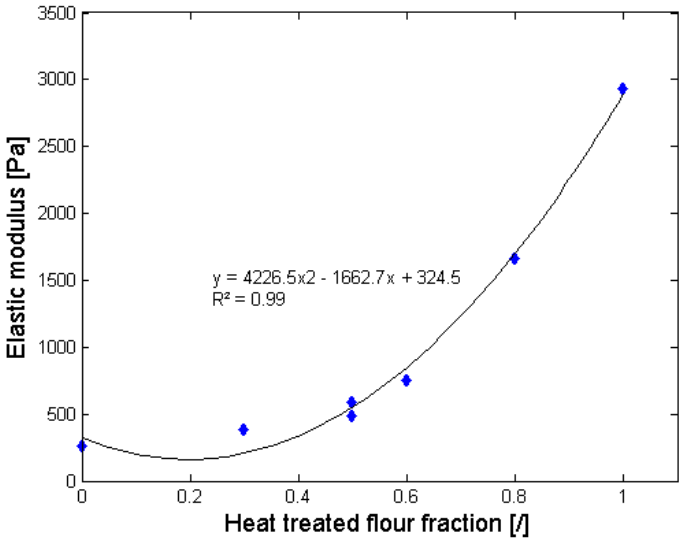

Figure 3-24: Elastic modulus of untreated flour, heat treated flour (190°C for 5 min) and combinations; with best-fit line

3.3.5 Rheomixer

The gluten proteins are responsible for the unique viscoelastic properties of wheat dough (Mann et al., 2014). Their three-dimensional structure unfolds upon mixing and water addition and a transient network is formed, comprised of mainly disulphide bonds, the most favourable arrangement of hydrogen bonds, hydrophobic interactions, and entanglements (Mann et al., 2014). Thermal treatments can alter protein conformation, their ability to take part in these processes and hence, the dough formation process is greatly modified (Mann et al., 2014). The effect of heat treatment on the gluten protein of flour I is discussed in the following.

Figure 3-25 shows the mixing curves in the rheomixer of flour samples treated at various temperatures for 5 min:

- In the untreated sample the gluten is hydrated and a network is developed upon mixing. The curves of the flour samples treated between 110°C (data not shown) and 135°C look similar suggesting a gluten network is formed.
- The curves of samples treated between 140°C and 160°C are marked by a significant drop in mixing torque after 5 - 8 min of mixing time. A gluten network might be developed in the beginning of the mixing phase, but the drop in mixing torque indicated the instability of the dough and its sensitivity to mechanical treatment.
- The profiles at 170°C and 180°C show no drop in mixing torque indicating a stable dough. However, the shape of the mixing curve is different from the ones at lower temperatures. The maximum torque is lower and the curve is not increasing, but constant with mixing time.

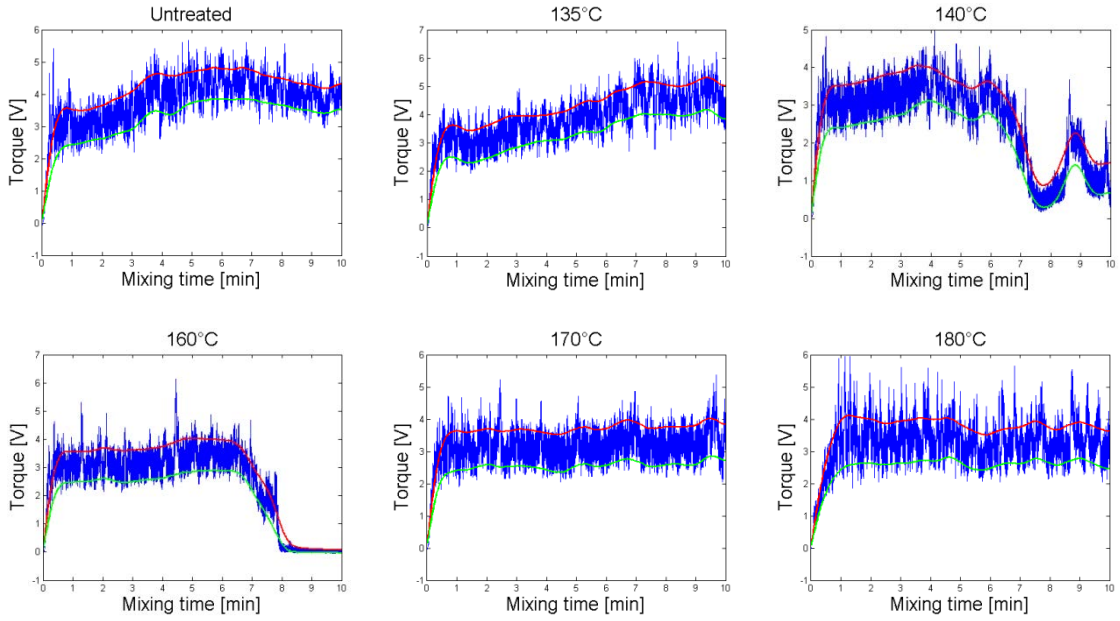

Figure 3-25: Mixing curves of samples of flour I treated at different temperatures for 5 min; red and green lines show upper and lower envelope lines.

Van Steertegem et al. (2013) reported a drastic impact of heat treatment on gluten hydration and dough development due to cross-linked proteins. At some level of heat treatment a complete lack of gluten network formation was seen (Van Steertegem et al. 2013). Hence, it is expected that the shape of the curves at 170°C and 180°C in this study (see Figure 3-25) is not because of the formation of a gluten network, but is due to a different phenomenon that dominates at high temperatures. This is supported by the fact that it was not possible to wash out the gluten of these samples (data not shown).

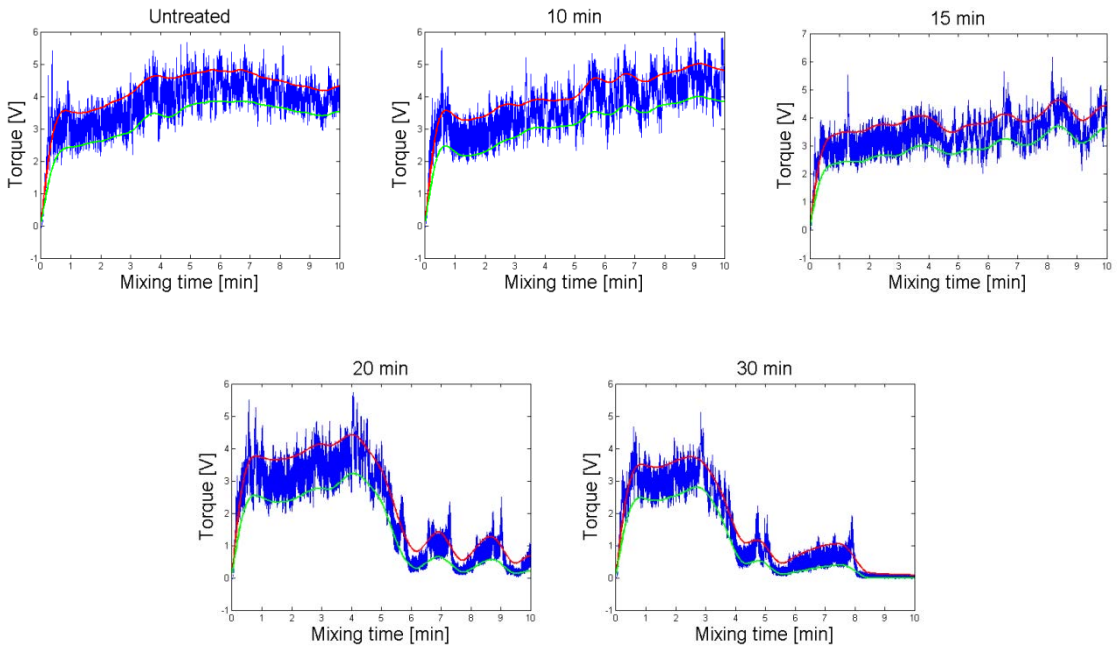

Figure 3-26: Mixing curves of samples of flour I treated at 130°C for different times; red and green lines show upper and lower envelope lines.

Figure 3-26 shows the mixing curves of flour samples treated at 130°C for different times. Up to a treatment time of 15 min, the development of a gluten network could be observed. At

longer times, the system destabilised after a certain mixing time as indicated by the sharp decrease in torque.

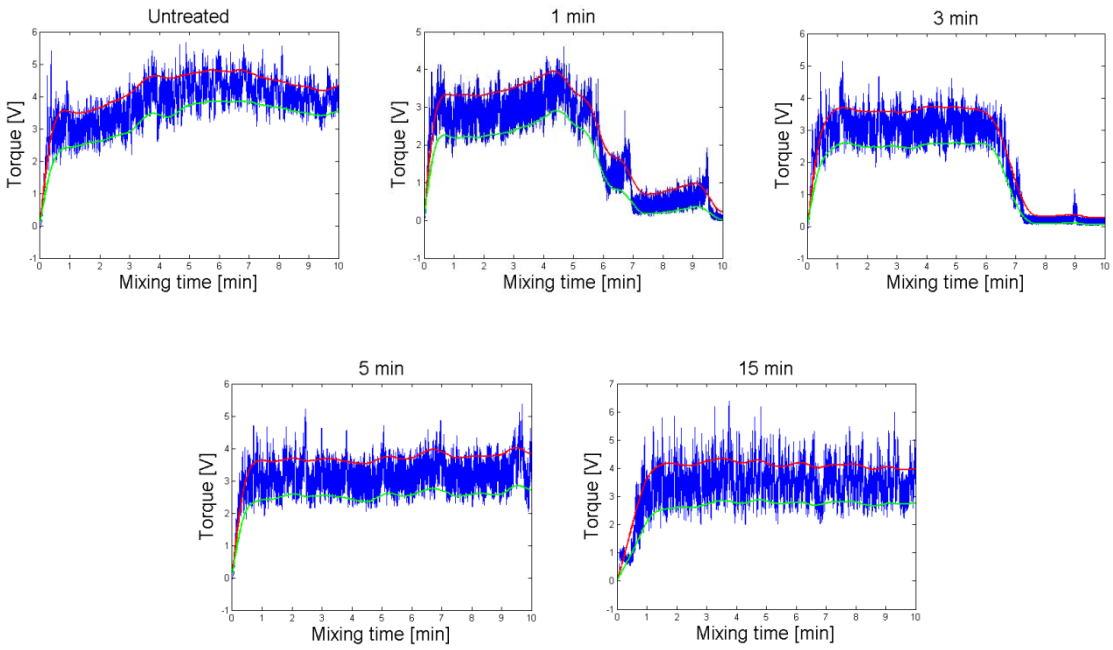

Figure 3-27: Mixing curves of samples of flour I treated at 170°C for different times; red and green lines show upper and lower envelope lines.

Figure 3-27 shows the mixing curves of flour samples treated at 170°C for different times. Up to treatment times of 3 min, a gluten network was formed but was mechanically destroyed after mixing times of 4 - 7 min. However, for treatment times between 5 min and 15 min, the rheomixer traces were stable, but the underlying mechanism will not be gluten development.

The findings show a significant impact of flour heat treatment on the hydration of protein and gluten network formation.

3.4 Conclusions

An accurate method for the heat treatment of flour was shown here. The effect of heat treatment on a number of functional aspects of flour was investigated.

Scanning electron microscope studies showed no differences in superficial structure of flour components in untreated and heat treated flour samples: differences in physical and chemical properties result from changes at a smaller scale than visible under SEM.

The overall swelling behaviour of flour polymers increased after heat treatment as shown by SRC tests at ambient conditions. In addition, the elastic moduli of heat treated flour-water slurries increased with increasing heat treatment intensity. These findings suggest enhanced interactions of flour components after heat treatment. In baking a cake, this can help to entrap and stabilise air bubbles in the cake batter.

The swelling behaviour of starch granules at elevated temperatures generally increased after heat treatment as measured by the RVA. The resulting interactions may strengthen the structure of a cake during baking and cause the expanding air bubbles to burst, so that the desired texture can be achieved (see chapter 2).

A model was developed to accurately calculate the RVA peak viscosity of flour in water after a stepwise temperature profile was applied to the flour. This was based on the data at constant temperature conditions. It may be used to predict the peak viscosity in processes where the temperature is not constant.

Different flours exhibited different starch granule swelling properties in different solvents. Untreated flours II and III showed facilitated starch granule swelling in 50% sucrose solution

in comparison to water in the RVA. However, the extent of starch granule swelling after heat treatment was found to be lower in 50% sucrose solution compared to water. Flour I showed the opposite trend in both aspects.

A different development of the peak viscosity with heat treatment time was observed in different RVA solvents. Excessive heat treatment of flour resulted in a decreased RVA peak viscosity in water. This was not observed when 50% sucrose solution or 5% lactic acid solution were used as solvents. The findings show a stabilising or delaying effect of the solutes on the swollen starch granules against shear. No difference was found in the RVA profiles of heat treated flour in alkaline solution indicating that

- changes in flour that occur during heat treatment are reversed by 5% sodium carbonate solution, or
- changes that are induced by heat treatment can also be achieved by the alkaline environment in a short time. Thereby, all transformations are accomplished to a maximum in the RVA solution causing identical traces; or
- the RVA test in sodium carbonate is insensitive to changes induced by heat treatment.

Key findings regarding the hypotheses for the impact of dry heat treatment on flour are:

i) Facilitation of starch granule swelling:

- Heat treatment of flour generally increased the peak viscosity in the RVA suggesting a higher degree of starch granule swelling at elevated temperatures.

- The formation of a stronger network of heat treated flour-water slurries was shown by small deformation oscillatory measurements at ambient temperatures. An increased elastic modulus of heat treated flour slurries represents a greater ability to store energy and may be due to higher starch granule swelling, possibly due to denaturation of the granule surface proteins.

ii) Impact on gluten proteins:

- An increased peak viscosity of heat treated flour samples in the RVA (in water) could be due to delayed granule disruption by external shear forces giving the granules more time to swell. This could be due to cross linking of the gluten proteins resulting in a more polymerised flour particle.
- A lack of gluten network formation was found after severe heat treatments by means of the rheomixer.
- SRC tests indicated an optimum treatment time for protein hydration and gluten network formation.

iii) Impact on solvent accessibility of arabinoxylans:

- Swelling behaviour of arabinoxylans as indicated by SRC tests increased by approx. 40% after flour heat treatment of 20 min at 150°C.
- The reason for the increased elastic modulus of heat treated flour slurries in small deformation oscillatory measurements may also be caused by the increased swelling behaviour of arabinoxylans after heat treatment.

4 Residence time of flour and grains in the Revtech

4.1 Introduction

This chapter investigates residence times of flour and grains through the Revtech system. The importance of processing time on flour functionality during the heat treatment of flour was shown in lab-scale experiments in chapter 3. Typical treatment times and temperatures of flour for the production of high-ratio cake flour have been summarized in chapter 2.

In addition to the heat treatment of flour, the process of microbial inactivation of grains is investigated here. This is due to the increased attention of microbial inactivation of low water activity, particulate products such as nuts, seeds, and pulses in recent years as foodborne pathogen infections were associated with these products (Beuchat et al., 2013). The primary pathogen of concern is *Salmonella* spp. (Beuchat et al., 2011; Codex Alimentarius Commisson, 2013). Even though a low water activity generally inhibits microbial growth, cells can remain viable at these conditions (Mattick et al., 2000; Penaloza Izurieta and Komitopoulou, 2012). Additionally, microorganisms can be more resistant to heat in matrices with reduced water activity (Barrile and Cone, 1970; Penaloza Izurieta and Komitopoulou, 2012; Podolak et al., 2010; Villa-Rojas et al., 2013). Pathogenic cells can cause sickness and consequently, measures like processing interventions that lead to a minimum 4 log reduction of Salmonella in almonds have been adopted to ensure the safety of these products (Almond Board of California, 2007). Technological solutions have focused on steam pasteurisation. The microbial count in the material commonly decreases with increasing treatment times. Therefore, the Revtech system can be used for the continuous heat treatment of these products.

Hence, the residence times of two types of particles are studied here:

i) *Flour:* The heat treatment of flour is necessary for the production of cake flour (see chapter 2).

ii) *Grains:* The heat treatment of grains is implemented to ensure microbiological safety.

In both processes, understanding of the particle motion and the accurate predictability of the residence time are critical for the design of a thermal process that results in high quality and safe products. The investigation of residence times was performed at ambient temperature to exclude complex interactions. The impact of temperature is investigated in chapter 5.

The aims of this study were:

- To investigate the influence of various process parameters on the residence time of grains and flour through the equipment, and
- to characterise the development of residence time with time, and
- to identify areas where the residence time is stable with time, and
- to develop a theoretical model to estimate the pasteurising effect of the heat treatment of grains in the Revtech equipment.

Work on this subject has been published (Keppler et al., 2016a; Keppler et al., 2016b).

4.2 Materials and methods

4.2.1 Materials

4.2.1.1 Grains

One batch of 200 kg of barley grains was used for the experiments. This was provided by Campden BRI (Gloucestershire, UK).

The median (by volume) of the particle size was calculated to be 5210 ± 430 μm with a sphericity of 0.81 ± 0.01 on a QICPIC system (Sympatec GmbH, D) with a measurable particle size of 30 - 10000 μm (Gradis disperser, M9 lense). The bulk density was measured to be 687 ± 2 kg/m^3.

4.2.1.2 Flour

Commercially available high ratio cake flour (wheat, protein content 8.6%) with the particle size distribution shown in Figure 4-1 was used for the experiments. The mean particle size was 86.5 ± 1.2 μm. One batch of 120 kg was used for the experiments. It was occasionally topped up to compensate for losses during sample taking. Bulk density and tap density were measured to be 510 ± 3 kg/m^3 and 810 ± 10 kg/m^3.

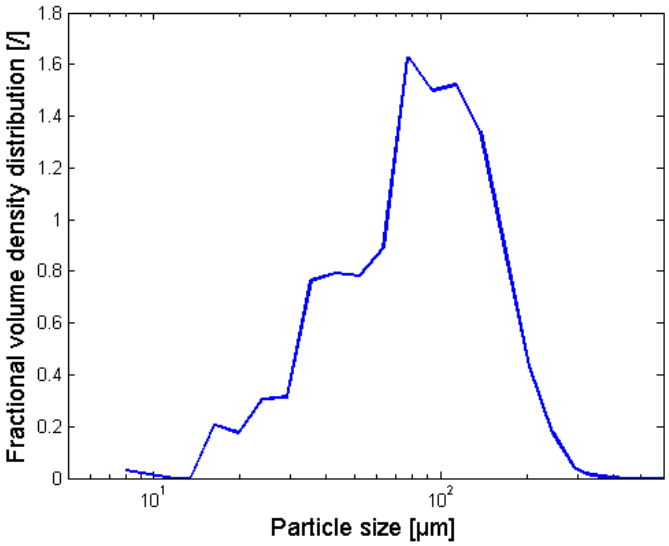

Figure 4-1: Particle size distribution of high ratio cake flour

4.2.2 Processing equipment

The equipment used for the experiments is a continuous, thermal processing unit provided by Revtech Process Systems (Loriol-sur-Drôme, France). It is described in detail in chapter 2.

The hopper and the heating spiral were used for the experiments here (see Figure 4-2). The product exits the helical pipe via a flexible plastic tube connected to the top and is collected in a plastic container. In a real process, the flexible pipe would be connected to the second spiral which cools down the product.

For the experiments here, the off balance motor setting was set to 65% resulting in an amplitude of vibrations of 4 - 5 mm.

A dry and a wet cleaning method can be applied to the spiral. A cleaning pig is used in both cases to push the remaining product out of the pipe. Compressed air is used in one case and

water in the other to drive the cleaning pig through the pipe. In one case the hand dishwashing liquid Suma Star plus D1 plus (JohnsonDiversey, Inc.) was added to clean the pipe.

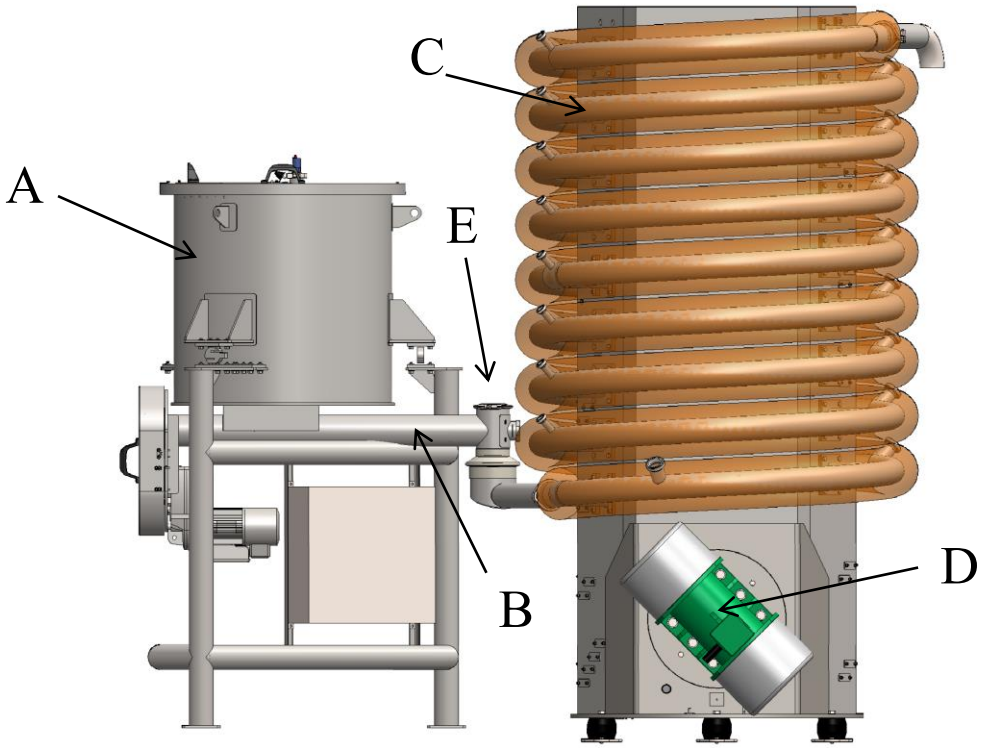

Figure 4-2: Experimental setup for residence time measurements: Hopper (A), screw feeder (B), insulated helical pipe (C), motor at an angle β with the horizontal (D), insertion point for marker particles (E)

4.2.3 Measurement of residence times

4.2.3.1 Grains

The residence time of barley grains was measured by a colorimetric method. Single grains were coloured with a permanent marker and left to dry overnight at ambient conditions. They were then individually added to a constant product flow (100 kg/h) into the machine (at point

E in Figure 4-2) and the time was taken with a stopwatch from the time when the grain entered the spiral until it was detected by eye at the exit in the collection container. Grains were added in parallel in 1.5 - 2 min intervals. Experiments were typically of 2 hour duration after which the hopper was empty and the residence time of approx. 55 - 80 grains was measured per experiment. A constant flow rate was ensured from approximately 5 minutes after the start of the machine until the end of the experiment.

Design of experiments

The motor angles of the machine were set to 20°, 30°, and 40°. Preliminary experiments were carried out to identify suitable motor speeds:

- At 20°, no significant differences in residence time could be detected between the minimal and the maximal value of the motor speed range. Hence, no values were tested in between.
- At 30°, the difference between the results at 600 rpm and at 740 rpm was larger and thus, 660 rpm was investigated as well.
- At 40°, different magnitudes and dynamics of the residence time were observed depending on the motor speed. An attempt was made to find a motor speed at which the residence time was constant over the entire timescale of the experiment. By trial-and-error method, motor speeds of 600 rpm, 710 rpm, 723 rpm, and 740 rpm were investigated.

Generally, the pipe was not cleaned between experiments, but the effect of cleaning is assessed in section 4.3.4.1. At least 3 and up to 11 experiments were carried out for each set of processing conditions.

4.2.3.2 Flour

For the measurement of residence time distributions (RTD) of flour, 25 g of burnt flour (15 min at 250°C in a convection oven) was used as a marker that was introduced instantaneously to a constant flour flow of 100 kg/h (insertion point E in Figure 4-2). The time was taken with a stopwatch and the marker was collected at the outlet of the flexible tube in 1 s bins. This was accomplished by moving the device in Figure 4-3 by one plastic dish per second manually. The approximate residence time at which the marker was to be expected was determined in preliminary experiments.

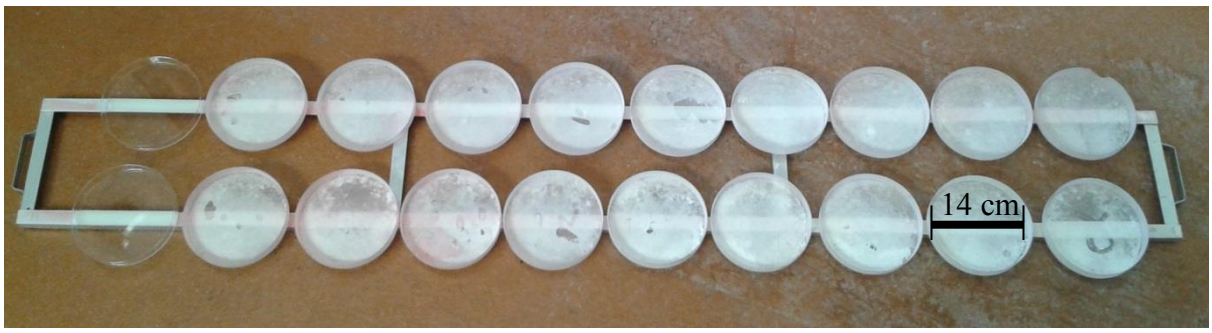

Figure 4-3: Flour collecting device for the determination of residence time distributions of flour passing through the Revtech

The mass as well as the colour values *X*, *Y*, *Z* (Konica Minolta spectrophotometer CM-5, reflectance mode, observer angle 10°, illuminant D65) of all collected bins were identified. The concentration (wt.%) of marker in each flour sample was calculated by means of a calibration curve. By multiplication of sample mass and marker concentration, the marker mass per bin was generated and related to the total marker mass collected at the outlet. Subsequently, residence time distributions were created in Minitab 17 ®.

Calibration curve

To create the calibration curve, the *X*- and *Z*-values of known concentrations (wt.%) of burnt flour within a burnt flour-fresh flour-mixture were studied. Two parameters were used instead of one to increase the accuracy. *X*- and *Z*-values of the known concentrations (0 - 30%) were plotted in a 2D graph and a linear regression was performed (Figure 4-4a). The distance δ along the regression curve was calculated for the known concentrations. As the data points do not lie perfectly on the calibration line, the nearest point was found by dropping a perpendicular onto the line. δ is calculated by the dot product of the unit vector of the regression curve and the vector of the measured sample (Eq.3 - 4, m: gradient of regression line).

$$\delta = \frac{1}{\sqrt{1+m^2}}\begin{pmatrix}1\\ m\end{pmatrix} \circ \begin{pmatrix}X\\ Z\end{pmatrix} \qquad \textbf{Eq. 3 – 4}$$

δ is then plotted against the corresponding concentrations of burnt flour mixtures. A third order polynomial can be fitted to the data (Figure 4-4b).

For the residence time experiments, *X* and *Z* values were found experimentally, δ calculated and the marker concentration found from the calibration curve.

a)

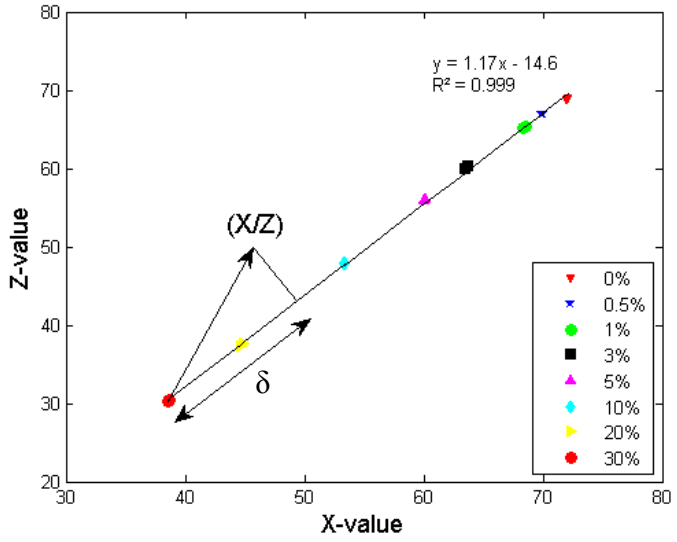

b)

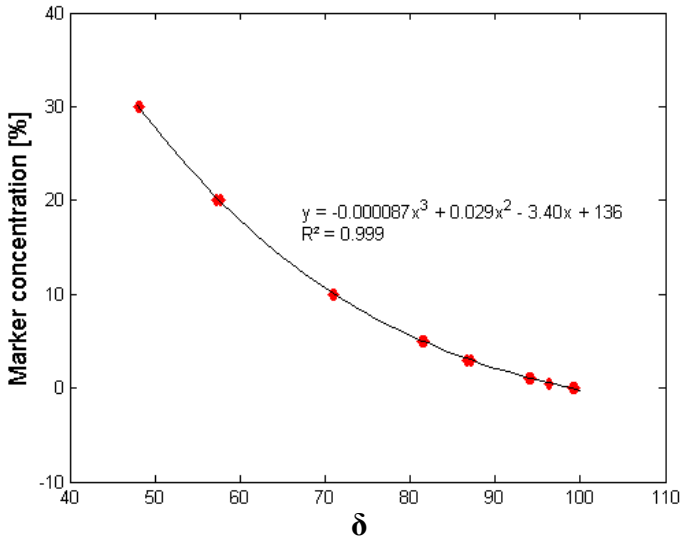

Figure 4-4: Calibration curves for burnt flour-fresh flour-mixtures of various concentrations. a) *Z*-values against *X*-values with best-fit line. b) Marker concentration (wt%) against δ with fitted third order polynomial.

Design of experiments

The residence time of flour was measured at the maximal motor speed of 740 rpm for motor angles of 20°, 30°, and 40°. At the minimal motor speed of 600 rpm, the residence time was determined for motor angles of 30° and 40°. At 20°, the horizontal component of acceleration of the vibrations was not sufficiently high to convey the particles up the spiral and the flour overflowed at the inlet.

4.2.4 Residence time dynamics

4.2.4.1 Grains

Changes in residence time were investigated during both single experiments as well as over the course of several experiments. This was done to identify time periods when residence time was stable, and to suggest reasons for any drift.

Single experiment

Different processing conditions resulted in different residence time dynamics over the timescale of one experiment. To characterise stable and unstable periods, two different methods were used.

i) Generally, the residence time data was analysed in Minitab 17®. Control charts in Minitab were used to establish whether the residence time was constant with time. Three standardised tests were applied and if the data failed one of them, the point was taken as transition point or stabilisation time. Here, these tests were:

- 1 point > 3 standard deviations from centre line (overall average of data)
- 9 points in a row on same side of centre line
- 6 points in a row, all increasing or all decreasing

The stable subset of the data was tested again. Sporadic outliers were neglected; in case one data set failed one of the tests, but none of the other sets at the same conditions did, it was still pooled to include variability.

ii) At motor angles of 40° and motor speeds of 600 rpm and 710 rpm, an initial start-up phase was observed before the residence time stabilised. However, even in the stable phase, the residence time showed a small, but continuous increase. This drift meant that control charts could not be used to find the stable phase, because as the data is not constant, it repeatedly failed the tests. Therefore, the 'stable' phase was taken to be after 2500 s of the experiment.

Multiple experiments

With the aim of presenting the dynamics of the residence time over the course of several experiments, the residence time data of the stable phases of all experiments of one day was connected and plotted versus a cumulative machine run-time. The first point of the stable phase of one experiment was connected to the last point plus 1 s of the stable phase of the previous experiment. Two or three experiments were performed per day. One dataset was created for each set of processing conditions and regressions were performed in Microsoft Excel (2010).

At 40°, the starting transient of the first 2500 s was removed for all motor speeds to allow data to be better compared. As the residence time was stable at a motor speed of 600 rpm and motor angles of 20° and 30°, all data was used in both cases.

Expression of results

Mean and standard deviation of the residence time was calculated for the stable phases of at least 3 and up to 11 data sets per processing condition with Minitab 17®. Results are expressed as mean ± standard deviation. The effect of different runs of the same day could be identified by examining different individual data sets.

Different data sets at the same processing conditions were generally not identical as proven by an analysis of variance (data not shown). Still, the data was pooled and thus, the variability between experiments was included in the results. However, due to the differences between the individual data sets, overall residence time distributions were not created.

4.2.4.2 Flour

To evaluate the development of the residence time with time, the residence time is taken to be the point when the marker starts to emerge at the outlet of the spiral. This avoids the need to measure full RTDs; results discussed below show that the distributions are very narrow at all processing conditions, so the approach is justified. Thus, the first sample bin that contains marker particles is determined by eye and the corresponding time is referred to as residence time. Hence, this represents a measure of the shortest residence time. Generally, marker samples were introduced every 10 minutes, which allowed for 5 samples per experiment (100

kg/h). 3 to 4 experiments were performed per day. The residence time of one day is then plotted versus a cumulative machine run-time. The dynamics of the residence time were studied at motor angles of 40° and a motor speed of 740 rpm.

Minitab 17® was used for standard statistics, ANOVA, correlation tests, histograms and Q-Q plots. Regressions were performed in Matlab®.

4.2.5 Particle size measurements and fractionation

Flour samples were taken at the outlet of the flexible tube and particle size distributions were determined. To avoid segregation in the sample bags, the samples were poured onto heaps and divided in 4 equal quarters. Three of these quarters were used individually to measure particle size distributions on a QICPIC system (Sympatec GmbH, D) with a measurable particle size of 10 - 3410 µm (Oasis Rodos disperser, M7 lense). The 10%, 50%, and 90% quantiles of the sample volume were calculated.

Furthermore, 60 kg of flour was sifted on a Sievmaster (Farleygreene Ltd, UK) on a sieve with a hole size of 75 µm and a diameter of 52 cm. Approx. 4 kg were sifted at once for 2 hours. Subsequently, the residence times of the resultant fine and coarse fraction were measured.

4.2.6 Determination of flour water content and air humidity

The water content of flour samples was determined in a convection oven at 130°C according to AACCI International Method 44-15.02 (1999) (note: silica gel was used as desiccant).

Ambient temperature and relative air humidity were measured with a Protimeter MMS (General Electric). Relative humidity is the ratio between partial water vapour pressure and the saturation vapour pressure at a given temperature.

4.2.7 Measurements of electrostatic effects

Charge dissipation properties of flour on an earthed surface were assessed in lab-scale experiments by measuring its surface potential.

The product charge was measured during experiments in the Revtech machine. Surface potential measurements were not possible because of the high moisture content of the flour (12.1%) that accelerates charge dissipation.

Lab-scale experiments of electrostatics

Flour was dried in a thin layer (< 1 mm) on a hotplate at 60°C, 80°C, 100°C, and 120°C for 2 min to moisture contents of 7.9%, 3.9%, 2.2% and 0.9% (moisture content determination, see section 4.2.6). It was then rolled down a 1 m long plastic gutter pipe and directly collected in a conductive metal cup (inner cup of the Faraday pail JCI 150 (Chilworth Technology Ltd., UK, see Figure 4-6, left)). The cup had a diameter of 60 mm and was shielded from the environment with aluminium foil (see Figure 4-5). The setup was placed on an earthed table to allow for the charges to dissipate. The surface voltage was measured with a JCI 140 static monitor (Chilworth Technology Ltd., UK) mounted on a stand and it was moved as close to the cup's surface as possible without touching.

Figure 4-5: Setup for surface voltage measurements of flour. JCI 150 pail (60 mm diameter) shielded with aluminium foil on earthed surface. Earthed JCI 140 static monitor on top.

Revtech experiments of electrostatics

A flour sample was collected at the outlet of the flexible pipe of the Revtech machine with the Faraday pail JCI 150 (see Figure 4-6, left). A self-built Faraday pail (see Figure 4-6, right) was used to take samples at the inlet of the spiral due to the narrow dimensions between screw feeder and spiral inlet. Typically, a Faraday pail consists of a metal cup located within a metal shield. Both are separated by an insulator like PTFE or Teflon. The core of a coax cable is connected to the pail and the outer conducting sheath to the shield. The charge measuring unit JCI 178 (Chilworth Technology Ltd., UK) was connected to either of the pails via a bnc connector. In preliminary experiments, it was assured that both pails read comparable values. The flour mass in the cup was measured and correlated with the charge.

The unit was zeroed briefly before the measurements and movements of the cable were avoided as this affects the charge reading. To avoid further disturbances during the measurements, full cotton clothes were worn by the person performing the experiments and additionally, the person was earthed by a wristband connected to earth with a crocodile clip.

Figure 4-6: Left: Commercial Faraday pail JCI 150 with lid. Right: Self-built Faraday pail with lid.

4.3 Residence time of barley grains

The particles travel through the vibrating system at a flow rate of 100 kg/h in a homogenous layer with a bed depth of about two particles, with a surface length of 4 - 5 cm across the pipe. The particles do not fill the entire cross-section of the pipe; they only bounce a few millimetres high. At a setpoint of 100 kg/h, the flow rate at the inlet of the spiral is accurately controlled at 99.5 ± 1.0 kg/h, which is measured by a checkweigher. The flow rate at the outlet was measured to be 99.2 kg/h ± 1.0 kg/h by collection of product for 60 s over runs of 2 hours and weighing it. Control charts in Minitab 17® confirmed no increasing or decreasing trend of the flow rate with time.

The average residence times of the stable phases of various processing conditions are depicted in Table 4-1 and Figure 4-7 and discussed below. Data of more than 150 passes of tracer was collected for each processing condition and the residence time was measured to accuracy of ± 1s. Therefore, accurate RTDs can be identified. For example, Figure 4-8a shows the residence time distribution of barley grains (723 rpm, 40°) with a fitted normal distribution. The probability plot indicates that deviations from Normality are small. However, the observed shift in residence times over time discussed below skews the overall distribution and hence, plotting RTDs is not appropriate for all processing conditions.

Table 4-1: Mean residence times of barley grains passing through the Revtech in seconds of the stable phases at motor angles of 20°, 30°, and 40° and motor speeds between 600 rpm and 740 rpm

		Motor angle [°]		
		20	**30**	**40**
Motor speed [rpm]	**600**	389 ± 10	298 ± 6	306 ± 13
	660	-	297± 6	-
	710	-	-	332 ± 8
	723	-	-	244 ± 6
	740	406 ± 13	261 ± 6	195 ± 3

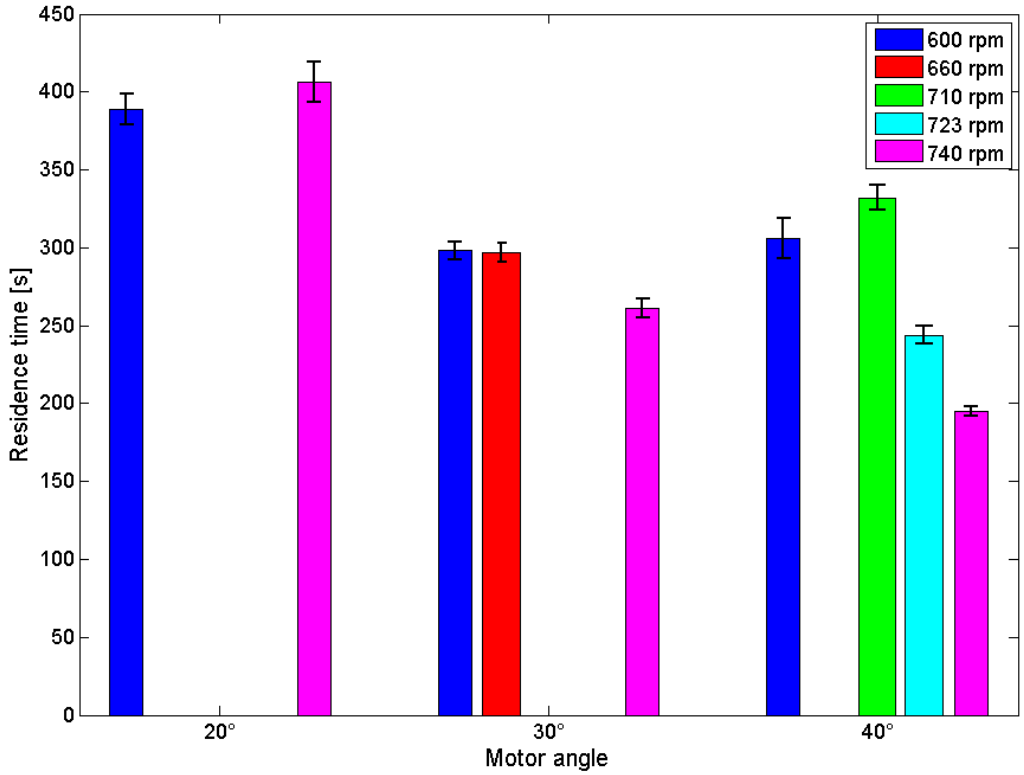

Figure 4-7: Average residence times of barley grains passing through the Revtech of the stable phases at motor angles of 20°, 30°, and 40° and motor speeds between 600 rpm and 740 rpm

Experiments were performed at ambient temperatures. At elevated temperatures, moisture migrates from the product into the atmosphere of the pipe. Many properties of the particles are thereby affected (e.g. surface properties, density, coefficient of restitution). It also renders the air more conductive and reduces electrostatic effects. Therefore, it is difficult to predict the effect of temperature on the residence time. The temperature effect on residence time is discussed in chapter 5.

Note that the experiments were performed on a pilot plant device and the results do not directly apply to industrial machines.

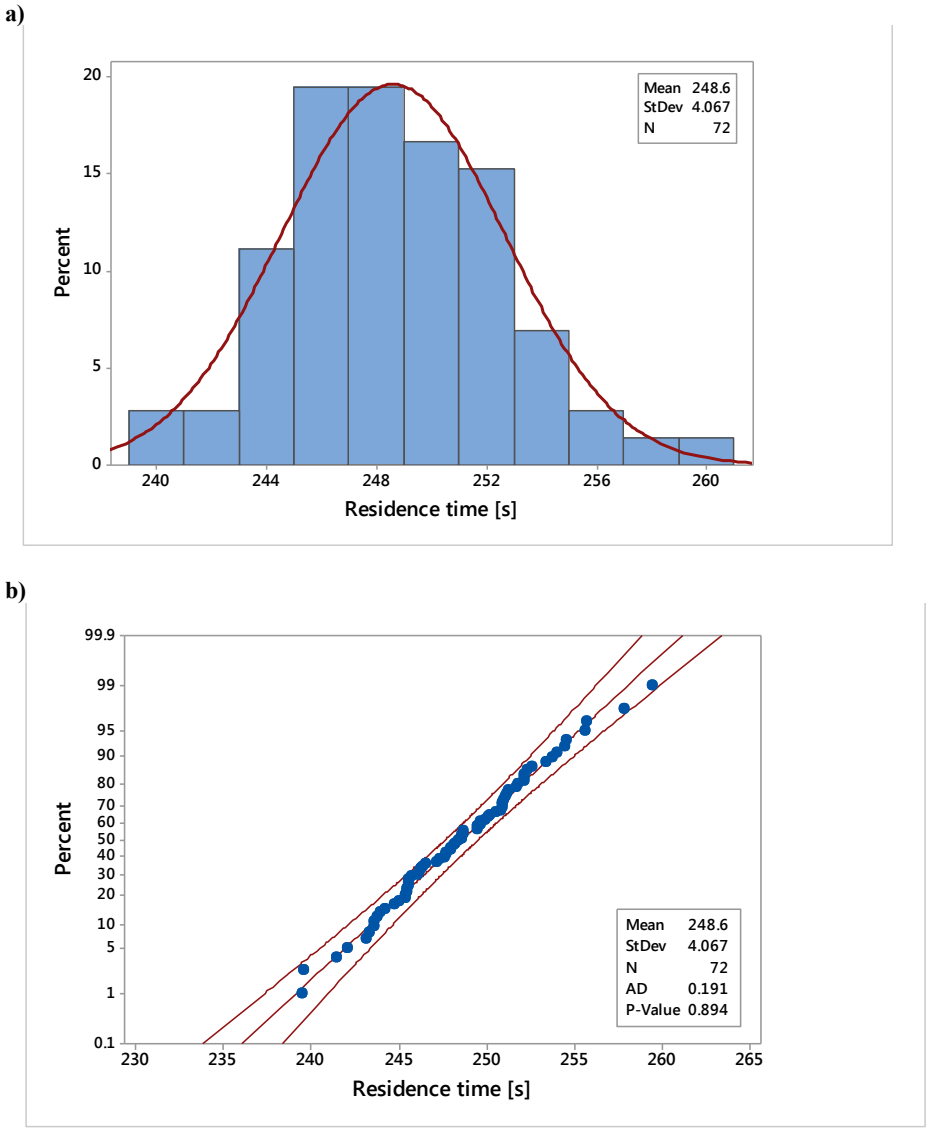

Figure 4-8: a) Residence time distribution of barley grains passing through the Revtech at a motor speed of 723 rpm and a motor angle of 40° and overlaid normal distribution. b) Probability plot with 95% confidence intervals.

4.3.1 Effect of motor speed

The motor speed controls the vibrational frequency of the spiral and it is associated with the amplitude of the vibrating bed. The spiral drives the particle flow to vibrate with the maximum amplitude at its resonance frequency. Macroscopically, it can be observed that at some frequencies, the flow is homogenous and regular and at others, the particle bed does not

move as one and the flow looks chaotic. The motor speed affects the mean residence time, but as it is constant over time (data not shown) it is not responsible for changes in residence time over time. The vibrational frequency was measured in preliminary experiments with a vibration meter.

The development of the residence time over the timescale of one experiment can be divided into two types of effects:

i) A characteristic time after the start of the machine for the system to stabilise as a function of motor speed and motor angle.

ii) Other effects like electrostatic forces that cause the residence time to shift after the stabilisation time.

4.3.1.1 Motor angle 20°

Figure 4-9a shows the residence time of barley grains at motor angles of 20° for motor speeds of 600 rpm and 740 rpm. Time 0 corresponds to the instant where the equipment is turned on and the product flow is started. The residence time is plotted against the time instant that the coloured grain enters the system. At 600 rpm, the residence time is stable over the timescale of the experiment as proven with control charts in Minitab (see section 4.2.4). In contrast, at 740 rpm, the residence time initially increases then stabilises before increasing again in the very end. The duration of the initial phase was determined with control charts. In three experiments, it took on average 1937 ± 146 s for the system to stabilise. The stable phase then lasted for 4529 ± 117 s. The variation in residence time between the smallest and the largest measured value was approx. 21.5% (79 s) (3 experiments). This is significantly higher than

the standard deviation of 13 s for the stable phase (see Table 4-1) and demonstrates the importance of identifying stable and unstable phases.

The mean residence time is 389 ± 10 s at 600 rpm and 406 ± 13 s at 740 rpm (see Figure 4-9a). This is calculated from all the data at 600 rpm and from the data for the stable system at 740 rpm. There is only a slight difference of the mean residence time over the motor speed range (< 4.4%).

The effect of the motor speed at angles of 20° is predominantly on the dynamics of the system rather than on the magnitude of the residence time. The stable data at 600 rpm facilitates the design of a thermal process. The difference between the average residence times at both motor speeds is small.

a)

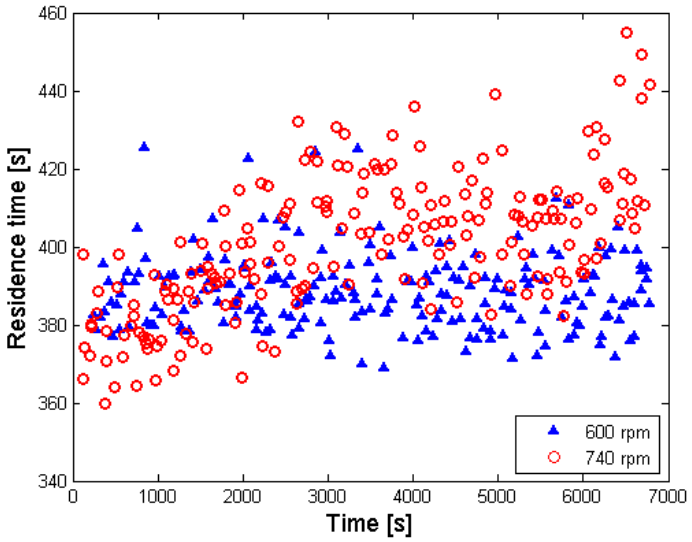

Figure 4-9: Residence time of barley grains passing through the Revtech: a) Motor angles of 20° and motor speeds of 600 rpm and 740 rpm. b) Motor angles of 30° and motor speeds of 600 rpm, 660 rpm, and 740 rpm. c) Motor angles of 40° and motor speeds of 600 rpm, 710 rpm, 723 rpm, and 740 rpm.

b)

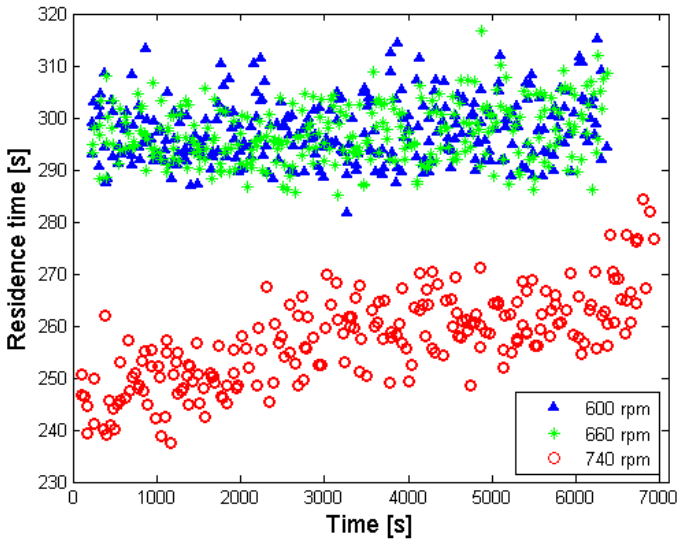

c)

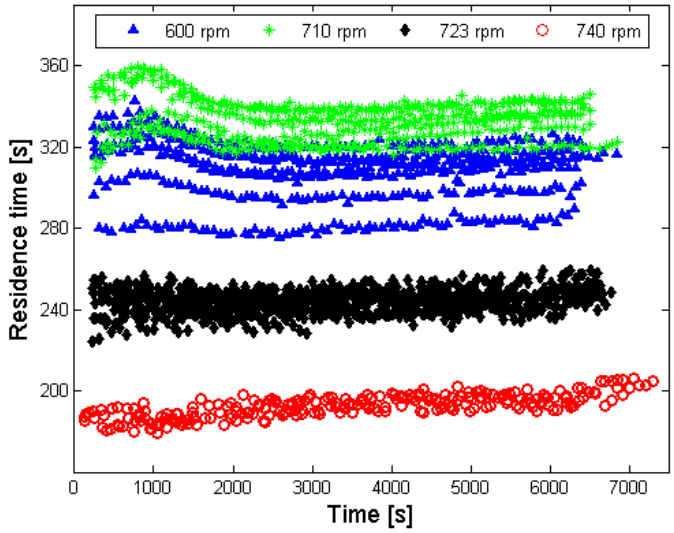

Figure 4-9 (continued): Residence time of barley grains passing through the Revtech: a) Motor angles of 20° and motor speeds of 600 rpm and 740 rpm. b) Motor angles of 30° and motor speeds of 600 rpm, 660 rpm, and 740 rpm. c) Motor angles of 40° and motor speeds of 600 rpm, 710 rpm, 723 rpm, and 740 rpm.

4.3.1.2 Motor angle 30°

The influence of the motor speed at motor angles of 30° is presented in Figure 4-9b. Motor speeds of 600 rpm, 660 rpm, and 740 rpm were tested. At 600 rpm and 660 rpm the residence time is stable over the timescale of the experiment, whereas at 740 rpm it increases in the beginning of the experiment before it levels off and increases again in the end. The transition between initial and stable phase was found at 2452 ± 260 s and the duration of the stable phase was 4208 ± 259 s. In three experiments, the variation between the smallest and the largest measured value was approx. 17% (40 s), which is comparable to the results at 20°.

In contrast to motor angles of 20°, different motor speeds also result in different magnitudes of the residence time. For 600 rpm and 660 rpm, the behaviour was not a function of time and average residence times of 298 s ± 6 s and 297 s ± 6 s were measured. However, at a motor speed of 740 rpm, the residence time of the stable phase was determined to be 261 s ± 6 s.

4.3.1.3 Motor angle 40°

Motor speeds of 600 rpm, 710 rpm, 723 rpm, and 740 rpm were tested at motor angles of 40°. Results are depicted in Figure 4-9c. It was found empirically that only at 723 rpm was the residence time approximately constant over the timescale of the experiment. For the other investigated motor speeds, there is an initial, unstable phase before the residence time stabilises. At 600 rpm and 710 rpm, the residence time increases and decreases before it levels off. At 740 rpm, it increases, levels off and increases again in the end of the experiment. In this case, it took 2495 ± 190 s for the system to stabilise and the stable period lasted for

4840 s ± 364 s. The variation in residence time between the smallest and the largest measured value was approx. 12% (22 s) (3 experiments).

By comparison to motor angles of 20° and 30°, changing the motor speed at 40° had a significant effect on the residence time. The mean was measured to be 306 ± 13 s, 332 ± 8 s, 244 ± 6 s, and 195 ± 3 s for motor speeds of 600 rpm, 710 rpm, 723 rpm, and 740 rpm, respectively (see Table 4-1). With exception of 600 rpm, the mean decreases with increasing motor speeds of 710 rpm, 723 rpm, and 740 rpm. Over the whole range of motor speeds between 600 rpm and 740 rpm, the standard deviation decreases from 13 s to 3 s with increasing motor speed. In the narrow range of motor speeds between 710 rpm and 740 rpm, the residence time decreases by approx. 137 s (41%). It is worth noting that the decrease in standard deviation was observed for the pooled data. The standard deviation of the individual data sets was similar for all motor speeds (2 s, 3 s, 4 s, 3 s for 600 rpm, 710 rpm, 723 rpm, 740 rpm). This indicates that the variability between experiments was higher for lower motor speeds, but the dispersion of the grains during each experiment was comparable.

4.3.2 Effect of motor angle

4.3.2.1 Motor speed 600 rpm

Figure 4-10a depicts the residence time of barley grains at a motor speed of 600 rpm for motor angles of 20°, 30°, and 40°. For 20° and 30°, it is constant over the timescale of the experiment as identified with control charts, whereas at 40° it increases and decreases in the initial phase before it stabilises.

Values of mean residence time distributions of 389 ± 10 s, 298 ± 6 s, and 306 ± 13 s were measured for motor angles of 20°, 30°, and 40°. While the data for 30° and 40° is in a similar range, residence time is about 29% higher for motor angles of 20°. There is no trend in the overall standard deviation from the pooled data sets. However, the standard deviation of the individual data sets decreases with increasing motor angle (9.4 s, 5.5 s, and 2.2 s for 20°, 30°, and 40°). This demonstrates that the dispersion of the barley grains decreases with increasing motor angle, but the variability between experiments increases.

a)

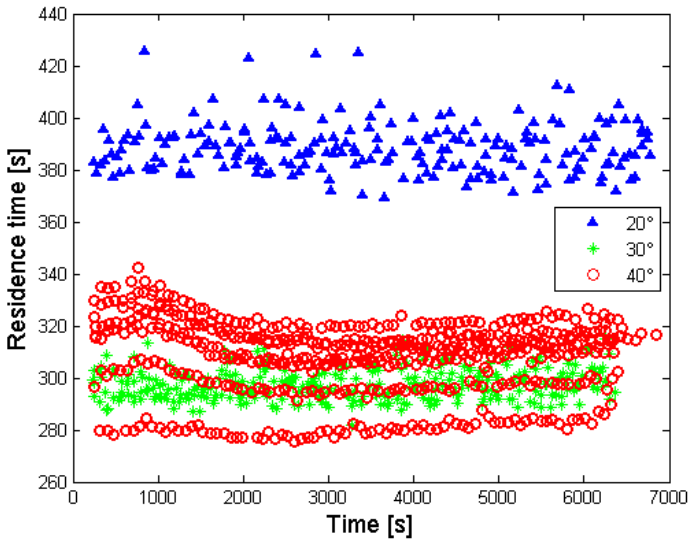

b)

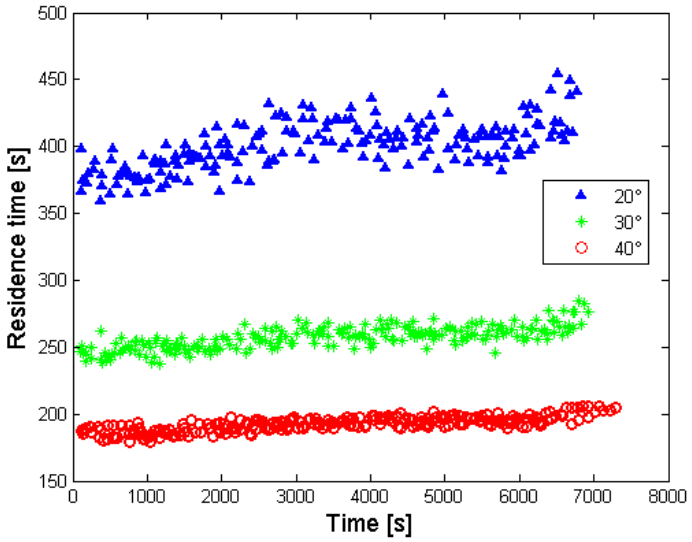

Figure 4-10: Residence time of barley grains passing through the Revtech: a) Motor speed of 600 rpm and motor angles of 20°, 30°, and 40°. b) Motor speed of 740 rpm and motor angles of 20°, 30°, and 40°.

4.3.2.2 Motor speed 740 rpm

The influence of the motor angle at a motor speed of 740 rpm is presented in Figure 4-10b. At all three angles, there is an initial stage where the residence time increases. It stabilises subsequently and increases again in the end. The stabilisation times were found by means of control charts and determined to be 1937 ± 146 s, 2452 ± 259 s, and 2495 ± 190 s for motor angles of 20°, 30°, and 40°. The duration of the stable phases was 4529 ± 117 s, 4208 ± 259 s, and 4840 ± 364 s for motor angles of 20°, 30°, and 40°. The overall residence time range between maximal and minimal value calculated from three experiments each is 22%, 17%, and 12% in relation to the minimal value for 20°, 30°, and 40°. It shows that the overall variation of residence time decreases with increasing motor angle.

The results of the pooled data of the stable phases are 406 ± 13 s, 261 ± 6 s, and 195 ± 3 s for motor angles of 20°, 30°, and 40°. The residence time at 20° is approx. 109% higher than at 40° which illustrates the importance of the effect of the motor angle. It is visible that mean and standard deviation decrease with increasing motor angle. This is also true for the individual data sets.

4.3.3 Summary of effects

For each motor angle, at least one motor speed was found at which the residence time of barley grains was constant over the entire timescale of the experiment. It would thus be possible to define a combination of angle and speed to deliver a uniform process.

At motor angles of 20° and 30°, the motor speed affected the dynamics of the system rather than the magnitude of the residence time; however motor speed at 40° influenced both the

mean and standard deviation to a much greater extent. It was also observed that the variability between experiments was higher at lower motor speeds for angles of 40°.

The effect of the motor angle on the average residence time is more significant at 740 rpm than at 600 rpm. A constant residence time was only observed at 600 rpm and motor angles of 20° and 30°. The standard deviation of the individual data sets and therefore the dispersion of the barley grains during one experiment generally decreased with increasing motor angle.

4.3.4 Residence time dynamics

It was found that under some conditions the residence time evolved over the course of several test runs. Such behaviour might make it difficult to specify a thermal process. For example, Figure 4-11 describes the dynamics of the residence time during one day for motor angles of 40°. The stable phases of all experiments during one day were connected. Each experiment took approx. 2 hours and subsequently, data of 2 (600 rpm) or 3 (710 rpm, 723 rpm) experiments was connected. Residence time at 600 rpm and 710 rpm increases with time and follows a quadratic curve. At 723 rpm, the data is more scattered and the increase is smaller. In this case, the data can be approximated by a linear equation. Over 12000 s of cumulative machine run-time (stable residence time phases), the average residence time increases by 19.6 s, 23.2 s, and 9.3 s which is 6.5%, 7.3%, and 3.9% of the initial value for motor speeds of 600 rpm, 710 rpm, and 723 rpm. The fitted curves were used for these calculations; at 600 rpm it was extrapolated. The change in particle holdup in the pipe results in a change in residence time. Only a small change in holdup is needed for the residence time to drift. The residence time in Figure 4-11 increases from approximately 320 s to 340 s over a time period

of 12000 s at a motor speed of 710 rpm. The holdup can be calculated as (flowrate · residence time) assuming no dead spaces. At a flow rate of 100 kg/h, this means a change of particle holdup in the pipe of 0.5 kg from ca. 8.9 kg to 9.4 kg and a change in flow rate of 0.15 kg/h. Therefore, the change in holdup in the pipe is smaller than the accuracy at which the flow rate can be measured (see section 4.3).

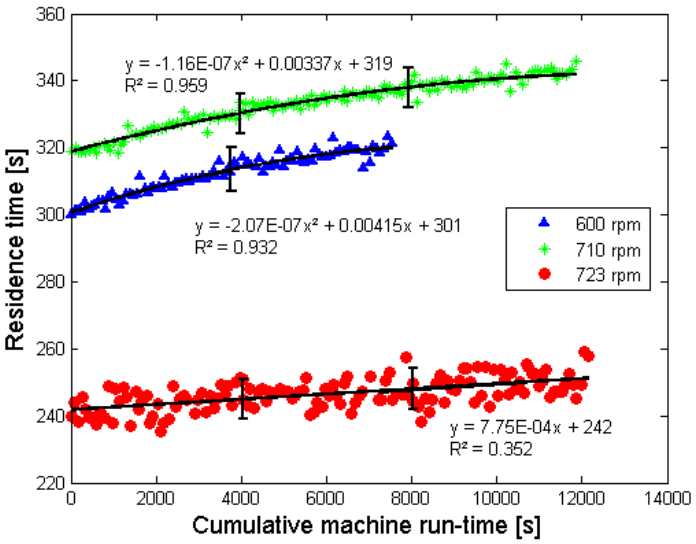

Figure 4-11: Development of the residence time of barley grains passing through the Revtech during the course of a day at motor angles of 40° and motor speeds of 600 rpm, 710 rpm, and 723 rpm. The vertical line indicates the connection points between consecutive experiments.

The residence time also increased during the day at motor angles of 20° and 30° at 600 rpm (data not shown). The extent of the linear increase was 4.5 s and 4.3 s after 12000 s, which represents 1.2% and 1.4% of the initial value at motor angles of 20° and 30°, respectively.

The data indicates that the increase of the residence time at motor angles of 20° and 30° is negligible, whereas it is much more significant at 40°. Furthermore at 40°, it increases to a higher extent at motor speeds of 600 rpm and 710 rpm than at 723 rpm.

Several factors might affect the residence time:

i) *Product effects*. The formation of a thin powder layer inside the pipe due to damage of the product may influence friction, the coefficient of restitution, or electrostatic effects.

ii) *Machine effects*. These could include warming up of the motors, the suspensions, or other parts that might have an impact on the vibrations over time and hence on the residence time of the grains.

iii) *Environmental parameters* like ambient temperature and humidity might have an influence. In preliminary experiments, no effect of ambient temperature could be found in the process range of 16 - 24°C.

These hypotheses were tested at motor angles of 40° and a motor speed of 600 rpm (see sections 4.3.4.1 and 4.3.4.2). Future work should focus on reasons why the increase in residence time only occurs at certain conditions and to variable extents.

This work was designed to demonstrate the use of the device at a flow rate of 100 kg/h. Careful experiments would be needed to confirm the residence time in practice, and to ensure minimal drift during processing time. The methods described here would be useful for such determination.

4.3.4.1 Hypothesis (i): Deposition of a powder layer inside the pipe

To test the hypothesis whether the formation of a powder layer inside the pipe due to material damage causes the residence time to increase during the day, a cleaning experiment was performed.

i) Two experiments (2 hours each) were performed per day for four consecutive days. At the end of each day, the pipe was cleaned with a cleaning pig and water. The data is shown in Figure 4-12a. The first and second runs of all four days fall into two repeatable groups. The residence time increases over the course of each day as it is clearly higher in the second run than in the first one.

ii) Two experiments (2 hours each) were performed per day for two consecutive days without cleaning the pipe. This is shown in Figure 4-12b. The first and second run of the first day match the data in Figure 4-12a. However, on the second day, the residence time of the first run is higher than that of the first run of the first day, but the second run on the second day behaves identically to that on the first day.

Hence, it is shown that the cleaning has an influence on residence time. Without cleaning, the residence time appears to increase.

On the other hand, if the residence time was solely due to the powder layer, it might be expected that the residence time at the start of the second day (point A in Figure 4-12b) would be the same as at the end of the previous day (point B in Figure 4-12b). However, the start point for the residence time decreases, perhaps due to alterations in the powder layer over night, e.g. humidity loss or gain or electrostatic charging. The experiments show that the formation of a powder layer inside the pipe affects the residence time of barley grains; more work would be needed to identify the precise cause.

a)

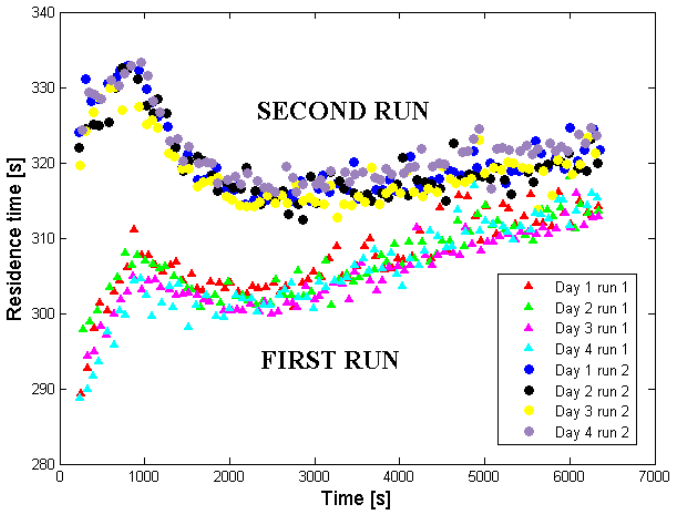

b)

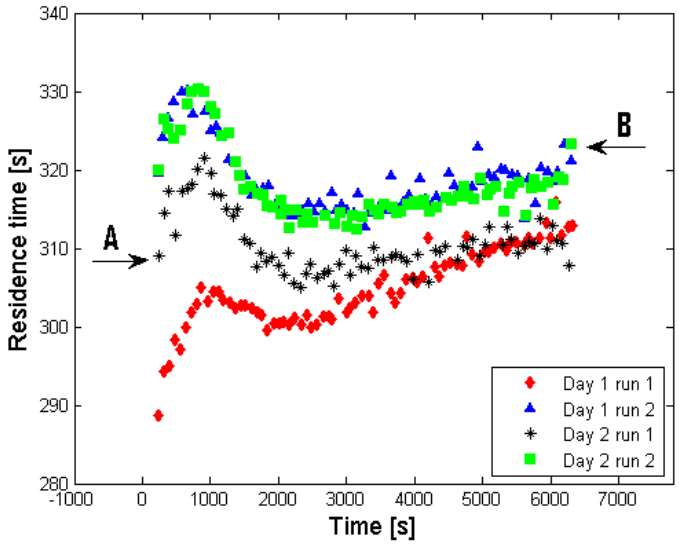

Figure 4-12: a) Residence time of barley grains passing through the Revtech at motor angles of 40° and a motor speed of 600 rpm at four consecutive days (2 runs each day). Cleaning after each day. b) Residence time of barley grains at motor angles of 40° and a motor speed of 600 rpm at two consecutive days (2 runs each day). No cleaning.

4.3.4.2 Hypothesis (ii): Warming up of the machine

The possible effect of warming up of the motors or other parts of the machine on the residence time of barley grains was tested. The machine was run for the period of one experiment (2 hours) without product to exclude product effects. Subsequently, product was

added and two more experiments were performed. The data can be compared to days where the machine was started with product from the beginning and two experiments were completed.

The results are presented in Figure 4-13 and show that data for experiments run after 2 hours of operation are identical to data from the first and second experiments of the control days. If the warming up of the motors caused the increase of the residence time the two data sets would be different.

Hence it is concluded that the vibrations are controlled accurately and the warming up of the machine does not influence the residence time of barley grains.

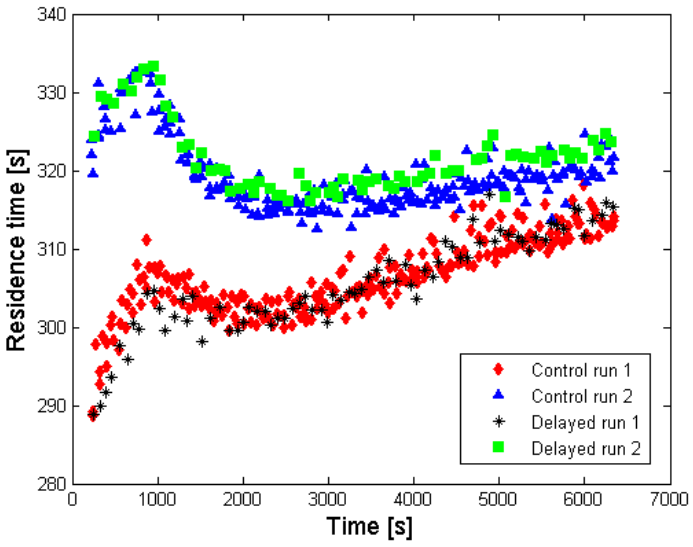

Figure 4-13: Residence time of barley grains passing through the Revtech at motor angles of 40° and a motor speed of 600 rpm. Two sets are shown (i) control run 1 and 2 where the machine was started at the start of run 1 and (ii) delayed run 1 and 2 where the machine was run for 2 hours without product before the start of run 1.

4.3.5 Model development for process validation

The work above has demonstrated a wide range of residence times of barley grains for different processing conditions. It is unclear whether the observed variations are of practical significance. To assess this issue, a model was developed that calculates the pasteurisation effect of the process as it is needed for example for the pasteurisation of almonds (Almond Board of California, 2007; Silva and Gibbs, 2012) .

Three inputs are required for the model:

i) Residence time data

ii) Temperature profiles along the axial direction of the pipe

iii) Microbial inactivation parameters

Residence time data from the experiments described in the previous sections (20°, 600 rpm) were used as the basis for the model.

The temperature profiles of the pipe are taken from preliminary experiments as measured by the 8 built-in temperature probes (see section 2.5). As the pipe is heated via resistive heating and is open to atmosphere, the temperature is not constant over the total length of the pipe. The temperature is controlled so that at least one of the probes is held at the temperature setpoint, whereas the temperature of the other probes depends on product flow rate and thermal properties of the product. This is explained in detail in chapter 5. Figure 4-14 shows a temperature profile of the pipe at a setpoint of 120°C. Straight line fits were drawn (i) between the first two temperatures, and (ii) to represent the mean of subsequent temperature probes. This profile is then used in the model as defined below.

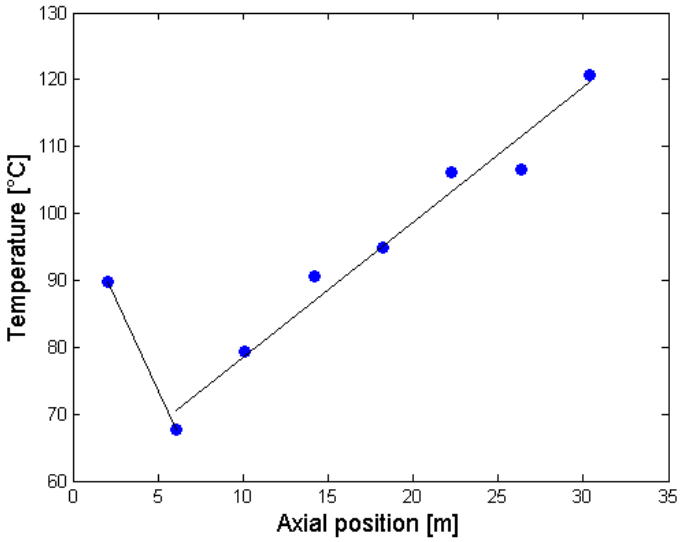

Figure 4-14: Temperature profile of the pipe wall in the axial direction of the Revtech tube. Setpoint 120°C.

The microbial input data comprises the D-value, its reference temperature, and the z-value. These are highly dependent on the microorganism and its environment and furthermore the processing history and the processing conditions (Podolak et al., 2010; Silva and Gibbs, 2012). Candidate organisms and their thermal behaviour are given in Table 4-2. As an example *Salmonella* Tennessee with D_{105} = 2.4 min and z = 11.9°C relevant to particulate grains is used.

Table 4-2: Kinetic data for the inactivation of microorganisms relevant to low moisture products

Microorganism	Product	D-value [min]	z-value [°C]	Conditions	Reference
Salmonella Tennessee	Toasted oat cereal	D_{85}=133.9 D_{105}=2.4	11.86	Dry heat treatment	(Chick, 2011)
Salmonella Agona		D_{85}=117 D_{105}=5.2	14.90		
Salmonella Enteritidis PT 30	Almond flour	D_{80}=1.63	8.28	Dry heat treatment a_w=0.610	(Villa-Rojas et al., 2013)
Salmonella weltevreden	Wheat flour	$D_{60\text{-}62}$=875 $D_{63\text{-}65}$=29	15.2 53.9	Initial a_w=0.4 Initial a_w=0.5	(Podolak et al., 2010)
Salmonella Enteritidis PT 30	Almonds	D_{60}=2.6 D_{80}=0.75	35	Hot water treatment	(Harris et al., 2012)
Salmonella Enteritidis	Almonds	D_{93}=0.27	-	Steam treatment	(Lee et al., 2006)

D-values and reaction rates are calculated at each temperature in the observed temperature range in the Revtech. The temperature of the particles' surface is assumed to be equal to the pipe wall and only the surface of the particles is microbiologically contaminated. The measured residence time data is used instead of fitted continuous distributions because of the observed shift in residence time over time. The microbial survivors are determined by a general first order expression for microbial evolution and log reductions are established.

The model calculates the thermal process by the following:

1) The D-value is calculated for all temperatures in the observed range by linear regression and by means of the z-value.

2) Reaction rates (φ(T)) of microbial inactivation are calculated for the observed range of temperatures in the Revtech tube:

$$\varphi(T) = \frac{2.303}{D(T)} \cdot \frac{1}{60} \quad [1/s] \qquad \textbf{Eq. 4 - 1}$$

3) Particles are assumed to travel at constant velocity, calculated by dividing the pipe length by the observed residence time.

4) The pipe length is divided in 344 small segments, each 0.1 m long.

   The residence time that a particle takes to pass one segment (Δt) is calculated by dividing the segment length by the velocity.

5) The temperature profile in the axial direction of the pipe is determined from the linearised temperature profile shown in Figure 4-14.

6) The reaction rate is found for each segment depending on the calculated temperature.

7) A general first order expression is used for microbial inactivation. The fractional microbial kill in each segment is calculated by applying the exponential function to the product of residence time per segment and reaction rates (Heldman, 2011).

$$S_{Segment} = \frac{N_{Segment,outlet}(t)}{N_{Segment,inlet}} = \exp(\varphi(T) \cdot \Delta t) \qquad \textbf{Eq. 4 - 2}$$

   The survivors of all segments are combined by multiplying the sequence.

$$S_{total} = \prod S_{segment} \qquad \textbf{Eq. 4 - 3}$$

8) The overall log-reduction is calculated.

Microbial reduction should be calculated individually for each application. As an example Figure 4-15 shows microbial reduction varies between 1.34 and 1.55 log reductions (overall mean calculated from RTD = 1.41 log reductions) for motor angles of 20° and a motor speed of 600 rpm (data of Figure 4-9a). Microbiological parameters of D_{105}=2.4 min and z =11.86°C

for *Salmonella* Tennessee (see Table 4-2) were assumed and the temperature profile of Figure 4-14 was applied.

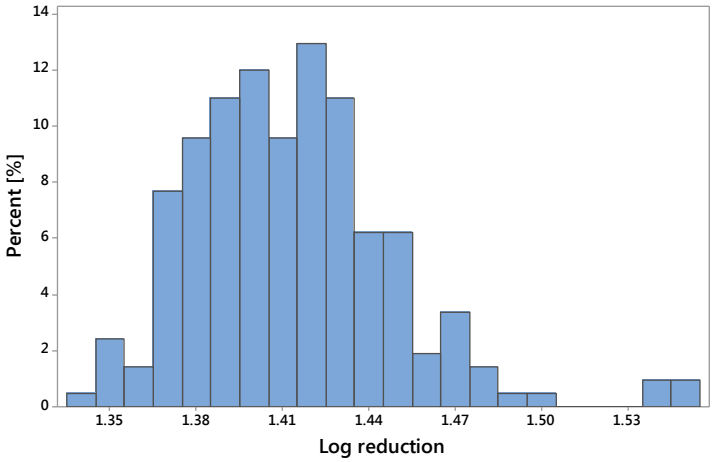

Figure 4-15: Calculation of microbial inactivation on particles which have been treated in the Revtech equipment. Distribution of log reductions of S. Tennessee (D_{105} = 2.4 min, z = 11.86°C) at motor angles of 20° and a motor speed of 600 rpm and a temperature setpoint of 120°C

It is evident that the variation in residence time relates to the microbial reduction linearly. In this case, the residence time ranges between 369 s and 426 s with a mean of 389 s. The difference between minimal and maximal value is 15% for the residence time as well as the microbial log reduction.

Table 4-3 shows both the mean and the range of microbial inactivation for different motor angles and motor speeds. The highest inactivation results from the highest residence time (motor angles of 20° and a motor speed of 740 rpm) whilst the smallest was calculated for the shortest residence time (motor angles of 40° and a motor speed of 740 rpm). The table also shows the relative differences in microbial inactivation and in residence times with respect to

their means at all tested processing conditions. The most precise treatment is achieved at 40° and 740 rpm (spread of 9%), but this might be different when individual runs are considered rather than the entirety of all experiments. In contrast, the highest spread was observed for 40° and 600 rpm (19%).

Table 4-3: Calculation of microbial inactivation on particles which have been treated in the Revtech equipment. Table of (i) Mean log microbial reductions and (ii) Range of log reductions; difference between maximum and minimum, written as % (range/mean).

		Motor angle [°]					
		20		30		40	
		Mean [log]	Range [%]	Mean [log]	Range [%]	Mean [log]	Range [%]
Motor speed [rpm]	600	1.41	15.7	1.08	11.7	1.11	19
	660	-	-	1.08	10.6	-	-
	710	-	-	-	-	1.21	9.6
	723	-	-	-	-	0.89	14.6
	740	1.48	17.7	0.95	13.5	0.71	9

Future work is needed to improve the model by making the following changes:

i) More complex heat transfer models can be chosen; convection and steam condensation may be taken into account.

ii) Dynamic D-values depending on the water status at the surface of the particles may be included (Jeong et al., 2009).

The calculations serve to assess the impact of the variation in residence time on microbial inactivation. An arbitrary model organism was chosen and the model does not reflect the possible magnitude of microbial reduction achievable with the machine; for example the D-

value changes significantly when steam is added. The Revtech equipment has been validated for a number of applications with a kill of well over 5 log reductions of *Enterococcus faecium*. The narrower the residence time distribution, the smaller the variation in log reduction will be.

4.4 Residence time of flour

For all experiments, the particles travel through the vibrating system at a flow rate of 100 kg/h in a homogenous layer with a low bed depth. The flow does not take up the entire space of the pipe, but the particles only bounce a few millimetres high.

Note that the experiments were performed on a pilot plant device and the results do not directly apply to industrial machines.

4.4.1 Residence time distributions

This section investigates the residence time distributions of flour at motor angles of 20°, 30°, and 40° at a motor speed of 740 rpm. Figure 4-17 shows examples of collected data and fitted normal distributions. By means of Q-Q plots (probability plots, 'Q' stand for quantile) it was established that in all cases deviations from Normality are small (see Figure 4-17). For 30° and 40°, the normal distribution overestimates the proportion of short times in the end of the distribution and the measured data shows greater residence times than predicted.

Typical normal distributions are shown in Figure 4-16 standardised by dividing by the mean residence time. For 20° and 30°, the standard deviation is between 0.45% and 0.70% of the mean, whereas for 40° it is 0.70% - 0.99%. Thus, the residence time distributions are narrower at lower motor angles with respect to the mean. However, the absolute spread in seconds is smaller at 40° because the residence time is shorter.

The overall mean for the data of Figure 4-16 was calculated to be 548.9 s, 311.2 s, and 218.5 s for 20°, 30°, and 40°. The residence time decreases by approx. 43% (238 s) from 20° to 30°

and by approx. 30% (93 s) from 30° to 40°. As the residence time was observed to shift over time as analysed below, this data only serves as an indication rather than as being fully representative of the range of data possible at the particular condition.

In conclusion, a method was established to accurately measure the residence time distributions of flour in the Revtech equipment. The RTDs can be approximated by normal distributions. The residence time decreases considerably with increasing motor angle and the distribution is narrower and thus more precise for 20° and 30° in comparison to 40° with respect to the mean.

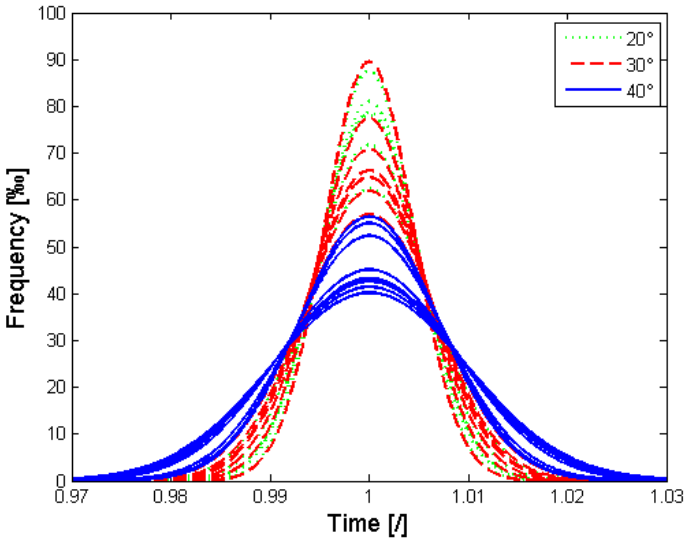

Figure 4-16: Approximated normal distributions of the residence time of flour passing through the Revtech at motor angles of 20°, 30°, and 40° at 740 rpm. Standardised by dividing by the mean residence time.

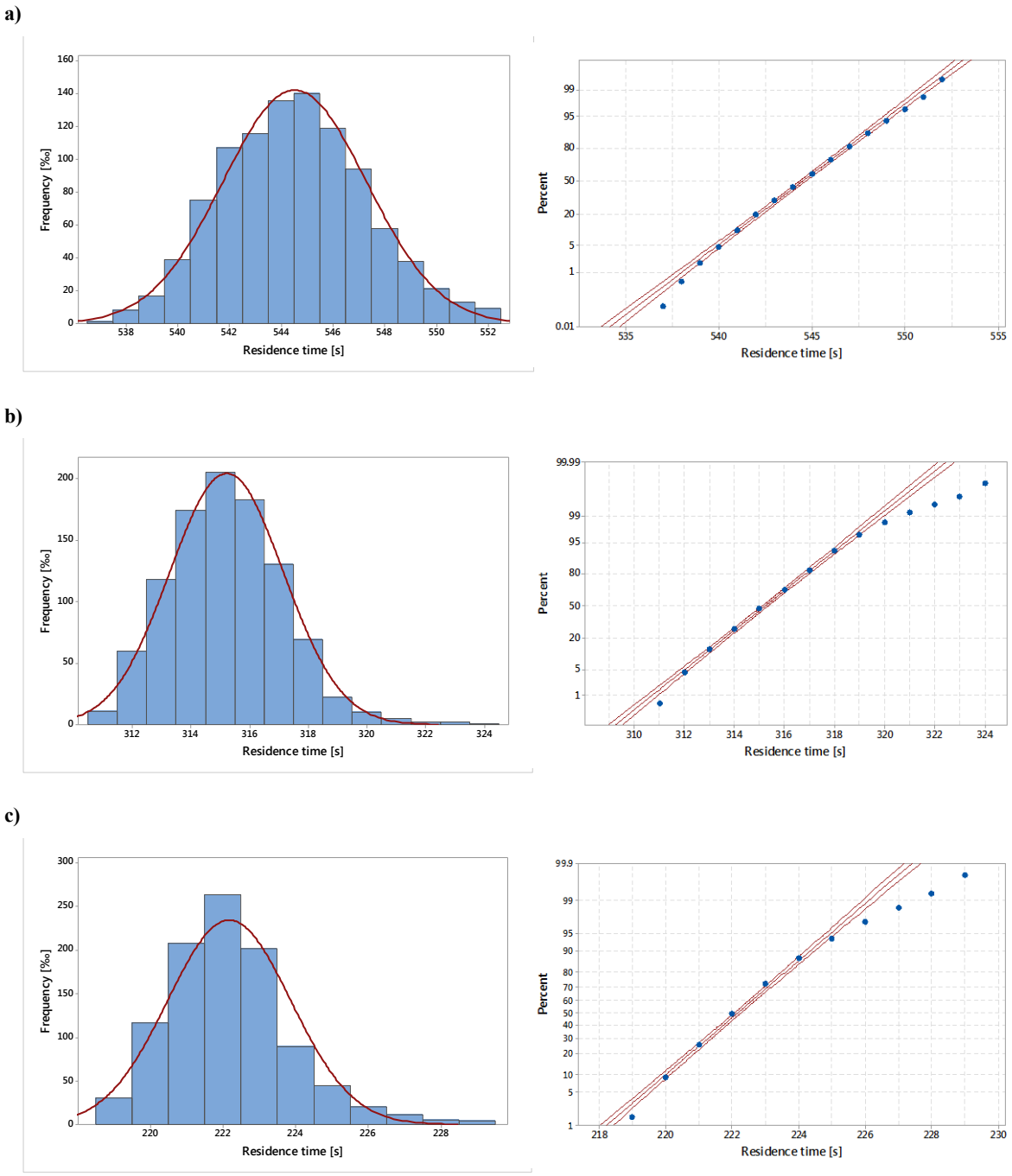

Figure 4-17: Typical measured residence time distributions of flour passing through the Revtech at a motor speed of 740 rpm in 1 s intervals and overlaid normal distributions. Probability plots with 95% confidence intervals. a) Motor angle: 20° b) Motor angle: 30° c) Motor angle: 40°.

4.4.2 Residence time dynamics

The residence time of flour was tested for motor angles of 20°, 30°, and 40° and motor speeds of 600 rpm and 740 rpm over a time period of ca. 3.5 h. Each experiment took approx. 1 hour. A marker sample was introduced to the product flow (100 kg/h) in intervals of 10 minutes and the shortest residence time, when the first marker particles appeared at the exit, was measured. Generally, between 3 and 4 experiments were performed per day and after each experiment, the flour was recirculated. Hence, the machine run-time is not continuous, but the cumulative run-length from the individual experiments per day is known. Before each day's experiments, the pipe was cleaned with a cleaning pig and water.

Figure 4-18 shows that at motor speed of 740 rpm, the residence time increases over the period of 3.5 h for all motor angles. The data can be approximated with first order polynomials and the gradients increase from 0.09 s/min and 0.08 s/min at 40° and 30° to 0.3 s/min at 20°. The initial level of the residence time increases from 200 s to 260 s to 445 s for motor angles of 40°, 30°, and 20°, respectively. Within 3.5 h, the residence time increases by 62 s, 17 s and 15 s (calculated from the 2 samples over 210 min) for motor angles of 20°, 30°, and 40°, which is an increase of 13.9%, 6.5%, and 7.7% of the initial value, respectively. Thus, changing the motor angles from 20° to 30° has a bigger effect on initial level and slope of the residence time than varying them from 30° to 40°.

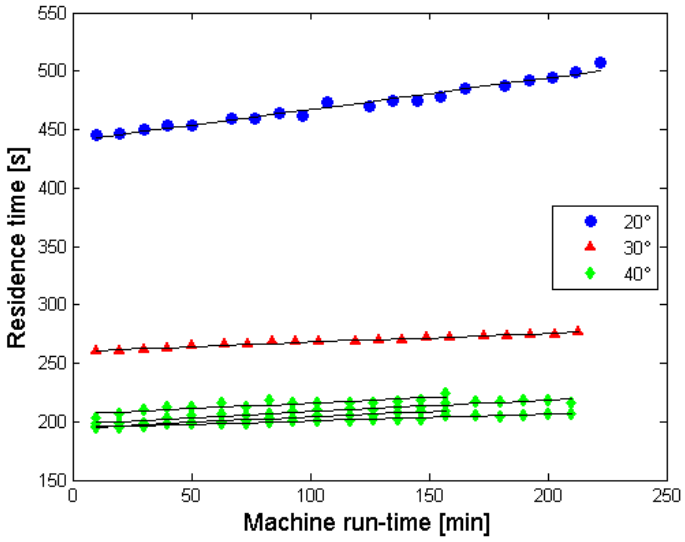

Figure 4-18: Residence time of flour passing through the Revtech at motor angles of 20°, 30°, and 40° and a motor speed of 740 rpm with fitted 1st order polynomials

At a motor speed of 600 rpm, results are more complex. At motor angles of 20°, the flour did not move up the spiral, but overflowed at the inlet. This demonstrates that as the acceleration at low motor angles is mainly vertical, the horizontal component of the acceleration can be insufficient to transport the flour. Figure 4-19a presents the residence time for motor angles of 30° and 40° at 600 rpm. In contrast to 740 rpm, the residence time does not increase constantly over time. At 30°, the shortest residence time decreases by 12 s over the timescale of the experiment whereas at 40°, the residence time decreases slightly at first before it increases again in the end changing by 4 s. In both cases, the data can be described accurately by second order polynomials. This suggests different residence time dynamics at 600 rpm from those at 740 rpm. However, similar to results at 740 rpm, the initial residence time decreases with increasing motor angle from 315 s at 30° to 250 s at 40°.

a)

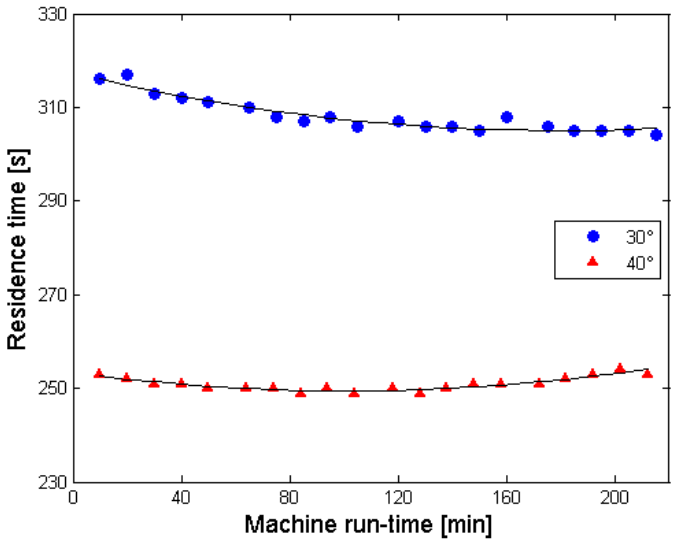

b)

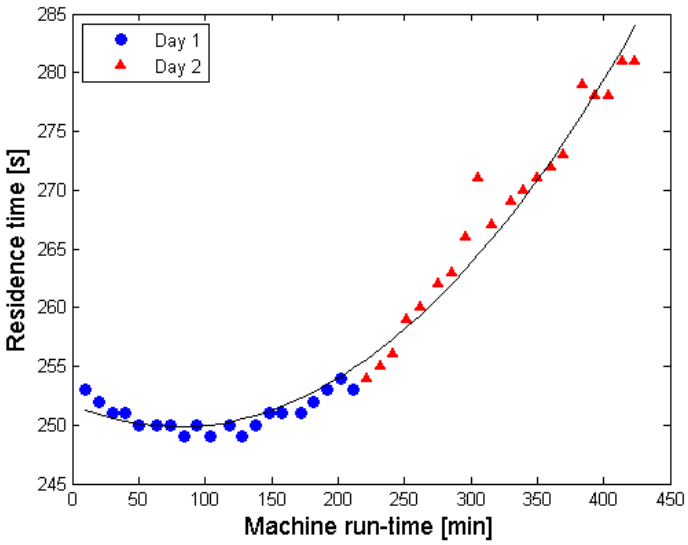

Figure 4-19: Residence time of flour passing through the Revtech at a) Motor angles of 30° and 40° and a motor speed of 600 rpm with fitted 2nd order polynomials. b) Motor angles of 40° and 600 rpm, showing (i) Day 1, starting with a clean pipe followed by (ii) Day 2, continuing without cleaning

When experiments at motor angles of 40° were continued for another 3.5 h on a second day (without cleaning the pipe), the residence time maintained its increase (see Figure 4-19b). The

residence time on the second day at 600 rpm shows an increasing trend, similar to the results at 740 rpm.

Figure 4-20 depicts the influence of the motor speed on the residence time at a motor angle of 30°. While the dynamics are different at 600 rpm and 740 rpm as explained above, the initial level of the residence time increases from 260 s at 740 rpm to 315 s at 600 rpm. The same was observed at 40° with residence times of 200 s and 253 s for 740 rpm and 600 rpm, respectively (data not shown). Hence, the residence time decreases with increasing motor angle and increasing motor speed. The dynamics are affected by the motor speed.

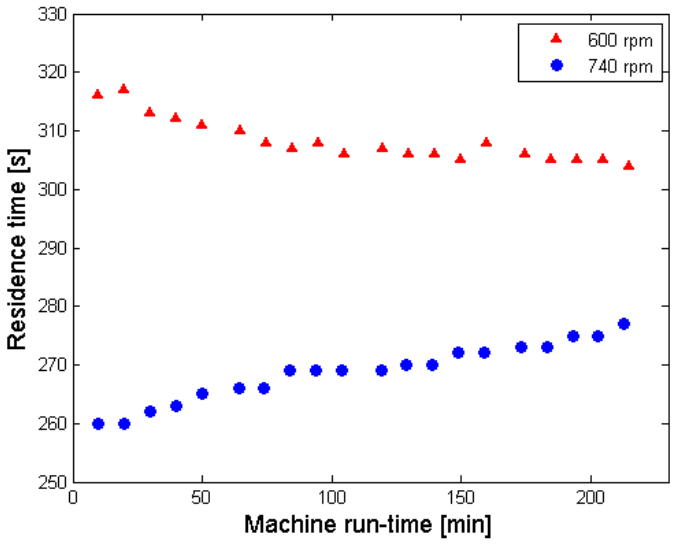

Figure 4-20: Residence time of flour passing through the Revtech at a motor angle of 30° and motor speeds of 600 rpm and 740 rpm

To demonstrate residence time dynamics, data from experiments run over 18 experimental days under the same conditions of 40° and 740 rpm is shown in Figure 4-21. In this case both clean and used pipes were used. In all cases the residence time increased over time with a

gradient of 0.07 ± 0.03 s/min. In addition Figure 4-21 shows that the initial residence time varies between 192 s and 228 s. The average increase over 3.5 h of cumulative machine run-time was 13.8 ± 5.0 s, equivalent to 6.6 ± 2.2 % of the initial value (calculated from the days with 20 samples). The overall spread of residence time (56 s) was between 192 s and 248 s, which represents 29% of the minimum and 23% of the maximum residence time. This spread is much larger than that observed in the individual distributions (i.e. standard deviation 2 s at 40°, see Figure 4-17c). It is necessary to identify the causes of this effect to accurately control and correctly operate the device.

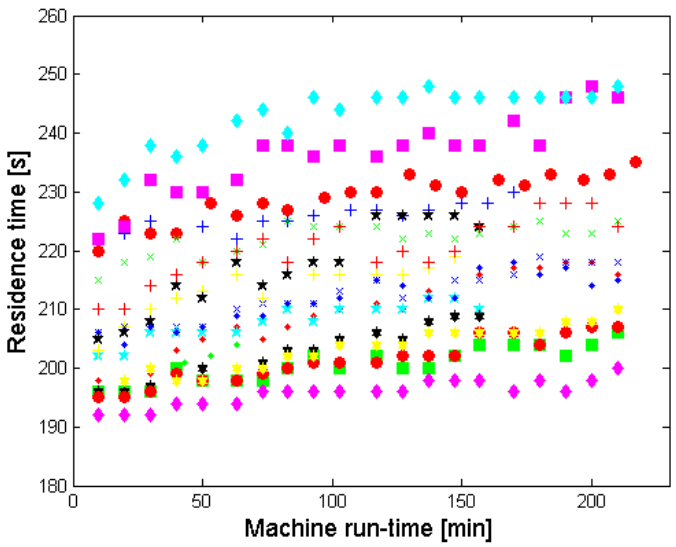

Figure 4-21: Results from 18 different experiments for the residence time of flour passing through the Revtech over time at motor angles of 40° and a motor speed of 740 rpm. Different markers relate to different experimental days.

From this data, three major questions arise:

i) What are the influences on the initial level of the residence time?

ii) What is responsible for the extent of the increase in residence time?

iii) Is there a plateau, where the residence time levels off?

Preliminary experiments showed no correlation between the residence time and ambient temperature. Potential influences related to the product, the machine, and environmental air humidity are discussed below.

4.4.3 Investigation of variation in residence time

4.4.3.1 Influence of particle size

Separation of the product in the hopper or the vibrating tube could affect the residence time during an experiment. As the flour is recirculated after each experiment, any change of particle size distribution throughout the day could affect the residence time, for example by deposition of fine particles in the pipe or their loss at the outlet of the pipe, where the product is collected.

Table 4-4 presents the 10^{th}, 50^{th}, and 90^{th} percentile of the particle size distribution of (i) the first flour sample of the day after 10 min of machine run-time and (ii) the last sample after 160 min. The p-values of an ANOVA between the samples are 0.03, 0.1, and 0.8 for x_{10}, x_{50}, and x_{90}, respectively. The results indicate no significant differences in particle size and that the particle size distribution remains constant throughout the day. Hence, product separation does not occur and does not cause the increase in residence time.

To assess the effect of different sized fractions on the residence time, the flour was sifted to a fine fraction (largely < 75 μm) and a coarse fraction (largely > 75 μm) (see Figure 4-22a). The results are shown in Figure 4-22b, which also shows the scattered data of Figure 4-21.

The fine fraction was more cohesive than the coarse fraction, whereas the coarse fraction was particularly dusty and free flowing. This might explain why the average residence time is greater for the fine fraction (191 s) compared to the coarse fraction (187 s).

a)

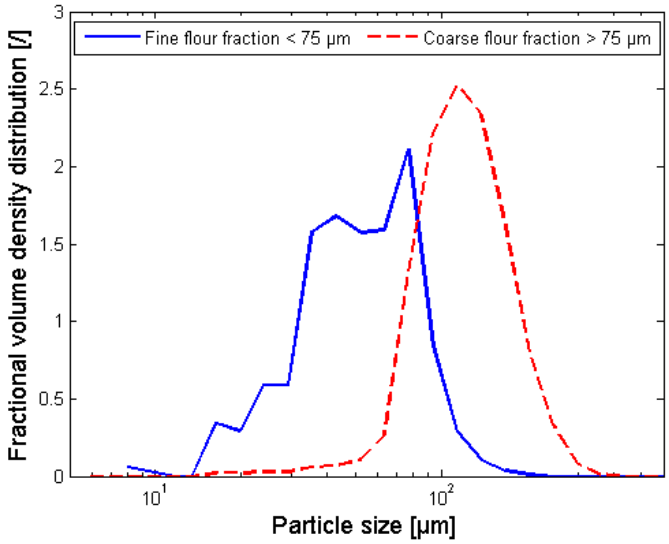

b)

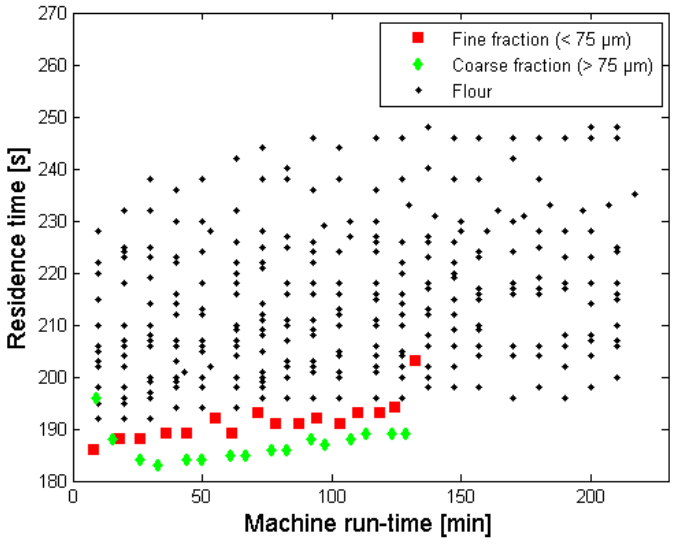

Figure 4-22: a) Particle size distribution of fine and coarse flour fractions after sieving (hole size 75 µm). b) Residence time of flour, fine flour fraction (< 75 µm), and coarse flour fraction (> 75 µm) passing through the Revtech at motor angles of 40° and a motor speed of 740 rpm.

Figure 4-22b shows that both fractions exhibit residence times below all data points measured for flour, apart from at the beginning and the end of the traces. The findings suggest it is not a particular size fraction that causes the observed phenomenon of increasing residence time. Yet, the results indicate complex interactions between particles of different sizes as the residence times of both size fractions are dissimilar to that of flour.

Table 4-4: Particle size distributions of flour passing through the Revtech after 10 min and 160 min of machine run-time

	Particle size		
Machine run-time [min]	x_{10} [µm]	x_{50} [µm]	x_{90} [µm]
10	32.70 ± 0.23	86.98 ± 0.76	171.53 ± 0.90
160	33.22 ± 0.13	88.00 ± 0.32	171.69 ± 0.67

4.4.3.2 Influence of water content of the product

Untreated flour

Changes in water content of the flour could affect cohesion properties or the coefficient of restitution between the flour and the vibrating tube. The moisture content was determined of 15 samples within 3 experiments of 1 day. The average moisture content of all samples was 12.12 ± 0.03 % (wet basis) and the data was randomly distributed. These findings show that the water content of the product is not responsible for the increase in residence time.

Dried flour

Flour was dried at a temperature setpoint of 120°C in the Revtech machine to a moisture content of 2.8%. The next day, the residence time of the dried flour was measured at ambient temperature and it was allowed to pick up ambient moisture. Figure 4-23 shows a linear increase in moisture content of the flour from 2.8% to 3.2% over a time period of approx. 3 h. The magnitude of the residence time is comparable with that of untreated flour (see Figure 4-21). In contrast to results of untreated flour, the residence time remains at a constant level for approx. 1 h before it follows a linearly increasing trend.

As discussed in section 4.3.4.1 and below, the build-up of a powder layer inside the pipe plays an important role for the residence time. It is possible that it takes longer for the dried flour to establish that layer, which could explain the initial lag phase and the delayed increase in residence time.

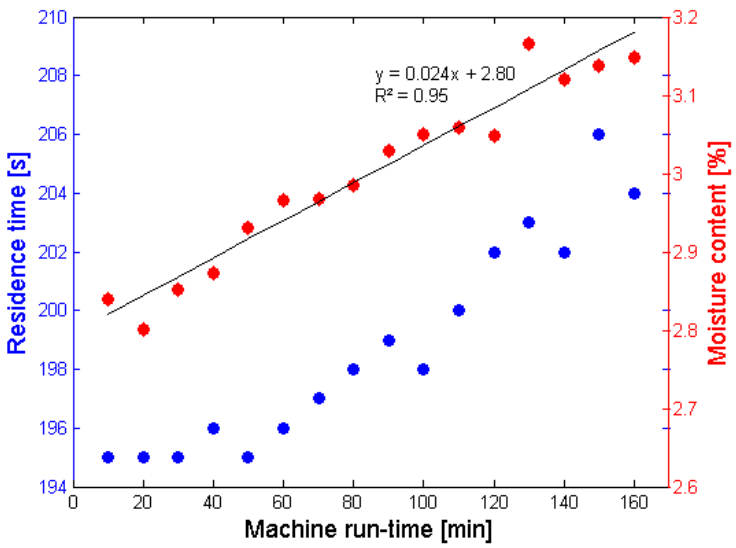

Figure 4-23: Residence time of dried flour passing through the Revtech at motor angles of 40° and a motor speed of 740 rpm and development of moisture content over time with approximated first order polynomial

4.4.3.3 Influence of air humidity

Figure 4-24 shows the relationship between flour residence time and relative humidity of the environment. There is no strong correlation (Spearman's Rho = -0.16), but there might be a trend. Reasons to reject a correlation include:

- At a relative humidity of 35%, all residence times between 190 s and 235 s could be achieved, and
- the data points around 70% relative humidity were collected on only one experimental day.

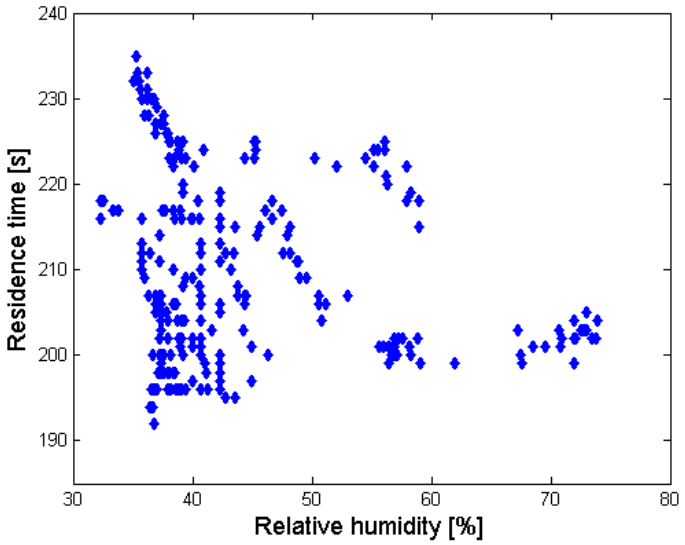

Figure 4-24: Correlation between residence time of flour passing through the Revtech and relative humidity of the environment

Figure 4-25 shows the correlation between the gradient of residence time of flour (calculated from the linear regression lines) and the average relative humidity of the environment. The correlation seems more distinct (Spearman's Rho = -0.59).

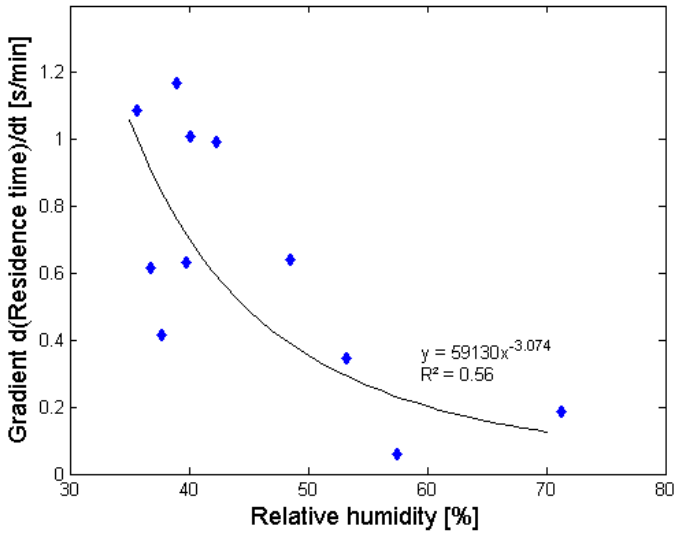

Figure 4-25: Correlation between the gradient of the residence time of flour passing through the Revtech and the relative humidity of the environment

The correlation between relative humidity in the air and the gradient of the residence time of flour is higher than for the absolute residence time. Air humidity might contribute to the trend in residence time development over time, but no clear conclusions can be drawn.

It is shown below in section 4.4.3.4 that air humidity affects dissipation of charge in the product. This could explain the potential correlation of air humidity and residence time during Revtech experiments. Charge effects might delay the flow due to attraction forces. The reason for the weak correlation might be the high moisture content of the flour (12.1%) that causes

very short dissipation times. The results suggest that many factors and interactions play a role in the phenomenon of increasing residence times.

4.4.3.4 Influence of static electricity

Lab-scale experiments

Lab-scale experiments have been performed to get a better understanding of electrostatic properties of flour. Figure 4-26 shows the charge dissipation of flours with different moisture content over time. The surface potential was measured and it shows the ability of charge to migrate through the flour. It takes longer for the surface voltage to decrease and the charge to dissipate with decreasing moisture content. This is due to water facilitating the migration of charges. Motion of the ions in the water will allow surplus charge to flow through the flour to the grounded surface. The initial magnitude of the surface charge was between 0.1 and 1.3 kV. The time it took for the surface voltage to decrease to 37% or 10% of its initial value could be approximated by exponential curves (R^2 = 0.98) for flour with increasing moisture contents between 0.9% and 7.9% (data not shown).

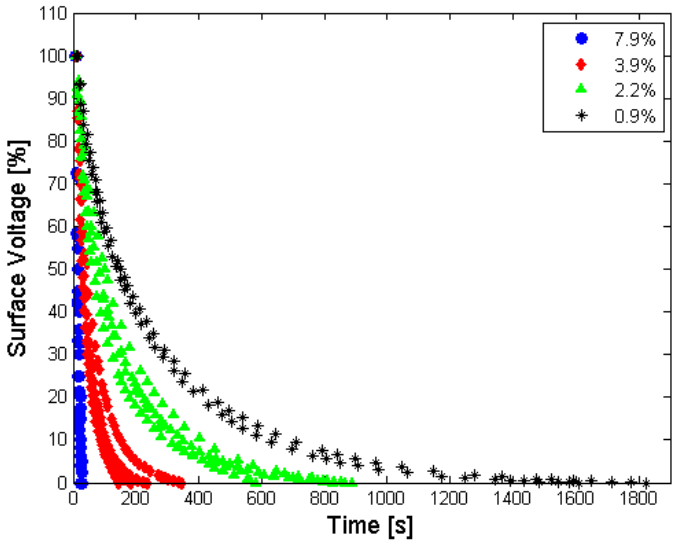

Figure 4-26: Surface voltage of flours with different moisture contents (0.9%, 2.2%, 3.9%, and 7.9%) over time

The influence of air humidity on charge dissipation was measured by monitoring the surface voltage of flour at 0.9% moisture content on different days with different relative humidities. The time after which the surface voltage decreased to 10% of its initial value was 350 s at a relative humidity of 55% and 670 s at 40%. The moisture in the air affects charge dissipation in flour because of adsorption by the flour particles. The results demonstrate the importance of air humidity in charge dissipation.

The local decay time constant is calculated as the decay time to 1/e or to 10% of the initial peak surface voltage. Figure 4-27 shows the variation of local decay time constant with time. In agreement with findings of Chubb and Walmsley (2010), it increases linearly with time. It can be used to predict decay times from short study times, which may be helpful in products with very slow charge decay times.

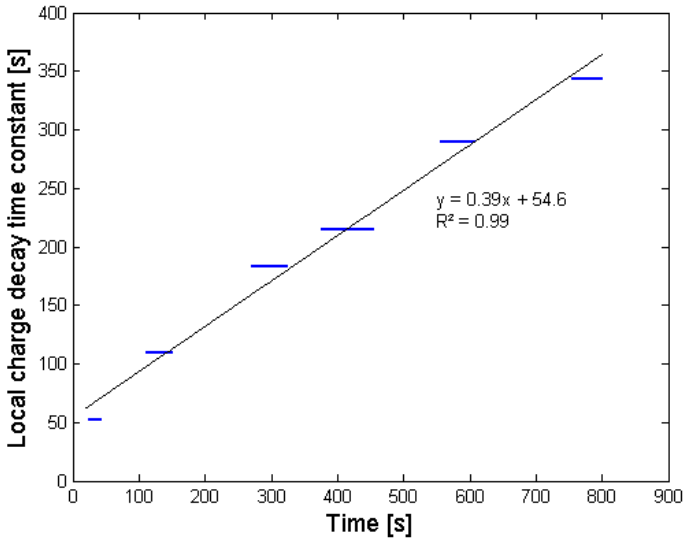

Figure 4-27: Variation of local decay time constant of flour with time with approximated first order polynomial

Revtech experiments

Charge effects are well known to cause problems in the flow of particles (Chubb, 2010). Interactions between flour and steel pipe may create static electricity. The flour might become charged over time. Alternatively, a thin layer of flour might deposit inside the pipe and become charged. The metal pipe cannot get charged as it has an electrical resistance of only 2.8 MΩ, which is easily overcome by the charge, and no change in the residence time was detected when the pipe was earthed.

Measurements of flour samples from the inlet of the pipe showed that the charge is close to zero (27 ± 23 pC/g) throughout the day (data not shown). In contrast, charge measurements of flour at the outlet of the spiral were 220 ± 160 pC/g (see Figure 4-29a). The findings prove that static charging of the material takes place in the pipe. However, no correlation could be established between residence time and outlet charge (Spearman's Rho = 0.033). No build-up

of static charge in the product may be observed because charging and discharging effects overlap.

Figure 4-29b shows the correlation between the gradient of the residence time of flour (calculated from the linear regression lines) and the outlet charge. A trend can be observed; it suggests that electrostatic charging plays a role in the increasing development of the residence time, but it is not the only factor causing the residence time to increase.

The outlet charge of the dried flour (see section 4.4.3.2) was 1297 ± 92 pC/g, which is significantly higher than for the untreated flour. This is to be expected as the mobility of charge is facilitated by water as explained above. However, the level of residence time was comparable. These findings do not support the theory that a high charge causes a larger increase in residence time.

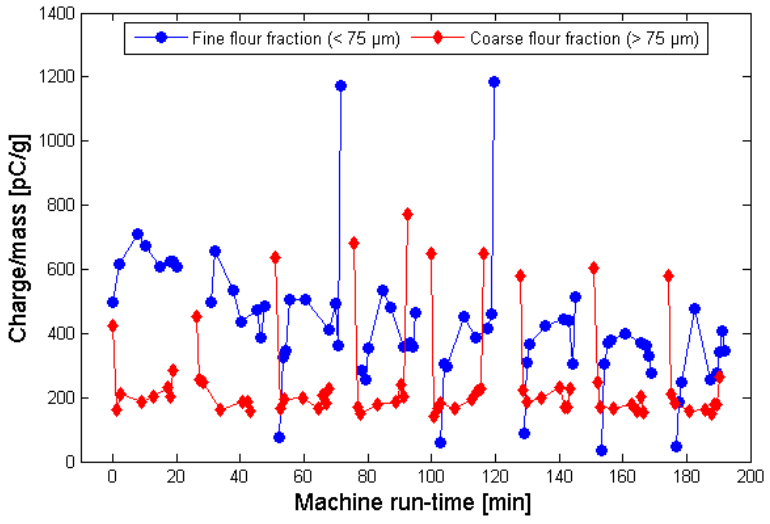

Figure 4-28: Charge development of fine and coarse flour fractions passing through the Revtech over time. Markers of samples within one experiment are connected.

a)

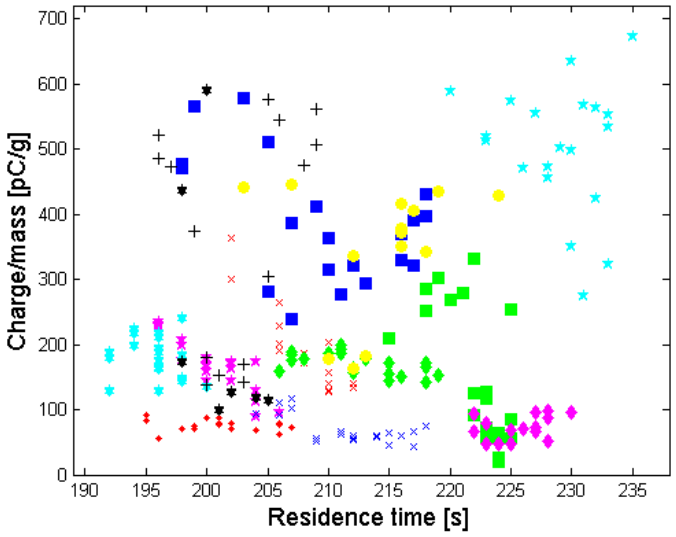

b)

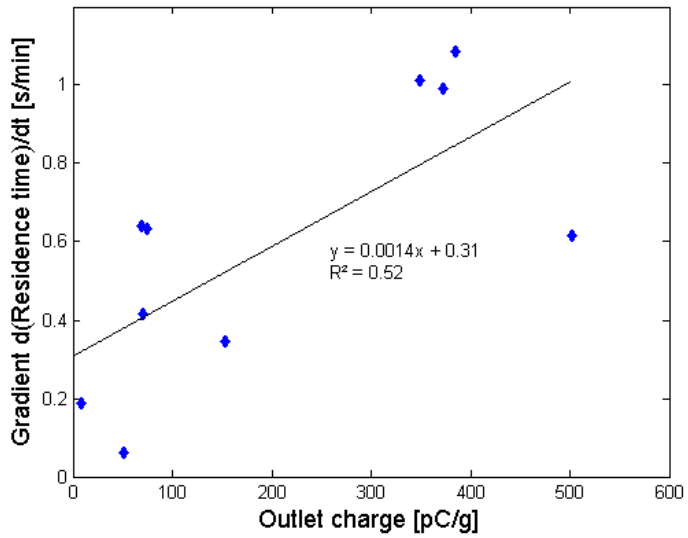

Figure 4-29: a) Charge of flour samples from the outlet of the flexible pipe of the Revtech in correlation with the measured residence time. Different markers relate to different experimental days. b) Correlation of outlet charge and the gradient of the residence time of flour passing through the Revtech with approximated first order polynomial.

Figure 4-28 illustrates the development of the outlet charge during the day for the fine flour fraction (< 75 µm) and the coarse flour fraction (> 75 µm) (see section 4.4.3.1). The results indicate that the fine fraction is generally higher charged than the coarse fraction, which can

be expected due to a larger surface area per unit mass where charge may be separated. It is worth noting that during each experiment, the charge progresses in u-shaped curves for the coarse fraction. This behaviour is approximately mirrored by the fine fraction. The first and the last particles of each experiment have more contact with the wall than the flow in between, which could play a role in this context. Furthermore, the overall charge is approximately constant during the day for the coarse fraction, whereas it decreases for the fine fraction. The reasons for this phenomenon are not clear.

4.4.3.5 Influence of recirculation of the product

Generally, the product is recirculated after each experiment (1 hour). This could cause errors in the results if the product is changed by the process in any way (e.g. particle size, electrostatic charge, etc.).

Figure 4-30 shows the residence time of 3 fresh batches of flour together with the experiments of Figure 4-21 where only one batch of flour was recirculated. The initial level of residence time of the first batch was measured at 203 s, which is amongst the control data (192 - 228 s). The residence time of all three flour batches can be approximated by a first order polynomial. The slope of the first order polynomial is 0.1 s/min, which is comparable to the control data (0.07 ± 0.03 s/min).

This in combination with findings about particle size, water content, and charge suggests that alterations of the material do not cause the shift in residence time.

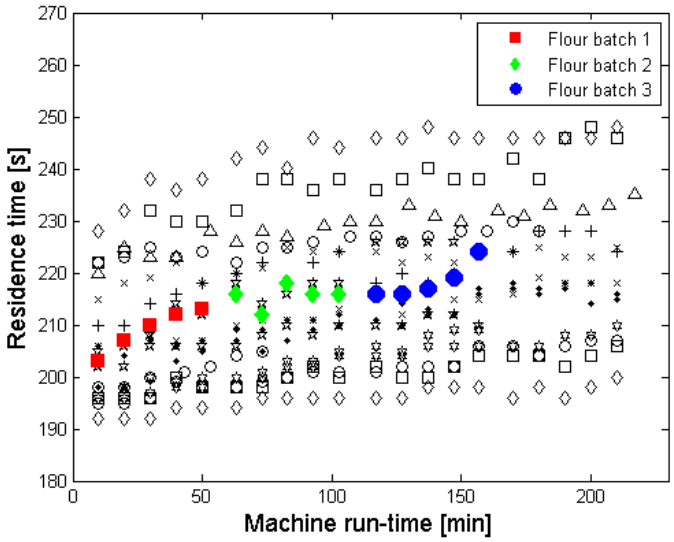

Figure 4-30: Residence time of 3 fresh flour batches passing through the Revtech in comparison to recirculated flour at motor angles of 40° and a motor speed of 740 rpm. Different marker symbols in black relate to different experimental days.

4.4.3.6 Influence of the cleanliness of the pipe

Deposition of product in the pipe might either obstruct the product flow or become electrostatically charged. To investigate this matter, 3 different cleaning methods were applied to the pipe and the residence time of flour was measured:

i) Cleaning with a cleaning pig and compressed air

ii) Cleaning with a cleaning pig and water

iii) Cleaning with a cleaning pig, water, and hand dishwashing liquid

A dirty pipe is defined as one that has been used for flour and has not been cleaned before new experiments started.

First, the pipe was cleaned with a cleaning pig and compressed air after each 1 hour experiment (3 times per day). This did not affect either the initial level of the residence time

or the extent of the increase during the day (data not shown). Hence, flour accumulations as physical obstructions can be excluded to be the cause for the shift in residence time.

Second, Figure 4-31 presents the residence times of flour for the pipe cleaned with a cleaning pig and water compared to a dirty pipe. Using a clean pipe reduces the initial level of the residence time, but to various extents as the starting points are not identical. The gradient of the increase in residence time was determined to be 0.09 ± 0.02 s/min for the clean pipe (4 data sets) and 0.07 ± 0.03 s/min for the dirty pipe (14 data sets). Analysis of variance indicates no differences between both conditions ($p = 0.29$). The results show that cleaning with water has a more significant effect on the initial residence time than cleaning with air.

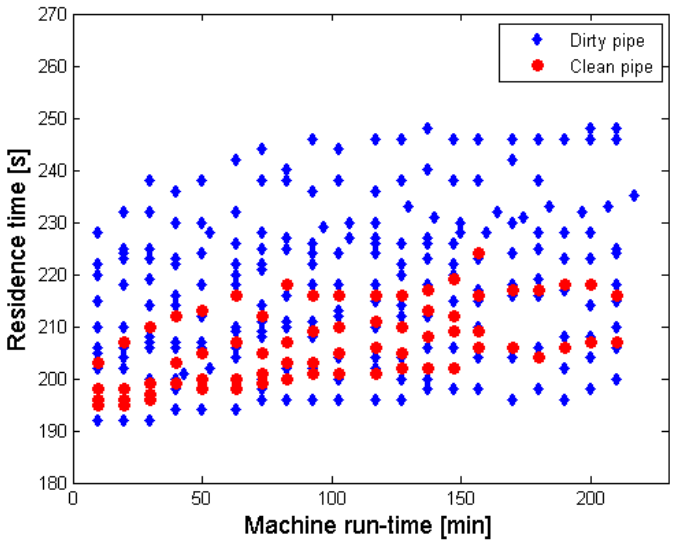

Figure 4-31: Residence time of flour passing through the Revtech at motor angles of 40° and a motor speed of 740 rpm using a clean and a dirty pipe

A line or deposit axially along the pipe could be seen in the pipe after flour had passed through (see Figure 4-32). This supports the theory of the build-up of a thin, but visible flour

layer. This line is not observable after cleaning, but flour particles could still be adhering to the pipe wall. It may be that minor deposits of particles resulting from differences in cleaning effect might account for dissimilar initial levels of the residence time.

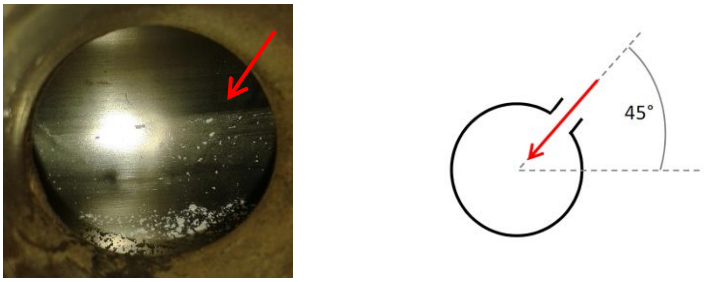

Figure 4-32: Left: Picture of a flour layer inside the Revtech pipe after flour has been passing through. Right: Schematic of the cross section of the pipe to clarify the perspective

Third, the pipe was cleaned with a hand dishwashing liquid, water, and a cleaning pig to ensure that all particles were removed. The results were similar to those obtained by cleaning with water only (data not shown). The slope of the increase in residence time was equivalent. This suggests that either the adhesion of fine particles in the pipe is not the problem or the chosen method is inappropriate to remove the remaining particles.

4.4.3.7 Machine performance

The motors or other parts of the machine might warm up over time, which can potentially affect the vibrational frequency or deflection. This in turn could impact on the development of the residence time over the course of the day.

Tests were carried out in which the machine was run without product for 2 hours before product flow was started. Results were compared to those where the machine was run with product from the beginning. The underlying hypothesis is that if the warming up of the machine is responsible for the increase in residence time, it would be expected to start at a higher initial residence time.

The results are presented in Figure 4-33, and show that the residence time started at a lower level after the machine ran idle for 2 h in comparison to the control run on the previous day. In agreement with observations in section 4.3.4.2, the findings suggest that the warming up of the machine does not cause the residence time to increase.

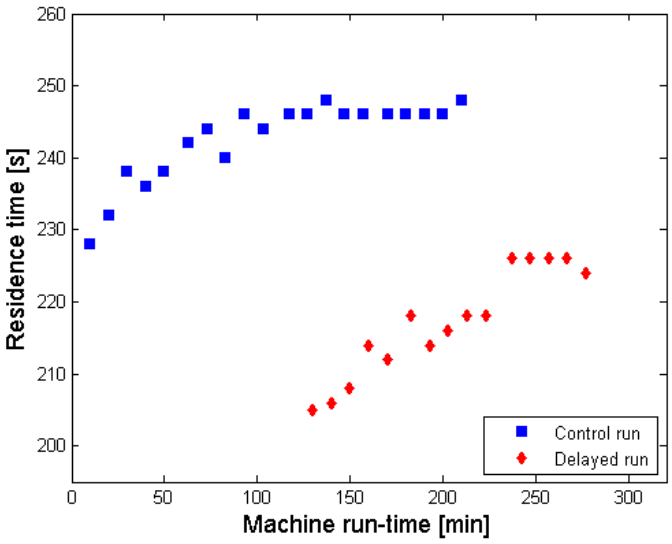

Figure 4-33: Residence time of flour passing through the Revtech at motor angles of 40° and a motor speed of 740 rpm. (i) control run where machine and product flow were started at the same time and (ii) delayed run where the machine was run for 2 hours without product before the product flow.

4.4.3.8 Extended run-length experiments

Figure 4-34 shows the development of the residence time of flour over 4 consecutive experimental days and a further day of measurements after a weekend. No cleaning was applied. It is evident that the residence time increases continuously over the first four days. This can be approximated with a second order polynomial (R^2 = 0.97). The slope decreases over the last 2 of the 4 consecutive days. After the 2-days break, the residence time drops visibly and the subsequent increase over the course of the day is comparable with the first day of the experimental data set.

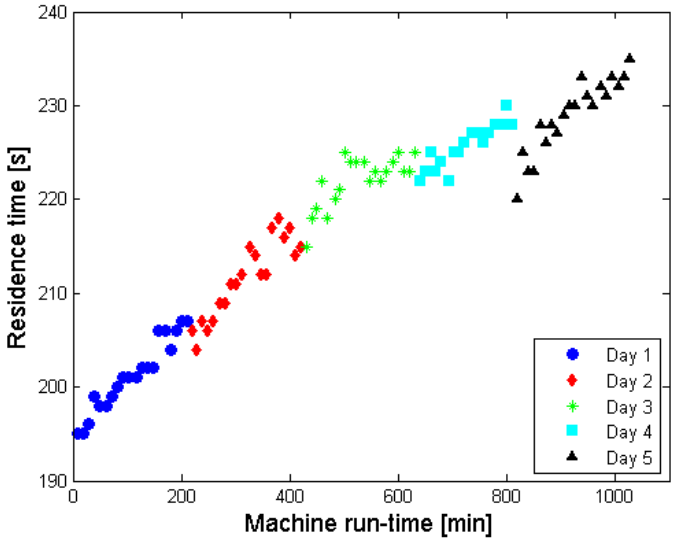

Figure 4-34: Residence time of flour passing through the Revtech at motor angles of 40° and a motor speed of 740 rpm over a time period of 5 experimental days

No constant value of the residence time was found. If the residence time increase is due to built-up of a thin flour layer inside the pipe, it would be expected to reach a saturation

thickness at which the residence time levels off. Thus, the phenomenon appears more complex than a simple correlation between the residence time and the thickness of the layer on the inside of the pipe.

4.5 Conclusions

The residence time of flour and grains passing through the Revtech system was characterised in both single experiments and over the period of multiple experiments. Both process parameters motor speed and motor angle had a significant impact on magnitude and development of residence time.

Methods were established to accurately determine residence time distributions of flour particles and grains. The RTDs can be approximated by normal distributions in both cases.

Effect of motor speed

The motor speed greatly affected the behaviour of the residence time of flour over time. At 740 rpm, the residence time of flour increased linearly at all motor angles, whereas at 600 rpm, the residence time decreased at first, before an increase was observed and a second order polynomial was approximated. The level of residence time was typically higher at lower motor speeds.

For grains, the motor speed affected the dynamics of the system rather than the magnitude of the residence time at 20° and 30°, whereas at 40° it influenced the mean and standard deviation to a much bigger extent. At least one motor speed was found for each motor angle at which the residence time was constant over the entire timescale of the experiment. Additionally, it was observed at angles of 40° that the variability between experiments was higher at low motor speeds.

Effect of motor angle

The motor angle had a significant impact on the magnitude of residence time of flour and grains. The residence time decreased considerably with increasing motor angle from 406 s to 261 s to 195 s for grains and from 445 s to 260 s to 200 s for flour at motor angles of 20°, 30°, and 40° at a motor speed of 740 rpm.

The motor angle also showed an effect on the accuracy of the treatment. RTDs were narrower and thus more precise for motor angles of 20° and 30° in comparison to 40° (with respect to the mean) for flour. The opposite was observed for grains, for which the process was more precise at larger motor angles. The standard deviation of the individual data sets and therefore the dispersion of the grains during one experiment decreased with increasing motor angle. The width of the RTDs is a critical factor for the accuracy of a thermal process.

Residence time dynamics

Generally, the residence time increased during the course of one day. At motor angles of 40°, the residence time of grains increased by 0.05 - 0.11 s/min and it increased by 0.07 ± 0.03 s/min for flour. The increase in residence time of flour decreases with increasing motor angle. In contrast, the data for grains suggests that the increase of the residence time at motor angles of 20° and 30° is negligible, whereas it is much more significant at 40°. The change is difficult to detect by measuring flow rate; holdup changes by less than a kg over several hours. Several hypotheses concerning the product, the machine, and the environment were tested regarding the cause for this phenomenon. Two factors were found to have a significant effect on the residence time:

i) Deposition of a powder layer inside the pipe as indicated by:
   - A wet cleaning procedure reduced the residence time of grains and flour.
   - A dry cleaning procedure of the pipe did not show any effect in case of flour particles. The results suggested that only few particles or a fine layer adhering to the pipe wall was sufficient for the increase in residence time.

ii) Alteration of the layer's properties over extended periods of time as indicated by:
   - The residence time of grains started on a lower level on a second experimental day than where it ended on the previous day indicating that the residence time cannot only be related to the thickness of the deposited powder layer.
   - Electrostatic charging of flour was proven to take place.
   - The residence time of flour increased over four consecutive days. After a 2 days break, it started on a lower level.

The results show that the formation of a powder layer on the inside of the pipe plays a significant role for the residence time of particles, but the residence time cannot simply be related to the thickness of the layer.

In addition, it was disproved that changes in the bulk material passing through the spiral were the cause for the increase in residence time. It is therefore sensible to assume the reason for the increase in residence time is within the pipe. The mechanical performance of the machine was shown to be constant over time. No correlation could be found between ambient temperature and residence time, but a possible correlation was found between the gradient of the increase in residence time of flour and relative air humidity. As air humidity is closely interlinked with electrostatic charging, this is a further indicator for electrostatic charging

being an important factor. It is likely that electrostatic charging is relevant to the average time particles spend in transit.

Overall, whichever process causes the residence time to increase during the day is reversible by cleaning the pipe or by idle time.

A simple model for pasteurisation of particles has been developed that characterises the impact of the variation in residence time on microbial inactivation in the Revtech device. Across all tested processing conditions for grains, the variation between minimal and maximal log reduction was between 9% and 19%. In this way, precise treatments can be identified.

More work is needed to identify the cause for the drift in residence time and to predict the residence time over periods of extended operation. The data does suggest that cleaning reduces the overall effect, and that frequent cleaning can allow relatively uniform behaviour. In practice, tests need to be done to confirm the residence time and ensure process uniformity.

5 Heat treatment of flour in the Revtech

5.1 Introduction

The effects of heat treatment on flour depend on treatment time and temperature. The impact of treatment on flour functionality under accurately controlled lab-scale conditions was investigated in chapter 3. In chapter 4, the development of the residence time of flour in the Revtech equipment was characterised in detail at ambient conditions.

The overall goal of this work is to implement the heat treatment of flour on the Revtech system to produce high ratio cake flour. For this purpose, this chapter describes the integrated effects of residence times and temperature treatment of flour in the Revtech. Temperature profiles of the pipe wall, the flour, and the air were characterised and flour residence times at elevated temperature were measured. The product is evaluated both in terms of functionality (RVA peak viscosity) and its performance in high ratio cakes. The results after flour treatment in the pilot plant equipment are compared to lab-scale experiments (see chapter 3). The hypothesis is that constant time-temperature data at lab-scale can be extended to variable time-temperature data at pilot scale. In addition, the relevance of the findings to industry is presented; an approach is shown both towards the development of a cake flour specification and the facilitation of process validation.

5.2 Materials and methods

5.2.1 Materials

Commercially available soft wheat flour (flour III, see chapter 3) was used for lab-scale experiments and experiments in the Revtech. It had a protein content of 7.8%, a moisture content of 14.2% and a Hagberg falling number of 235 s. Flour III was generously provided by Heygates Ltd. (Northampton, UK). The particle size distribution is shown in Figure 5-1. The flour was stored at -20°C in 20 kg paper bags to limit functional changes over time. It was unfrozen over night at ambient temperature for experiments.

Commercially available high ratio cake flour (protein content 8.6%, moisture content 12.1%, see chapter 4) was used for the measurement of residence time in the Revtech at elevated temperature without extraction. The particle size distribution is shown in Figure 5-1.

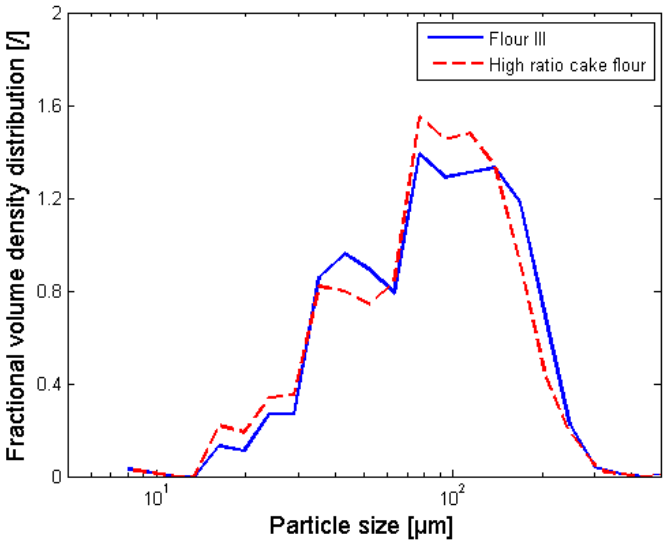

Figure 5-1: Particle size distributions of flour III and commercially available high ratio cake flour

It should be noted that finer flour (i.e. flour II of chapter 3) was found not to flow continuously through the Revtech equipment at elevated temperature, but discontinuities of up to 30 s were observed in the outlet flow.

5.2.2 Heat treatment of flour in the Revtech

The Revtech system is described in detail in chapter 2; hopper, heating spiral, and extraction were used for the experiments here (see section 4.2.2). Using conditions of 40°, 740 rpm, and 95% off balance motor setting, flour III passed continuously through the equipment at a flow rate of 100 kg/h. The temperature setpoints of the pipe were 110°C, 130°C, 150°C, and 170°C comparable to the conditions in lab-scale experiments (see chapter 3). A clean pipe was used for all experiments (cleaned with cleaning pig and water).

The empty pipe was heated up to the setpoint temperature before a flour flow of 100 kg/h was started. After the temperature in the pipe had stabilised, the product flow from the hopper was stopped and the plastic pipe at the outlet of the spiral (see Figure 5-2a) was reconnected to the inlet piece of the spiral. Longer treatment times could be achieved using this recirculation method.

To remove the moisture that migrated from the flour during heat treatment, the atmosphere inside the pipe was extracted via the top 6 extraction ports (1 in each loop) located 10.5 - 31 m in axial direction from the inlet. An underpressure of -20 mmH_2O was applied at the extraction manifold (see Figure 5-2b).

a) b)

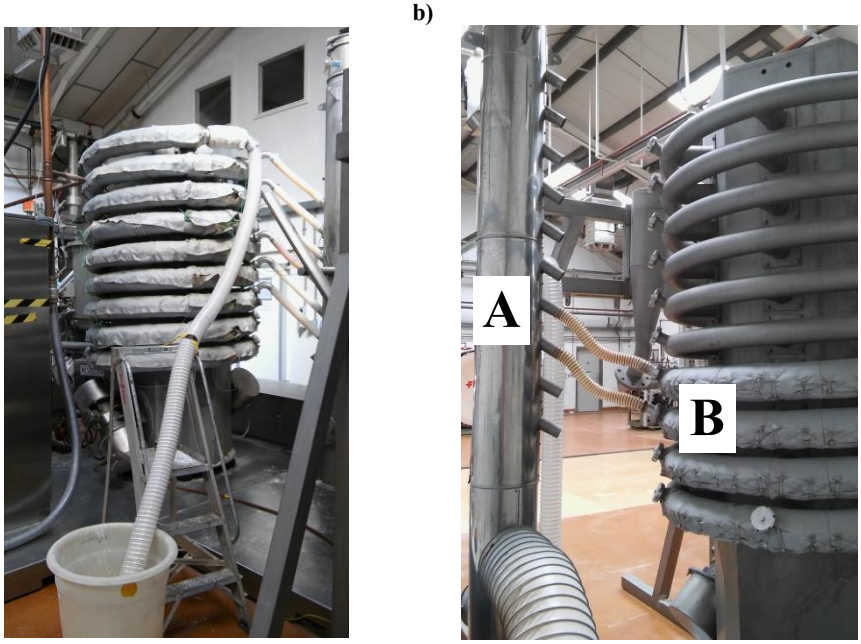

Figure 5-2: a) Experimental setup of the Revtech heating spiral with flexible recirculation pipe. b) Extraction ports (B) in the heating spiral and connection to extraction manifold (A).

5.2.2.1 Residence time measurements

During the heat treatment of flour in the Revtech equipment, the residence time was measured with a coloured marker, in the same way as described in chapter 4. The residence time was measured for 20 - 30 min during stable operation to monitor the development with time.

5.2.2.2 Sample taking

Heat treated flour samples were taken after several cycles of recirculation through the Revtech. Figure 5-3 shows the sequence of taking samples of flour that had been through the Revtech once, twice, and three times and that exhibited constant residence time of 2:00 - 2:15 min. The zero of time is an arbitrary one taken during the phase of stable operation:

i) The clock was started after 20 - 30 min of stable operation and the first sample was taken after 1 pass through the spiral.

ii) At a specific time (here 2:10 min), the product flow from the hopper was stopped and the recirculation pipe was connected from the outlet of the heating pipe to the inlet to allow multiple passes of flour through the system.

iii) The spread of residence time of the device had to be taken into account for subsequent sample taking. A minimum time and a maximum time for the first particles to exit the pipe was established for all cycles.

iv) Here, the first particles of the 2nd cycle exit the pipe between 4:10 min and 4:25 min, because the residence time was measured to be 2:00 - 2:15 min. The first particles of the 3rd cycle exit the pipe between 6:10 min and 6:40 min. Therefore, the sample treated for 2 cycles of recirculation had to be taken after 4:25 min and before the 3rd cycle starts at 6:10 min.

v) This was repeated for samples treated for various numbers of cycles of recirculation.

This principle was used for constant residence times at temperature setpoints of 110°C and 130°C. At temperature setpoints of 150°C and 170°C, the residence time was not constant with time (see section 5.6.1). The sample taking method was modified to include the linearly increasing residence time, but the principle remained the same: the minimum and maximum time was calculated for the first particles of each cycle to exit the pipe and the sample was taken after the maximum time of one cycle and the minimum time of the next cycle.

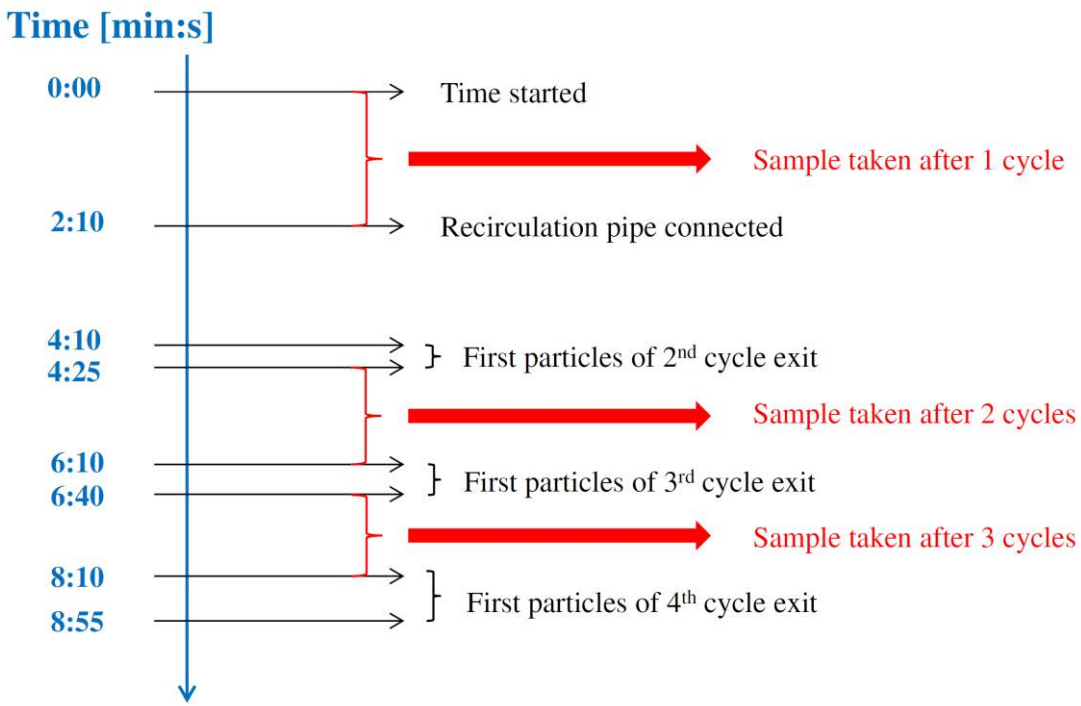

Figure 5-3: Method of sample taking during flour heat treatment in the Revtech after a certain number of recirculation cycles for flour with a constant residence time of 2:00 - 2:15 min.

Table 5-1 shows the time of sample taking, the number of recirculation cycles, and the average residence time for each temperature setpoint. All samples were taken after 20 - 30 min of stable operation. For each sample, approx. 250 g of flour was collected in plastic bags for approx. 10 - 15 s. After all samples were taken, they were cooled down to ambient temperature by shaking the plastic bags inside a walk-in refrigerator at 6°C for a few minutes. The heat treated samples were used to measure RVA peak viscosity in water and 50% sucrose solution and to bake high ratio cakes (see below).

Table 5-1: Time of sample taking, number of recirculation cycles and residence time a flour sample has received during heat treatment in the Revtech for different temperature setpoints.

Temperature setpoint[°C]	Sample taking time [min:s]	Cycles	Residence time [min]
110	2:10	1	2.2
	7:15	3	6.5
	13:00	5	10.8
130	2:10	1	2.2
	7:15	3	6.5
	7:15	3	6.5
	10:30	4	8.6
	11:30	5	10.8
150	2:10	1	2.2
	3:10	1	3.2
	7:45	3	6.7
	11:00	3	9.8
	17:50	5	16.7
	13:15	5	11.1
170	3:00	1	3.1
	7:15	2	6.2
	11:00	3	9.4
	17:00	5	15.9

5.2.3 Analysis for flour and cake quality

5.2.3.1 Rapid-Visco-Analyser (RVA) tests

Starch-pasting behaviour of heat treated flour was studied in the Rapid-Visco-Analyser (RVA 4500, Perten Instruments (Hägersten, Sweden)) in two different liquids: i) deionised water and ii) 50% w/w sucrose solution. The method is described in chapter 3.

5.2.3.2 Cake baking

Table 5-2 shows the high ratio cake formulation used in this work. 200 g flour at 14% moisture content was used as a reference. The recipe was adjusted depending on the moisture content of the flour in that water was added directly to the recipe. All liquids were placed into a Hobart bowl followed by the dry ingredients, fat, and paste emulsifier. The ingredients were mixed on speed 1 for 30 s. Subsequently, the batter sticking to the wall of the bowl was scraped down. Mixing was continued on speed 2 for 1 min and the batter was scraped down again. Finally, the batter was mixed on speed 3 for 4 min. The mixing time was set to be constant for all samples. Optimum mixing times might vary. The batter density was measured by filling a 100 ml cup with cake batter and measuring the mass. 300 g of batter were deposited into paper cases in 400 g rectangular bread tins. The cakes were baked in a deck oven (bottom heat level 3, top heat level 6) at 180°C for 40 min. Two cakes were baked per flour sample. The cake volume was measured the following day.

Table 5-2: High ratio yellow cake recipe (Campden BRI, 2012)

Ingredients	% on total flour weight
Flour (14% moisture)	100
Fat	58
Paste emulsifier	2
Caster sugar	115
Baking powder	3.75
Skimmed milk powder	7
Salt	1
Water	55
Glycerine	8
Liquid whole egg	80

5.2.3.3 Cake volume measurement

The cake volume was measured one day after the cake was baked to allow a stable structure to develop. It was measured with the BVM-L 370 Bread Volume Analyser (Perten Instruments (Hägersten, Sweden)). The instrument works on the principle of laser detection of the bread or cake shape. The sample was placed on a rotating stand and a laser travels around it. The cake weight is entered manually into a software, which calculates various parameters such as cake volume, dimensions, and cake density. The method is described in detail by Campden BRI (2015).

5.3 Temperature profile of the pipe wall in the heating spiral

The temperature profiles of the pipe wall in the heating spiral of the Revtech system during the heat treatment of flour were characterised for temperature setpoints of 110°C, 130°C, 150°C, and 170°C. As the steel pipe is heated via resistive heating and the pipe represents an open system, the temperature is not constant over the total length of the pipe. The temperature is controlled by adjusting the heating power that is delivered to the pipe between 0% (no heating) and 100% (maximal heating power), which is characterised by the output value. The temperature is controlled so that at least one of the 8 temperature probes is held at the temperature setpoint, whereas the temperature of the other probes depends on product flow rate, thermal properties of the product, and the injection and extraction of steam.

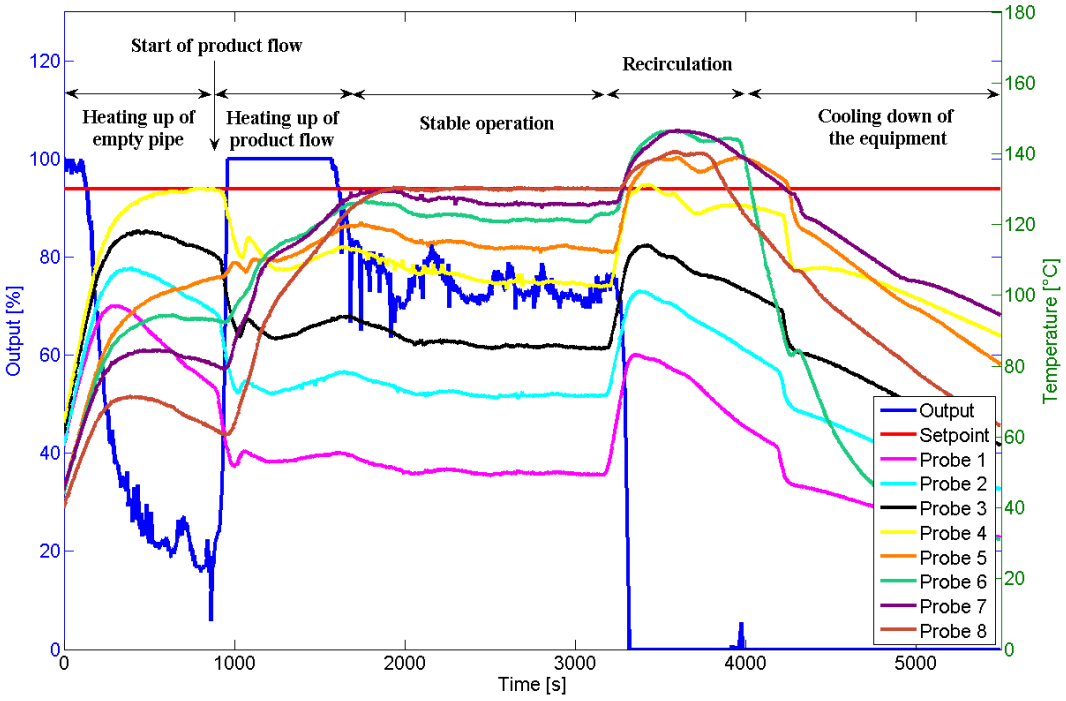

Figure 5-4: Heating power (output) and temperature profiles of built-in temperature probes located in axial direction of the Revtech heating spiral during the heat treatment of flour (100 kg/h). Temperature setpoint: 130°C. Probe 1 is located at the base of the spiral, probe 8 is located at the top.

Figure 5-4 shows a representative example of the temperature development of the pipe wall of the Revtech spiral during heat treatment (setpoint 130°C) of flour during continuous operation and recirculation as measured by built-in temperature probes. It includes the following stages:

i) Heating up of the empty pipe

0 - 900 s: The empty pipe is heated up until one probe reaches the setpoint temperature. The heating power (output) is controlled, so that the setpoint is not exceeded. In this case, probe 4 reaches the setpoint of 130°C.

ii) Start of product flow

900 s: The flour flow is started (100 kg/h), cooling down the pipe marked by a sharp decrease in temperature of the first four probes. The system reacts by increasing the heating power to 100%, when the hottest temperature probe (in this case Probe 4) starts to cool down.

iii) Heating up of the product flow

900 - 1700 s: The heating power remains at 100% and the temperature increases until one probe reaches the setpoint. In this case it is probe 8. This time period is taken as stabilisation time. The stabilisation time increases linearly with increasing temperature setpoint, which is shown in Figure 5-5.

iv) Stable operation

1700 - 3200 s: Temperatures and output value stabilise.

v) Start of recirculation

3200 s: The hopper feed is stopped and the recirculation pipe at the outlet of the heating spiral is connected to the inlet.

vi) Recirculation

3200 - 4000 s: The product recirculates within the spiral. The output value decreases to 0. The temperature increases quickly and exceeds the setpoint. Figure 5-6 shows the overshoot of the hottest probe for all setpoints. At setpoints of 110°C and 130°C, probe 6 (in the 6^{th} loop of the spiral) was the hottest. At setpoints of 150°C and 170°C, probe 7 was the hottest. The maximal overshoot is 11.9 - 16.3°C across all temperature setpoints. The reason for this is a relatively slow reaction of the proportional-integral-derivative (PID) controller. As the

temperature of the flour is higher during recirculation, less heat is being transferred from the pipe to the flour and the system heats up.

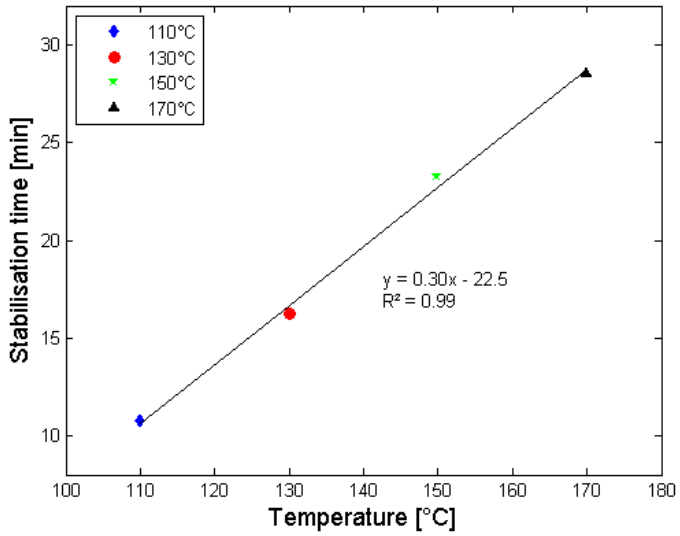

Figure 5-5: Stabilisation times of the pipe wall temperature during flour treatment (100 kg/h) in the Revtech at different temperature setpoints with best-fit line

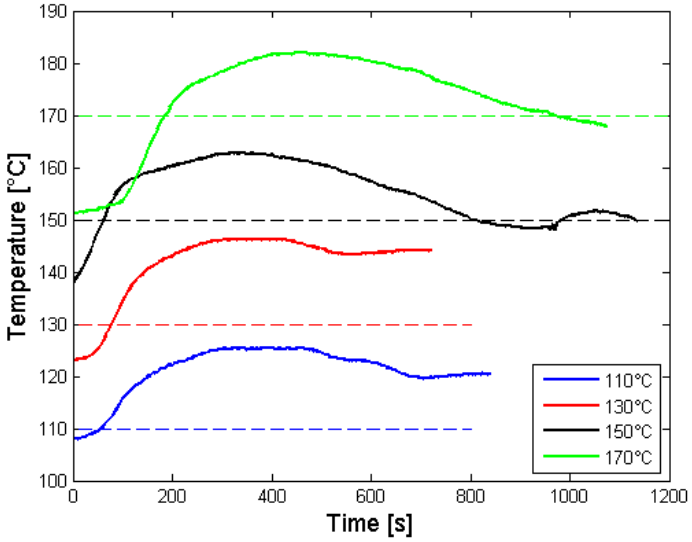

Figure 5-6: Temperature overshoot of the hottest temperature probe during flour recirculation (100 kg/h) in the Revtech system. Dashed lines mark temperature setpoints.

Figure 5-7 shows temperature profiles of the pipe wall in axial direction for setpoints of 110°C, 130°C, 150°C, and 170°C as measured by built-in probes during stable phases of operation. Second order polynomials can be fitted. Temperatures were measured over a time period of 1000 - 1500 s and the standard deviation was 0.2 - 1.8°C for all probes at all setpoints. Hence, the temperature is controlled accurately in the pipe during continuous operation.

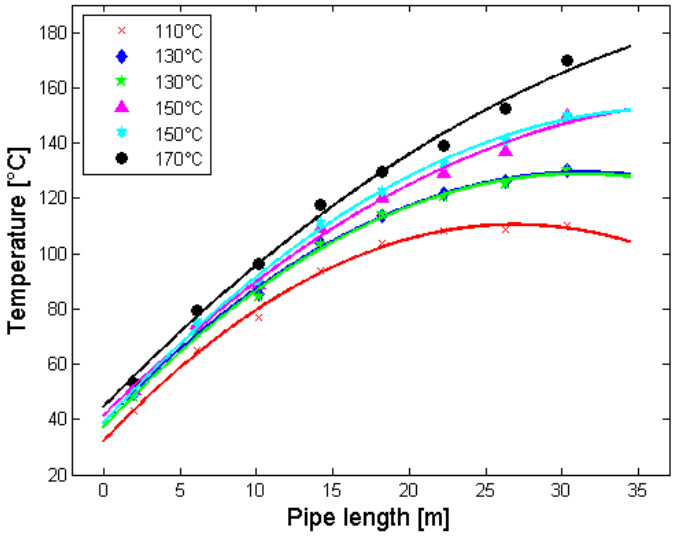

Figure 5-7: Pipe wall temperature profiles in axial direction of the Revtech pipe for setpoints of 110°C, 130°C, 150°C, and 170°C with fitted second order polynomials

5.4 Modelling of flour and air temperature in the heating spiral

5.4.1 Development of the model

The temperature profiles of the product and the air flow passing through the Revtech pipe are not easily measured. Hence, these profiles were mathematically modelled. For this purpose, energy balances were made for flour and air in a simplified system. Boundary conditions and input parameters were given and the resulting equations were solved. The following assumptions were made:

- Flour and air velocities are constant and only in axial direction of the pipe
- Conduction in the materials is negligible
- The temperatures of flour and air are constant in radial direction of the pipe

The nomenclature used in this section is listed in Table 5-3.

Table 5-3: Nomenclature for calculation of flour and air temperature profiles in the Revtech tube

Symbol	Parameter	Unit
a	Thermal diffusivity	m^2/s
c_p	Specific heat	J/kgK
h	Heat transfer coefficient	$W/(m^2K)$
k	Thermal conductivity	W/(m K)
m	Mass	kg
$\dot{m}$	Flow rate	kg/h
r	Radius	m
v	Velocity	m/s
x	Axial pipe length	m
L	Length	m
T	Temperature	K
$\dot{Q}$	Heat flux	W
V	Volume	m^3
α	Angle	°
μ	Dynamic viscosity	Pas
ν	Kinematic viscosity	m^2/s
ρ	Bulk density	kg/m^3

The system under consideration is shown in Figure 5-8a-b. Energy balances for flour and air layers are made over a thin shell of the cross-section of the pipe according to Bird et al. (2005) (see Figure 5-8c-d). Equations 5-1 - 5-4 describe the temperature profile of the flour layer and equations 5-5 - 5-7 describe the air temperature profile in axial direction of the pipe.

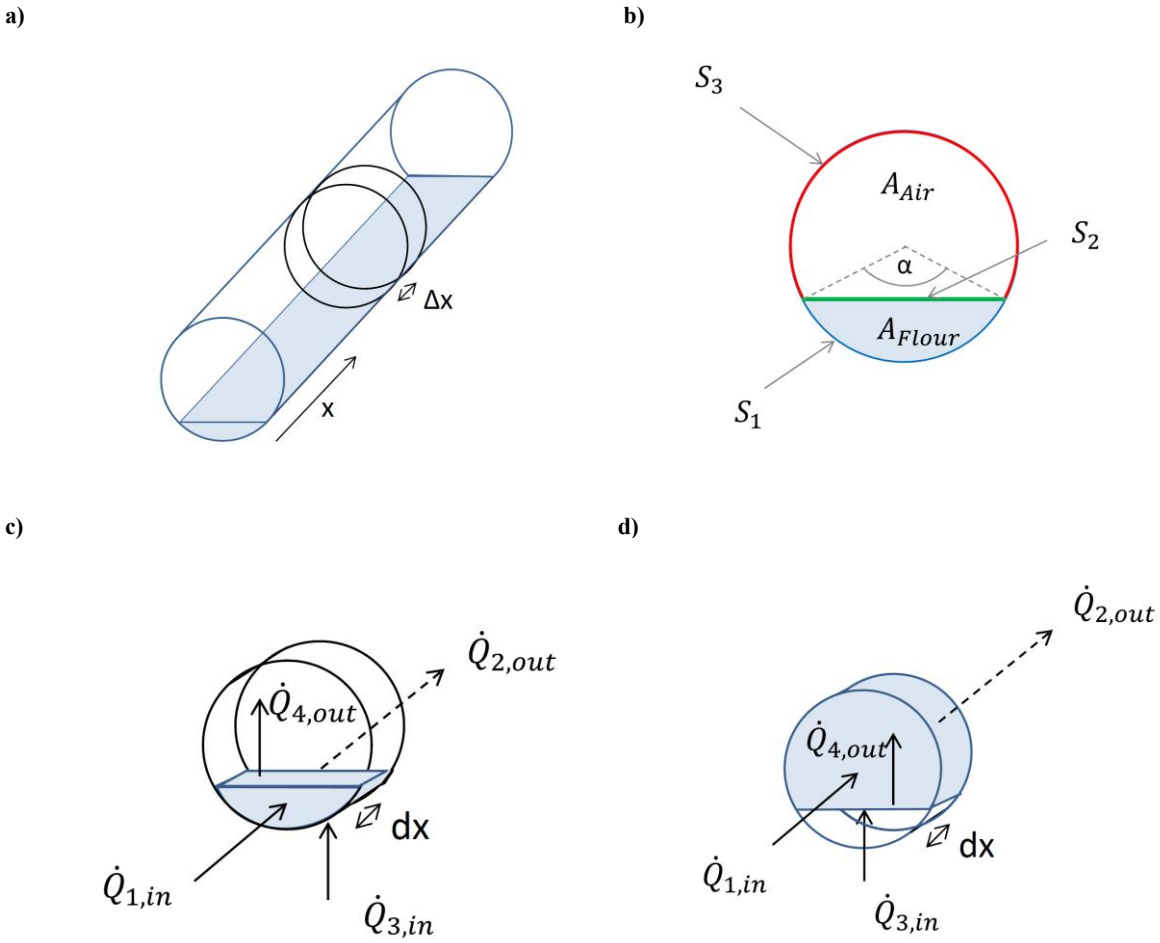

Figure 5-8: a) Model system of the Revtech heating pipe. The blue section depicts the flour layer, the transparent section shows the air layer. x: axial direction of the pipe. b) Cross section of the pipe with flour and air and cross-sectional areas and lines of heat transfer S_1, S_2, S_3 c) Thin shell of the system in a) and heat fluxes for the flour layer. d) Thin shell of the system in a) and heat fluxes for the air layer. The blue section depicts the air layer.

$$\dot{Q}_{1,in} - \dot{Q}_{2,out} + \dot{Q}_{3,in} - \dot{Q}_{4,out} = 0 \qquad \textbf{Eq. 5-1}$$

$$\rho_{Flour} \cdot c_{p,Flour} \cdot v_{Flour} \cdot A_{Flour} \cdot T_{Flour}|_x -$$

$$\rho_{Flour} \cdot c_{p,Flour} \cdot v_{Flour} \cdot A_{Flour} \cdot T_{Flour}|_{x+dx} + h_{Flour-Wall} \cdot S_1 \cdot dx \cdot (T_{Wall} - T_{Flour}) -$$

$$h_{Flour-Air} \cdot S_2 \cdot dx \cdot (T_{Flour} - T_{air}) = 0 \qquad \textbf{Eq. 5-2}$$

After division by dx and consideration of Eq. 5-3, the differential equation of the flour temperature profile is shown in Eq. 5-4.

$$\lim_{x\to 0} \frac{\rho \cdot c_p \cdot v \cdot T|_x - \rho \cdot c_p \cdot v \cdot T|_{x+dx}}{dx} = -\frac{d}{dx}\left(\rho \cdot c_p \cdot v \cdot T\right) \qquad \textbf{Eq. 5-3}$$

$$\frac{dT_{Flour}}{dx} + \frac{h_{Flour-Air} \cdot S_2 + h_{Wall-Flour} \cdot S_1}{\rho_{Flour} \cdot c_{p,Flour} \cdot V_{Flour} \cdot A_{Flour}} \cdot T_{Flour} =$$

$$\frac{h_{Flour-Air} \cdot S_2}{\rho_{Flour} \cdot c_{p,Flour} \cdot v_{Flour} \cdot A_{Flour}} \cdot T_{Air} + \frac{h_{Wall-Flour} \cdot S_1}{\rho_{Flour} \cdot c_{p,Flour} \cdot v_{Flour} \cdot A_{Flour}} \cdot T_{Wall}(x) \qquad \textbf{Eq. 5-4}$$

$$\dot{Q}_{1,in} - \dot{Q}_{2,out} + \dot{Q}_{3,in} - \dot{Q}_{4,out} = 0 \qquad \textbf{Eq. 5-5}$$

$$\rho_{Air} \cdot c_{p,Air} \cdot v_{Air} \cdot A_{Air} \cdot T_{Air}|_x - \rho_{Air} \cdot c_{p,Air} \cdot v_{Air} \cdot A_{Air} \cdot T_{Air}|_{x+dx} + h_{Wall-Air} \cdot S_3 \cdot dx \cdot$$

$$(T_{Wall} - T_{Air}) - h_{Flour-Air} \cdot S_2 \cdot dx \cdot (T_{Air} - T_{Flour}) = 0 \qquad \textbf{Eq. 5-6}$$

$$\frac{dT_{Air}}{dx} + \frac{h_{Flour-Air} \cdot S_2 + h_{Wall-Air} \cdot S_3}{\rho_{Air} \cdot c_{p,Air} \cdot v_{Air} \cdot A_{Air}} \cdot T_{Air} = \frac{h_{Flour-Air} \cdot S_2}{\rho_{Air} \cdot c_{p,Air} \cdot v_{Air} \cdot A_{Air}} \cdot T_{Flour} +$$

$$\frac{h_{Wall-Air} \cdot S_3}{\rho_{Air} \cdot c_{p,Air} \cdot v_{Air} \cdot A_{Air}} \cdot T_{Wall}(x) \qquad \textbf{Eq. 5-7}$$

Equations 5-4 and 5-7 lead to a system of differential equations in Eq. 5-8 that describes the temperature distributions of flour and air in axial direction of the pipe.

$$\begin{bmatrix} \frac{dT_{Flour}}{dx} \\ \frac{dT_{Air}}{dx} \end{bmatrix} == \begin{bmatrix} -\left(\frac{h_{Flour-Air}\cdot S_2 + h_{Wall-Flour}\cdot S_1}{\rho_{Flour}\cdot c_{p,Flour}\cdot v_{Flour}\cdot A_{Flour}}\right) & \frac{h_{Flour-Air}\cdot S_2}{\rho_{Flour}\cdot c_{p,Flour}\cdot v_{Flour}\cdot A_{Flour}} \\ \frac{h_{Flour-Air}\cdot S_2}{\rho_{Air}\cdot c_{p,Air}\cdot v_{Air}\cdot A_{Air}} & -\left(\frac{h_{Flour-Air}\cdot S_2 + h_{Wall-Air}\cdot S_3}{\rho_{Air}\cdot c_{p,Air}\cdot v_{Air}\cdot A_{Air}}\right) \end{bmatrix} \begin{bmatrix} T_{Flour} \\ T_{Air} \end{bmatrix} +$$

$$\begin{bmatrix} \frac{h_{Wall-Flour}\cdot S_1}{\rho_{Flour}\cdot c_{p,Flour}\cdot v_{Flour}\cdot A_{Flour}} \cdot T_{Wall}(x) \\ \frac{h_{Wall-Air}\cdot S_3}{\rho_{Air}\cdot c_{p,Air}\cdot v_{Air}\cdot A_{Air}} \cdot T_{Wall}(x) \end{bmatrix} \quad \textbf{Eq. 5-8}$$

The following boundary conditions are applied:

Boundary condition I: $T_{Flour}(x = 0) = 293\ \text{K}$ **Eq. 5-9**

Boundary condition II: $T_{Air}(x = 0) = 293\ \text{K}$ **Eq. 5-10**

Calculation of input parameters:

i) The flour velocity in the axial direction of the pipe is calculated by dividing the pipe length by the measured residence time. An average residence time was taken in case residence time was not constant.

ii) The heat transfer coefficient of air can be calculated in two ways:

- By using Equation 5-11. The heat transfer coefficient is a function of the air velocity ("Convective Heat Transfer", 2016):

$$h = 10.45 - v + 10 \cdot v^{0.5} \quad \textbf{Eq. 5-11}$$

Assuming a velocity of 2 m/s, the heat transfer coefficient is 22.6 W/m^{2}K.

- By using Reynolds, Prandtl, and Nusselt number (Incropera and DeWitt, 2007):

$$Re = \frac{v \cdot L \cdot \rho}{\mu} \quad \textbf{Eq. 5-12}$$

$$Pr = \frac{\nu}{a} \quad \textbf{Eq. 5-13}$$

$$Nu = 0.644 \cdot Re^{\frac{1}{2}} \cdot Pr^{\frac{1}{3}} = \frac{h \cdot L}{k} \quad \textbf{Eq. 5-14}$$

With $v = 2$ m/s, $L = 0.084$ m, $\rho = 1.2922$ kg/m^3, $\mu = 1.983 \cdot 10^{-5}$ Pas, $\nu = 1.535 \cdot 10^{-5}$ m^2/s, $a = 1.9 \cdot 10^{-5}$ m^2/s, $k = 2.428 \cdot 10^{-2}$ W/m K, a heat transfer coefficient of 18.2 W/m^{2}K is calculated.

Taking both approaches into account, an estimate of 20 W/m^{2}K was used in following calculations for the heat transfer coefficient between air and the pipe wall and air and flour.

iii) Areas and lines of heat transfer (see Figure 5-8b.):

- $r = 0.042$ **Eq. 5-15**
- $A_{Flour} = \frac{r^2}{2} \cdot (\alpha - \sin(\alpha))$ **Eq. 5-16**
- $A_{Air} = r^2 \cdot \pi - A_{Flour}$ **Eq. 5-17**
- $S_1 = r \cdot \alpha$ **Eq. 5-18**
- $S_2 = 2 \cdot r \cdot sin\left(\frac{\alpha}{2}\right)$ **Eq. 5-19**
- $S_3 = 2 \cdot \pi \cdot r - S_1$ **Eq. 5-20**

Angle α is calculated from the flour mass in the pipe:

- The flour mass in the pipe is calculated by Eq. 5-21

$$m = \dot{m} \cdot Residence\ time \qquad \textbf{Eq. 5-21}$$

- The volume of the flour is calculated by $V_{Flour} = \frac{m}{\rho}$ **Eq. 5-22**
- The volume of the trough of the pipe that is filled with flour is calculated by multiplying the cross-section filled with flour (A_{Flour}) and the pipe length (L):

  $$V_{Trough} = A_{Flour} \cdot L \qquad \textbf{Eq. 5-23}$$

  The cross sectional area (A_{Flour}) is calculated by Eq. 5-16. The angle α is adjusted, so that the trough volume (see Eq. 5-23) equals the flour volume (see Eq. 5-22). Values of α are shown in Table 5-5.

Model input parameters are listed in Table 5-4 and Table 5-5. The length (x) of the pipe length is 34.4 m from the inlet to the outlet of the spiral. The temperature profiles of the pipe are taken from the fitted second order polynomials in Figure 5-7.

Table 5-4: Material properties of flour and air for calculation of temperature profiles in the Revtech device

Parameter	Symbol	Value	Reference
Flour			
Bulk density	ρ	500 kg/m^3	Measurements
Specific heat capacity	c_p	1600 J/kgK	Klingler (2010) Wheelock and Lancaster (1970)
Air			
Bulk density	ρ	1.2922 kg/m^3	"Density of Air", (2016)
Specific heat capacity	c_p	1000 J/kgK	"Air Properties", (2016)
Velocity	v	2 m/s	(Revtech Process Systems, 2016)

Table 5-5: Model input parameters for the calculation of flour and air temperature profiles and measured outlet temperature of flour depending on the temperature setpoint of the Revtech pipe. x is the axial distance of the pipe.

Temperature setpoint [°C]	α [rad]	v_{flour} [m/s]	Temperature profile of the pipe [K]	$T_{flour, outlet}$ [°C]
110	1.1519	0.27	$-0.1086\,x^2 + 5.8366\,x + 305.22$	-
130	1.1519	0.27	$-0.0915\,x^2 + 5.7576\,x + 312.06$	85.5 ± 1.9
150	1.2741	0.20	$-0.0668\,x^2 + 5.5173\,x + 314.49$	97.9 ± 2.8
170	1.2741	0.20	$-0.0543\,x^2 + 5.6590\,x + 317.64$	111.7 ± 5.4

The heat transfer coefficient between the pipe wall and the flour layer is unknown. However, the temperature of the flour at the outlet of the pipe[1] is known (see Table 5-5). Hence, the heat transfer coefficient was fitted to be 22 W/m^2K using a temperature setpoint of the pipe of 150°C.

5.4.2 Calculated temperature profiles

Temperature profiles of the pipe wall during flour heat treatment could be measured for different temperature setpoints (see section 5.3). The temperature profiles of the product and the air flow passing through the pipe are not easily measured. Hence, these profiles were mathematically modelled. For this purpose, energy balances were made for flour and air in a simplified system. Boundary conditions and input parameters were given and the resulting equations were solved.

[1] The flour temperature was measured after 3.1 m of flexible, plastic pipe (recirculation pipe) from the outlet of the heating spiral. Due to increased flour velocity and insulation properties of the plastic pipe, heat losses in the recirculation pipe were assumed to be negligible.

The system of differential equations in Eq. 5-8 was solved simultaneously in Wolfram Mathematica® using the boundary conditions and input parameters given. The resulting temperature profiles of flour and air are shown in Figure 5-10a-d for temperature setpoints of 110°C, 130°C, 150°C, and 170°C. Both flour and air temperatures remain below the wall temperature, which was expected as flour outlet temperatures were measured to be approx. 45 - 60°C below the setpoint temperatures. The air temperature heats up more quickly than the flour temperature due to a significantly lower specific heat capacity and density. The measured outlet temperature of the flour is in agreement with the modelled temperature at the end of the pipe at all temperature setpoints (see Figure 5-9). A first order polynomial can be fitted to the data. Hence, the assumptions made for the model and the estimate of the fitted heat transfer coefficient of 22 W/m^{2}K between the pipe wall and the flour layer are adequate.

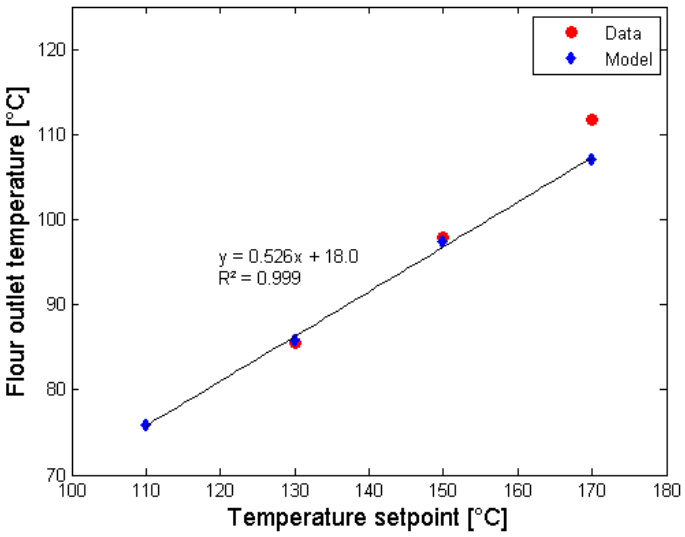

Figure 5-9: Flour temperature at the outlet of the Revtech pipe for different temperature setpoints. Model and data with best-fit line.

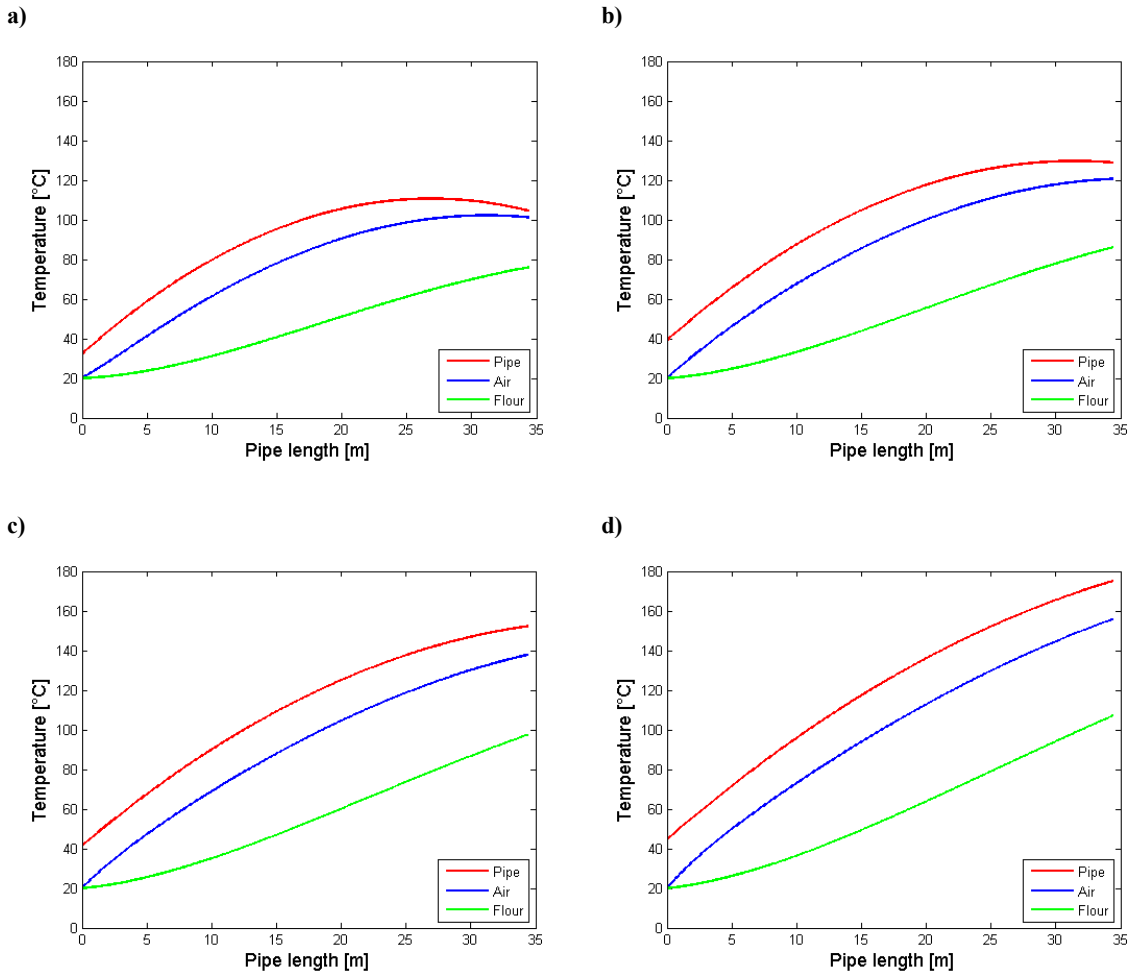

Figure 5-10: Flour, air, and pipe wall temperature profiles in axial direction of the Revtech pipe for different temperature setpoints: a) 110°C b) 130°C c) 150°C d) 170°C

5.5 Comparison of RVA results between lab-scale and Revtech experiments

The effect of constant temperature and stepwise temperature profiles on the RVA peak viscosity of flour in water has been studied in lab-scale experiments (see chapter 3). In the Revtech machine, a continuous, non-constant temperature profile was applied to flour (see section 5.3). The objective here is to develop an algorithm to estimate RVA peak viscosity of heat treated flour from the Revtech based on results from lab-scale experiments. This is done in three steps:

i) The RVA peak viscosity of flour is fitted from lab-scale experiments at constant temperature depending on treatment time and temperature.

ii) Temperature profiles are created for flour passing through the Revtech tube depending on time.

iii) An algorithm is developed to estimate peak viscosity based on the development of peak viscosity after stepwise temperature profiles were applied in lab-scale experiments.

5.5.1 Lab-scale experiments: Fitting of RVA peak viscosity of heat treated flour

Based on data in chapter 3 (see Figure 3-6), the peak viscosity of heat treated flour is approximated depending on treatment time (1 s time step) and constant temperatures between 110°C and 170°C (2°C temperature step). The following assumptions were made:

- No viscosity value below the initial value (1405 cP for untreated flour) can be taken.
- There is no increase in peak viscosity for heating temperatures below 110°C (see chapter 3).
- Data from Figure 3-6 (Flour III) was fitted as straight lines between 110°C and 120°C ($R^2 = 0.99$).
- Data from Figure 3-6 was fitted as logarithmic curves for treatment temperatures above 120°C and after 2 min treatment time ($R^2 = 0.97$). Straight lines were fitted between 0 - 2 min.

The resulting fitted RVA peak viscosity of heat treated flour in lab-scale experiments is shown in Figure 5-11.

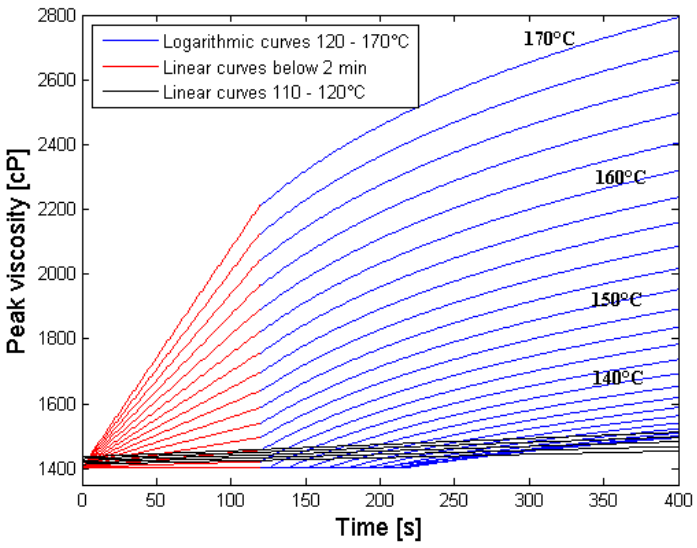

Figure 5-11: Fitted RVA peak viscosity in water of heat treated flour depending on treatment time and temperature (results from lab-scale experiments, chapter 3, Figure 3-6). Temperature contours are 2°C apart.

5.5.2 Revtech experiments: Flour temperature profiles

The temperature profile of flour passing through the Revtech machine can be determined in different ways. It can be measured or mathematically modelled (see section 5.4). Results show that even at high temperature setpoints of the pipe wall, the average flour temperature does not significantly exceed 110°C. It is likely that the flour near the wall will reach the wall temperature, but individual flour granules do not spend much time at the wall because of the continual mixing of the flour as it travels up the tube. Hence, due to the assumption made based on lab-scale experiments that there is no increase in peak viscosity below 110°C (see section 5.5.1), the modelled flour temperature profiles cannot be used to estimate peak viscosity.

To demonstrate the principle of the algorithm, the flour temperature was taken to be equal to the pipe temperature. This is equivalent to the maximum temperature profile possible in the Revtech, but it overestimates reality.

Hence, the flour temperature is calculated from the pipe temperature in the axial direction (see section 5.3). Different temperature profiles were taken for different cycles of recirculation as the temperature was not constant in recirculation mode (see section 5.3). The pipe temperature of the first cycle represents the temperature distribution during stable operation. For the following cycles, the temperature of all probes was taken at the time of reconnection plus residence time at the respective temperature setpoints.

The flour temperature profiles as taken from the pipe wall profiles for different cycles of recirculation during recirculation at a temperature setpoint of 130°C are shown in Figure 5-12. The temperature of the probes is shown over time. The temperature profile of flour passing

through the pipe results by reading the graph from the bottom to the top (Probe 1 - Probe 8). The blue dashed lines represent the points in time, at which the temperature profiles were taken for different cycles of recirculation.

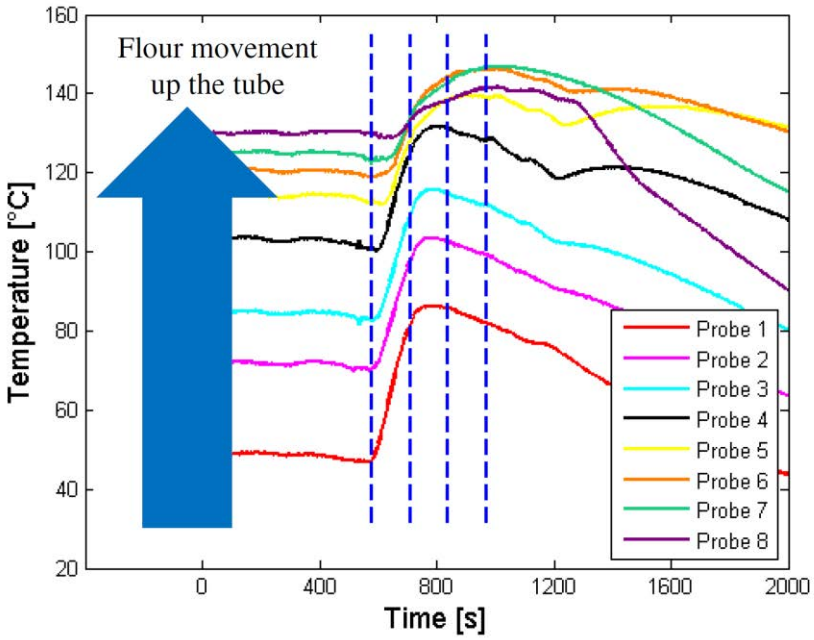

Figure 5-12: Wall temperature profiles during flour recirculation at 100 kg/h and a temperature setpoint of 130°C in the Revtech. Blue dashed lines are the temperature profiles in the axial direction of the pipe taken as model input. Probe 1 is at the base of the tube, probe 8 at the top. Flour passes the probes in sequence as it moves up the tube.

To calculate RVA peak viscosity after Revtech treatment, flour temperature profiles were used at temperature setpoints of 130°C and 150°C. At 110°C, the flour temperature is too low to calculate peak viscosity and at 170°C, the flour temperature exceeds the data available from lab-scale experiments.

Residence time at 130°C is 129 s and it is linearly increasing between 192 s and 208 s (increment of 4 s per cycle) at 150°C (see section 5.6.1.2). By combination of residence time and temperature profile (depending on the axial position of the pipe), the time period can be calculated for which flour was exposed to a certain temperature.

The resulting flour temperature profiles depend on time and second order polynomials can be fitted to the data ($R^2 = 0.99$). This is shown in Table 5-6 for 1 - 5 recirculation cycles and setpoint temperatures of 130°C and 150°C.

Table 5-6: Temperature profiles of flour depending on time for setpoints of 130°C and 150°C in the Revtech equipment and for different cycles of recirculation

Cycles	Temperature setpoint: 130°C	Temperature setpoint: 150°C
1	$-0.0067 \cdot t^2 + 1.5685 \cdot t + 37.184$	$-0.0055 \cdot t^2 + 1.5781 \cdot t + 38.742$
2	$-0.0066 \cdot t^2 + 1.2919 \cdot t + 69.531$	$-0.0048 \cdot t^2 + 1.4864 \cdot t + 39.990$
3	$-0.0081 \cdot t^2 + 1.4921 \cdot t + 73.508$	$-0.0054 \cdot t^2 + 1.2564 \cdot t + 78.747$
4	$-0.0078 \cdot t^2 + 1.5390 \cdot t + 68.847$	$-0.0076 \cdot t^2 + 1.5617 \cdot t + 80.323$
5	$-0.0073 \cdot t^2 + 1.5266 \cdot t + 64.397$	$-0.0077 \cdot t^2 + 1.6555 \cdot t + 73.929$

5.5.3 Algorithm to calculate RVA peak viscosity

To estimate the peak viscosity of flour after heat treatment in the Revtech, the following algorithm was developed based on lab-scale results for stepwise temperature profiles (see section 3.3.2.1). The final peak viscosity of the flour is assumed to result from the time-temperature history to which it has been exposed. Eq. 5-24 calculates the peak viscosity (PV) of flour after the n-th cycle of recirculation in the Revtech with T = temperature and t = time.

$$PV_n = PV_{n-1}|_{T_n} + \left(\frac{\Delta PV}{\Delta t}\right)\Big|_{T_n, PV_{n-1}} \cdot \Delta t \qquad \textbf{Eq. 5-24}$$

The algorithm is illustrated in Table 5-7 for the case where flour at 110°C and of a viscosity of 10 (arbitrary units) is heated at 2°C/s to 120°C.

1) A matrix is created for the peak viscosity (see Table 5-7) depending on time and temperature based on lab-scale experiments and assumptions in section 5.5.1. Figure 5-11 is presented as a matrix.
2) The temperature closest to 110°C (there is no increase in peak viscosity below) is found in the flour temperature profile in the Revtech (see section 5.3).
3) All peak viscosities at 110°C are found in the lab-scale matrix and the peak viscosity is selected at the starting time plus a time step of 1 s, i.e. 20 in the matrix.
4) The next temperature is selected in the flour temperature profile (112°C) and the corresponding peak viscosities are found in the lab-scale experiments matrix; i.e. 12 - 102.
5) The closest peak viscosity to the final peak viscosity at the previous temperature (i.e. 20) is selected on the peak viscosity curve of the new temperature and taken as a starting point; i.e. 22.
6) The new peak viscosity is found at the given temperature after a time step of 1 s from the selected peak viscosity; i.e. from 22 to 32.
7) Points 4 - 6 are repeated for the entire temperature profile of the flour. Table 5-7 shows a temperature profile between 110°C and 120°C with a temperature step of 2°C and a time step of 1 s is applied; the final peak viscosity is ca. 90. Vertical lines

represent lines of constant viscosity; horizontal lines show the effect of increasing time on peak viscosity.

Table 5-7: Illustration of the principle of the algorithm to calculate peak viscosity of flour after a non-constant temperature profile was applied. The path of the algorithm is highlighted in yellow for a system which spends 1 s at each temperature from 110°C to 120°C.

		Peak viscosity [arbitrary units]									
Time [s]		1	2	3	4	5	6	7	8	9	10
Temperature [°C]	110	10	20	30	40	50	60	70	80	90	100
	112	12	22	32	42	52	62	72	82	92	102
	114	16	26	36	46	56	66	76	86	96	106
	116	20	30	40	50	60	70	80	90	100	110
	118	30	40	50	60	70	80	90	100	110	120
	120	45	60	75	90	105	120	135	150	175	190

5.5.4 Results

It was shown in lab-scale experiments that the RVA peak viscosity in water of flour treated with a non-constant, stepwise temperature profile could be predicted accurately (see section 3.3.2.1). In the Revtech equipment, a continuous, non-constant temperature profile was applied to flour (see section 5.3). An algorithm was developed to estimate the RVA peak viscosity of flour treated in the Revtech based on results from lab-scale experiments. The algorithm was applied to maximum flour temperature profiles at setpoints of 130°C and

150°C in the Revtech. The modelled temperature profiles of section 5.4 could not be used because the temperature is too low to compare them to lab-scale experiments.

The resulting peak viscosities calculated with the developed algorithm are shown in Figure 5-13. It shows the increase in peak viscosity during each cycle of recirculation using the last peak viscosity of the previous cycle as the starting point for the new cycle. The black lines show peak viscosity at constant temperatures with increasing temperature from the right, bottom corner to the left, top corner. Hence, the traces of increasing peak viscosity for each cycle can be followed from the right side to the left side in the figure.

Table 5-8 shows the estimated peak viscosities in comparison to the measured data. It shows that the algorithm does not predict the peak viscosity of flour after heat treatment in the Revtech to satisfactory accuracy.

Table 5-8: RVA peak viscosity (data and model) for flour heat treated in the Revtech at temperature setpoints of 130°C and 150°C for different cycles of recirculation

	RVA peak viscosity [cP]			
	Temperature setpoint 130°C		**Temperature setpoint 150°C**	
Cycles	Data	Model	Data	Model
1	1436	1468	1728	1560
3	1940	1603	3139	1824
4	2217	1675	-	-
5	2221	1729	3051	2259

The results obtained here indicate that the peak viscosity depends not only on temperature and time as suggested by lab-scale experiments, but that other factors are important. The slow and

continuous increment of temperature in the Revtech tube might play a role. It leads to slow removal of moisture from the flour in the beginning of the process, which might have an effect on peak viscosity. To investigate this phenomenon, two tests were performed in lab-scale experiments:

i) Flour was dried at a low temperature of 80°C for 10 min leading to a moisture content of approx. 2.5% before it was treated at 170°C for 7 min. The resulting peak viscosity of 2725 cP was comparable to results without drying (see Figure 5-17a).

ii) Flour was treated at 185°C for 3 - 5 min and a maximum peak viscosity of 2700 cP was obtained.

In lab-scale experiments, the maximum peak viscosity that could be reached for heat treated flour III was approx. 2750 cP, which is significantly lower than the values reached after heat treatment in the Revtech. Further studies about drying time and temperature in lab-scale experiments are needed to examine this phenomenon. Once the mechanism is clear and included in the algorithm, the temperature profiles modelled in section 5.4 can be used as input profiles.

a)

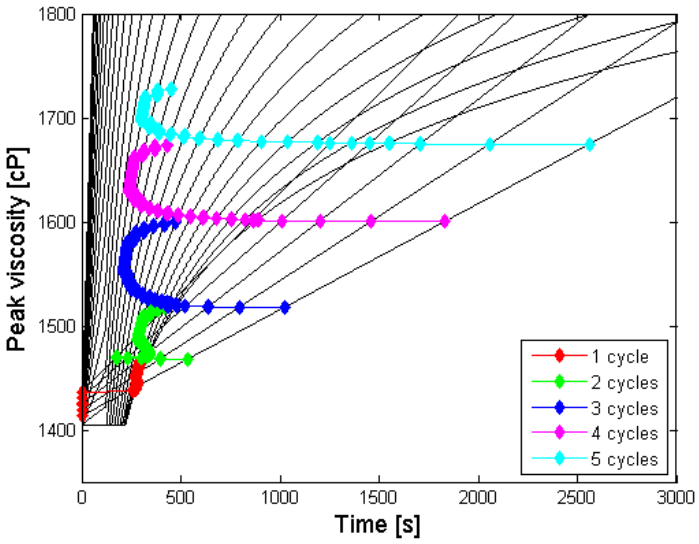

b)

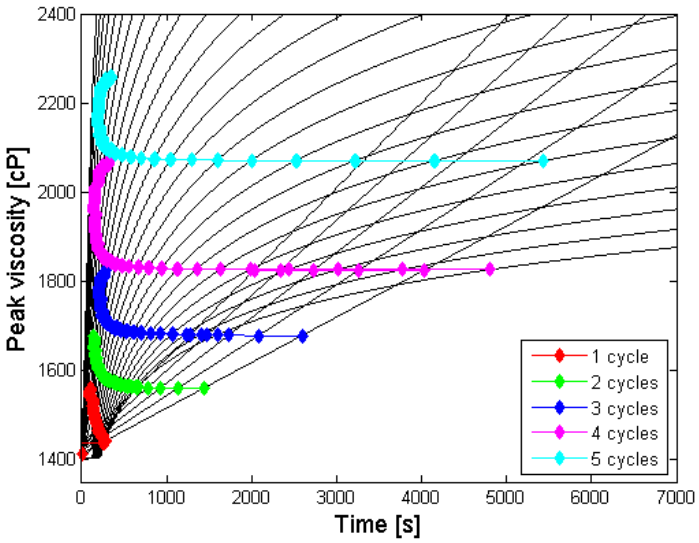

Figure 5-13: Estimated RVA peak viscosity of flour after heat treatment in the Revtech after different cycles of recirculation at temperature setpoints of a) 130°C and b) 150°C[2]

[2] For the 5th cycle at 150°C, lab-scale peak viscosity curves were used above 130°C (below 130°C, peak viscosity curves were too flat to find the peak viscosity from the previous cycle).

5.6 Results and discussion

5.6.1 Residence times of flour in the Revtech at elevated temperatures

Residence times have been investigated at ambient conditions in chapter 4. However, the development of the residence time at higher temperatures is of great importance for the design and the validation of a thermal process.

5.6.1.1 Without extraction

Figure 5-14 shows the residence time of a commercially available high ratio cake flour passing through the Revtech equipment at a temperature setpoint of 120°C in comparison to ambient conditions without extraction of the atmosphere inside the pipe. At elevated temperature, the residence time is considerably higher than at ambient temperature. The initial residence time is 313 s at 120°C in comparison to an average of 206.2 ± 10.9 s at ambient temperature, representing an increase of approx. 52% from ambient temperature to 120°C. Furthermore, the gradient at which the residence time increases during the experiment is increased at high temperature. It was measured to be 0.77 s/min in comparison to 0.12 ± 0.08 s/min at ambient temperature (see Figure 5-14). Over a time period of 40 min, the residence time increased by 30 s (9.6% of initial value) at elevated temperatures compared to an increase of 4.7 ± 3.2 s (2.2 ± 1.5% of initial value) at ambient temperature.

Two factors are involved in the observed phenomenon:

i) The dynamics of residence time at ambient temperature (see chapter 4) are still likely to play a role at conditions of elevated temperature.

ii) Water evaporates from the flour due to high temperature. The flour had an initial moisture content of approx. 12.1%. The humid environment in the pipe affects parameters like cohesion properties and the coefficient of restitution, which in turn may slow down product flow and increase residence time. This was confirmed by the experimental observation that the treated product was partially clumped together as spheres (see Figure 5-15).

It is difficult to distinguish between both effects. However, the second effect can be significantly reduced by extraction of the moist atmosphere through extraction ports in the pipe.

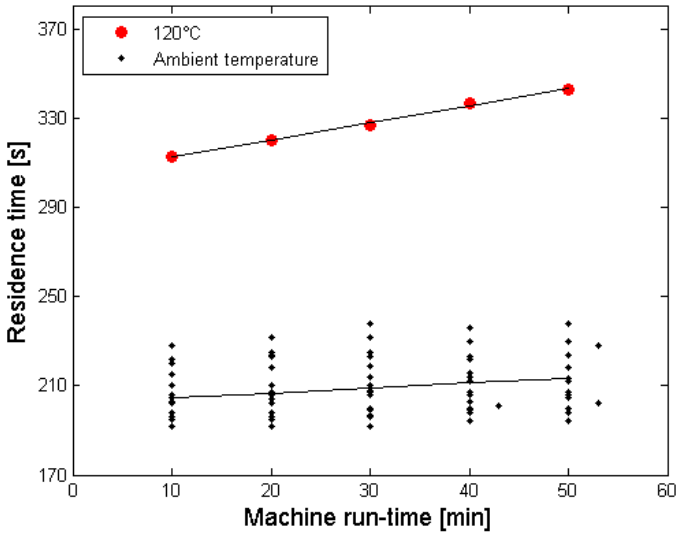

Figure 5-14: Residence time of flour passing through the Revtech equipment at 120°C and ambient temperature. Motor angles: 40°. Motor speed: 740 rpm. Off balance motor setting 65%.

Figure 5-15: Agglomerated flour spheres after flour heat treatment in the Revtech (120°C, 40°, 740 rpm) without extraction of the atmosphere

5.6.1.2 With extraction

In contrast to the previous section, the residence time was measured here whilst moist air was extracted from the pipe through the top 6 extraction pipes (see section 5.2.2).

Figure 5-16 shows the residence time of flour at different temperature setpoints. The residence time was constant during the observed time period at setpoints of 110°C and 130°C. It was measured to be 129 ± 1 s and 129 ± 6 s respectively. At 150°C and 170°C, the residence time increased linearly (gradient approx. 1.2 s/min) from a starting level of approx. 161 s.

The magnitude of residence times measured here is comparable to the residence time measured at ambient temperature without extraction (see Figure 5-14). The findings suggest that the moisture removal via extraction is efficient and the flow characteristics of the flour are similar to ambient conditions.

The increase in residence time was observed in previous experiments at ambient temperature. Details about this phenomenon are discussed in chapter 4. The reasons for constant residence time at 110°C and 130°C are not clear.

The results highlight the importance of defining process parameters for each individual industrial application, so that the desired outcome can be achieved. The magnitude of residence time and the dynamics can be different at different temperature setpoints.

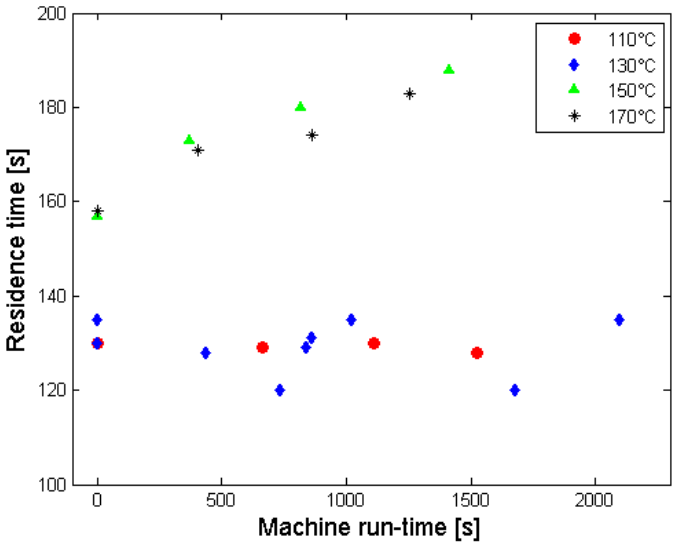

Figure 5-16: Residence time of flour (100 kg/h) passing through the Revtech spiral over time at different temperature setpoints

5.6.2 Effect of heat treatment in the Revtech on flour

To evaluate the effect of heat treatment in the Revtech on flour, the RVA peak viscosity was measured in water and in 50% sucrose solution. In addition, high ratio cakes were baked and the cake volume was measured.

5.6.2.1 RVA peak viscosity in water and 50% sucrose solution

The RVA peak viscosity of heat treated flour in the Revtech equipment compared to that of lab-scale experiments (see chapter 3) is shown in Figure 5-17a in deionised water and in Figure 5-17b in 50% sucrose solution. Samples were held at a constant temperature for a specific time during lab-scale experiments. During heat treatment in the Revtech, a setpoint temperature was defined (see section 5.2.2) and the total treatment time (residence time) is shown. Hence, the sample was treated below the setpoint temperature for most of the treatment time.

The overall development of peak viscosity in both liquids of samples treated in the Revtech is similar to lab-scale results; it increases with increasing intensity of heat treatment to a certain point and decreases after prolonged treatment. Details are shown in chapter 3.

The magnitude of peak viscosity in both liquids is significantly different for samples treated in the Revtech in comparison to lab-scale results. Even though the sample is mostly treated below setpoint temperature in the Revtech, the peak viscosity generally exceeds the lab-scale results for equivalent setpoint temperatures. Reasons were discussed in section 5.5.4. It was suggested that peak viscosity not only depends on treatment temperature and time as indicated

by lab-scale experiments, but other factors are important. The slow and continuous increment of temperature in the Revtech tube might play a role.

a)

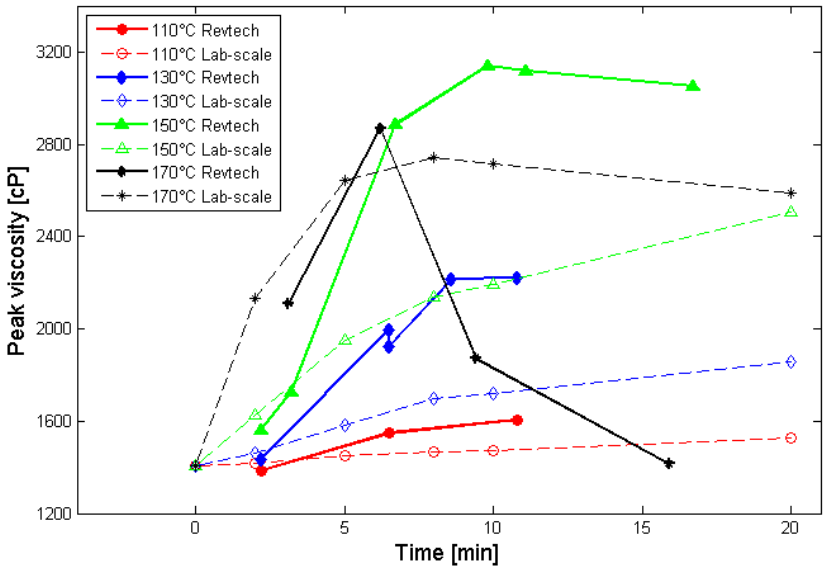

b)

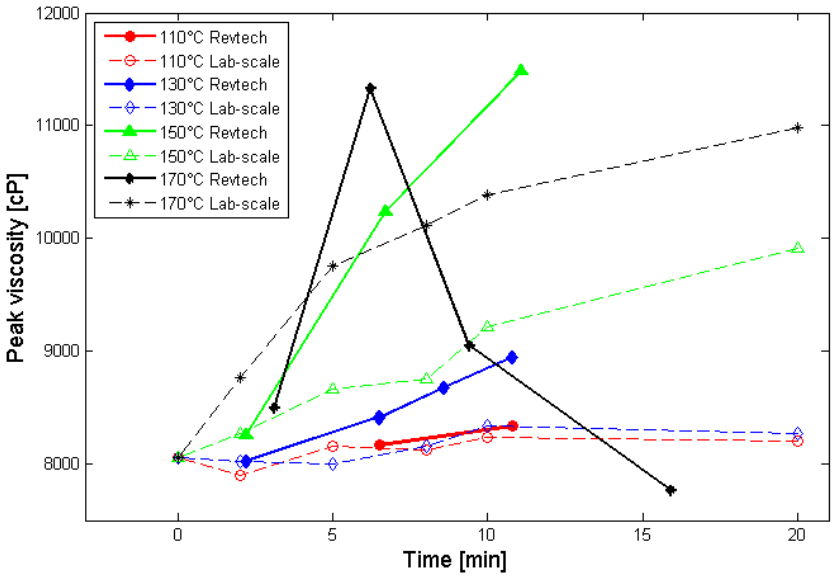

Figure 5-17: RVA peak viscosity of heat treated flour in lab-scale experiments and Revtech experiments. a) In water. b) In 50% sucrose solution.

5.6.2.2 High ratio cake quality

Baking good quality cakes is the overall objective of the heat treatment of flour. Cake quality can be defined in many ways such as cake volume, taste, texture, or colour. This work focuses on cake volume measurements.

High ratio cakes were baked after the heat treatment of flour in the Revtech. Figure 5-18 shows cross sections of cakes made with untreated and heat treated flour. Figure 5-20 presents volumes of cakes baked with untreated flour and heat treated flour from the Revtech at temperature setpoints between 110°C and 170°C depending on treatment time.

Cakes baked with untreated flour collapsed after removal from the oven resulting in a small cake volume as explained in chapter 2 (see Figure 5-18a and Figure 5-20).

For cakes baked with heat treated flour, cake volume generally increased with increasing treatment time at all temperature setpoints (see Figure 5-18b-e and Figure 5-20). The surface of the cakes rises showing a dome shaped cake. Figure 5-19 shows the top view of a collapsed cake made with untreated flour and a cake made with successfully treated flour. It is in agreement with literature that flour heat treatment prevents cake collapse and increases cake volume (Chesterton et al., 2015; Doe and Russo, 1968; Neill et al., 2012; Nicholas et al., 1978).

In addition, heat treatment of flour affects cake texture. Cakes made with untreated flour exhibit a coarser texture than cakes prepared with heat treated flour. The more intense the heat treatment, the finer the texture appears in Figure 5-18.

a) Untreated

b) 110°C: **6:25 min** **10:45 min**

c) 130°C: **6:25 min** **10:45 min**

Figure 5-18: High ratio cakes baked with untreated flour (a) and flour heat treated in the Revtech at different temperature setpoints b) 110°C c) 130°C d) 150°C e) 170°C) and residence times

d) 150°C: **3:10 min** **6:40 min**

9:50 min **16:40 min**

e) 170°C **3:05 min** **6:10 min**

15:50 min

Figure 5-18 (continued): High ratio cakes baked with untreated flour (a) and flour heat treated in the Revtech at different temperature setpoints b) 110°C c) 130°C d) 150°C e) 170°C) and residence times

Figure 5-19: Top view of a cake made with untreated flour (left) and a cake made with flour heat treated in the Revtech (170°C, 15.9 min) (right)

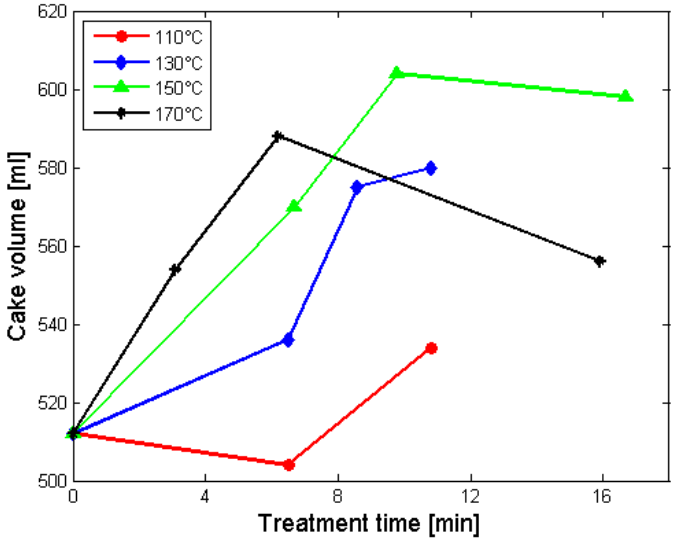

Figure 5-20: Volumes of cakes baked with untreated and heat treated flour from the Revtech (110°C - 170°C) depending on treatment time. Data with connected lines

The batter density was measured to be 84 - 89 g/100 ml after the standard mixing time. No correlation was found between batter density and cake volume or RVA peak viscosity.

As cake collapse is prevented by heat treatment, cake volume increases and cake density decreases with increasing treatment intensity. The more common parameter of specific cake volume in ml/g is defined as the reciprocal of the cake density. Figure 5-21 shows a linear correlation between cake volume and specific cake volume (ml/g).

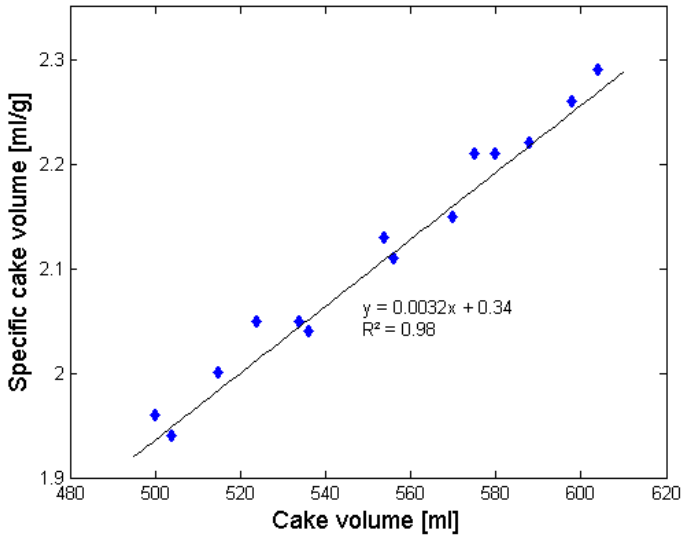

Figure 5-21: Correlation of cake volume and specific cake volume with best-fit line

Figure 5-22 plots the relationship between the measured cake volume and the RVA peak viscosity of flour in water. The figure shows a reasonable correlation (R^2 = 0.75). No such correlation could be found in literature; this is the first indication of it.

Optimal heat treatment of flour stabilises the cake batter during baking and results in high volume cakes (Guy et al., 2007; Guy and Pithawala, 1981; Neill et al., 2012). In addition it facilitates starch granule swelling and increases the RVA peak viscosity (Guy et al., 2007; Guy and Pithawala, 1981; Van Steertegem et al., 2013). Over-treatment also stabilises the

cake batter during baking and results in high volume cakes, however, the RVA peak viscosity can be low (see chapter 3).

The over treated points, if included in the figure, would obscure the correlation shown in Figure 5-22. A wide range of cake volumes can be achieved by under treated as well as over treated samples with a low peak viscosity. The data suggests that heat treatment first increases cake volume and peak viscosity, giving the correlation of Figure 5-22. At some point, the flour is over treated and the peak viscosity decreases significantly while the cake volume remains relatively high as shown in one point in Figure 5-22.

These findings suggest that there might be a correlation between cake volume and peak viscosity of flour after heat treatment, but before over-treatment.

The decrease in RVA peak viscosity indicates less swelling of the over treated starch granules, however cake volumes remain high. Hence the results show that the reason for the improvement of cake baking after the heat treatment of flour cannot only be the facilitation of starch granule swelling, but it may alter interactions of flour with other cake ingredients.

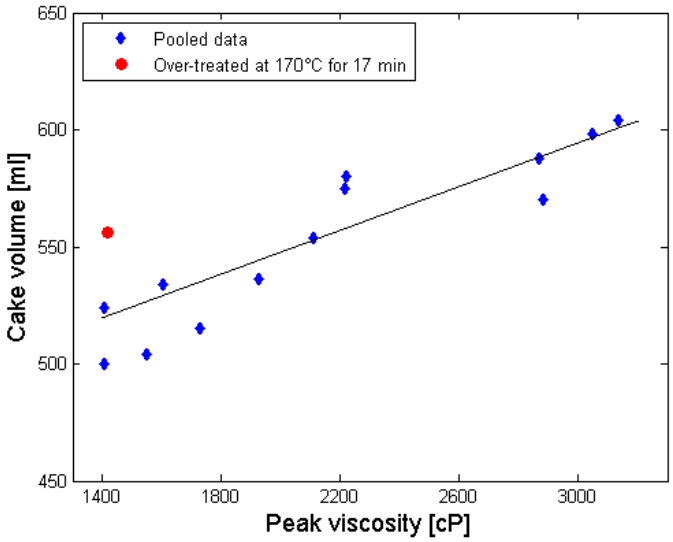

Figure 5-22: Correlation of RVA peak viscosity of heat treated flour in water and cake volume

5.6.3 Industrial relevance

So far, the success of flour heat treatment on cake quality is assessed by baking and evaluating a cake (Neill et al., 2012; Thomasson et al., 1995). No correlation between a simple analytical method of flour testing and cake quality has been found yet. The problem with testing flour by analytical methods is that various processing conditions (e.g. time-temperature combinations) result in identical levels of response (e.g. RVA, rheometer, SRC tests). However, only specific treatment conditions result in an acceptable cake.

A series of experiments has been carried out to characterise the effect of heat treatment on flour functionality (see chapter 3). The findings may be used to uniquely identify any time-temperature history a flour sample may have been exposed to, which may then be correlated with cake quality attributes. This could be valuable for the development of a cake flour specification and for process validation.

Combination of the appropriate measurements may create the ability to identify heat effects. Such a method is presented in Figure 5-23, which plots contour lines[3] of

i) Rapid-Visco-Analyser (RVA) peak viscosity of heat treated flour III in water, and

ii) Rapid-Visco-Analyser (RVA) peak viscosity of heat treated flour III in 50% sucrose solution

depending on treatment time and temperature.

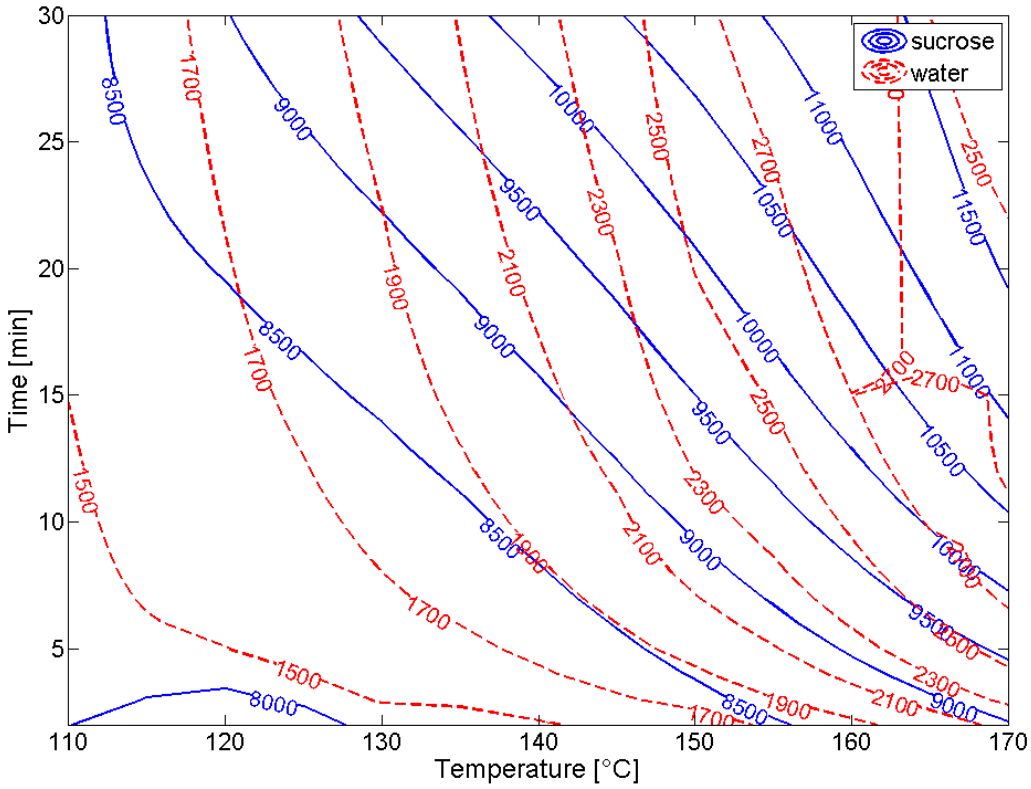

Figure 5-23: Contour lines of RVA peak viscosity in water and in 50% sucrose solution of heat treated flour III in lab-scale experiments as a function of treatment time and temperature

[3] The response surface of peak viscosity in water of flour III was modelled in analogy to the response surface of flour I in chapter 3 (R^2 = 0.99). The response surface of peak viscosity in 50% sucrose solution was modelled as peak viscosity over treatment temperature for different times. A coefficient of determination of 0.87 was obtained.

Figure 5-23 shows that a peak viscosity of e.g. 8500 cP in 50% sucrose solution can be achieved at all temperatures between 110°C and 155°C. A unique characterisation of the time-temperature history that a sample has received is not possible with only one set of contour lines. However, after combining the contour lines of the peak viscosity in water and in 50% sucrose solution, there are regions in the diagram in which the contour lines cross. That means that a combination of the two measures can position a sample precisely on the time-temperature plot.

Table 5-9: Cake volume and RVA peak viscosity in water and 50% sucrose solution of flour after heat treatment in the Revtech and equivalent treatment time and temperature from lab-scale experiments

Temperature setpoint [°C]	Treatment time [min]	Peak viscosity in water [cP]	Peak viscosity in 50% sucrose solution [cP]	Cake volume [ml]	Equivalent time [min]	Equivalent temperature [°C]
110	6.5	1549	8167	504	10 3	116 140
110	10.8	1607	8335	534	17 2	116 150
130	6.5	1926	8411	536	Contour lines do not cross	
130	8.6	2217	8678	575	Contour lines do not cross	
130	10.8	2221	8948	580	Contour lines do not cross	
150	6.7	2884	10236	570	Contour lines do not cross	
170	3.1	2110	8500	554	Contour lines do not cross	
170	6.2	2869	11330	588	29	161
170	15.9	1415	7768	556	Contour lines do not cross	

Table 5-9 shows the data for peak viscosities and cake volumes obtained from the heat treatment of flour in the Revtech equipment (see section 5.6.2). These peak viscosities were

compared to lab-scale results obtained at constant treatment times and temperatures. The corresponding contour lines from Figure 5-23 are shown in Figure 5-24. The contour lines of the peak viscosity in water and in 50% sucrose solution cross for conditions of 110°C and 170°C and 6.2 min (see Figure 5-24a-b), but there are also cases where the contour lines do not cross in the operating window considered (see Figure 5-24c).

a)

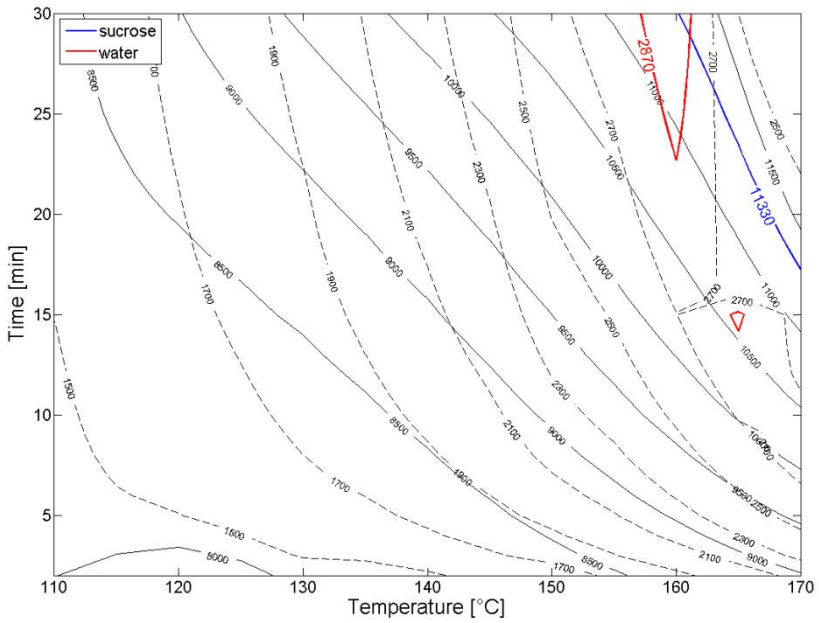

Figure 5-24: Contour lines of RVA peak viscosity in water and in 50% sucrose solution of heat treated flour III depending on treatment time and temperature in lab-scale experiments (black) with highlighted values (blue and red) obtained after flour heat treatment in the Revtech at different processing conditions: a) 170°C, 6.2 min, b) 110°C, 10.8 min, and c) 130°C, 8.6 min

b)

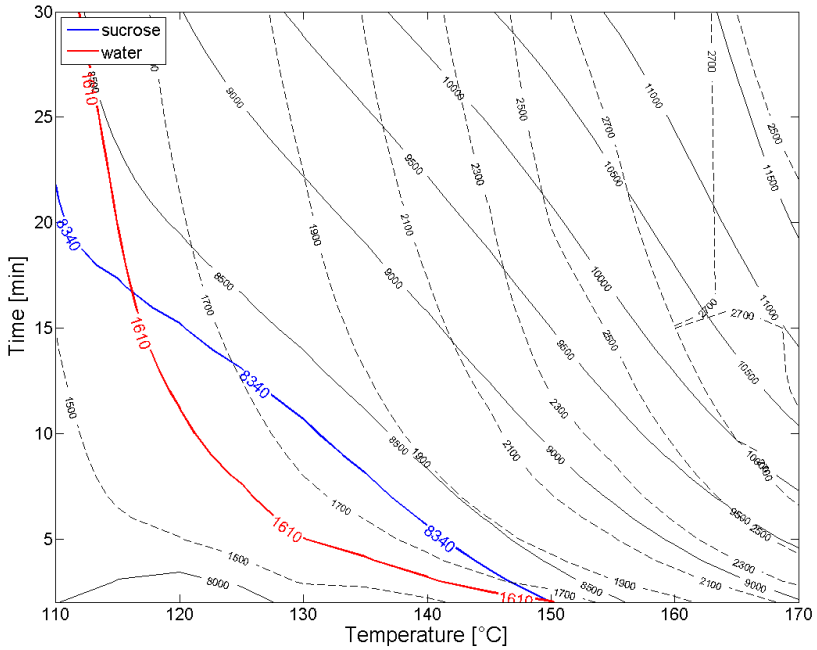

c)

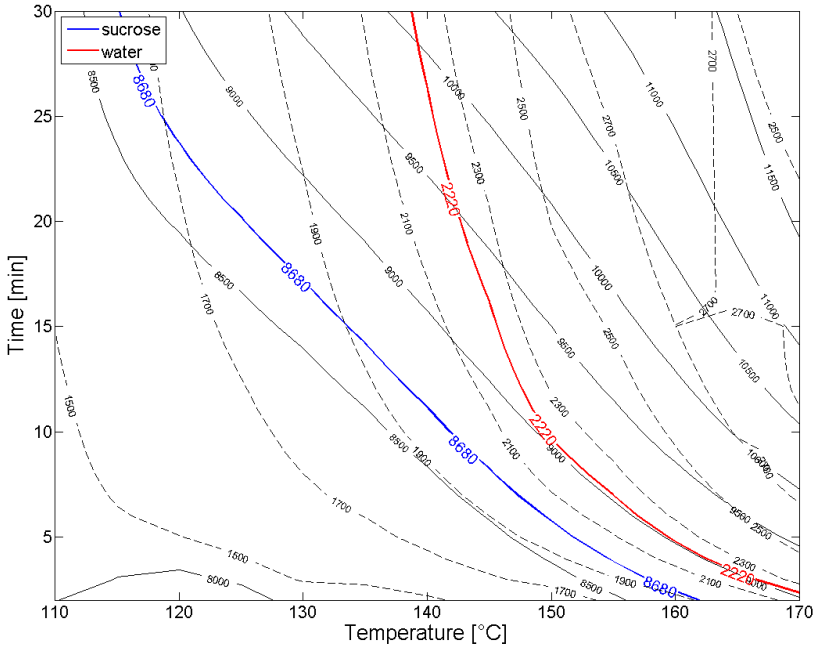

Figure 5-24 (continued): Contour lines of RVA peak viscosity in water and in 50% sucrose solution of heat treated flour III depending on treatment time and temperature in lab-scale experiments (black) with highlighted values (blue and red) obtained after flour heat treatment in the Revtech at different processing conditions: a) 170°C, 6.2 min, b) 110°C, 10.8 min, and c) 130°C, 8.6 min

Should contour lines cross, an equivalent constant treatment temperature and time from lab-scale experiments can be assigned to the flour sample treated in the Revtech. For example, flour that has been treated in the Revtech at a setpoint temperature of 110°C for 10.8 min can be compared to an equivalent, constant treatment temperature of 116°C for 17 min or 150°C for 2 min.

These points may be used to correlate cake quality (e.g. cake volume) with the treated flour sample. This is shown in Figure 5-25. It plots cake volume with equivalent, constant times and temperatures obtained from lab-scale experiments. The correlation seems good, but more data is needed. This may also be done for other cake quality attributes such as texture, colour, or taste. This method suggests that it may not be necessary to bake a cake to evaluate the outcome of a heat treatment process, but 2 types of analytical methods such as RVA tests may suffice. By using this approach, a flour specification could be established.

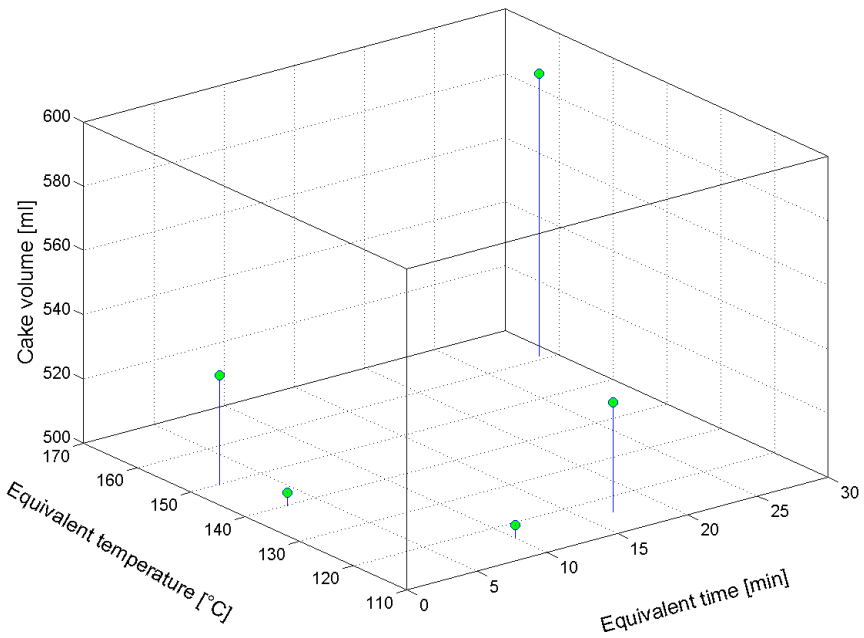

Figure 5-25: Relationship between cake volume and equivalent treatment times and temperatures from Table 5-9

In addition to establishing a flour specification, this method can help to facilitate process validation when new equipment is considered for the heat treatment of flour. It is not always easy to measure the accurate temperature distribution in a device and therefore the temperature experienced by the product (see sections 5.3 and 5.4 for the Revtech equipment). By using Figure 5-23, only the two peak viscosities need to be measured and an equivalent treatment time and temperature can be assigned from lab-scale experiments, which then may be correlated with cake quality.

However, a combination of analytical method is needed that results in less similar contour lines. Furthermore, the contour lines only cross for 3 out of 8 treatment conditions in this case. The reason for this is likely to be the observed phenomenon in section 5.6.2.1. The peak viscosity develops faster and to higher extents for flour after heat treatment in the Revtech in comparison to lab-scale experiments. It may be that another mechanism (e.g. gradual moisture loss) is involved in the development of the peak viscosity and that it is not only a function of time and temperature. Hence, the results of lab-scale experiments and Revtech experiments that only take treatment time and temperature into account might not always be comparable.

The method would need to be repeated for different flour batches, but if the shape of a surface is known, only a small experimental design will be necessary.

The correlation between cake volume and RVA peak viscosity in the previous section would suggest that the approach taken here is not needed. However, no such correlation has been found in literature and the correlation may only be valid before over treatment. Hence, the approach shown here for the development of a cake flour specification is justified.

5.7 Conclusions

The heat treatment of flour in the Revtech equipment was investigated here. The temperature profile in axial direction of the pipe was characterised for different temperature setpoints during stable operation and recirculation mode. The temperature profiles of flour and air passing through the heating pipe were mathematically modelled. The model results are in agreement with measurements of the flour outlet temperature.

The residence time of flour passing through the device at elevated temperature was examined. A continuous product flow without lumping was ensured by extraction of the humid environment in the pipe.

The effect of both treatment time and treatment temperature in the Revtech was evaluated by measuring RVA peak viscosities in water and in 50% sucrose solution and by baking high ratio cakes:

i) The qualitative development of peak viscosity is comparable to lab-scale experiments in that it increases with increasing treatment time and temperature until a certain point, after which it decreases. However, the peak viscosity increases significantly faster and to higher extents after heat treatment in the Revtech in comparison to lab-scale experiments. These findings indicate that peak viscosity does not only depend on time and temperature, but another mechanism is involved. This was suggested to be the gradual water loss that differentiates the treatment in the pilot plant equipment from the lab-scale treatment.

ii) Baking high ratio cakes showed collapsed cakes when baked with untreated flour and an increase in cake volume with increasing flour heat treatment. A correlation

between cake volume and RVA peak viscosity in water was shown. In addition, the results suggest that heat treatment does not only cause the facilitation of the swelling of starch granules (see chapter 3), but it also alters the interactions between flour and other cake ingredients.

To highlight the industrial relevance of the findings in this study, a method was shown to help developing a cake flour specification and to facilitate validation of new processing equipment. The method suggests that it may not be necessary to bake a cake to evaluate the outcome of a heat treatment process, but 2 types of analytical methods such as RVA tests can suffice.

6 Conclusions and future work

The dry heat treatment of flour for the production of high ratio cake flour was successfully implemented on the Revtech system. The objectives of the study were:

i) to investigate changes in flour functionality induced by heat treatment, and

ii) to characterise residence times of particles in the Revtech equipment, and

iii) to examine temperature profiles in the system, and

iv) to evaluate integrated effects of time and temperature after the heat treatment of flour in the Revtech device.

The key outcomes are summarized below and recommendations for future work are given.

6.1 Effect of temperature and time on flour functionality

The alterations in flour functionality after heat treatment were assessed in accurately controlled lab-scale experiments. The most significant findings were:

i) Increased swelling behaviour of flour polymers at ambient conditions as shown by solvent retention capacity tests.

ii) Increased swelling behaviour of starch granules at elevated temperature was found in the Rapid-Visco-Analyser (RVA).

iii) Increased elastic modulus of heat treated flour-water slurries in the rheometer.

iv) Denaturation of proteins after heat treatment. No gluten network formation was found in the rheomixer after severe heat treatments. Solvent retention capacity tests indicated an optimum treatment time for protein hydration.

The results suggest the facilitation of starch granule swelling and enhanced interactions of flour components after heat treatment. In this way, a cake batter made with heat treated flour can be stabilised during baking and the desired cake structure can develop.

No differences in superficial structure of flour components in untreated and heat treated flour samples were observed under the scanning electron microscope (SEM); differences in physical and chemical properties result from changes at a smaller scale than visible under SEM.

The swelling behaviour of starch granules was further investigated in the Rapid-Visco-Analyser in different solvents; water, 50% sucrose solution, 5% lactic acid solution, and 5% sodium carbonate solution. Different effects of the solutes on the starch granules were observed.

In addition, a model was developed to accurately calculate the RVA peak viscosity of flour in water after a stepwise temperature profile was applied to the flour. This was based on the data at constant temperature conditions. It may be used to predict the peak viscosity in industrial processes.

Results from lab-scale experiments may be useful in the development of a cake flour specification or the facilitation of process validation (see below).

6.2 Residence time of flour and grains in the Revtech

The implementation of the heat treatment of flour on the Revtech equipment requires the understanding of treatment times in the tube and the factors impacting on it. The residence time of flour and grains passing through the Revtech system at ambient conditions was characterised in both single experiments and over the period of multiple experiments.

Residence time distributions (RTDs) were accurately determined for flour and grains and could be approximated by normal distributions. The width of the RTDs was generally narrow, which is a critical factor for the accuracy of a thermal process.

Both process parameters motor speed and motor angle had a significant impact on the level of residence time and the development of residence time over extended periods of operation. For example, the residence time decreased considerably with increasing motor angle from 406 s to 261 s to 195 s for grains and from 445 s to 260 s to 200 s for flour at motor angles of 20°, 30°, and 40°.

The residence time was generally found to increase during extended periods of operation at a rate of 0.05 - 0.11 s/min. Several hypotheses concerning the product, the machine, and the environment were tested regarding the cause for this phenomenon. The findings indicate that the formation of a powder layer on the inside of the pipe plays a significant role for the residence time of particles, but the residence time cannot simply be related to the thickness of the layer. Instead, it was suggested that the properties of the layer change over time and influence residence time. Alterations in the layer might be changes in moisture content or electrostatic charge. Electrostatic charging of flour passing through the Revtech system was proven to take place. The data suggests that cleaning reduces the overall effect of increasing

residence times, and that frequent cleaning can allow relatively uniform behaviour. In practice, tests need to be done to confirm the residence time and ensure process uniformity.

A simple model for pasteurisation of particles was developed that characterises the impact of the variation in residence time on microbial inactivation in the Revtech device.

6.3 Heat treatment of flour in the Revtech

The integrated effects of treatment temperature and time on flour during processing in the Revtech system were investigated.

Temperature profiles of flour, air, and the pipe wall were characterised and residence times of flour passing through the device at elevated temperatures were determined. The effect of treatment was evaluated by measuring peak viscosities in the Rapid-Visco-Analyser in water and in 50% sucrose solution and by baking high ratio cakes:

i) The qualitative development of the RVA peak viscosity was comparable to lab-scale experiments. However, the peak viscosity increased more rapidly and to higher extents after heat treatment in the Revtech in comparison to lab-scale experiments. The findings indicate that peak viscosity does not only depend on time and temperature, but other factors are involved. This was suggested to be the gradual water loss that differentiates the treatment in the pilot plant equipment from the lab-scale treatment.

ii) Baking high ratio cakes showed collapsed cakes when baked with untreated flour and an increase in cake volume with increasing intensity of flour heat treatment. A

correlation between cake volume and RVA peak viscosity in water was shown before over-treatment.

To highlight the industrial relevance of the findings in this work, a method was shown to help in developing a cake flour specification and to facilitate validation of new processing equipment. The approach combines results from lab-scale experiments with Revtech experiments. The findings indicate that it may not be necessary to bake a cake to evaluate the outcome of a heat treatment process, but 2 types of analytical methods such as RVA tests suffice.

6.4 Future work

Based on the conclusions developed from this thesis, it is recommended that the emphasis of further studies is on the development of a cake flour specification as demonstrated in this work, which will also facilitate the validation of new processing equipment. Such a standard would be beneficial to bakeries as well as to equipment manufacturers. The following aspects may be considered:

i) The RVA peak viscosity of flour in water was shown to depend on treatment time and temperature in lab-scale experiments. However, results from flour heat treatment in the Revtech system suggest other factors might be involved such as slow moisture removal from the flour. This should be further studied in lab-scale experiments.

ii) It was shown that the time-temperature history of flour may be uniquely characterised by combination of analytical methods, which is significant for the

development of a cake flour specification. Future work should focus on identifying such methods that deliver contour lines which are less similar than those from the two RVA methods presented here.

iii) Once i) and ii) are accomplished, cakes should be baked from flour that has been heat treated in the Revtech equipment and a correlation might be found between the equivalent treatment conditions from lab-scale experiments and cake quality attributes (see section 5.6.3), which would then characterise a cake flour specification.

iv) The residence time of flour and grains in the Revtech device was shown to increase over extended periods of operation. Reasons for the increase and the extent at different processing conditions should be further investigated.

List of References

"Air Properties" (2016). http://www.engineeringtoolbox.com/air-properties-d_156.html. *(accessed 09/2016)*.

"Convective Heat Transfer" (2016). http://www.engineeringtoolbox.com/convective-heat-transfer-d_430.html. *(accessed 09/2016)*.

"Density of Air" (2016). https://en.wikipedia.org/wiki/Density_of_air. *(accessed 09/2016)*.

AACCI Approved Method 44-15.02 (1999). AACC International. Approved Methods of Analysis, 11th Ed., Moisture - Air oven methods. *Available online. AACCI: St. Paul, MN*.

AACCI Approved Method 54-40.02 (1999). AACC International. Approved Methods of Analysis, 11th Ed., Mixograph Method. *Available online. AACCI: St. Paul, MN*.

AACCI Approved Method 56-11.02 (2009). AACC International. Approved Methods of Analysis, 11th Ed., Solvent Retention Capacity Profile. *Available online. AACCI: St. Paul, MN* **11**.

AACCI Approved Method 76-21.01 (1999). AACC International. Approved Methods of Analysis, 11th Ed., General Pasting Method for Wheat or Rye Flour or Starch Using the Rapid Visco Analyser. *Available online. AACCI: St. Paul, MN*.

Al-Dmoor, H.M. (2013). Cake flour: Functionality and quality (Review). *European Scientific Journal* **9,** 166-180.

Alexander, G.L. (1939). Soft-Wheat Testing Problems. *Cereal Chemistry* **16,** 197-208.

Almond Board of California (2007). http://www.almonds.com/sites/default/files/content/attachments/proprietary-processes.pdf. *(accessed 02/2017)*.

Anderson, C. Characterising wheat flour protein quality from rheomixer traces. Rep. no. 324. 2003. HGCA.

Anson, M.L. and Mirsky, A.E. (1932). The effect of denaturation on the viscosity of protein systems. *The Journal of General Physiology* **15,** 341-350.

Barrile, J.C. and Cone, J.F. (1970). Effect of added moisture on the heat resistance of Salmonella anatum in milk chocolate. *Applied Microbiology* **19,** 177-178.

Bean, M.M. and Yamazaki, W.T. (1973). Wheat starch gelatinization in sugar solutions. I. Sucrose: Microscopy and viscosity effects. *Cereal Chemistry* **55,** 936-944.

Bent, A.J., Bennion, E.B., and Bamford, G.S.T. (1997). *The Technology of Cake Making*. Springer US.

Beuchat, L., Komitopoulou, E., Betts, R., Beckers, H., Bourdichon, F., Joosten, H. et al. Persistence and Survival of Pathogens in Dry Foods and Dry Food Processing Environments. 2011. International Life Sciences Institute Europe.

Beuchat, L.R., Komitopoulou, E., Beckers, H., Betts, R., Bourdichon, F., Fanning, S., Joosten, H., and ter Kuile, B. (2013). Low-Water Activity Foods: Increased Concern as Vehicles of Foodborne Pathogens. *Journal of Food Protection* **76,** 150-172.

Bird, R.B., Stewart, W.E., and Lightfoot, E.N. (2005). *Transport phenomena*. Singapore: John Wiley & Sons, Inc.

Buleon, A., Colonna, P., Planchot, V., and Ball, S. (1998). Starch granules: structure and biosynthesis. *International Journal of Biological Macromolecules* **23,** 85-112.

Campden BRI (2012). Biscuit & Flour Confectionary Recipe. Cake: High ratio yellow cake. *Recipe No. 34*.

Campden BRI (2015). *Machine Guide: TecVol BVM-L370 Bread Volume Analyser*.

Catterall, P.F. The production of cakes from non-chlorinated cake flour. Rep. no. 20. 2000. Campden & Chorleywood Food Research Association Group, Campden BRI (Chipping Campden, UK).

Catterall, P.F. (2014). *Personal Communication (Campden BRI, UK)*.

Cauvain, S.P. (2001). Breadmaking. In *Cereals processing technology*. (ed. Owens,G.), pp. 204-230. Woodhead Publishing Limited.

Cauvain, S.P., Hodge, D.G., Muir, D.D., and Dodds, N.J.H. Improvements in and relating to treatment of grain. 1976. UK Patent No. 1,444,173.

Cauvain, S.P. and Muir, D.D. High-ratio yellow cakes: the effect of flour particle size. Rep. no. 61. 1974. Flour Milling and Baking Research Association, Chorleywood (UK).

Cauvain, S.P. and Young, L.S. (2009). *The ICC Handbook of Cereals, Flour, Dough & Product Testing*. Lancaster, Pennsylvania, USA: DEStec Publications, Inc.

Chamberlain, N. (1962). Research on flour confectionery. *BBIRA Bulletin* **6,** 160-167.

Chesterton, A.K.S., Wilson, D.I., Sadd, P.A., and Moggridge, G.D. (2015). A novel laboratory scale method for studying heat treatment of cake flour. *Journal of Food Engineering* **144,** 36-44.

Chick, M. Thermal Inactivation Kinetics of Salmonella Serovars on Dry Cereal. 2011. M.S. thesis. Retrieved from the University of Minnesota Digital Conservancy. http://purl.umn.edu/116854

Chubb, J. (2010). *An introduction to electrostatic measurements*. New York: Nova Science Publishers, Inc.

Chubb, J. and Walmsley, H. (2010). Analysis of long corona charge decay times. *Journal of Electrostatics* **68,** 284-286.

Clements, R.L. and Donelson, J.R. (1982). Role of Free Flour Lipids in Batter Expansion in Layer Cakes. I. Effects of "Aging". *Cereal Chemistry* **59,** 121-124.

Codex Alimentarius Commisson . Proposed Draft Code of Hygienic Practice for Low-Moisture Foods CX/FH 13/45/7. 2013. Food and Agriculture Organization of the United Nations, World Health Organization.

Collyer, D.M. High-ratio cake - a review of the literature. Rep. no. 18. 1968. Flour Milling and Baking Research Association, Chorleywood (UK).

Cook, S. Factors affecting the production of cakes from heat-treated cake flour. Rep. no. 20 - Supplement 1. 2002. Campden & Chorleywood Food Research Association Group, Campden BRI (Chipping Campden, UK).

Cornell, H.J. (2012). 3 - The chemistry and biochemistry of wheat. In *Breadmaking (Second edition)Woodhead Publishing Series in Food Science, Technology and Nutrition*. pp. 35-76. Woodhead Publishing.

Cornford, S.J. (1961). The mechanism of fruit holding in high-ratio cake batters. *Journal of the Science of Food and Agriculture* **12,** 693-700.

Crosbie, G.B. and Ross, A.S. (2007). *The RVA Handbook*. American Association of Cereal Chemists.

Da Rosa Zavareze, E. and Guerra Dias, A.R. (2011). Impact of heat-moisture treatment and annealing in starches: A review. *Carbohydrate Polymers* **83,** 317-328.

Doe, C.A.F. and Russo, J.V.B. Flour Treatment Process. 1968. UK Patent No. 1110711.

Doe, C.A.F. and Russo, J.V.B. Flour treatment process. 1970. US Patent 3490917.

Donelson, J.R., Yamazaki, W.T., and Kissell, L.T. (1984). Functionality in White Layer Cake of Lipids from Untreated and Chlorinated Patent Flours. II. Flour Fraction Interchange Studies. *Cereal Chemistry* **61,** 88-91.

FAOSTAT (2016). http://faostat.fao.org/. *(accessed 09/2016)*.

Flick, D., Doursat, C., Grenier, D., and Lucas, T. (2015). Modelling of baking processes. In *Modeling Food Processing Operations*. (ed. Bakalis,S., Knoerzer,K., and Fryer,P.J.), pp. 129-161. Woodhead Publishing.

Germaine, K., Quail, K., and Walker, C. (2004). Use of the RVA for Measuring Cake Flour Heat Treatment. *The technical journal of Newport Scientific*.

Gil, A.M. (2012). 4 - Techniques for analysing wheat proteins. In *Breadmaking (Second edition)Woodhead Publishing Series in Food Science, Technology and Nutrition*. pp. 77-99. Woodhead Publishing.

Gough, B.M., Greenwood, C.T., and Whitehouse, M.E. The role and function of chlorine in the preparation of high-ratio cake flour. Rep. no. 75. 1977. Flour Milling and Baking Research Association, Chorleywood (UK).

Greatbatch, S. (2015). *Personal Communication (Bowmans)*.

Gusek, T.W. Microwave treatment of unchlorinated cake flour. 1994. International Patent WO 94/00018.

Guy, R.C.E. Starch Handbook. Rep. no. 51. 2006. Campden & Chorleywood Food Research Association Group.

Guy, R.C.E. and Mair, C. The Improvement of wheat flours for use in high-ratio cakes product - Heat moisture treatments. Unpublished work (Campden BRI). 1993.

Guy, R.C.E. and Pithawala, H.R. (1981). Rheological studies of high ratio cake batters to investigate the mechanism of improvement of flour by chlorination or heat treatment. *International Journal of Food Science & Technology* **16,** 153-166.

Guy, R.C.E., Skinner, K., and Sahi, S. Effects of manufacturing processes on the performance of starch: Heat-treated flours and starches. 2007. Campden & Chorleywood Research Association.

Hanamoto, M. and Bean, M. Process for improving baking properties of unbleached cake flour. 1979. US Patent No. 4,157,406.

Harrel, C.G. (1952). Maturing and bleaching agents used in producing flour. *Ind. Eng. Chem.* **44,** 95-100.

Harris, L.J., Uesugi, A.R., Abd, S., and McCarthy, K.L. (2012). Survival of Salmonella Enteritidis PT 30 on inoculated almond kernels in hot water treatments. *Food Research International* **45,** 1093-1098.

Hatcher, D.W. (2001). Asian noodle processing. In *Cereals processing technology*. (ed. Owens,G.), pp. 131-157. Woodhead Publishing Limited.

Heldman, D.R. (2011). Kinetic Models for Food Systems. In *Food Preservation Process Design*. pp. 19-48.

Hesso, N., Loisel, C., Chevallier, S., Le-Bail, A., Queveau, D., Pontoire, B., and Le-Bail, P. (2015). Monitoring cake baking by studying different ingredient interactions: From a model system to a real system. *Food Hydrocolloids* **51,** 7-15.

Hodge, D.G. (1975). Alternatives to chlorination for high ratio cake flours. *Baking Industries Journal* 12-19.

Hoseney, R.C. (1984). Functional properties of pentosans in baked foods. *Journal of Food Technology* **38,** 114-117.

Hutkins, R.W. (2008). Bread fermentation. In *Microbiology and Technology of Fermented Foods*. (ed. Hutkins,R.W.), pp. 261-299. Wiley-Blackwell Publishing.

Incropera, F.P. and DeWitt, D.P. (2007). *Fundamentals of Heat and Mass Transfer*. John Wiley & Sons.

Izydorczyk, M.S. and Biliaderis, C.G. (1995). Cereal arabinoxylans: advances in structure and physicochemical properties. *Carbohydrate Polymers* **28,** 33-48.

Jacobsberg, F.R. and Daniels, N.W.R. (1974). Gelatinisation properties of high-ratio cake flours. *Chemistry and Industry* **21,** 1007-1008.

Jeong, S., Marks, B.P., and Orta-Ramirez, A. (2009). Thermal Inactivation Kinetics for Salmonella Enteritidis PT30 on Almonds Subjected to Moist-Air Convection Heating. *Journal of Food Protection* **72,** 1602-1609.

Johnson, A.C. and Hoseney, R.C. (1980). Chlorine Treatment of Cake Flours. IV. Effects of Storing and Heating Nondefatted and Defatted Flours. *Cereal Chemistry* **57,** 92-93.

Kent, N.L. (1994). *Kent's Technology of Cereals*. Woodhead Publishing.

Keppler, S., Bakalis, S., Leadley, C.E., and Fryer, P.J. (2016a). A Systematic Study of the Residence Time of Flour in a Vibrating Apparatus Used for Thermal Processing. *Innovative Food Science and Emerging Technologies* **33,** 462-471.

Keppler, S., Bakalis, S., Leadley, C.E., and Fryer, P.J. (2016b). Processing of barley grains in a continuous vibrating conveyor. *Journal of Food Engineering* **187,** 114-123.

Kiszonas, A.M., Fuerst, E.P., and Morris, C.F. (2013). Wheat Arabinoxylan Structure Provides Insight into Function. *Cereal Chemistry* **90,** 387-395.

Klingler, R.W. (2010). *Grundlagen der Getreidetechnologie*. Hamburg: Behr's Verlag.

Kulp, K., Olewnik, M., and Bachofer, C. (1985). Functional Effects of Chlorinated Flour on Cookie Spread and Quality of Sugar Snap Cookies. *American Institute of Baking - Technical Bulletin* **VII**.

Kulp, K. and Tsen, C.C. Effect of Chlorine on the Starch Component of Soft Wheat Flour. AACC Annual Meeting. 1972.

Kweon, M., Slade, L., and Levine, H. (2011). Solvent Retention Capacity (SRC) Testing of Wheat Flour: Principles and Value in Predicting Flour Functionality in Different Wheat-Based Food Processes and in Wheat Breeding -A Review. *Cereal Chemistry* **88,** 537-552.

Kweon, M., Slade, L., Levine, H., Martin, R., Andrews, L., and Souza, E. (2009). Effects of Chlorination, Extraction Rate, and Particle Size Reduction on Flour and Gluten Functionality Explored by Solvent Retention Capacity (SRC) and Mixograph. *Cereal Chemistry* **86,** 221-224.

Kweon, M., Slade, L., Levine, H., and Souza, E. (2010). Application of RVA and Time-Lapse Photography to Explore Effects of Extent of Chlorination, Milling Extraction Rate, and Particle-Size Reduction of Flour on Cake-Baking Functionality. *Cereal Chemistry* **87,** 409-414.

Lee, S.-Y., Oh, S.-W., Chung, H.-J., Reyes-De-Corcuera, J.I., Powers, J.R., and Kang, D.-H. (2006). Reduction of Salmonella enterica Serovar Enteritidis on the Surface of Raw Shelled Almonds by Exposure to Steam. *Journal of Food Protection* **69,** 591-595.

Mangels, C.E. (1934). Some effects of heat exposure on wheat starches. *Cereal Chemistry* **11,** 86-94.

Manley, D., Pareyt, B., and Delcour, J.A. (2011). Wheat flour and vital wheat gluten as biscuit ingredients. In *Technology of biscuits, crackers and cookies*. (ed. Manley,D.), pp. 109-133.

Mann, J., Schiedt, B., Baumann, A., Conde-Petit, B., and Vilgis, T.A. (2014). Effect of heat treatment on wheat dough rheology and wheat protein solubility. *Food Science and Technology International* **20,** 341-351.

Marchylo, B.A. (2001). Pasta production. In *Cereals processing technology*. (ed. Owens,G.), pp. 109-130. Woodhead Publishing Limited.

Mattick, K.L., Jorgensen, F., Legan, J.D., Cole, M.B., Porter, J., Lappin-Scott, H.M., and Humphrey, T.J. (2000). Survival and filamentation of Salmonella enterica Serovar Enteritidis PT4 and Salmonella enterica Serovar Typhimurium DT104 at low water activity. *Applied and environmental microbiology* **66,** 1274-1279.

Meza, B.E., Chesterton, A.K.S., Verdini, R.A., Rubiolo,A.C., Sadd, P.A., Moggridge, G.D., and Wilson, D.I. (2011). Rheological characterisation of cake batters generated by planetary mixing: Comparison between untreated and heat-treated wheat flours. *Journal of Food Engineering* **104,** 592-602.

Mills, C.E.N., Wellner, N., Salt, L.A., Robertson, J., and Jenkins, J.A. (2012). 5 - Wheat proteins and bread quality. In *Breadmaking (Second edition) Woodhead Publishing Series in Food Science, Technology and Nutrition*. pp. 100-122. Woodhead Publishing.

Miri, T. (2010). Viscosity and Oscillatory Rheology. In *Practical Food Rheology: An Interpretive Approach*. (ed. Norton,I.T., Spyropoulos,F., and Cox,P.), pp. 7-28.

Miskelly, D., Batey, I.L., and Suter, D.A.I. (2010). Processing wheat to optimise product quality. In *Cereal Grains. Assessing and Managing Quality*. (ed. Wrigley,C.W. and Batey,I.L.), pp. 431-457. Woodhead Publishing Limited.

Montzheimer, J.W. (1931). A study of methods for testing cake flour. *Cereal Chemistry* **8,** 510-517.

Morrison, W.R. (1978). The Stability of Wheat Starch Lipids in Untreated and Chorine-treated Cake Flours. *Journal of the Science of Food and Agriculture* **29,** 365-371.

Neill, G., Al-Muhtaseb, A.H., and Magee, T.R.A. (2012). Optimisation of time/temperature treatment, for heat treated soft wheat flour. *Journal of Food Engineering* **113,** 422-426.

Nicholas, E.M., Boynton, G.E., Russo, J.V., and Totty, R. Flour Treatment Process. [US 1499986]. 1978. US 1499986.

Ozawa, M., Kato, Y., and Seguchi, M. (2009). Investigation of Dry-Heated Hard and Soft Wheat Flour. *Starch* **61,** 398-406.

Penaloza Izurieta, W. and Komitopoulou, E. (2012). Effect of moisture on salmonella spp. heat resistance in cocoa and hazelnut shells. *Food Research International* **45,** 1087-1092.

Perten Instruments . Rapid Visco Analyser RVA SUPER 4 Installation and Operation Manual. 2010.

Podolak, R., Enache, E., Stone, W., Black, G., and Elliott, P.H. (2010). Sources and Risk Factors for Contamination, Survival, Persistance, and Heat Resistance of Salmonella in Low-Moisture Foods. *Journal of Food Protection* **73,** 1919-1936.

Poole,M. (2014). *Personal Communication (Campden BRI, UK)*.

Revtech Process Systems (2016). *Personal Communication*.

Riganakos, K.A. and Kontominas, M.G. (1994). GC study of the effect of specific heat treatment on water sorption by wheat and soy flour. *Zeitschrift fur Lebensmittel-Untersuchung und -Forschung* **198,** 47-51.

Ross, A.S. (2012). Starch in Foods. In *Food Carbohydrate Chemistry*. (ed. Wrolstad,R.E.), pp. 107-131.

Russo, J.V. and Doe, C.A. (1970). Heat treatment of flour as an alternative to chlorination. *Journal of Food Technology* **5,** 363-374.

Sahi, S. (2015). *Personal Communication (CampdenBRI, UK)*.

Sahin, S. (2008). Cake Batter Rheology. In *Food Engineering Aspects of Baking Sweet Goods*. pp. 99-120. CRC Press.

Saulnier, L., Sado, P.-E., Branlard, G., Charmet, G., and Guillon, F. (2007). Wheat arabinoxylans: Exploiting variation in amount and composition to develop enhanced varieties. *Journal of Cereal Science* **46,** 261-281.

Seguchi, M. and Yamada, Y. (1988). Hydrophobic Character of Heat-Treated Wheat Starch. *Cereal Chemistry* **65,** 375-376.

Shelke, K., Faubion, J.M., and Hoseney, R.C. (1990). The Dynamics of Cake Baking as Studied by a Combination of Viscometry and Electrical Resistance Oven Heating. *Cereal Chemistry* **67,** 575-580.

Shewry, P.R. (2009). Wheat. *Journal of Experimental Botany* **60,** 1537-1553.

Silva, F.V.M. and Gibbs, P.A. (2012). Thermal pasteurization requirements for the inactivation of Salmonella in foods. *Food Research International* **45,** 695-699.

Stewart, B.A. The suitability of English wheat for the production of high ratio cake flour. Technologists' Conference of the Cake and Biscuit Alliance Ltd. 1969.

Telloke, G.W. Chlorination of cake flour. Rep. no. 131. 1986. Flour Milling and Baking Research Association, Chorleywood (UK).

Thomasson, C.A., Miller, R.A., and Hoseney, R.C. (1995). Replacement of Chlorine Treatment for Cake Flour. *Cereal Chemistry* **72,** 616-620.

Tsen, C.C., Kulp, K., and Daly, C.J. Effects of Chlorine on Flour Proteins, Dough Properties, and Cake Quality. AACC 54th Annual Meeting. 1971.

Van Steertegem, B., Pareyt, B., Slade, L., Levine, H., Brijs, K., and Delcour, J.A. (2013). Impact of Heat Treatment on Wheat Flour Solvent Retention Capacity (SRC) Profiles. *Cereal Chemistry* **90,** 608-610.

Villa-Rojas, R., Tang, J., Wang, S., Gao, M., Kang, D.-H., Mah, J.-H., Gray, P., Sosa-Morales, M.E., and Lopez-Malo, A. (2013). Thermal Inactivation of Salmonella Enteritidis PT 30 in Almond Kernels as Influenced by Water Activity. *Journal of Food Protection* **76,** 26-32.

Wheelock, T.D. and Lancaster, E.B. (1970). Thermal Properties of Wheat Flour. *Starch* **22,** 44-48.

Whistler, R.L., Mittag, T.W., and Ingle, T.R. (1966). Mechanism of starch depolymerization with chlorine. *Cereal Chemistry* **43,** 371.

Whistler, R.L., Spencer, W.W., Goatley, J.L., and Nikuni, Z. (1958). Effect of drying on the presence of cavities in corn starch granules. *Cereal Chemistry* **35,** 331-336.

Zeeman, S.C., Kossmann, J., and Smith, A.M. (2010). Starch: its metabolism, evolution, and biotechnological modification in plants. *Annu. Rev. Plant. Biol.* **61,** 209-234.

Appendix

The work presented in this thesis has been published in scientific journals. The publications are provided here in full length:

- Palgan, I., Limburn, R., Maguire, E., Keppler, S. (2015). “Challenges in validation of processes for low water activity foods.” *New Food Magazine*, 18 (3), 58-62
- Keppler, S., Bakalis, S., Leadley, C.E., and Fryer, P.J. (2016). “A systematic study of the residence time of flour in a vibrating apparatus used for thermal processing.” *Innovative Food Science and Emerging Technologies*, 33, 462-471.
- Keppler, S., Bakalis, S., Leadley, C.E., and Fryer, P.J. (2016). “Processing of barley grains in a continuous vibrating conveyor.” *Journal of Food Engineering*, 187, 114-123.

Izabela Palgan, Rob Limburn and Emma Maguire
Campden BRI

Silvia Keppler
School of Chemical Engineering, University of Birmingham

Challenges in validation of processes for low water activity foods

Herbs, spices, nuts, seeds and other dry ingredients such as cereal or dried vegetables can contribute significantly to the nutritional quality of products. A variety of these ingredients have been increasing in popularity in recent years due to consumers' palates becoming more sophisticated, interests in healthy alternative ingredients and international food recipes spreading globally. Many of these dry ingredients commonly contain a high natural microbiological load, including those microorganisms that cause food poisoning.

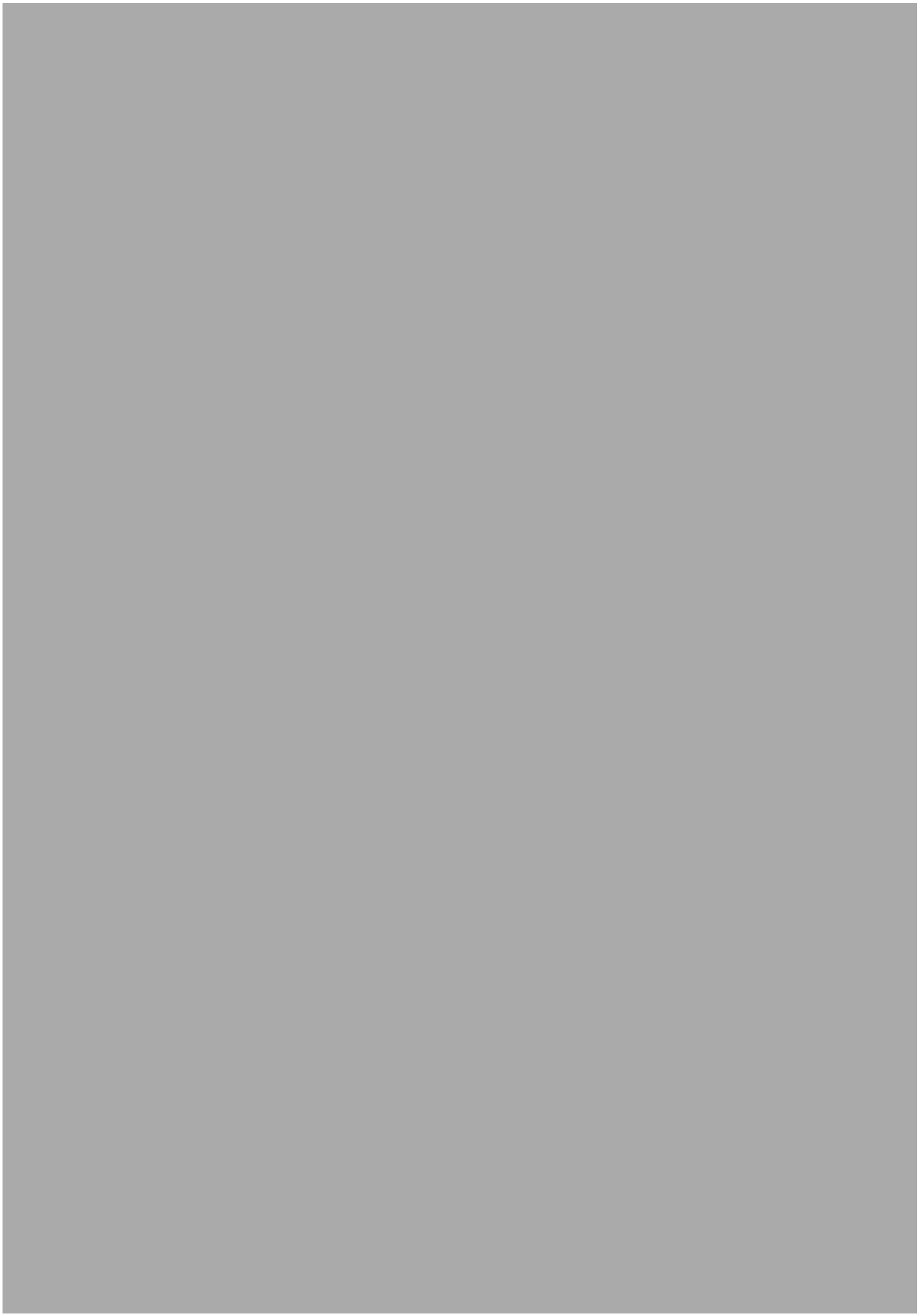

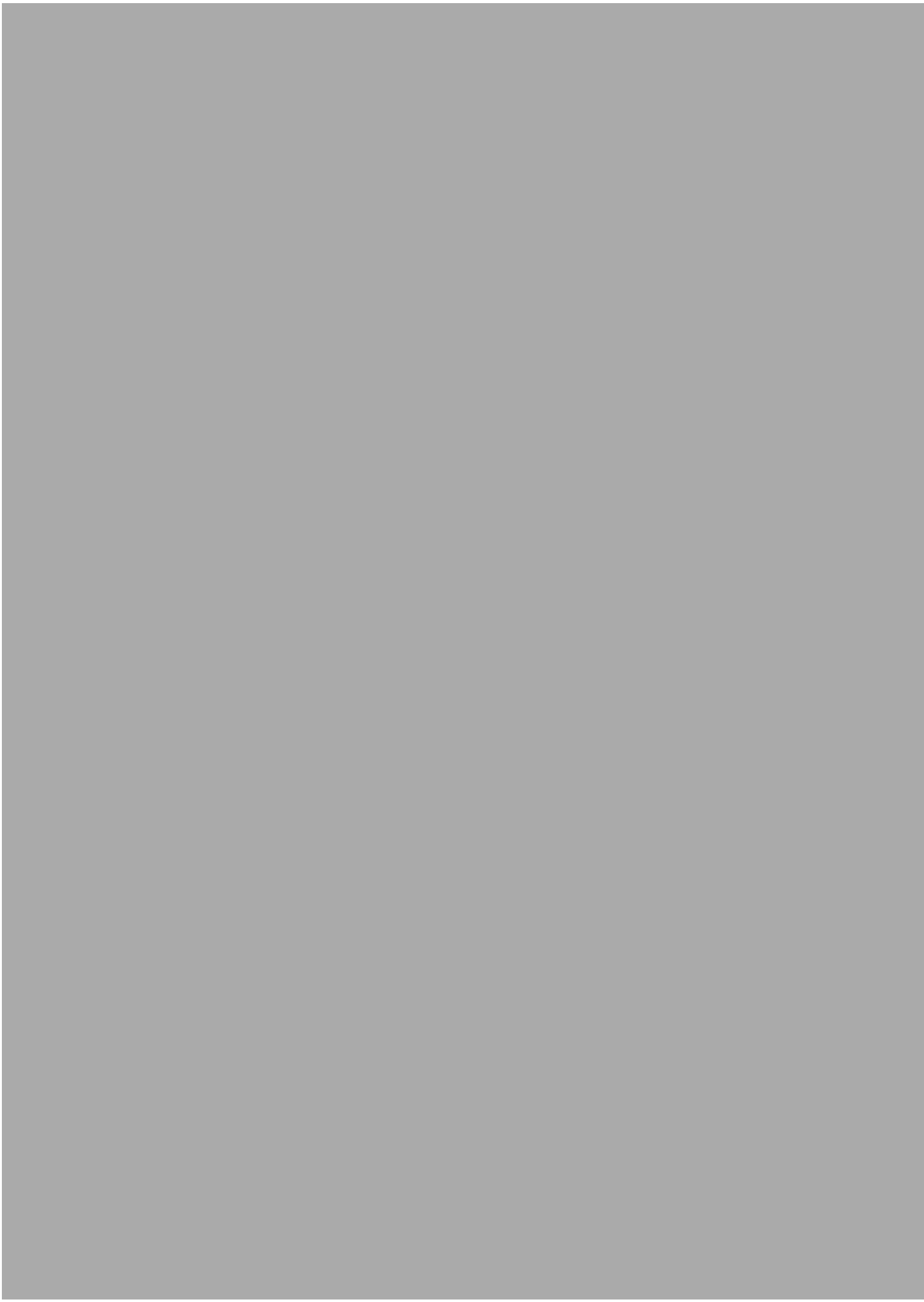

Innovative Food Science and Emerging Technologies 33 (2016) 462–471

Contents lists available at ScienceDirect

Innovative Food Science and Emerging Technologies

journal homepage: www.elsevier.com/locate/ifset

A systematic study of the residence time of flour in a vibrating apparatus used for thermal processing

S. Keppler [a,*], S. Bakalis [a], C.E. Leadley [b], P.J. Fryer [a]

[a] University of Birmingham, School of Chemical Engineering, Edgbaston, Birmingham, B15 2TT, UK
[b] Campden BRI Gloucestershire, UK

ARTICLE INFO

Article history:
Received 1 October 2015
Accepted 2 December 2015
Available online 17 December 2015

Keywords:
Vibrating apparatus
Residence time distributions
Heat treatment of flour
Particle flow

ABSTRACT

The dry heat treatment of flour is well established for the production of cake flour for high ratio cakes. This study investigates a new tubular apparatus in which flour is conveyed by vibrations through a helical pipe. Residence time distributions (RTDs) of flour were characterised for various processing conditions and the development of the residence time in extended operation was analysed.

A method was developed to accurately determine the RTDs, which could be approximated by normal distributions. The width of the distributions is a critical factor for the accuracy of a thermal process and was identified for different processing conditions. The distributions were narrow, with variations of $\pm 1\%$ at most.

In some cases, the residence time increased over 3.5 h of machine run-time by 7.7%–13.9%. To explain this phenomenon, several hypotheses have been tested. The machine performance was constant with time and no influence of ambient temperature or humidity could be found. It was furthermore shown that changes in the bulk material passing through the apparatus were not the cause of the increase. However, electrostatic charging of the material was observed.

Two things led to a reduction in residence time: i) cleaning the pipe with a cleaning pig and water and ii) time, during which the machine is not running. It was suggested that a thin layer of particles inside the pipe in combination with electrostatics effects could be the reason for the residence time increase. Frequent cleaning can therefore allow relatively uniform behaviour and control of residence time.

Industrial relevance: This work investigates the potential application of a novel, vibrating device for the dry heat treatment of flour as a replacement for chlorination in the production of cake flour. Since chlorination was banned in the EU in the year 2000, there is an industrial interest for alternative treatments and equipment to produce flour for high ratio cakes.

1. Introduction

High ratio cake formulations are widespread in the UK in the production of sponges (e.g. Madeira cake), Angel cake, gateaux, slab cakes, or cupcakes (Hodge, 1975). Their sweet and moist characteristics achieved by a sugar to flour ratio of 1.0–1.4 are well appreciated by the market (Chesterton, Wilson, Sadd, & Moggridge, 2015; Guy & Pithawala, 1981; Magee & Neill, 2011). In comparison, cakes with lower or equal amounts of sugar and flour refer to low ratio cakes (Wilderjans, Luyts, Brijs, & Delcour, 2013). To achieve the desired attributes in high ratio cakes, it is required to use flour with a distinctive functionality to carry more water and sugar compared to flour used in low ratio cakes (Collyer, 1968). This was formerly accomplished by treating flour with chlorine gas (Collyer, 1968; Hodge, 1975).

During the baking process of a high ratio cake, the viscosity of the batter increases due to starch gelatinisation and protein coagulation (Cook, 2002). The key element is that previously introduced bubbles by water vapour, heat expansion, and CO_2 expand and eventually burst due to increasing internal pressure transforming the viscous foam structure into a solid foam with uniform air cells distributed evenly throughout the cake (Cook, 2002; Meza et al., 2011). Untreated flour does not provide the necessary batter viscosity for the bubbles to rupture and the cake collapses when the temperature falls on removal from the oven (Cook, 2002). In contrast, chlorination increases the swelling capacity of the starch granules and the hydration capacity of gluten ensuring the mutual contact between starch granules after gelatinisation, increasing batter viscosity, allowing the cake structure to solidify in the final stages of baking and thus preventing the cake from collapsing (Collyer, 1968; Gough, Greenwood, & Whitehouse, 1977; Guy & Pithawala, 1981).

Whereas chlorination of flour is still used in the US, the process was banned in the EU in 2000 after concerns about health risks were raised

* Corresponding author. Tel.: +44 7557651407.
E-mail address: sxk250@bham.ac.uk (S. Keppler).

http://dx.doi.org/10.1016/j.ifset.2015.12.003

(Catterall, 2000). Two general alternatives appeared to be other treatment processes or the modification of cake formulations (Gough et al., 1977).

In this context, Mangels in 1934 had discovered that the dry heat treatment of starch increased its rate of swelling in dilute sodium hydroxide solution (Hodge, 1975). This is the basis of the current heat treatment process of flour in industry, which generally involves 3 thermal steps followed by rehydration and milling (Chesterton et al., 2015). Specific details of flour heat treatments are not readily available in the public domain. In a first drying step, the flour is heated up and the moisture content is reduced, preferably below 4% in a stream of hot air (Chesterton et al., 2015; Neill, Al-Muhtaseb, & Magee, 2012). In a second heat treatment step, the flour is held at high temperatures by contact heating in rotated drums or heated conveyors (e.g. 120 °C–140 °C, 20–30 min) (Chesterton et al., 2015; Doe & Russo, 1970). After a cooling step to interrupt the heat treatment, the flour is rehydrated to a moisture content of e.g. 7%–12% (Chesterton et al., 2015; Neill et al., 2012). A final milling step is generally applied to break up agglomerates formed during rehydration (Chesterton et al., 2015).

As the dry heat treatment of flour is a physical modification, it is broadly accepted in public in contrast to chemical methods (Hodge, 1975; Thomasson, Miller, & Hoseney, 1995). Little is published about the alterations in flour generated by heat treatment, but the key effect of flour improvement appears to relate to the surface of the starch granules and its neighbouring layers (Guy & Pithawala, 1981; Magee & Neill, 2011). Two major effects of flour improvement by heat treatment were specified (Cook, 2002; Guy & Pithawala, 1981):

i) Improved swelling power of the starch granules and thereby increasing the batter viscosity
ii) Increased interaction between the starch and egg proteins, increasing the gel firmness for batters of treated flours.

In this study, a novel machine (Revtech, 2015) is presented that can potentially be used for the continuous heat treatment of flour. The core piece consists of a helical tube that is heated via resistive heating and that conveys the product from the bottom to the top of the spiral by vibrations. With the aim of designing a uniform and efficient process it is essential to investigate residence time distributions of the product passing through the machine as well as to examine the applied temperature profiles. The present work focuses on the residence time distributions depending on various processing conditions and their peculiarities with respect to the dynamics of the system.

2. Materials and methods

2.1. Material

Commercially available high ratio flour (protein content 8.6%) with the particle size distribution shown in Fig. 1 (calculated from triplicates) was used for the experiments. Bulk density and tap density were measured to be 0.51 ± 0.003 g/ml and 0.81 ± 0.01 g/ml.

2.2. Equipment

The equipment used for the experiments is a continuous, thermal processing unit manufactured by Revtech process systems (Loriol-sur-Drome, France). It consists of three major parts, a hopper, a heating spiral, and a cooling spiral. In this study only the hopper and the heating spiral were used for simplicity. As shown in Fig. 2, particles are conveyed by a screw feeder (B) from the hopper (A) into the spiral. It is a helical, steel pipe (C) with an internal diameter of 84.5 mm, a slope of 2.83° to the horizontal, and a length of approximately 34.4 m. It is possible both to heat the pipe by resistive heating and to inject steam. The screw speed controls the overall particle flow, whilst the behaviour in the tubing is controlled by

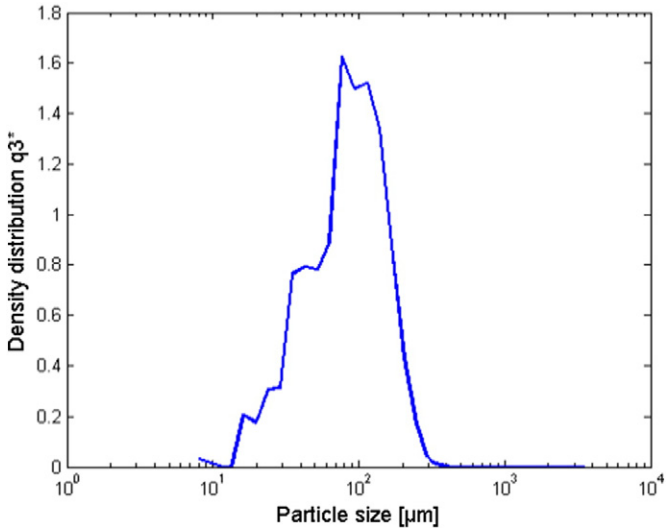

Fig. 1. Particle size distribution of high ratio flour.

the vibrations of the motors. Two off-balance motors (D) are attached on opposite sides of the spiral and at an adjustable angle with the horizontal. They create vibrations of different amplitudes and frequencies. The vibrations can be controlled by changing:

- *Motor angle*. The movement of the motor is perpendicular to the motor axis. Adjustment of the motor angle β affects the velocity components of the motors in horizontal and vertical direction. This is shown in Fig. 3 and the components are defined as Eqs. (1) and (2). With increasing angle β, which ranges between 0° and 90° ($\alpha = 90° - \beta$), the horizontal velocity component increases, whereas the vertical one decreases.

$$v_x = v \cdot cos(\alpha) \quad (1)$$

$$v_y = v \cdot sin(\alpha) \quad (2)$$

- *Motor speed*. This controls the vibrational frequency of the oscillations and can be adjusted between 600 rpm (10 Hz) and 740 rpm (12.3 Hz).

The vibrations cause particles to move from the bottom to the top of the spiral. The product leaves the helical pipe via a flexible plastic tube that is connected to the top and it is collected in a plastic container.

For the experiments, the hopper of the machine was typically filled with approximately 100 kg of flour, which allowed for a 1 h experiment (100 kg/h). The flour was recirculated and the fraction lost (ca. 5%) through sample taking was topped up prior the next experiment (recirculation method).

A dry and a wet cleaning method can be applied to the spiral. A cleaning pig is used in both cases to push the remaining product out of the pipe. Compressed air is used in one case and water in the other to drive the cleaning pig through the pipe. In one case the hand dishwashing liquid Suma Star plus D1 plus (JohnsonDiversey, Inc.) was added to clean the pipe.

2.3. Determination of residence times

2.3.1. Residence time distributions

The residence time distributions of flour in the vibrating machine were measured at ambient temperature. Twenty-five grams of burnt flour (15 min at 250 °C in a convection oven) was used as a marker that was introduced instantaneously to a constant flour flow of 100 kg/h (insertion point E in Fig. 2). The time was taken with a

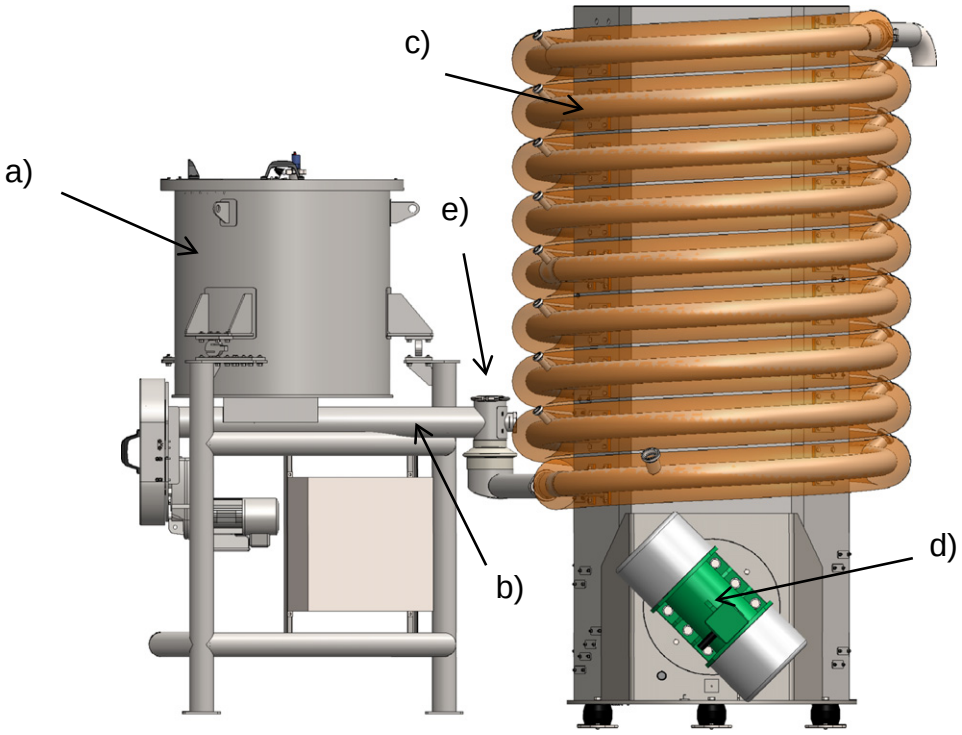

Fig. 2. Experimental setup: hopper (a), screw feeder (b), insulated helical pipe (c), motor at an angle with the horizontal (d), and insertion point for marker sample (e).

stopwatch and the marker was collected at the outlet of the flexible tube in 1 s bins. This was accomplished by moving the unit with the plastic dishes (cf. Fig. 4) by one plastic dish per second manually. The approximate residence time at which the marker was to be expected was determined in preliminary experiments.

The mass as well as the colour values *X*, *Y*, and *Z* (Konica Minolta spectrophotometer CM-5, reflectance mode, observer angle 10°, illuminant D65) of all collected bins were identified. The concentration (wt.%) of marker in each flour sample was calculated by means of a calibration curve. By multiplication of sample mass and marker concentration, the marker mass per bin was generated and related to the total marker mass collected at the outlet. Subsequently, residence time distributions were created in Minitab 17®.

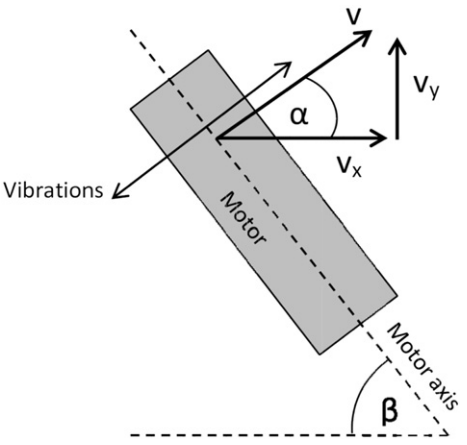

Fig. 3. Relation between total velocity (v) of the motor movement, velocity components in horizontal and vertical direction (v_x, v_y), and motor angle to the horizontal (β).

2.3.1.1. Calibration curve. To create the calibration curve, the *X*- and *Z*-values of known concentrations (wt.%) of burnt flour within a burnt flour-fresh flour-mixture were studied. Two parameters were used instead of one to increase the accuracy. *X*- and *Z*-values of the known concentrations (0–30%) were plotted in a 2D graph and a linear regression was performed (Fig. 5a). The distance α along the regression curve was calculated for the know concentrations. As the data points do not lie perfectly on the calibration line, the nearest point was found by dropping a perpendicular onto the line. α is calculated by the dot product of the unit vector of the regression curve and the vector of the measured sample (Eq. (3) m:gradient of regression line).

$$alpha = \frac{1}{\sqrt{1+m^2}}\begin{pmatrix}1\\ m\end{pmatrix}\circ\begin{pmatrix}X\\ Z\end{pmatrix} \tag{3}$$

α is then plotted against the corresponding concentrations of burnt flour-mixtures. A third order polynomial can be fitted to the data (Fig. 5b).

For the residence time experiments, *X* and *Z*-values were found experimentally, α calculated and the marker concentration found from the calibration curve.

2.4. Residence time dynamics

In the study of the development of the residence time with time, the residence time is taken to be the point when the marker starts to

Fig. 4. Flour collecting device for the determination of residence time distributions.

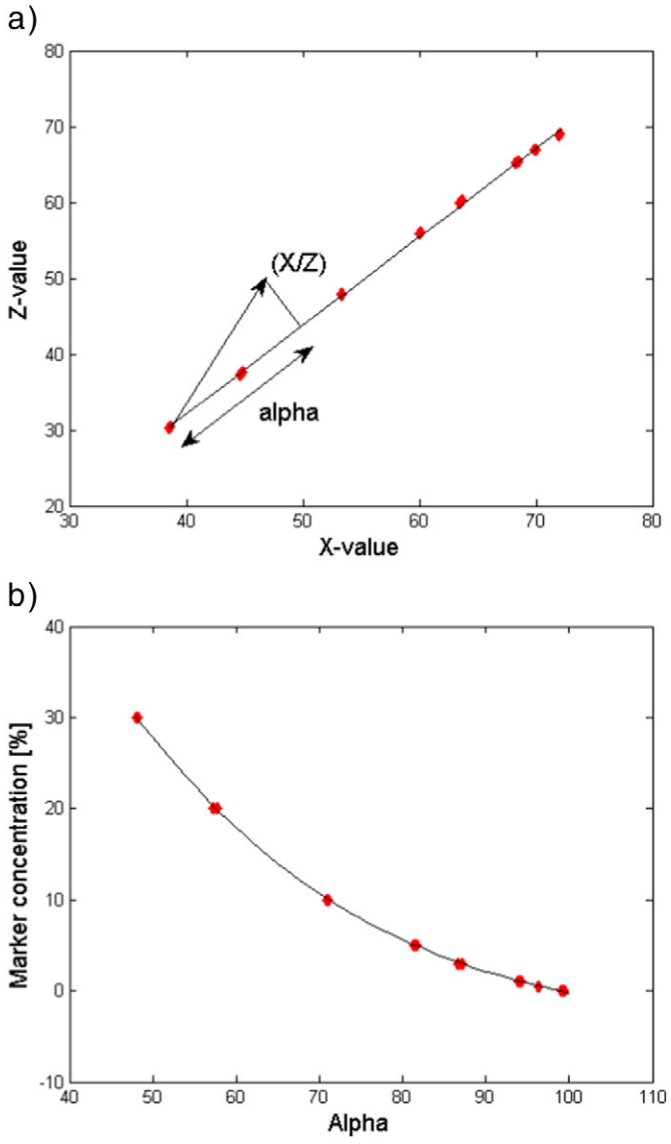

Fig. 5. Calibration curves for burnt flour-fresh flour-mixtures of concentration of 0%, 0.5%, 1%, 3%, 5%, 10%, 20%, 30%. a) *Z*-values against *X*-values. b) Concentration (wt.%) against alpha.

emerge at the outlet of the spiral. This avoids the need to measure full RTDs; Fig. 8 shows that the distributions are very narrow at all processing conditions, so the approach is justified. Thus, the first sample bin that contains marker particles is determined by eye and the corresponding time is referred to as residence time. Hence, this represents a measure of the shortest residence time. Generally, marker samples were introduced every 10 min, which allowed for 5 samples per experiment (100 kg/h). Three to 4 experiments were performed per day.

2.5. Particle size measurements and fractionation

Flour samples were taken at the outlet of the flexible tube. To avoid segregation in the sample bags, the samples were poured onto neat heaps and divided in 4 equal quarters. Three of these quarters were used individually to measure the particle size distributions on a QICPIC (Sympatec GmbH, D) with a measurable particle size of 10 μm–3410 μm (Oasis Rodos disperser, M7 lense). The 10%, 50%, and 90% quantiles of the sample volume were calculated.

Furthermore, 60 kg of flour was sifted on a Sievmaster (Farleygreene Ltd., UK) on a sieve with a hole size of 75 μm and a diameter of approximately 52 cm. Approximately 4 kg was sifted at once for 2 h. Subsequently, the residence times of the resultant fine and coarse fraction were measured.

2.6. Determination of water content

The water content of flour samples was determined in a convection oven at 130 °C according to AACC International Method 44–15.02 (note: silica gel was used as desiccant).

2.7. Charge measurements

A flour sample was collected at the outlet of the flexible pipe with a commercially available Faraday pail JCI 150 (Chilworth Technology Ltd., UK). A self-built Faraday pail was used to take samples at the inlet of the spiral due to the narrow dimensions between screw feeder and spiral inlet. Typically, a Faraday pail consists of a metal cup located within a metal shield. Both are separated by an insulator like PTFE or Teflon. The core of a coax cable is connected to the pail and the outer conducting sheath to the shield. The charge measuring unit JCI 178 (Chilworth Technology Ltd., UK) was connected to either of the pails via a bnc connector. In preliminary experiments, it was assured that both pails read comparable values. The flour mass in the cup was measured and put in relation to the charge.

The unit was zeroed briefly before the measurements and movements of the cable were avoided as this affects the charge reading. To avoid further disturbances during the measurements, full cotton clothes were worn by the person performing the experiments and additionally, the person was earthed by a wristband that is connected to earth with a crocodile clip.

2.8. Statistics

Minitab 17® was used for standard statistics, ANOVA, correlation tests, histograms and *Q*–*Q* plots. Regressions were performed in Matlab®.

3. Residence time results and preliminary discussion

For all experiments, the particles travel through the vibrating system at a flow rate of 100 kg/h in a homogenous layer with a low bed depth. The flow does not take up the entire space of the pipe, but the particles only bounce a few millimetres high.

Note that the experiments were performed on a pilot plant device and the results do not directly apply to industrial machines.

3.1. Residence time distributions

This section investigates the residence time distributions of flour at motor angles of 20°, 30°, and 40° at a motor speed of 740 rpm. Fig. 6 shows examples of collected data and fitted normal distributions. By means of *Q*–*Q* plots it was established that in all cases deviations from Normality are small (cf. Fig. 6). For 30° and 40°, the Normal overestimates the proportion of short times in the end of the distribution and the measured data shows greater residence times than predicted.

Typical normal distributions are shown in Fig. 7 standardised by dividing by the mean residence time. For 20° and 30°, the standard deviation is between 0.45% and 0.70%, whereas for 40° it is 0.70%–0.99%. Thus, the residence time distributions are narrower at lower motor angles with respect to the mean. However, the absolute spread in seconds is smaller at 40° because the residence time is shorter.

The overall mean for the data of Fig. 7 was calculated to be 548.9 s, 311.2 s, and 218.5 s for 20°, 30°, and 40°. The residence time decreases by approximately 43% (238 s) from 20° to 30° and by approximately 30% (93 s) from 30° to 40°. As the residence time was observed to shift over time as analysed below, this data only serves as an indication

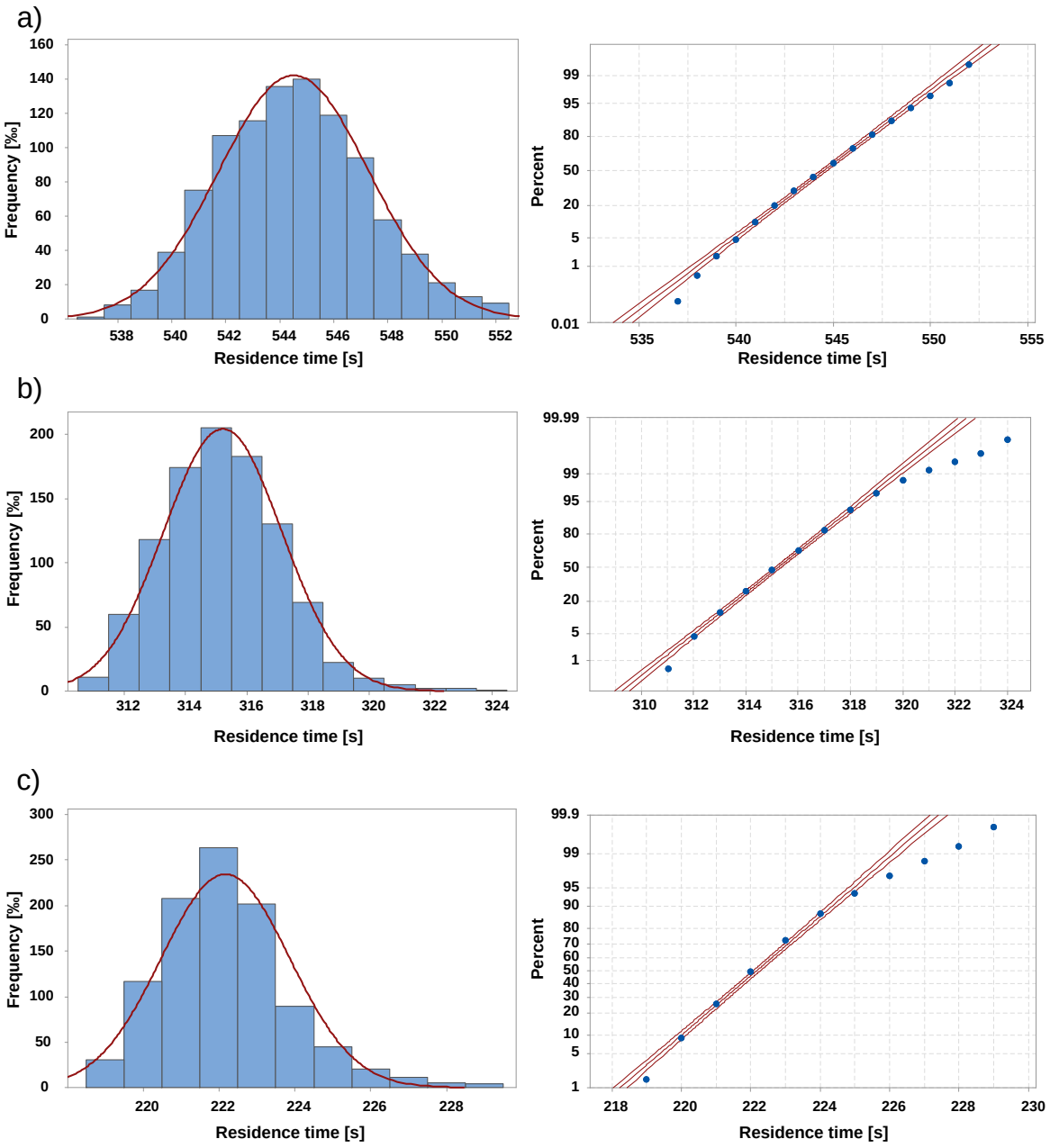

Fig. 6. Typical measured residence time distributions of flour at a motor speed of 740 rpm in 1 s intervals and overlaid normal distributions. Probability plots with 95% confidence intervals. a) Motor angle: 20°. b) Motor angle 30°. c) Motor angle: 40°.

rather than as being fully representative of the range of data possible at the particular condition.

In conclusion, a method was established to accurately measure the residence time distributions of flour in the vibrating machine. The RTDs can be approximated by normal distributions. The residence time decreases considerably with increasing motor angle and the distribution is narrower and thus more precise for 20° and 30° in comparison to 40° with respect to the mean.

3.2. Residence time development with time

The residence time of flour was tested for motor angles of 20°, 30°, and 40° and motor speeds of 600 rpm and 740 rpm over a time period of ca. 3.5 h. Each experiment took approximately 1 h. A marker sample was introduced to the product flow (100 kg/h) in intervals of 10 min and the shortest residence time was measured. Generally, between 3 and 4 experiments were performed per day and after each experiment, the flour was recirculated. Hence, the machine run-time is not continuous, but the cumulative run-length from the individual experiments per day is known. Before each day's experiments, the pipe was cleaned with a cleaning pig and water.

Fig. 8 shows that at motor speed of 740 rpm, the residence time increases over the period of 3.5 h for all motor angles. The data can be approximated with first order polynomials and the gradients increase from 0.09 s/min and 0.08 s/min at 40° and 30° to 0.3 s/min at 20°. The initial level of the residence time increases from 200 s to 260 s to 445 s for motor angles of 40°, 30°, and 20°, respectively. Within 3.5 h, the residence time increases by 62 s, 17 s and 15 s (calculated from the 2 samples over 210 min) for motor angles of 20°, 30°, and 40°, an increase of 13.9%, 6.5%, and 7.7% of the initial value, respectively. Thus, changing the motor angles from 20° to 30° has a bigger effect on initial level and slope of the residence time than varying them from 30° to 40°.

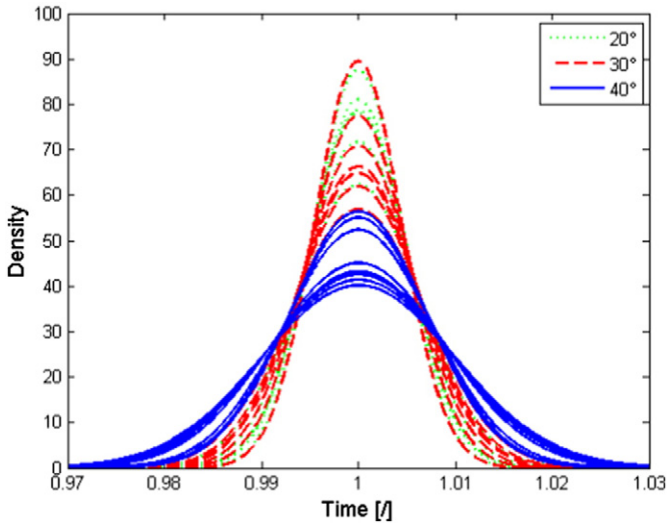

Fig. 7. Approximated normal distributions of the residence time of flour at motor angles of 20°, 30°, and 40° at 740 rpm.

At a motor speed of 600 rpm, results are more complex. At motor angles of 20°, the flour did not move up the spiral, but overflowed at the inlet. This demonstrates that as the acceleration at low motor angles is mainly vertical, the horizontal component of the acceleration can be insufficient to transport the flour. Fig. 9a presents the residence time for motor angles of 30° and 40° at 600 rpm. In contrast to 740 rpm, the residence time does not increase constantly over time. At 30°, the lowest residence time decreases by 12 s over the timescale of the experiment whereas at 40°, the residence time decreases slightly at first before it increases again in the end changing by 4 s. In both cases, the data can be described accurately by second order polynomials. This suggests different residence time dynamics at 600 rpm from those at 740 rpm. However, as at 740 rpm, the initial residence time decreases with increasing motor angle from 315 s at 30° to 250 s at 40°.

When experiments at motor angles of 40° were continued for another 3.5 h on a second day (without cleaning the pipe), the residence time maintained its increase (cf. Fig. 9b). The residence time on the second days at 600 rpm shows an increasing trend, approaching the results at 740 rpm.

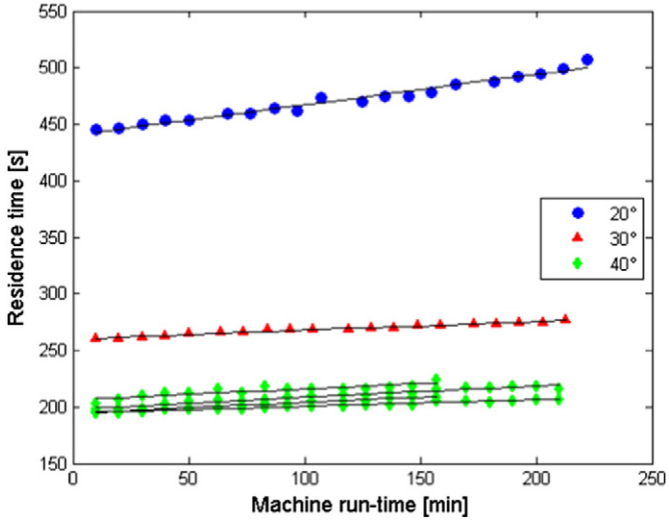

Fig. 8. Residence time of flour at motor angles of 20°, 30°, and 40° and a motor speed of 740 rpm with fitted 1st order polynomials.

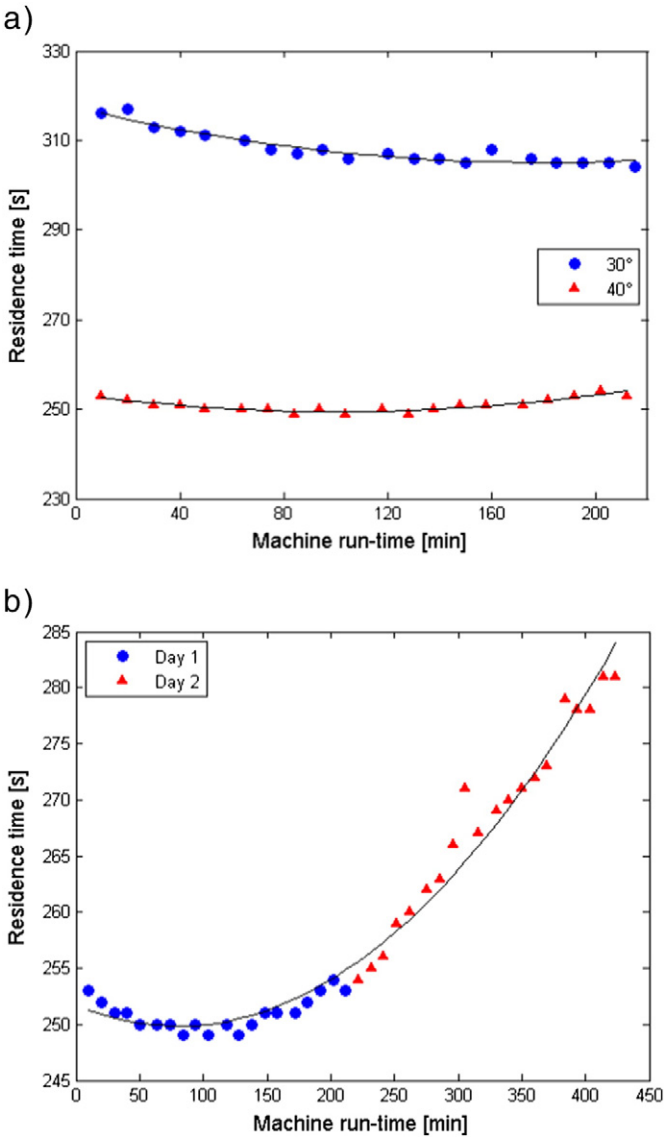

Fig. 9. a) Residence time of flour at motor angles of 30° and 40° and a motor speed of 600 rpm with fitted 2nd order polynomials. b) Motor angles of 40° and 600 rpm, showing (i) Day 1, starting with a clean pipe followed by (ii) Day 2, continuing without cleaning the pipe.

Fig. 10 depicts the influence of the motor speed on the residence time at a motor angle of 30°. Whilst the dynamics are different at 600 rpm and 740 rpm as explained above, the initial level of the residence time increases from 260 s at 740 rpm to 315 s at 600 rpm. The same was observed at 40° with residence times of 200 s and 253 s for 740 rpm and 600 rpm, respectively (data not shown). Hence, the residence time decreases with increasing motor angle and increasing motor speed. The dynamics are affected by the motor speed.

To demonstrate residence time dynamics, data from experiments run over 18 experimental days under the same conditions of 40° and 740 rpm is shown in Fig. 11. In this case both clean and used pipes were used. In all cases the residence time increased over time, in addition Fig. 11 shows that the initial residence time varies between 192 s and 228 s. The average increase over 3.5 h of machine run-time was 13.8 ± 5.0 s, equivalent to 6.6 ± 2.2% of the initial value (calculated from the days with 20 samples). The spread of residence time (56 s) was between 192 s and 248 s, which represents 29% of the minimum and 23% of the maximum

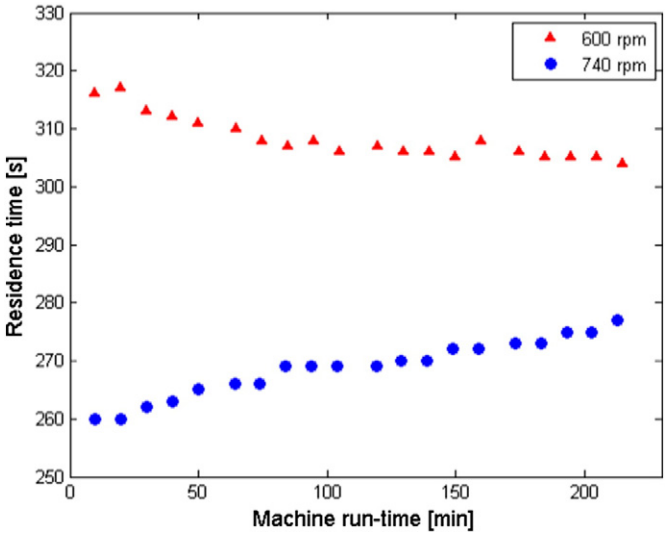

Fig. 10. Residence time of flour at a motor angle of 30° and motor speeds of 600 rpm and 740 rpm.

residence time. This spread is much larger than that observed in the individual distributions (i.e. standard deviation 1.88 s at 40°). It is necessary to identify the causes of this effect to accurately control and correctly operate the device.

From this data, three major questions arise:

i) What are the influences on the initial level of the residence time?
ii) What is responsible for the extent of the increase in residence time?
iii) Is there a plateau, where the residence time levels off?

Preliminary experiments showed no correlation between the residence time and ambient temperature, relative and specific humidity. Potential influences related to the product and the machine are discussed below.

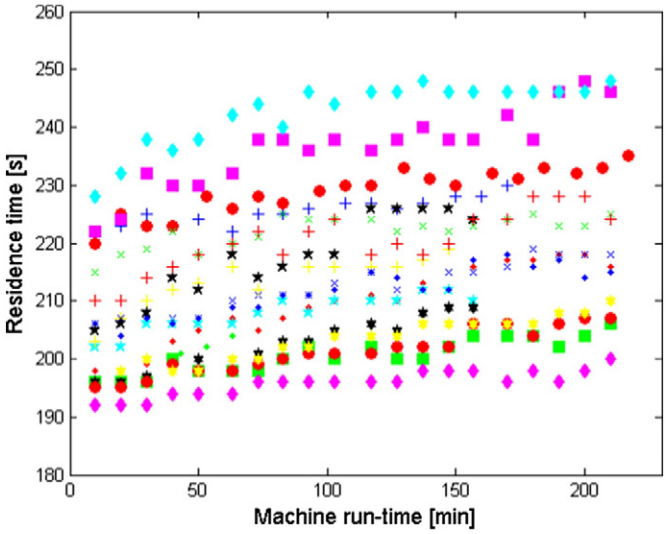

Fig. 11. Results from 18 different experiments for the residence time of flour over time at motor angles of 40° and a motor speed of 740 rpm. Different markers relate to different experimental days.

4. Investigation of variation in residence time

4.1. Influence of particle size

Separation of the product in the hopper or the vibrating tube could affect the residence time during an experiment. As the flour is recirculated after each experiment, any change of particle size distribution throughout the day could affect the residence time, for example by deposition of fine particles in the pipe or their loss at the outlet of the pipe, where the product is collected.

Table 1 presents the 10th, 50th, and 90th percentile of the particle size distribution of (i) the first flour sample of the day after 10 min of machine run-time and (ii) the last sample after 160 min. The *p*-values of an ANOVA between the samples are 0.03, 0.1, and 0.8 for x_{10}, x_{50}, and x_{90}, respectively. The results indicate no significant differences in particle size and that the particle size distribution remains constant throughout the day. Hence, product separation does not occur and does not cause the increase in residence time.

The flour used was sifted to a fine fraction (largely <75 μm) and a coarse fraction (largely >75 μm) (cf. Fig. 12a) to assess the effect of different sized fractions on the residence time. The results are shown in Fig. 12b, which also shows the scattered data of Fig. 11. The fine fraction was more cohesive than the coarse fraction, whereas the coarse fraction was particularly dusty and free flowing. This might explain why the average residence time is greater for the fine fraction (191 s) compared to the coarse fraction (187 s).

Both fractions however exhibit residence times below all data points measured for flour, apart from at the beginning and the end of the traces. The findings suggest it is not a particular size fraction that causes the observed phenomenon. Yet, the results suggest complex interactions between particles of different sizes as the residence times of both size fractions are dissimilar to that of flour.

4.2. Influence of water content of the product

Changes in water content of the flour could affect cohesion properties or the coefficient of restitution between the flour and the vibrating tube. The moisture content was determined of 15 samples within 3 experiments of 1 day. The average moisture content of all samples was 12.12 ± 0.03% (wet basis) and the data was randomly distributed. These findings prove that the water content of the product is not responsible for the increase in residence time.

4.3. Influence of static electricity

Charge effects are well known to cause problems in the flow of particles (Chubb, 2010). Interactions between the flour and the steel pipe may create static electricity. The flour might become charged over time. Alternatively, a thin layer of flour might deposit inside the pipe and become charged. The metal pipe cannot get charged as it has an electrical resistance of only 2.8 MΩ, which is easily overcome by the charge, and no change in the residence time was detected when the pipe was earthed.

Measurements of flour samples from the inlet of the pipe showed that the charge is close to zero (27 ± 23 pC/g) throughout the day

Table 1
Particle size distributions of flour with time.

Machine run-time [min]	Particle size		
	x_{10} [μm]	x_{50} [μm]	x_{90} [μm]
10	32.70 ± 0.23	86.98 ± 0.76	171.53 ± 0.90
160	33.22 ± 0.13	88.00 ± 0.32	171.69 ± 0.67

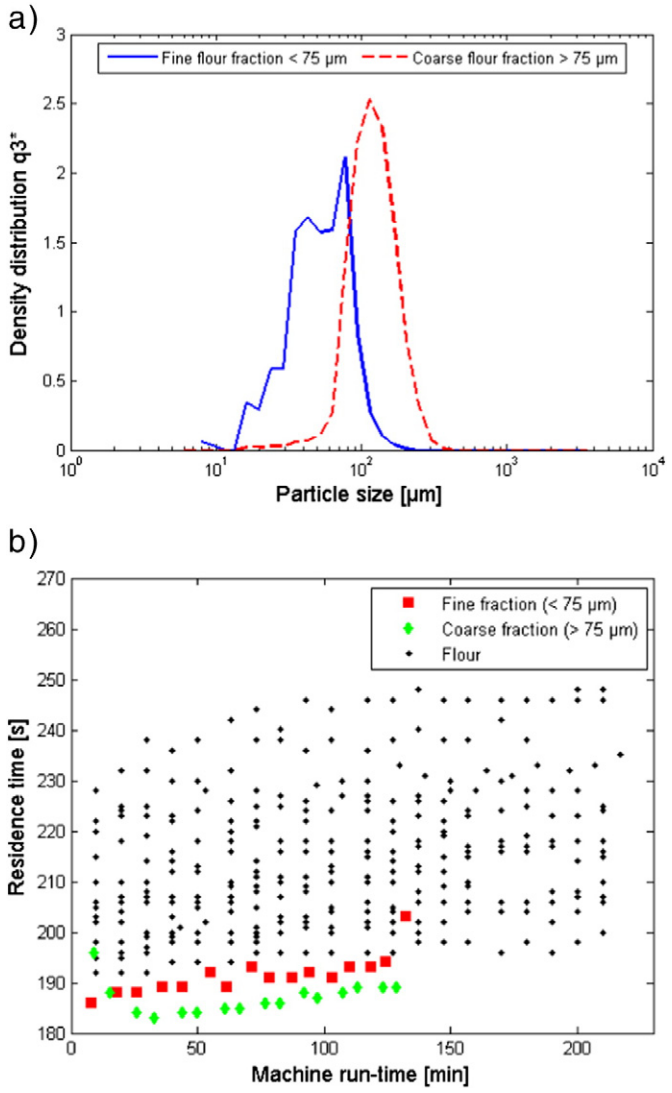

Fig. 12. a) Particle size distribution of fine and coarse flour fractions after sieving (hole size 75 µm). b) Residence time of flour, the fine flour fraction (<75 µm), and the coarse flour fraction (>75 µm) at motor angles of 40° and a motor speed of 740 rpm. Small points are the residence time data for flour shown in Fig. 11.

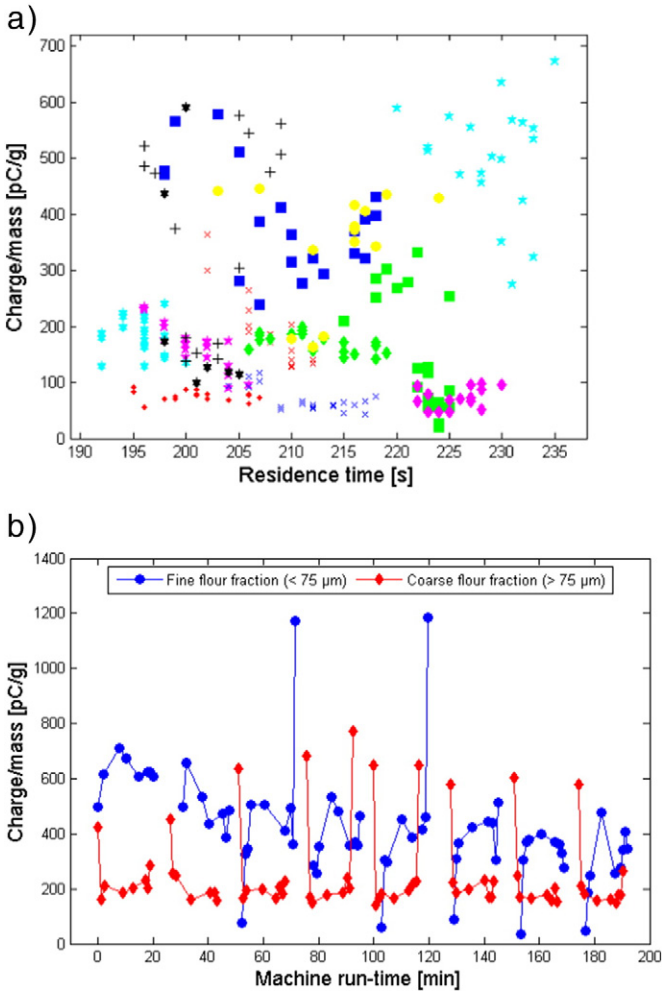

Fig. 13. a) Charge of flour samples from the outlet of the flexible pipe in correlation with the measured residence time. Different markers relate to different experimental days. b) Charge development of fine and coarse flour fractions over time. Markers of samples within one experiment are connected.

(data not shown). In contrast, charge measurements of flour at the outlet of the spiral were 220 ± 160 pC/g (cf. Fig. 13a). This proves that static charging of the material takes place in the pipe. However, no correlation could be established between the residence time and the outlet charge (Spearman's rho = 0.033). The findings suggest that the build-up of static charge in the bulk material does not cause the increase in residence time.

Fig. 13b illustrates the development of the outlet charge during the day for the fine flour fraction (<75 µm) and the coarse flour fraction (>75 µm) (cf. Section 4.1). The results indicate that the fine fraction is generally higher charged than the coarse fraction, which can be expected due to a larger surface area where charge may be separated. It is worth noting that during each experiment, the charge progresses in u-shaped curves for the coarse fraction. This behaviour is roughly mirrored by the fine fraction. The first and the last particles of each experiment have more contact with the wall than the flow in between, which could play a role in this context. Furthermore, the overall charge is rather constant during the day for the coarse fraction, whereas it decreases for the fine fraction. The reasons for this phenomenon are not clear.

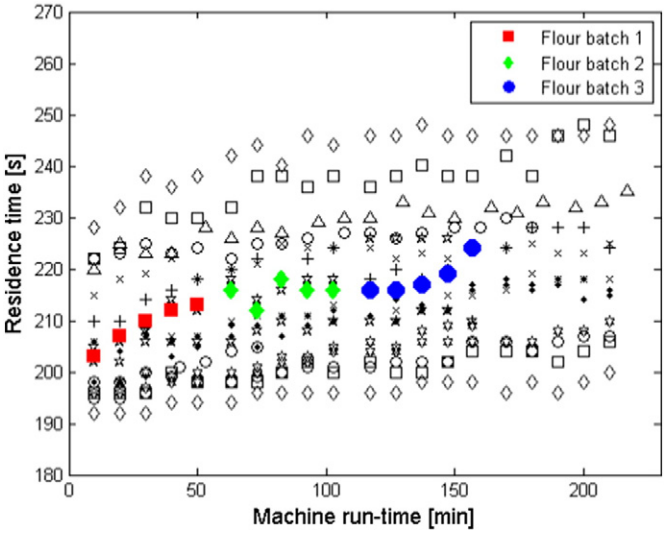

Fig. 14. Residence time of 3 fresh flour batches in comparison to recirculated flour at motor angles of 40° and a motor speed of 740 rpm. Different markers relate to different experimental days.

4.4. Influence of recirculation of the product

In the experiments, the product is recirculated for each experiment (1 h). This could cause errors in the results if the product is changed by the process in any way (e.g. particle size, electrostatic charge, etc.).

Fig. 14 shows the residence time of 3 fresh batches of flour together with the experiments of Fig. 11 where only one batch of flour was recirculated. The initial level of the residence time of the first batch was measured at 203 s, which is amongst the control data (192 s–228 s). Furthermore, the slope of a first order polynomial through the curve described by the 3 flour batches is 0.1 s/min. This is similar to the average gradient of the control data of 0.07 ± 0.03 s/min.

This in combination with the findings about particle size, water content, and charge suggests that alterations of the material do not cause the shift in residence time.

4.5. Influence of the cleanliness of the pipe

Deposition of product in the pipe might either obstruct the product flow or become electrostatically charged. To investigate this matter, 3 different cleaning methods were applied to the pipe and the residence time of flour was measured:

i) Cleaning with a cleaning pig and compressed air,
ii) Cleaning with a cleaning pig and water,
iii) Cleaning with a cleaning pig, water, and hand dishwashing liquid.

In the following, a dirty pipe is defined as one that has been used for flour and has not been cleaned before new experiments started.

First, the pipe was cleaned with a cleaning pig and compressed air after each 1 h experiment (3 times per day). This did not affect either the initial level of the residence time or the extent of the increase during the day (data not shown). Hence, flour accumulations as physical obstructions can be excluded to be the cause for the shift in residence time.

Second, Fig. 15 presents the residence times of flour for the pipe cleaned with a cleaning pig and water compared to a dirty pipe. Using a clean pipe reduces the initial level of the residence time, but to various extents as the starting points are not identical. Additionally, the gradient of the increase in residence time was determined to be 0.09 ± 0.02 s/min for the clean pipe (4 data sets) and 0.07 ± 0.03 s/min for the dirty pipe (14 data sets). Analysis of variance indicates no differences between both conditions ($p = 0.29$).

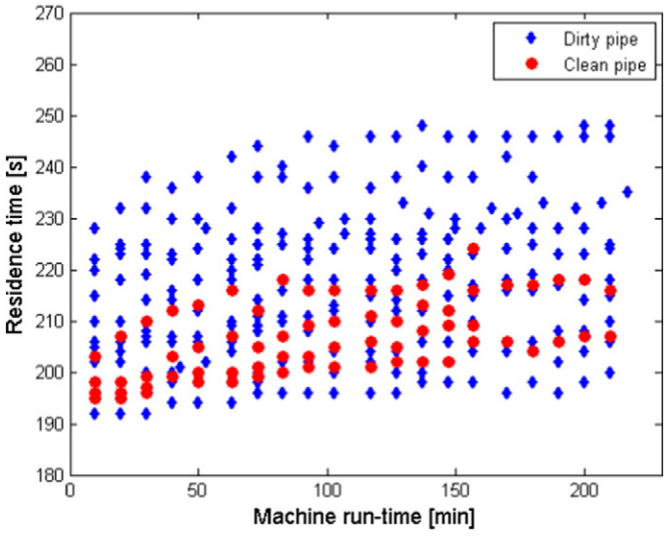

Fig. 15. Residence time of flour at motor angles of 40° and a motor speed of 740 rpm using a clean and a dirty pipe.

Cleaning with water has a more significant effect on the initial residence time than cleaning with air.

A line or deposit axially along the pipe could be seen in the pipe after flour had passed through. This supports the theory of the build-up of a thin, but visible flour layer. This line is not observable after cleaning. This does not mean that there cannot be a few particles adhering to the pipe wall. It may be that minor deposits of particles resulting from differences in cleaning effect might account for dissimilar initial levels of the residence time.

Third, judging from these outcomes, the pipe was cleaned with a hand dishwashing liquid, water, and a cleaning pig to ensure that all particles were removed. The results were similar to those obtained by cleaning with water only (data not shown). The slope of the increase in residence time was equivalent as well. This suggests either the adhesion of fine particles in the pipe is not the problem or the chosen method is inappropriate to remove the remaining particles.

4.6. Machine performance

The motors or other parts of the machine might warm up over time, which can potentially affect the vibrational frequency or deflection. This in turn could impact on the development of the residence time over the course of the day.

Tests were carried out in which the machine was run without product for 2 h before product flow was started. Results were compared to those where the machine was run with product from the beginning. The underlying hypothesis is that if the warming up of the machine is responsible for the increase in residence time, the latter would be expected to start at a higher initial residence time.

The results are shown in Fig. 16, and show that the residence time started at a lower value after the machine ran idle for 2 h in comparison to the control day. This suggests that the warming up of the machine does not cause the residence time to increase.

4.7. Extended run-length experiments

Fig. 17 shows the development of the residence time of flour over 4 consecutive experimental days and a further day of measurements after a weekend. It is evident that the residence time increases continuously over the first 4 days. This can be approximated with a second order polynomial ($R^2 = 0.97$). The slope decreases over the last 2 of the 4

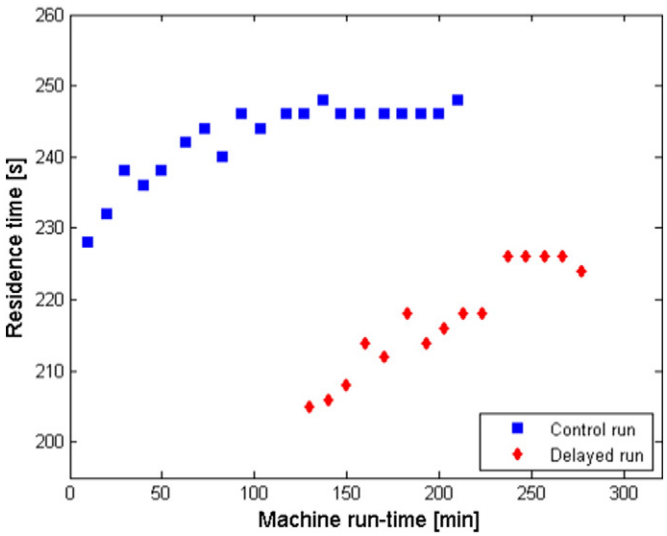

Fig. 16. Residence time of flour at motor angles of 40° and a motor speed of 740 rpm. (i) Control run where machine and product flow were started at the same time and (ii) delayed run where the machine was run for 2 h without product before the product flow was started.

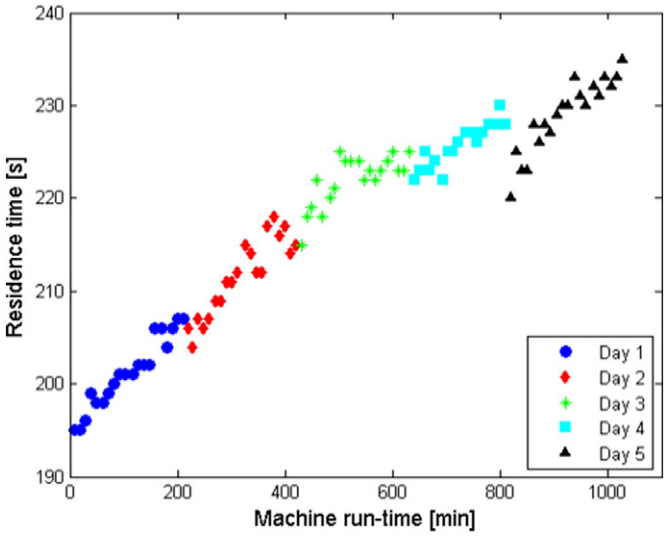

Fig. 17. Residence time of flour at motor angles of 40° and a motor speed of 740 rpm over a time period of 5 experimental days.

consecutive days. After the 2-day break, the residence time drops visibly and the subsequent increase over the course of the day is comparable with the first day of the experimental data set.

No constant value of the residence time was found. If the residence time increase is due to built-up of a thin flour layer inside the pipe, it would be expected to reach a saturation thickness at which the residence time levels off. Thus, the phenomenon appears more complex than a simple correlation between the residence time and the thickness of the layer on the inside of the pipe.

5. Conclusions

A novel tubular apparatus for the continuous heat treatment of flour has been studied. The residence time distributions of flour were characterised for various processing conditions and the development of the residence time in extended operation was analysed.

A method was established to accurately determine the residence time distributions. The RTDs can be approximated by normal distributions. The residence time decreases considerably with increasing motor angle and the distribution is narrower and thus more precise for 20° and 30° in comparison to 40° with respect to the mean. The width of the distribution is a critical factor for the accuracy of a thermal process.

The dynamics of the residence time were greatly affected by the motor speed. The systematically increasing residence time at 740 rpm could be fitted by a first order polynomial, whereas at 600 rpm, the residence time decreased at first, before an increase was observed and a second order polynomial was approximated.

The residence time increases over the course of approximately 3.5 h of machine run-time by 13.9%, 6.5%, and 7.7% for motor angles of 20°, 30°, and 40° and a motor speed of 740 rpm at room temperature. Several hypotheses concerning the product, the machine, and the environment were tested regarding the cause for this phenomenon.

Changes in the bulk material passing through the spiral were not the cause of the increase. This was established by the fact that the same trend was observed whether 3 fresh batches of product were used or the same product was recirculated during the day. Furthermore, particle size distributions and water contents were constant throughout the day. Electrostatic charging of the flour does take place during the process, but no correlation between charge of the material and residence time could be found. It is likely that electrostatic charging is relevant to the average time particles spend in transit.

The mechanical performance of the machine is constant over time and no correlation between residence time and ambient temperature and humidity could be found. It is sensible to assume the reason for the increase in residence time is in the pipe. It was found that two things led to a reduction in initial residence time: i) cleaning the pipe with a cleaning pig and water and ii) time, during which the machine is not running.

Cleaning the pipe with the pig and water reduces the initial residence time in contrast to cleaning with the pig and air. This suggests that it must be a very thin layer or few particles that stick firmly to the walls of the pipe that cause the residence time to shift. Overall, whichever process causes the residence time to increase during the day is reversible by cleaning the pipe or by idle time.

These observations suggest that a layer of few particles on the inside of the pipe wall causes the residence time to change. That the effect decreases when the equipment is left idle suggests an effect of something like electrostatics which discharges slowly over time.

More work is needed to identify the cause for the drift in residence time and to predict the residence time over periods of extended operation. The data does suggest that cleaning reduces the overall effect, and that frequent cleaning can allow relatively uniform behaviour. In practise, tests need to be done to confirm the residence time and ensure process uniformity.

Acknowledgments

This research was done as part of a PhD project supported by the University of Birmingham (Birmingham, UK) in collaboration with Campden BRI (Gloucestershire, UK). The authors would like to thank Revtech process systems (Loriol-sur-Drome, FR) for providing the equipment and BBSRC for financial support.

The work is part of the RCUK National Centre for Sustainable Energy in Food Chains (EP/K011820/1).

References

Catterall, P. F. (2000). The production of cakes from non-chlorinated cake flour. *Rep. No. 20*. Chipping Campden, UK: Campden & Chorleywood Food Research Association Group, Campden BRI.

Chesterton, A. K. S., Wilson, D. I., Sadd, P. A., & Moggridge, G. D. (2015). A novel laboratory scale method for studying heat treatment of cake flour. *Journal of Food Engineering, 144*, 36–44.

Chubb, J. (2010). *An introduction to electrostatic measurements*. New York: Nova Science Publishers, Inc.

Collyer, D. M. (1968). High-ratio cake—A review of the literature. *Rep. No. 18*. Chorleywood (UK): Flour Milling and Baking Research Association.

Cook, S. (2002). Factors affecting the production of cakes from heat-treated cake flour. *Rep. No. 20 - supplement 1*. Chipping Campden, UK: Campden & Chorleywood Food Research Association Group, Campden BRI.

Doe, C. A. F., and Russo, J. V. B.(1970). "Flour treatment process." US Patent 3490917.

Gough, B. M., Greenwood, C. T., & Whitehouse, M. E. (1977). The role and function of chlorine in the preparation of high-ratio cake flour. *Rep. No. 75*. Chorleywood (UK): Flour Milling and Baking Research Association.

Guy, R. C. E., & Pithawala, H. R. (1981). Rheological studies of high ratio cake batters to investigate the mechanism of improvement of flour by chlorination or heat treatment. *International Journal of Food Science and Technology, 16*, 153–166.

Hodge, D. G. (1975). Alternatives to chlorination for high ratio cake flours. *Baking Industries Journal*, 12–19.

Magee, T. R. A., & Neill, G. (2011). Effects of heat treatment on protein denaturation and starch gelatinisation in wheat flour. *ICEF11*.

Meza, B. E., Chesterton, A. K. S., Verdini, R. A., Rubiolo, A. C., Sadd, P. A., Moggridge, G. D., & Wilson, D. I. (2011). Rheological characterisation of cake batters generated by planetary mixing: Comparison between untreated and heat-treated wheat flours. *Journal of Food Engineering, 104*, 592–602.

Neill, G., Al-Muhtaseb, A. H., & Magee, T. R. A. (2012). Optimisation of time/temperature treatment, for heat treated soft wheat flour. *Journal of Food Engineering, 113*, 422–426.

Revtech(2015). "http://www.revtech-process-systems.com/index.php/en/.".

Thomasson, C. A., Miller, R. A., & Hoseney, R. C. (1995). Replacement of chlorine treatment for cake flour. *Cereal Chemistry, 72*, 616–620.

Wilderjans, E., Luyts, A., Brijs, K., & Delcour, J. A. (2013). Ingredient functionality in batter type cake making. *Trends in Food Science & Technology, 30*, 6–15.

Journal of Food Engineering 187 (2016) 114–123

Contents lists available at ScienceDirect

Journal of Food Engineering

journal homepage: www.elsevier.com/locate/jfoodeng

Processing of barley grains in a continuous vibrating conveyor

S. Keppler [a, *], S. Bakalis [a], C.E. Leadley [b], P.J. Fryer [a]

[a] University of Birmingham, School of Chemical Engineering, Edgbaston, Birmingham, B15 2TT, UK
[b] Campden BRI, Gloucestershire, UK

ARTICLE INFO

Article history:
Received 9 October 2015
Received in revised form
8 April 2016
Accepted 13 April 2016
Available online 14 April 2016

Keywords:
Vibrating conveyer
Residence time distributions
Particle flow
Heat transfer

ABSTRACT

A novel tubular industrial apparatus for the surface pasteurization of particles has been studied. Particles are conveyed through a helical pipe by vibrations created by off-balance motors. The residence time of barley grains was characterized. The behaviour of the system was a function of motor angle and motor speed. The residence time could vary up to 21% during one experiment of 2 h (20°, 740 rpm). However, ranges of processing conditions were identified that produce stable operation and thus effective pasteurization of product. In some cases, residence time increased by up to 7% of the initial value over consecutive experiments (40°, 710 rpm). Some reasons for this phenomenon have been proposed and tested. The formation of a powder layer inside the pipe has been proven to affect the residence time of barley grains. A simple model for pasteurization of particles has been developed to characterise the impact of variation in residence time on microbial inactivation.

1. Introduction

Thermal processing is a major part of the food industry; it is carried out for a range of reasons, both to improve product quality but also to enhance the microbiological safety of products. It is essential to ensure that the thermal process does not damage the product. Careful selection of the correct temperature-time combination of the thermal process is thus critical in determining the success of the overall product.

In recent years, foodborne pathogen infections associated with the consumption of low water activity products such as almonds, peanut butter, or powdered infant formula have received increased attention (Beuchat et al., 2013). The primary pathogen of concern is *Salmonella* spp. (Codex Alimentarius Commission, 2013; Beuchat et al., 2011). Between 2000 and 2011, at least 1771 people were affected in Australia, New Zealand, Canada, USA and Europe by outbreaks of such infections (Beuchat et al., 2011). Even though a low water activity generally inhibits microbial growth, cells can remain viable at these conditions (Penaloza Izurieta and Komitopoulou, 2012; Mattick et al., 2000). Additionally, microorganisms can be more resistant to heat in matrices with reduced water activity (Barrile and Cone, 1970; Penaloza Izurieta and Komitopoulou, 2012; Podolak et al., 2010; Villa-Rojas et al., 2013). Depending on food preparation, portion size, and individual circumstances of the consumer, viable pathogenic cells can cause sickness. Consequently, measures like processing interventions that lead to a minimum 4 log reduction of Salmonella in almonds have been adopted to ensure the safety of these products (Almond Board of California, (2007)). Some kinetic data for relevant organisms is given in Table 1.

Technological solutions to the pasteurisation/sterilisation of particulates have focused on steam pasteurisation. This has proven to be more efficient than dry heat in inactivating microorganisms in low water activity, particulate products. Reasons include:

- Steam can penetrate small areas and cavities within the particles. Furthermore, steam has a greater specific enthalpy at 100 °C than water at that temperature and it increases the temperature of the particle's surface rapidly due to steam condensation (Lee et al., 2006).
- Microorganisms are more thermally sensitive at the increased moisture content on the product surface caused by steam condensation (Chang et al., 2010). Proteins are more stable at low water contents in the cells (Podolak et al., 2010; Neetoo and Chen, 2011). Hence, at low water content more energy is needed to unfold the protein structure, which leads to increased heat resistance (Podolak et al., 2010). In comparison, moist thermal treatment potentially destroys the proteins (Neetoo and Chen, 2011). Consequently, disulphide bonds and hydrogen bonds in

* Corresponding author.
E-mail address: sxk250@bham.ac.uk (S. Keppler).

http://dx.doi.org/10.1016/j.jfoodeng.2016.04.010

Table 1
Kinetic data for microorganisms relevant to low moisture products.

Microorganism	Product	D-value [min]	z-value [°C]	Conditions	Source
Salmonella Tennessee	Toasted oat cereal	$D_{85} = 133.9$ $D_{105} = 2.4$	11.86	Dry heat treatment	(Chick, 2011)
Salmonella Agona		$D_{85} = 117$ $D_{105} = 5.2$	14.90		
Salmonella Enteritidis PT 30	Almond flour	$D_{80} = 1.63$	8.28	Dry heat treatment $a_w = 0.610$	(Villa-Rojas et al., 2013)
Salmonella weltevreden	Wheat flour	$D_{60-62} = 875$ $D_{63-65} = 29$	15.2 53.9	Initial $a_w = 0.4$ Initial $a_w = 0.5$	(Podolak et al., 2010)
Salmonella Enteritidis PT 30	Almonds	$D_{60} = 2.6$ $D_{80} = 0.75$	35	Hot water treatment	(Harris et al., 2012)
Salmonella Enteritidis	Almonds	$D_{93} = 0.27$	–	Steam treatment	(Lee et al., 2006)

the surrounding protein weaken and break (Podolak et al., 2010).

The principle of controlled condensation is the base of a steam pasteurisation process. The goals of such a process are:

- The formation of a thin layer of moisture on the surface of each particle;
- Maintenance of those conditions for sufficiently long for the inactivation of pathogens;
- A short drying step in the end of the process to provide a safe, dry, and stable product.

Several methods are used for this purpose (Napasol, 2015; ETIA, 2014; Buhler, 2014). In batch systems, moist heat and reduced pressure are common to ensure high quality and safe products (Napasol, 2015; Buhler, 2014). Continuous systems such as electrical heated screw conveyors are also implemented (ETIA, 2014). The continuous system presented in this study (Revtech, 2015) conveys particles up a helical pipe by vibrations. The pipe is heated directly by resistive heating in which electrical current flows through the pipe at low voltages (approx. 30 V). The combination of the vibrations of the helix and a relatively low bed height of the product are considered to deliver quick and even heat transfer from the heated walls of the pipe to the particles. Steam can be added and extracted at various points throughout the process.

The design of any process to deliver a microbial reduction requires understanding of the variation of residence time of material within the process. In the process studied here, understanding of the particle motion and the accurate predictability of the residence time are critical for the design of a thermal process that results in high quality and safe products. The aims of this study were:

- To investigate the influence of various process parameters on the residence time of barley grains through the equipment, and
- To identify areas where the residence time is stable with time, and
- To develop a theoretical model to estimate the pasteurising effect of the process

Parallel work has studied the use of the device to process flour (Keppler et al., 2015).

2. Materials and methods

2.1. Material

One batch of 200 kg of barley grains was used for the experiments. This was provided by Campden BRI (Gloucestershire, UK).

The median (by volume) of the particle size was calculated to be 5210 ± 430 μm with a sphericity of 0.81 ± 0.01 on a QICPIC system (Sympatec GmbH, D) with a measurable particle size of 30 μm–10,000 μm (Gradis disperser, M9 lense). The bulk density was measured to be 687 ± 2 kg/m^3.

2.2. Equipment

The equipment used for the experiments is a continuous, thermal processing unit provided by Revtech (Loriol-sur-Drôme, France). It consists of three major parts, a hopper, a heating spiral, and a cooling spiral. In this study only the hopper and the heating spiral were used for simplicity. As shown in Fig. 1, particles are conveyed by a screw feeder (B) from the hopper (A) into the spiral. It is a helical, steel pipe (C) with an internal diameter of 84.5 mm, a slope of 2.83° to the horizontal, and a length of approx. 34.4 m. It is possible both to heat the pipe by resistive heating and to inject steam, but in this case, no thermal treatment was applied. The screw feeder speed is controlled by a check-weigher to keep the mass flow constant. This controls the overall particle flow, whilst the behaviour in the tubing is controlled by the vibrations of the motors. Two off-balance motors (D) are attached on opposite sides of the spiral and at an adjustable angle with the horizontal. They create vibrations of different amplitudes and frequencies. The vibrations can be controlled by changing:

- *Motor angle*. The movement of the motor is perpendicular to the motor axis. Adjustment of the motor angle β affects the velocity components of the motors in horizontal and vertical direction. This is shown in Fig. 2 and the components are defined as equations (1) and (2). With increasing angle β, which ranges

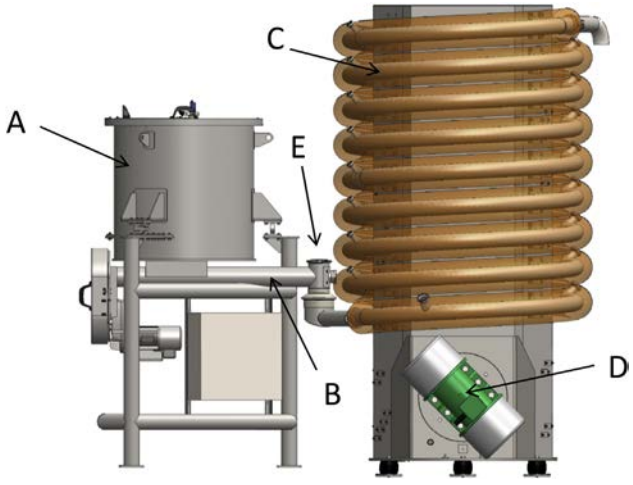

Fig. 1. Experimental setup: Hopper (A), screw feeder (B), insulated helical pipe (C), motor at an angle with the horizontal (D), insertion point for coloured grains (E).

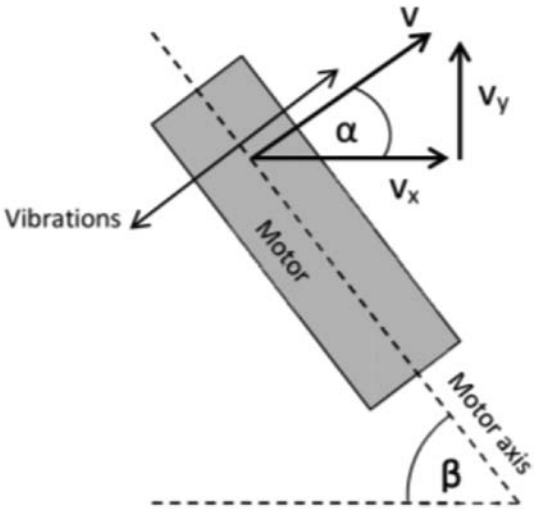

Fig. 2. Relation between total velocity (v) of the motor movement, velocity components in horizontal and vertical direction (v_x, v_y), and motor angle to the horizontal (β).

between 0° and 90° ($\alpha = 90° - \beta$), the horizontal velocity component increases, whereas the vertical one decreases.

$$v_x = v \cdot cos(\alpha) \quad (1)$$

$$v_y = v \cdot sin(\alpha) \quad (2)$$

- *Motor speed*. This controls the vibrational frequency of the oscillations and can be adjusted between 600 rpm (10 Hz) and 740 rpm (12.3 Hz).

The vibrations cause particles to move from the bottom to the top of the spiral. The product exits the helical pipe via a flexible plastic tube that is connected to the top and it is collected in a plastic container.

2.3. Measurement of residence times

The residence time of barley grains was measured by a colorimetric method. Single grains were coloured with a permanent marker and left to dry overnight at ambient conditions. They were then individually added to a constant product flow into the machine (at point E in Fig. 1) and the time was taken with a stopwatch from the time when the grain entered the spiral until it was detected by eye at the exit in the collection container. Grains were added in parallel at approx. 1.5–2 min intervals. Experiments were typically of 2 h duration after which the hopper was empty and the residence time of approx. 55–80 grains was measured per experiment. A constant flow rate was ensured from approximately 5 min after the start of the machine until the end of the experiment.

2.4. Design of experiments

The motor angles of the machine were set to 20°, 30°, and 40°. Preliminary experiments were carried out to identify suitable motor speeds.

- At 20°, no significant differences in residence time could be detected between the minimal and the maximal value of the motor speed range. Hence, no values were tested in between.
- At 30°, the difference between the results at 600 rpm and at 740 rpm was larger and thus, 660 rpm was investigated as well.
- At 40°, different magnitudes as well as dynamics of the residence time were observed depending on the motor speed. An attempt was made to find a motor speed at which the residence time is constant over the entire timescale of the experiment. By trial-and-error method, motor speeds of 600 rpm, 710 rpm, 723 rpm, and 740 rpm were investigated.

The flow rate for all experiments in this study was set using the screw feed to be 100 kg/h. The screw speed is adjusted by a checkweigher to keep the flow rate constant in the hopper as the bulk density decreases. Generally, the pipe was not cleaned between the experiments, but the effect of cleaning is assessed in section 2.5. At least 3 and up to 11 experiments were carried out for each set of processing conditions.

2.5. Identification of stable and unstable residence time

Changes in residence time were investigated during both single experiments as well as over the course of several experiments. This was done to identify time periods when the distribution was stable, and to suggest reasons for any drift.

2.5.1. Single experiment

Different processing conditions resulted in different residence time dynamics over the timescale of one experiment. To characterise stable and unstable periods, two different methods were used.

a. Generally, the residence time data was analysed in Minitab 17®. Control charts in Minitab were used to establish whether the residence time was constant with time. Three standardised tests were applied and if the data failed one of them, the point was taken as transition point or stabilisation time. Here, these tests were:
   - 1 point >3 standard deviations from centre line (overall average of data)
   - 9 points in a row on same side of centre line
   - 6 points in a row, all increasing or all decreasing

The stable subset of the data was tested again. Sporadic outliers were neglected and in case one data set failed one of the tests, but none of the other sets at the same conditions did, it was still pooled to include variability.

b. At motor angles of 40° and motor speeds of 600 rpm and 710 rpm, an initial start-up phase was observed before the residence time stabilised. However, even in the stable phase, the residence time showed a small, but continuous increase. This drift meant that control charts could not be used to find the stable phase, because as the data is not constant, it repeatedly failed the tests. Therefore, the stable phase was taken to be after 2500 s of the experiment.

2.5.2. Multiple experiments

With the aim of presenting the dynamics of the residence time over the course of several experiments, the residence time data of the stable phases of all experiments over one day was connected and plotted versus a cumulative machine run-time. The first point of the stable phase of one experiment was connected to the last point plus 1 s of the stable phase of the previous experiment. Two or three experiments were performed per day. One dataset was created for each set of processing conditions and regressions were

performed in Microsoft Excel (2010).

At 40°, the starting transient of the first 2500 s was removed for all motor speeds to allow data to be better compared. As the residence time was stable at a motor speed of 600 rpm and motor angles of 20° and 30°, all data was used in both cases.

2.6. Statistics

The mean and standard deviation was calculated for the stable phases of at least 3 and up to 11 data sets per processing condition. The results are expressed as mean ± standard deviation. The effect of different runs of the same day could be identified by examining different individual data sets.

Different data sets at the same processing conditions were generally not identical as proven by an analysis of variance (data not shown). Still, the data was pooled and thus, the variability between experiments was included in the results. However, due to the differences between the individual data sets, overall residence time distributions (RTD) were not created.

3. Results and discussion

The particles travel through the vibrating system at a flow rate of 100 kg/h in a homogenous layer with a bed depth of about two particles, with a surface length of 4–5 cm across the pipe. The particles do not fill the pipe; they only bounce a few millimetres high. At a setpoint of 100 kg/h, the flow rate at the inlet of the spiral is accurately controlled at 99.5 ± 1.0 kg/h, which is measured by a checkweigher. The flow rate at the outlet was measured to be 99.2 kg/h ± 0.98 kg/h by collection of product for 60 s over runs of 2 h and weighing it. Control charts in Minitab confirmed no increasing or decreasing trend of the flow rate with time.

The average residence times of the stable phases of various processing conditions are depicted in Table 2 and will be discussed below. Typical experiments involved more than 150 passes of tracer and measurement of the residence time to accuracy of ± 1s. It is possible therefore to identify the RTD to considerable accuracy. For example, Fig. 3a shows the residence time distribution of barley grains (723 rpm, 40°) with a fitted normal distribution. The probability plot indicates that deviations from Normality are small. However, the observed shift in residence times over time discussed below skews the overall distribution and hence, plotting RTDs is not appropriate for all processing conditions.

Experiments were performed at ambient temperatures. At elevated temperatures, moisture migrates from the product into the atmosphere of the pipe. Many properties of the particles are thereby affected (e.g. surface properties, density, coefficient of restitution). It also renders the air more conductive and reduces electrostatic effects. Therefore, it is difficult to predict the effect of temperature on the residence time. This needs to be determined in future studies.

Note that the experiments were performed on a pilot plant device and the results do not directly apply to industrial machines.

Table 2
Mean residence times in seconds of the stable phases at motor angles of 20°, 30°, and 40° and motor speeds between 600 rpm and 740 rpm.

		Motor angle [°]		
		20	30	40
Motor speed [rpm]	600	389 ± 10	298 ± 6	306 ± 13
	660	–	297 ± 6	–
	710	–	–	332 ± 8
	723	–	–	244 ± 6
	740	406 ± 13	261 ± 6	195 ± 3

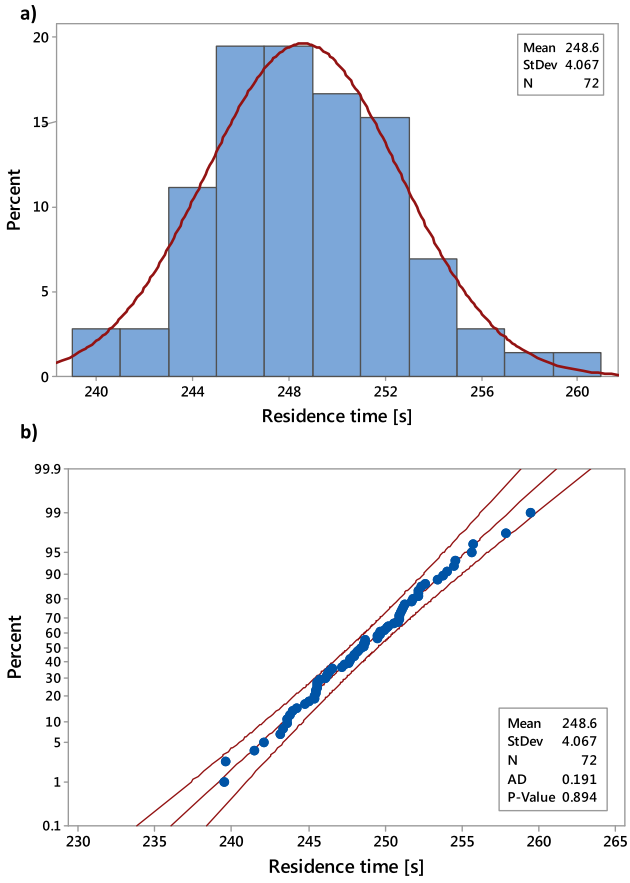

Fig. 3. a) Residence time distribution of barley grains at a motor speed of 723 rpm and a motor angle of 40° and overlaid normal distribution. b) Probability plot with 95% confidence intervals.

3.1. Effect of motor speed

The motor speed relates to the vibrational frequency of the spiral and it is associated with the amplitude of the vibrating bed. The spiral drives the particle flow to vibrate with the maximum amplitude at its resonance frequency. Macroscopically, it can be observed that at some frequencies, the flow is homogenous and regular and at others, the particle bed does not move as one and the flow looks chaotic. The motor speed affects the mean residence time, but as it is constant over time (data not shown) it is not responsible for changes in residence time over time.

The causes for the development of the residence time over time can be divided in.

i) A characteristic time after the start of the machine for the system to stabilise as a function of motor speed and motor angle
ii) Other effects like electrostatic forces that cause the residence time to shift after the stabilisation time.

3.1.1. Motor angle 20°

Fig. 4a shows the residence time of barley grains at motor angles of 20° for motor speeds of 600 rpm and 740 rpm. Time 0 corresponds to the instant where the equipment is turned on. The residence time is plotted against the time instant that the coloured grain enters the system. At 600 rpm, the residence time is stable over the timescale of the experiment as proven with control charts in Minitab (cf. section 2.5). In contrast at 740 rpm, the residence

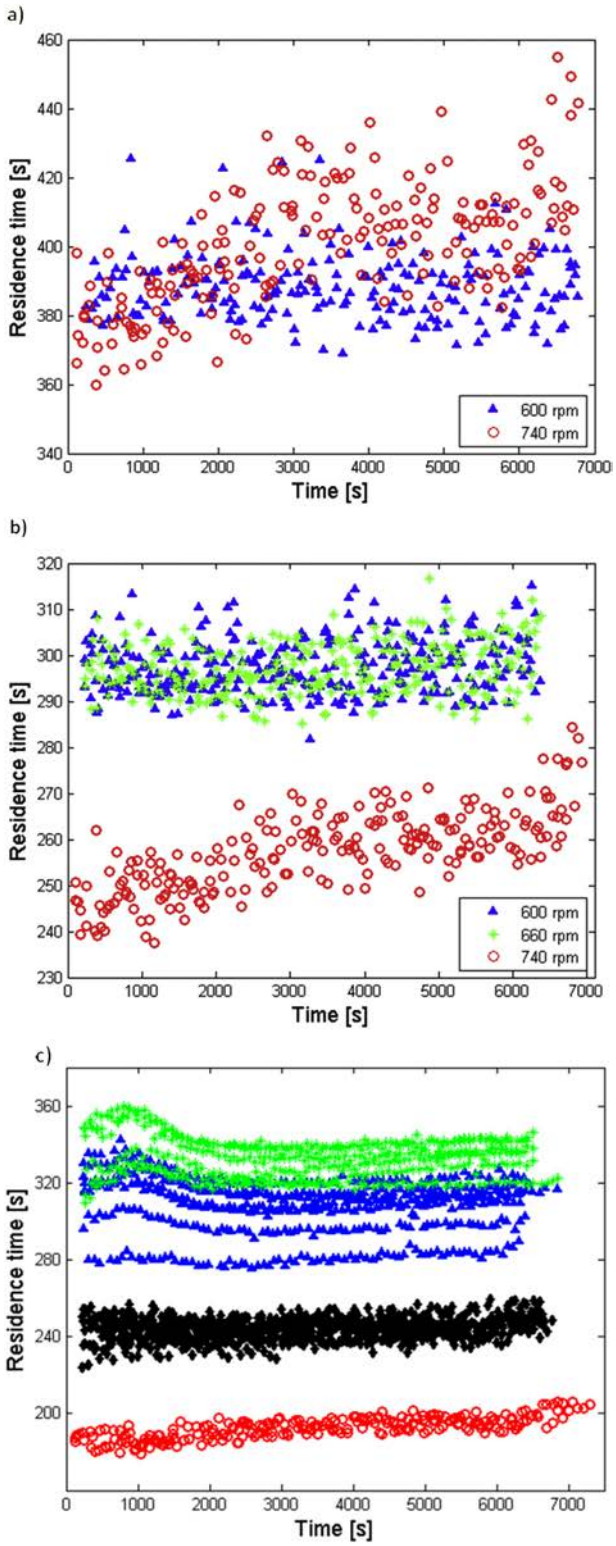

Fig. 4. Residence time of barley grains: a) Motor angles of 20° and motor speeds of 600 rpm and 740 rpm b) Motor angles of 30° and motor speeds of 600 rpm, 660 rpm, and 740 rpm. c) Motor angles of 40° and motor speeds of 600 rpm, 710 rpm, 723 rpm, and 740 rpm (Triangle: 600 rpm. Asterisk: 710 rpm. Diamonds: 723 rpm. Circle: 740 rpm.).

time initially increases then it stabilises before increasing again in the very end. The duration of the initial phase was determined with control charts. In three experiments, it took on average 1937 ± 146 s for the system to stabilise. The stable phase then lasted for 4529 ± 117 s. The variation in residence time between the smallest and the largest measured value was approx. 21.5% (79 s) (3 experiments). This is significantly higher than the standard deviation of 13 s for the stable phase and demonstrates the importance of identifying stable and unstable phases.

The mean residence time is 389 ± 10 s at 600 rpm and 406 ± 13 s at 740 rpm (cf. Fig. 4a). This is calculated from all the data at 600 rpm and from the data for the stable system at 740 rpm. There is only a slight difference of the mean residence time over the motor speed range (<4.4%).

The effect of the motor speed at angles of 20° is predominantly on the dynamics of the system rather than on the magnitude of the residence time. The stable data at 600 rpm facilitates the design of a thermal process. The difference between the average residence times at both motor speeds is small.

3.1.2. Motor angle 30°

The influence of the motor speed at motor angles of 30° is presented in Fig. 4b. Motor speeds of 600 rpm, 660 rpm, and 740 rpm were tested. At 600 rpm and 660 rpm the residence time is stable over the timescale of the experiment, whereas at 740 rpm it increases in the beginning of the experiment before it levels off and increases again in the end. The transition between initial and stable phase was found at 2452 ± 260 s and the duration of the stable phase was 4208 ± 259 s. In three experiments, the variation between the smallest and the largest measured value was approx. 17% (40 s), which is comparable to the results at 20°.

In contrast to motor angles of 20°, different motor speeds also result in different magnitudes of the residence time. For 600 rpm and 660 rpm, the behaviour was not a function of time and average residence times of 298 s ± 6 s and 297 s ± 6 s were measured. However, at a motor speed of 740 rpm, the residence time of the stable phase was determined to be 261 s ± 6 s.

3.1.3. Motor angle 40°

Motor speeds of 600 rpm, 710 rpm, 723 rpm, and 740 rpm were tested for motor angles of 40°. Results are depicted in Fig. 4c. It was found empirically that only at 723 rpm was the residence time approximately constant over the timescale of the experiment. For the other investigated motor speeds, there is an initial, unstable phase before the residence time stabilises. At 600 rpm and 710 rpm, the residence time increases and decreases before it levels off. At 740 rpm, it increases, levels off and increases again in the end of the experiment. In this case, it took 2495 ± 190 s for the system to stabilise and the stable period lasted for 4840 s ± 364 s. The variation in residence time between the smallest and the largest measured value was approx. 12% (22 s) (3 experiments).

By comparison to motor angles of 20° and 30°, changing the motor speed at 40° had a significant effect on the residence time. The mean was measured to be 306 ± 13 s, 332 ± 8 s, 244 ± 6 s, and 195 ± 3 s for motor speeds of 600 rpm, 710 rpm, 723 rpm, and 740 rpm, respectively. With the exception of 600 rpm, the mean and standard deviation decrease with increasing motor speeds of 710 rpm, 723 rpm, and 740 rpm. In this narrow range of motor speed, the residence time decreases by approx. 137 s (41%). It is worth mentioning that the decrease in standard deviation was observed for the pooled data. The standard deviation of the individual data sets was similar for all motor speeds (2 s, 3 s, 4 s, 3 s for 600 rpm, 710 rpm, 723 rpm, 740 rpm). This indicates that the variability between experiments was higher for lower motor speeds, but the dispersion of the grains during each experiment was comparable.

3.2. Effect of motor angle

3.2.1. Motor speed 600 rpm

Fig. 5a depicts the residence time of barley grains at a motor speed of 600 rpm for motor angles of 20°, 30°, and 40°. For 20° and 30°, it is constant over the timescale of the experiment as identified with control charts, whereas at 40° it increases and decreases in the initial phase before it stabilises.

Values of mean residence time distributions of 389 ± 10 s, 298 ± 6 s, and 306 ± 13 s were measured for motor angles of 20°, 30°, and 40°. While the data for 30° and 40° is in a similar range, residence time is about 29% higher for motor angles of 20°. There is no trend in the overall standard deviation from the pooled data sets. However, the standard deviation of the individual data sets decreases with increasing motor angle (data not shown). This demonstrates that the dispersion of the barley grains decreases with increasing motor angle, but the variability between experiments increases.

3.2.2. Motor speed 740 rpm

The influence of the motor angle at a motor speed of 740 rpm is presented in Fig. 5b. At all three angles, there is an initial stage where the residence time increases. It stabilises subsequently and increases again in the end. The stabilisation times were found by means of control charts and determined to be 1937 ± 146 s, 2452 ± 259 s, and 2495 ± 190 s for motor angles of 20°, 30°, and 40°. The duration of the stable phases was 4529 ± 117 s, 4208 ± 259 s, and 4840 ± 364 s for motor angles of 20°, 30°, and 40°. The overall residence time range between maximal and minimal value calculated from three experiments each is 22%, 17%, and 12% from the minimal value for 20°, 30°, and 40°. It shows that the overall variation of the residence time decreases with increasing motor angle.

The results of the pooled data of the stable phases are 406 ± 13 s, 261 ± 6 s, and 195 ± 3 s for motor angles of 20°, 30°, and 40°. The residence time at 20° is approx. 109% higher than at 40° which illustrates the importance of the effect of the motor angle. It is visible that mean and standard deviation decrease with increasing motor angle. This is also true for the individual data sets.

3.3. Summary of effects

For each motor angle, at least one motor speed was found at which the residence time of barley grains was constant over the entire timescale of the experiment. It would thus be possible to define a combination of angle and speed to deliver a uniform process.

At motor angles of 20° and 30°, the motor speed affected the dynamics of the system rather than the magnitude of the residence time; however motor speed at 40° influenced both the mean and standard deviation to a much greater extent. It was also observed that the variability between experiments was higher at lower motor speeds for angles of 40°.

The effect of the motor angle on the average residence time is more significant at 740 rpm than at 600 rpm. A constant residence time was only observed at 600 rpm and motor angles of 20° and 30°. The standard deviation of the individual data sets and therefore the dispersion of the barley grains during one experiment generally decreased with increasing motor angle.

3.4. Residence time dynamics

It was found that under some conditions the residence time evolved over the course of several test runs. Such behaviour might

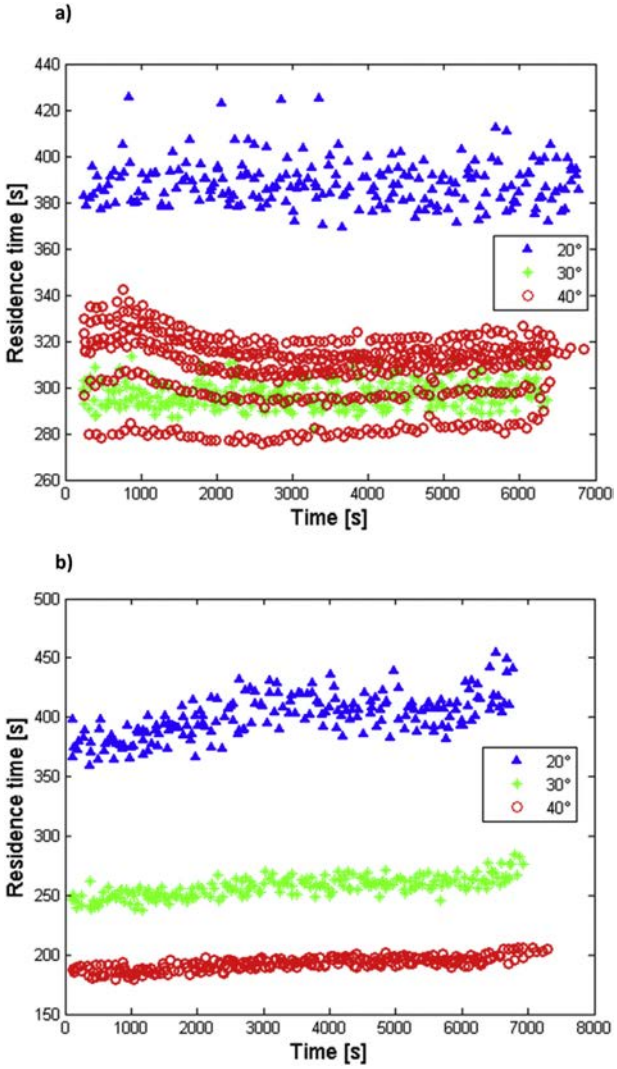

Fig. 5. Residence time of barley grains: a) Motor speed of 600 rpm and motor angles of 20°, 30°, and 40°. b) Motor speed of 740 rpm and motor angles of 20°, 30°, and 40°.

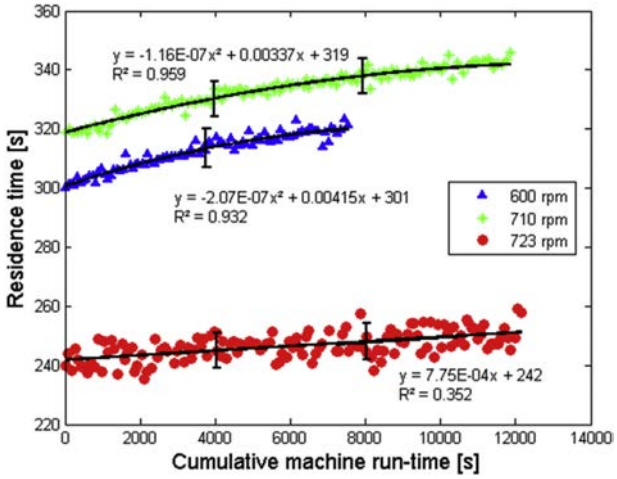

Fig. 6. Development of the residence time of barley grains during the course of a day at motor angles of 40° and motor speeds of 600 rpm, 710 rpm, and 723 rpm. The vertical line indicates the connection points between consecutive experiments.

make it difficult to specify a thermal process. For example, Fig. 6 describes the dynamics of the residence time during the day for motor angles of 40°. Results are given to three significant figures. The stable phases of all experiments during one day were connected. Each experiment took approx. 2 h and subsequently, the data of 2 (600 rpm) or 3 (710 rpm, 723 rpm) experiments was connected. Residence time at 600 rpm and 710 rpm increases with time and follows a quadratic curve quite accurately. At 723 rpm, the data is more scattered and the increase is smaller. In this case, the data can be approximated by a linear equation. Over 12,000 s, the average residence time increases by 19.6 s, 23.2 s, and 9.3 s which is 6.5%, 7.3%, and 3.9% of the initial value for motor speeds of 600 rpm, 710 rpm, and 723 rpm. The fitted curves were used for these calculations; at 600 rpm it was extrapolated. The change in residence time results in a change in particle holdup in the pipe. Only a small change in holdup is needed. The residence time in Fig. 6 increases from approximately 320 s–340 s over a time period of 12,000 s at a motor speed of 710 rpm. At a flow rate of 100 kg/h, this means a change of particle holdup in the pipe of 0.5 kg from ca. 8.9 kg–9.4 kg and a change in flow rate of 0.15 kg/h. Therefore, the change in holdup in the pipe is smaller than the accuracy at which the flow rate can be measured.

The residence time also increased during the day at motor angles of 20° and 30° at 600 rpm (data not shown). The extent of the linear increase was 4.5 s and 4.3 s after 12,000 s, which represents 1.2% and 1.4% of the initial value at motor angles of 20° and 30°, respectively. This data was calculated from the regression curve.

The data indicates that the increase of the residence time at motor angles of 20° and 30° is negligible, whereas it is much more significant at 40°. Furthermore at 40°, it increases to a higher extent at motor speeds of 600 rpm and 710 rpm than at 723 rpm.

Several factors might affect the residence time.

i) *Product effects*. The formation of a thin powder layer inside the pipe due to damage of the product may influence friction or the coefficient of restitution.
ii) *Machine effects*. These could include warming up of the motors, the suspensions or other parts might have an impact on the vibrations over time and hence on the residence time of the grains.
iii) *Environmental parameters* like ambient temperature and humidity might have an influence. In preliminary experiments, no effect of ambient temperature could be found in the process range of 16–24 °C.

These hypotheses were tested at motor angles of 40° and a motor speed of 600 rpm. It would be interesting to study why that increase only occurs at certain conditions and to variable extents. This is to be investigated in future work.

3.4.1. Hypothesis (i): deposition of a powder layer inside the pipe

To test the hypothesis whether the formation of a powder layer inside the pipe due to material damage causes the residence time to increase during the day, a cleaning experiment was performed.

i) Two experiments (2 h each) were performed per day for four consecutive days. At the end of each day, the pipe was cleaned with a cleaning pig and water. The data is shown in Fig. 7a. The first and second runs of all four days fall into two repeatable groups. The residence time increases over the course of each day as it is clearly higher in the second run than in the first one.
ii) Two experiments (2 h each) were performed per day for two consecutive days without cleaning the pipe. This is shown in Fig. 7b. The first and second run of the first day match the data in Fig. 7a. However, on the second day, the residence time of the first run is higher than that of the first run of the first day, but the second run on the second day behaves identically to that on the first day.

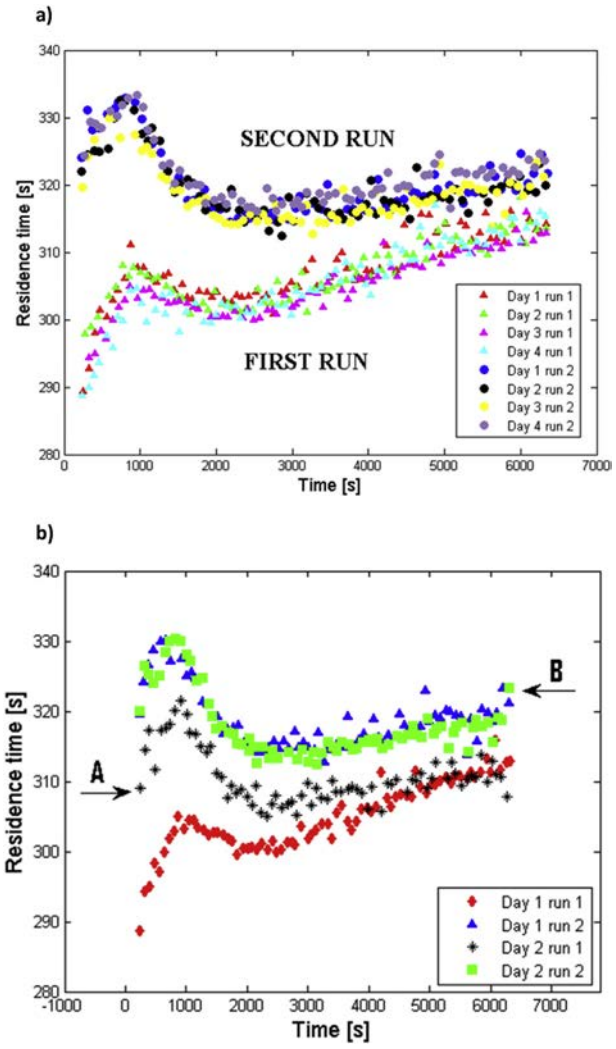

Fig. 7. a) Residence time of barley grains at motor angles of 40° and a motor speed of 600 rpm at four consecutive days (2 runs each day). Cleaning after each day. b) Residence time of barley grains at motor angles of 40° and a motor speed of 600 rpm at two consecutive days (2 runs each day). No cleaning.

Hence, it is obvious that the cleaning has an influence on the residence time. Without the cleaning, the residence time appears to increase.

On the other hand, if the residence time was solely due to the powder layer, it might be expected that the residence time at the start of the second day (point A in Fig. 7b) would be the same as at the end of the previous day (point B in Fig. 7b). However, the start point for the residence time decreases, perhaps due to alterations in the powder layer over night, e.g. humidity loss or gain or electrostatic charging. The experiments show that the formation of a powder layer inside the pipe affects the residence time of barley grains; more work would be needed to identify the precise cause.

3.4.2. Hypothesis (ii): warming up of the machine

The possible effect of warming up of the motors or other parts of the machine on the residence time of barley grains was tested. The machine was run for the period of one experiment (2 h) without

product to exclude product effects. Subsequently, product was added and two more experiments were performed. The data can be compared to days where the machine was started with product from the beginning and two experiments were completed.

The results are presented in Fig. 8 and show that data for experiments run after 2 h of operation are identical to data from the first and second experiments of the control days. If the warming up of the motors caused the increase of the residence time the two data sets would be different.

Hence it is concluded that the vibrations are controlled accurately and the warming up of the machine does not influence the residence time of barley grains.

4. Model development for process validation

The work above has demonstrated a wide range of residence times of barley grains for different processing conditions. It is unclear whether the observed variations are of practical significance. To assess this issue, a model was developed that calculates the pasteurisation effect of the process as it is needed for example for the pasteurisation of almonds (Almond Board of California, (2007); Silva and Gibbs, 2012).

Three inputs are required for the model:

i) Residence time distributions
ii) Temperature profiles along the axial direction of the pipe
iii) Microbial inactivation parameters

The residence time data from the experiments described in the previous sections were used as the basis for the model.

The temperature profiles along the axial direction of the pipe are determined by 8 temperature probes embedded between the outside of the steel pipe and the insulation layer. One probe is located in each loop, starting from half a loop after the inlet of the spiral to probe 8 towards the top of the spiral. As the pipe is heated via resistive heating and is open to atmosphere, the temperature is not constant over the total length of the pipe. The temperature is controlled so that at least one of the probes is held at the temperature setpoint, whereas the temperature of the other probes depends on product flow rate and thermal properties of the product. Fig. 9 shows a measured temperature profile for electrical heating

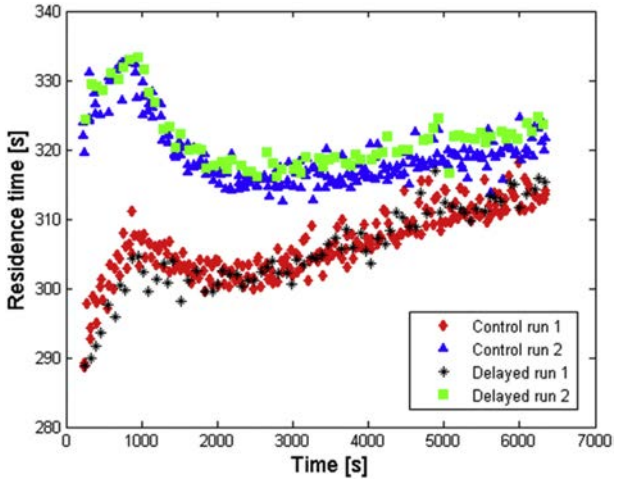

Fig. 8. Residence time of barley grains at motor angles of 40° and a motor speed of 600 rpm. Two sets are shown (i) control run 1 and 2 where the machine was started at the start of run 1 and (ii) delayed run 1 and 2 where the machine was run for 2 h without product before the start of run 1.

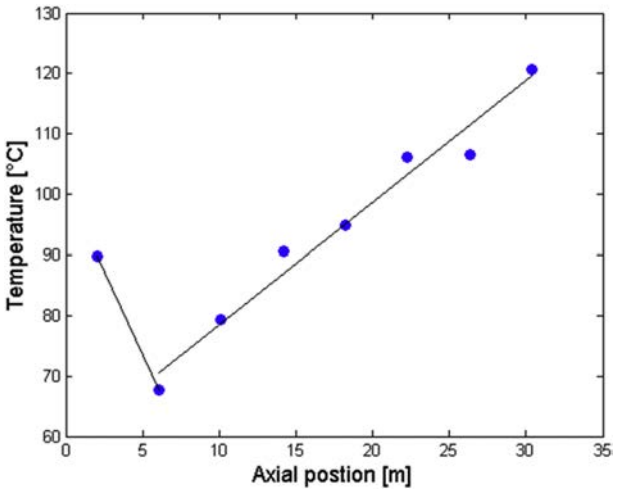

Fig. 9. Temperature profile along axial direction of the pipe. Setpoint 120 °C.

for a setpoint of 120 °C. The temperature profile down the tube is clear. Straight line fits were drawn (i) between the first two temperatures, and (ii) to represent the mean of subsequent temperature probes. This profile is then used in the model as defined below.

The microbial input data comprises the D-value, its reference temperature, and the z-value. These are highly dependent on the microorganism and its environment and furthermore the processing history and the processing conditions (Silva and Gibbs, 2012; Podolak et al., 2010). Candidate organisms and their thermal behaviour are given in Table 1. As an example *Salmonella* Tennessee with $D_{105} = 2.4$ min and $z = 11.9$ °C relevant to particulate grains is used.

D-values and reaction rates are calculated at each temperature in the observed range. The model assumes that the temperature of the surface of the particles is the same as the temperature profile of the probes and that only the surface is microbiologically contaminated. No fitted continuous distribution or minimum residence time was used because of the observed shift in residence time over time. The residence time data is used to calculate the velocity of individual particles. The survivors are determined by the general expression for microbial evolution and the log reductions are established.

The model calculates the thermal process by the following:

1) The D-value is calculated for the observed range of temperatures by linear regression and by means of the z-value.
2) Reaction rates (k(T)) are calculated for the observed range of temperatures.

$$k(T) = \frac{2.303}{D(T)} \cdot \frac{1}{60} \quad [1/s] \tag{3}$$

3) Particles are assumed to travel at constant velocity, calculated by dividing the pipe length by the observed residence time.
4) The pipe length is divided in 344 small segments, each 0.1 m long.

The residence time that a particle takes to pass one segment (Δt) is calculated by dividing the segment length by the velocity.

5) The temperature profile in the axial direction of the pipe is determined from the linearised temperature profile shown in Fig. 9.

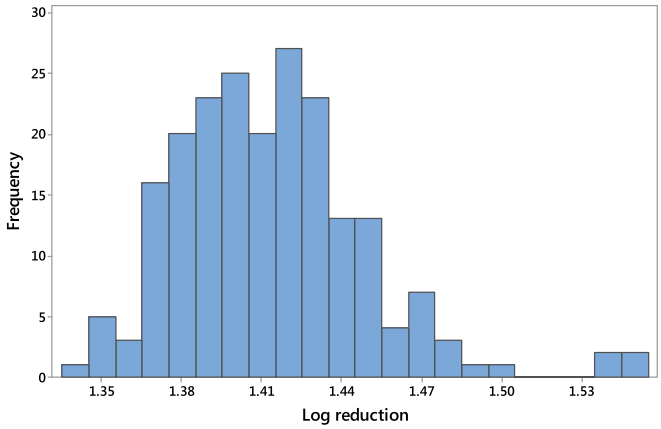

Fig. 10. Distribution of log reductions of S. Tennessee (D_{105} = 2.4 min, z = 11.86 °C) at motor angles of 20° and a motor speed of 600 rpm and a temperature setpoint of 120 °C.

6) The reaction rate is next found for each segment depending on the calculated temperature.
7) The integral $\int 10^{T-T_{ref}/z}dt$ which describes the inactivation effect can be approximated using the temperature profile and section residence time (Heldman, 2011). The fractional microbial kill in each segment is calculated by applying the exponential function to the product of residence time per segment and reaction rates (Heldman, 2011).

$$S_{Segment} = \frac{N_{Segment,outlet}(t)}{N_{Segment,inlet}} = \exp(k(T)\cdot\Delta t) \quad (4)$$

The survivors of all segments are combined by multiplying the sequence.

$$S_{total} = \prod S_{segment} \quad (5)$$

8) The overall log-reduction is calculated

Microbial reduction should be calculated individually for each application. As an example Fig. 10 shows for motor angles of 20° and a motor speed of 600 rpm (data of Fig. 5a), assuming microbiological parameters of D_{105} = 2.4 min and z = 11.86 °C for *Salmonella* Tennessee (cf. Table 1) and the temperature profile of Fig. 9, microbial reduction varies between 1.34 and 1.55 log reductions (overall mean calculated from RTD: 1.41 log reductions).

It is evident that the variation in residence time relates to the microbial reduction linearly. In this case, the residence time ranges between 369 s and 426 s with a mean of 389 s. The difference between minimal and maximal value is 15% for the residence time as well as the microbial log reduction.

Table 3 shows both the mean and the range of microbial inactivation for different motor angles and motor speeds. The highest inactivation results from the highest residence time (motor angles of 20° and a motor speed of 740 rpm) whilst the smallest was calculated for the shortest residence time (motor angles of 40° and a motor speed of 740 rpm). The table also shows the relative differences in microbial inactivation as well as in residence times with respect to their means at all tested processing conditions. The most precise treatment is achieved at 40° and 740 rpm (spread of 9%), but this might be different when individual runs are considered rather than the entirety of all experiments. In contrast, the highest spread was observed for 40° and 600 rpm (19%).

To improve the model and to make it more realistic, the following changes could be made:

i) More complex heat transfer models can be chosen and additionally convection and steam may be taken into account.
ii) Dynamic D-values depending on the water status at the surface of the particles may be included (Jeong et al., 2009).
iii) A more accurate measure of the distribution of temperature across the probes is needed, together with the relationship between wall and particle temperature.

The calculations serve to assess the impact of the variation in residence time on microbial inactivation. An arbitrary model organism was chosen and the model does not reflect the possible magnitude of microbial reduction achievable with the machine; for example the D-value changes significantly as soon as steam is added. The Revtech equipment has been validated for a number of applications with a kill of well over 5 log reductions of *Enterococcus faecium*. The narrower the residence time distribution, the smaller the variation in log reduction will be.

The mass holdup in the system is obviously important in the determination of the residence time. The holdup can be calculated as (flowrate × residence time) assuming no dead spaces and is in the region of 9 kg. The change in holdup that gives rise to the changes in residence time is small (ca. 0.5 kg). All of this work has used a flow of 100 kg/h, and was designed to demonstrate the use of the device. Careful experiments would be needed to confirm the residence time in practice, and to ensure minimal drift in the process time. The methods described here would be useful for such determination. The drift in residence time is less for barley than for flour (Keppler et al., 2015); different particles will show different effects.

5. Conclusion

A novel tubular apparatus for the pasteurisation of particles was investigated. The residence time was characterized in both single experiments and over the period of multiple experiments. The

Table 3
Table of (i) Mean log microbial reductions and (ii) Range of log reductions; difference between maximum and minimum, written as % (range/mean).

		Motor angle [°]					
		20		30		40	
		Mean [log]	Range [%]	Mean [log]	Range [%]	Mean [log]	Range [%]
Motor speed [rpm]	600	1.41	15.7	1.08	11.7	1.11	19
	660	–	–	1.08	10.6	–	–
	710	–	–	–	–	1.21	9.6
	723	–	–	–	–	0.89	14.6
	740	1.48	17.7	0.95	13.5	0.71	9

behaviour of the system was a function of two variables, motor angle and motor speed.

At motor angles of 20° and 30°, the motor speed affected the dynamics of the system rather than the magnitude of the residence time; at 40° it influenced the mean and standard deviation to a much bigger extent. At least one motor speed was found for each motor angle at which the residence time was constant over the entire timescale of the experiment. Additionally, it was observed at angles of 40° that the variability between experiments was higher at low motor speeds.

The effect of the motor angle on the average residence time was more significant at a motor speed of 740 rpm compared to 600 rpm. At 600 rpm the residence time was constant for motor angles of 20° and 30° in contrast to 40°, where an initial unstable phase occurred. Unstable dynamics were observed at 740 rpm for all motor angles. The standard deviation of the individual data sets and therefore the dispersion of the barley grains during one experiment decreased with increasing motor angle.

Generally, the residence time increased during the course of the day. The data suggests that the increase of the residence time at motor angles of 20° and 30° is negligible, whereas it is much more significant at 40°. Furthermore, at 40° it increases to a higher extent at motor speeds of 600 rpm and 710 rpm than at 723 rpm. The change is difficult to detect by measuring flow rate – holdup changes by less than a kg over several hours.

Some reasons for this phenomenon were proposed and tested. The formation of a powder layer inside the pipe has proven to affect the residence time of barley grains. It is unlikely that this is the only factor causing the residence time to increase during the day and it is suggested that the properties of that layer might change over time. The warming up of the machine does not influence the residence time. No correlation was found between ambient temperature and residence time.

A simple model for pasteurisation of particles has been developed that characterises the impact of the variation in residence time on microbial inactivation. Across all tested processing conditions, the variation between minimal and maximal log reduction was between 9% and 19%. In this way, precise treatments can be identified.

More work is needed to identify the cause of the drift in residence time, and to confirm or develop the mathematical model. Ranges of processing conditions have been identified that produce stable operation and thus effective pasteurisation of product.

Acknowledgement

This research was done as part of a PhD project supported by a BBSRC studentship in collaboration with Campden BRI (Gloucestershire, UK). The project is supported by the RCUK National Centre for Sustainable Energy Use in Food Chains: (EP/K011820/1). The authors would like to thank Revtech process systems (Loriol-sur-Drome, FR) for providing the equipment.

References

Almond Board of California, 2007. Considerations for Proprietary Processes Used for Almond Pasteurization and Treatment. Available: http://www.almonds.com/sites/default/files/content/attachments/proprietary-processes.pdf (Accessed: 04/2016).

Barrile, J.C., Cone, J.F., 1970. Effect of added moisture on the heat resistance of Salmonella anatum in milk chocolate. Appl. Microbiol. 19 (1), 177–178.

Beuchat, L., Komitopoulou, E., Betts, R., Beckers, H., Bourdichon, F., Joosten, H., Fanning, S., ter Kuile, B., 2011. Persistence and survival of pathogens in dry foods and dry food processing environments. Int. Life Sci. Inst. Eur. Rep. Ser. 1–48.

Beuchat, L.R., Komitopoulou, E., Beckers, H., Betts, R., Bourdichon, F., Fanning, S., Joosten, H., ter Kuile, B., 2013. Low-water activity foods: increased concern as vehicles of foodborne pathogens. J. Food Prot. 76 (1), 150–172.

Buhler AG, (2014). http://www.buhlergroup.com/northamerica/en/downloads/CCP.pdf (Accessed 04/2016).

Chang, S.-S., Han, A.R., Reyes-De-Corcuera, J.I., Powers, J.R., Kang, D.-H., 2010. Evaluation of steam pasteurization in controlling Salmonella serotype Enteritidis on raw almond surfaces. Lett. Appl. Microbiol. 50 (4), 393–398.

Chick, M., 2011. Thermal Inactivation Kinetics of Salmonella Serovars on Dry Cereal. M.S. thesis. Retrieved from the University of Minnesota Digital Conservancy. http://purl.umn.edu/116854.

Codex Alimentarius Commission, 2013. Proposed Draft Code of Hygienic Practice for Low-moisture Foods CX/FH 13/45/7. Food and Agriculture Organization of the United Nations, World Health Organization. Available: ftp://ftp.fao.org/codex/meetings/ccfh/ccfh45/fh45_07e.pdf (Accessed 04/2016).

ETIA(2014). "www.spirajoule.com." (Accessed 04/2016).

Harris, L.J., Uesugi, A.R., Abd, S., McCarthy, K.L., 2012. Survival of Salmonella Enteritidis PT 30 on inoculated almond kernels in hot water treatments. Food Res. Int. 45 (2), 1093–1098.

Heldman, D.R., 2011. Kinetic models for food systems. In: Food Preservation Process Design. Elsevier, Amsterdam, pp. 19–48.

Jeong, S., Marks, B.P., Orta-Ramirez, A., 2009. Thermal inactivation kinetics for Salmonella enteritidis PT30 on almonds subjected to moist-air convection heating. J. Food Prot. 72 (8), 1602–1609.

Keppler, S., Bakalis, S., Leadley, C.E., Fryer, P.J., 2015. A systematic study of the residence time of flour in a vibrating apparatus used for thermal processing. Innov. Food Sci. Emerg. Technol. 33, 462–471.

Lee, S.-Y., Oh, S.-W., Chung, H.-J., Reyes-De-Corcuera, J.I., Powers, J.R., Kang, D.-H., 2006. Reduction of Salmonella enterica Serovar Enteritidis on the surface of raw shelled almonds by exposure to steam. J. Food Prot. 69 (3), 591–595.

Mattick, K.L., Jorgensen, F., Legan, J.D., Cole, M.B., Porter, J., Lappin-Scott, H.M., Humphrey, T.J., 2000. Survival and filamentation of Salmonella enterica serovar enteritidis PT4 and Salmonella enterica serovar typhimurium DT104 at low water activity. Appl. Environ. Microbiol. 66 (4), 1274–1279.

Napasol(2015). "www.napasol.com." (Accessed 04/2016).

Neetoo, H., Chen, H., 2011. Individual and combined application of dry heat with high hydrostatic pressure to inactivate Salmonella and Escherichia coli O157:H7 on alfalfa seeds. Food Microbiol. 28 (1), 119–127.

Penaloza Izurieta, W., Komitopoulou, E., 2012. Effect of moisture on salmonella spp. heat resistance in cocoa and hazelnut shells. Food Res. Int. 45 (2), 1087–1092.

Podolak, R., Enache, E., Stone, W., Black, G., Elliott, P.H., 2010. Sources and risk factors for contamination, survival, persistance, and heat resistance of Salmonella in low-moisture foods. J. Food Prot. 73 (10), 1919–1936.

Revtech(2015). "http://www.revtech-process-systems.com/index.php/en/(Accessed 04/2016).

Silva, F.V.M., Gibbs, P.A., 2012. Thermal pasteurization requirements for the inactivation of Salmonella in foods. Food Res. Int. 45 (2), 695–699.

Villa-Rojas, R., Tang, J., Wang, S., Gao, M., Kang, D.-H., Mah, J.-H., Gray, P., Sosa-Morales, M.E., Lopez-Malo, A., 2013. Thermal inactivation of Salmonella enteritidis PT 30 in Almond Kernels as influenced by water activity. J. Food Prot. 76 (1), 26–32.